DEVELOPMENT OF A GRAPHITE HORIZONTAL STABILIZER

Interim Technical Report
1 May to 31 October 1971

February 1972

Prepared Under Contract N00156-70-C-1321

For

Vehicle Technology Department
Naval Air Development Center
Warminster, Pennsylvania, 18974

Approved for public release, distribution unlimited

McDonnell Douglas Corporation
Douglas Aircraft Company
Long Beach, California

UNCLASSIFIED
Security Classification

DOCUMENT CONTROL DATA – R & D

(Security classification of title, body of abstract and indexing annotation must be entered when the overall report is classified)

1. ORIGINATING ACTIVITY *(Corporate author)*

DOUGLAS AIRCRAFT COMPANY
MCDONNELL DOUGLAS CORPORATION
LONG BEACH, CALIFORNIA

2a. REPORT SECURITY CLASSIFICATION

UNCLASSIFIED

2b. GROUP

3. REPORT TITLE

DEVELOPMENT OF A GRAPHITE HORIZONTAL STABILIZER

4. DESCRIPTIVE NOTES *(Type of report and inclusive dates)*

INTERIM TECHNICAL REPORT (1 MAY 1971 TO 31 OCTOBER 1971)

5. AUTHOR(S) *(First name, middle initial, last name)*

GEORGE M. LEHMAN, ET AL.

6. REPORT DATE	7a. TOTAL NO. OF PAGES	7b. NO. OF REFS
FEBRUARY 1972	174	10

8a. CONTRACT OR GRANT NO.	9a. ORIGINATOR'S REPORT NUMBER(S)
N00156-70-C-1321 b PROJECT NO.	MDC J5317
c.	9b. OTHER REPORT NO(S) *(Any other numbers that may be assigned this report)*
d.	

10 DISTRIBUTION STATEMENT

APPROVED FOR PUBLIC RELEASE, DISTRIBUTION UNLIMITED.

11. SUPPLEMENTARY NOTES	12. SPONSORING MILITARY ACTIVITY
	VEHICLE TECHNOLOGY DEPARTMENT NAVAL AIR DEVELOPMENT CENTER WARMINSTER, PENNSYLVANIA 18974

13. ABSTRACT

THE STRUCTURAL WEIGHTS, STRESS-ANALYSIS RESULTS, AND MANUFACTURING METHODS ARE SUMMARIZED FOR AN A-4 AIRCRAFT HORIZONTAL STABILIZER UTILIZING NARMCO 5206 GRAPHITE-EPOXY LAMINATES IN THE PRIMARY STRUCTURE. THE ACTUAL WEIGHT OF THE FIRST UNIT PRODUCED WAS 178 POUNDS, A WEIGHT REDUCTION OF 30 PERCENT IN COMPARISON TO THE EQUIVALENT METAL STRUCTURE. THE FINISHED STRUCTURE WEIGHT WAS COMPRISED OF APPROXIMATELY 62 PERCENT GRAPHITE-EPOXY, 11 PERCENT FIBERGLASS-EPOXY, 10, 8, AND 5 PERCENT, RESPECTIVELY, OF ALUMINUM, STEEL, AND TITANIUM ALLOYS (INCLUDING ATTACHMENTS), AND 4 PERCENT ADHESIVE AND EPOXY FILLETS. RESULTS OF A DISCRETE ELEMENT STRESS-ANALYSIS ARE PRESENTED FOR THE THREE CRITICAL LOAD CONDITIONS ON THE STABILIZER. THE DISCRETE ELEMENT MODEL INCLUDED RECENT DESIGN CHANGES (DIMENSIONS AND ELASTIC PROPERTIES) TO THE STABILIZER AND PROVISIONS FOR RUNNING ASYMMETRIC LOAD CASES BUCKLING ALLOWABLE ARE PRESENTED FOR ACTUAL SKIN PANEL THICKNESSES AND MARGINS-OF-SAFETY ARE SUMMARIZED FOR ALL CRITICAL ELEMENTS OF THE STRUCTURE. TOOLING, FABRICATION, AND ASSEMBLY PROCEDURES USED DURING CONSTRUCTION OF THE FIRST STABILIZER ASSEMBLY AND THE SECOND SUBSTRUCTURE ASSEMBLY ARE DISCUSSED. DETAILS OF THE DISCRETE ELEMENT MODEL, INTERNAL STRESS DISTRIBUTIONS, INCOMING MATERIAL AND IN-PROCESS TEST RESULTS (INCLUDING NDT), AND FABRICATION PROCEDURES ARE CONTAINED IN APPENDICES

DD FORM 1 NOV 65 1473

UNCLASSIFIED
Security Classification

14. KEY WORDS	LINK A		LINK B		LINK C	
	ROLE	WT	ROLE	WT	ROLE	WT
AIRCRAFT STRUCTURES						
STRUCTURAL DESIGN						
STRUCTURAL ANALYSIS						
DISCRETE ELEMENT ANALYSIS						
ORTHOTROPIC PROPERTIES						
GRAPHITE/EPOXY COMPOSITES						
NARMCO 5206						
ALLOWABLE BUCKLING STRESSES						
FABRICATION PROCEDURES						
TOOLING						
STRUCTURAL TEST						
NONDESTRUCTIVE TEST						

DEVELOPMENT OF A GRAPHITE HORIZONTAL STABILIZER

Interim Technical Report
1 May to 31 October 1971

February 1972

Prepared Under Contract N00156-70-C-1321

For

Vehicle Technology Department

Naval Air Development Center

Warminster, Pennsylvania, 18974

McDonnell Douglas Corporation
Douglas Aircraft Company
Long Beach, California

FOREWORD

This report was prepared by the Douglas Aircraft Company, McDonnell Douglas Corporation, Long Beach, California, under the terms of contract N00156-70-C-1321. It is the fourth semi-annual interim technical report covering work completed between 1 May 1971 and 31 October 1971. The program is sponsored by the Vehicle Technology Department, Naval Air Development Center (NADC), Warminster, Pennsylvania 18974. Mr. Anthony Manno, Code STD-8, is the Project Engineer for NADC.

The following Douglas personnel were the principal contributors to the program during the reporting period: G. M. Lehman, Program Manager; A. V. Hawley, Structural Design Coordinator; F. C. Allen and P. T. Mikkelson, Structural Analysis; R. J. Palmer and H. M. Toellner, Material and Process Engineering; A. T. Tucci and R. L. Zwart, Manufacturing Development; D. J. Hagemaier, Nondestructive Test; and D. E. McCay, Instrumentation and Testing.

The Rohr Corporation, Riverside, California, is a subcontractor to Douglas for fabrication of the substructure assembly. Mr. R. A. Elkin is the subcontract program manager for Rohr.

This report was prepared under Douglas Report MDC-J5317. It was approved by NADC for distribution in February 1972.

THIS PAGE LEFT BLANK INTENTIONALLY.

SUMMARY

The structural weights, stress-analysis results, and manufacturing methods are summarized for an A4 aircraft horizontal stabilizer utilizing Narmco 5206 graphite-epoxy laminates in the primary structure. The actual weight of the first unit produced was 178 pounds, a weight reduction of 30% in comparison to the equivalent metal structure. The finished structure weight was comprised of approximately 62 percent graphite-epoxy, 11 percent fiberglass-epoxy, 10, 8, and 5 percent, respectively, of aluminum, steel, and titanium alloys (including attachments), and 4 percent adhesive and epoxy fillets. Results of a discrete element stress-analysis are presented for the three critical load conditions on the stabilizer. The discrete element model included recent design changes (dimensions and elastic properties) to the stabilizer and provisions for running asymmetric load cases. Buckling allowables are presented for actual skin panel thicknesses and margins-of-safety are summarized for all critical elements of the structure. Tooling, fabrication, and assembly procedures used during construction of the first stabilizer assembly and the second substructure assembly are discussed. Details of the discrete element model, internal stress distributions, incoming material and in-process test results (including NDT), and fabrication procedures are contained in Appendices.

THIS PAGE LEFT BLANK INTENTIONALLY.

TABLE OF CONTENTS

THIS PAGE LEFT BLANK INTENTIONALLY.

LIST OF ILLUSTRATIONS

LIST OF ILLUSTRATIONS (Continued)

LIST OF ILLUSTRATIONS (Continued)

LIST OF ILLUSTRATIONS (Continued)

LIST OF ILLUSTRATIONS (Continued)

LIST OF TABLES

LIST OF SYMBOLS

E	Young's Modulus of Elasticity	psi
G	Shear Modulus	psi
T	Temperature differential	degrees F
α	Coefficient of Thermal expansion	inches/inch/degree F
σ	Normal stress	psi
τ	Shear stress	psi
ν	Poisson's Ratio	
x,y,z	Cartesian (base) coordinate axes	
α, β	Discrete element coordinate axes	
1,2	Laminate axes of orthotropy	

Matrix Notation*

A	Matrix expression for Hooke's Law	psi
B	Matrix expression for thermal strain	inches/inch
b	Matrix relating strains to displacements	$inches^{-1}$
K	Generalized stiffness matrix	pounds/inch
K^i	Element stiffness matrix	pounds/inch
K_r	Stiffness matrix reduced to account for six rigid-body degrees-of-freedom	pounds/inch
K_w	Stiffness matrix reduced to account for degrees-of-freedom restrained by boundary conditions	pounds/inch
P	Load matrix	pounds
Q	Thermal force matrix	pounds
U	Generalized displacement matrix	inches
u	Element displacement matrix	inches
λ	Coordinate transformation matrix (base system to element system)	

*Superior bar (e.g., $\overline{U}$) signifies that the matrix elements are referenced to the base coordinate system.

THIS PAGE LEFT BLANK INTENTIONALLY.

SECTION 1

INTRODUCTION

The overall objective of the graphite composite structural development program is to obtain significant improvements in aircraft weapon system performance through structural applications of advanced composite materials. A primary requirement of the program is to demonstrate the structural performance and weight characteristics of graphite/epoxy composites in aircraft wing-type applications. This requirement will be met through the design, fabrication, and test of a graphite/epoxy horizontal stabilizer structure for the A-4 attack aircraft, and through analytical comparisons of its structural performance with the functionally equivalent metal component.

The program involves the design and development of two full-scale stabilizers and selected intermediate development components. The latter components were chosen to substantiate design and fabrication techniques used in the stabilizers. Design refinements to the stabilizer structure were accomplished at the conclusion of the intermediate component tests. The two full-scale stabilizers will include a static and vibration test article and a fatigue test article, both of which will be tested at the Naval Air Development Center (NADC).

The stabilizer was designed to take maximum advantage of the engineering properties of graphite reinforced composites in the primary structure. Other materials were used selectively in the design where their properties were advantageous (e.g., fiberglass leading-edge assembly, metal fittings and joint reinforcements). The design concept involved the use of solid laminate skins stabilized against buckling by a multi-shear web substructure made of bonded honeycomb panels. Machined metal fittings were utilized at the seven elevator hinge stations and at the stabilizer attach points to the fixed structure. Bonded metal reinforcing was also used to transmit concentrated elevator loads into the skin panels. However, graphite reinforced composites comprised approximately 62 percent of the finished stabilizer weight. A structural weight reduction of approximately 30 percent was attained on the first unit completed (the vibration and static test article).

This report describes work accomplished during the fourth six-month period of the program. Accomplishments during this period included:

- Completion of fabrication, assembly and instrumentation of the first stabilizer unit
- Completion of fabrication and assembly of the second stabilizer substructure assembly at Rohr
- Completion of the fabrication procedures for detail parts and assemblies
- Complete revision and updating of the discrete element analysis of the stabilizer structure.

These activities are described following under the headings Engineering Design and Analysis, and Manufacturing Development. Details of the stress analysis, fabrication procedures, incoming quality control test results, and in-process test results are presented in the Appendices.

SECTION 2

ENGINEERING DESIGN AND ANALYSIS

Design activity during the reporting period consisted primarily of engineering liaison with the tooling and manufacturing activities. Three intermediate component I-beams were also reworked by Douglas and retested at NADC to verify the combination bolted and bonded design approach adopted during the prior reporting period (see Reference 1). Weight estimates were revised based on the final design configuration of the stabilizer and the actual weight of the first unit was compared with the estimates. A discrete element analysis was conducted using an improved analysis model which included design changes to the upper skin panel resulting from the intermediate component tests. The analysis model also included revised elastic constants and provisions for running asymmetric load cases. The results of the reworked I-beam tests, the current weight summary, and the stress analysis results are presented in this section under the headings Structural Design and Structural Analysis.

STRUCTURAL DESIGN

Intermediate Component Tests

Three I-beam fatigue specimens were reworked to represent the combination bolted/bonded skin panel design adopted during the prior reporting period (see Reference 1). The beams were reworked to remove the fiberglass grid element and the graphite/epoxy upper attach-angles by means of a rough trim, disc-sand, and final hand-sand operation. The grid and attach-angles were removed without damaging the honeycomb shear panels or the lower skins. The new upper attach-angles with a revised fiber pattern were cocured and bonded to the shear-webs, and subsequently the upper skin was secondarily bonded to the attach-angles using an oven cure for the adhesive layer. The upper surface fasteners were installed using the standard installation torque prior to the adhesive cure. The resulting preload in the fasteners supplied the bond pressure during the oven cure operation.

To verify the validity of the bolted/bonded skin panel attachment, two of the reworked I-beams were tested statically and the third was fatigue tested at NADC. Static strength of 11,500 and 12,300 pounds were attained by the reworked I-beams, corresponding to 164 and 176%, respectively, of design limit load (DLL). The reworked fatigue I-beam was cycled under constant amplitude conditions at a maximum load of 7000 pounds (100% DLL) and a stress ratio R of + 0.05. After 330,000 cycles of limit load, the fatigue beam failed as shown in Figure 1. The fatigue failure occurred in the facings of the honeycomb sandwich shear-webs of the reworked I-beam. Failures of the original I-beam design always occurred in the tension flange (i.e., grid and/or skin panel). The shear-web failure was also characteristics of the reworked I-beam static test.

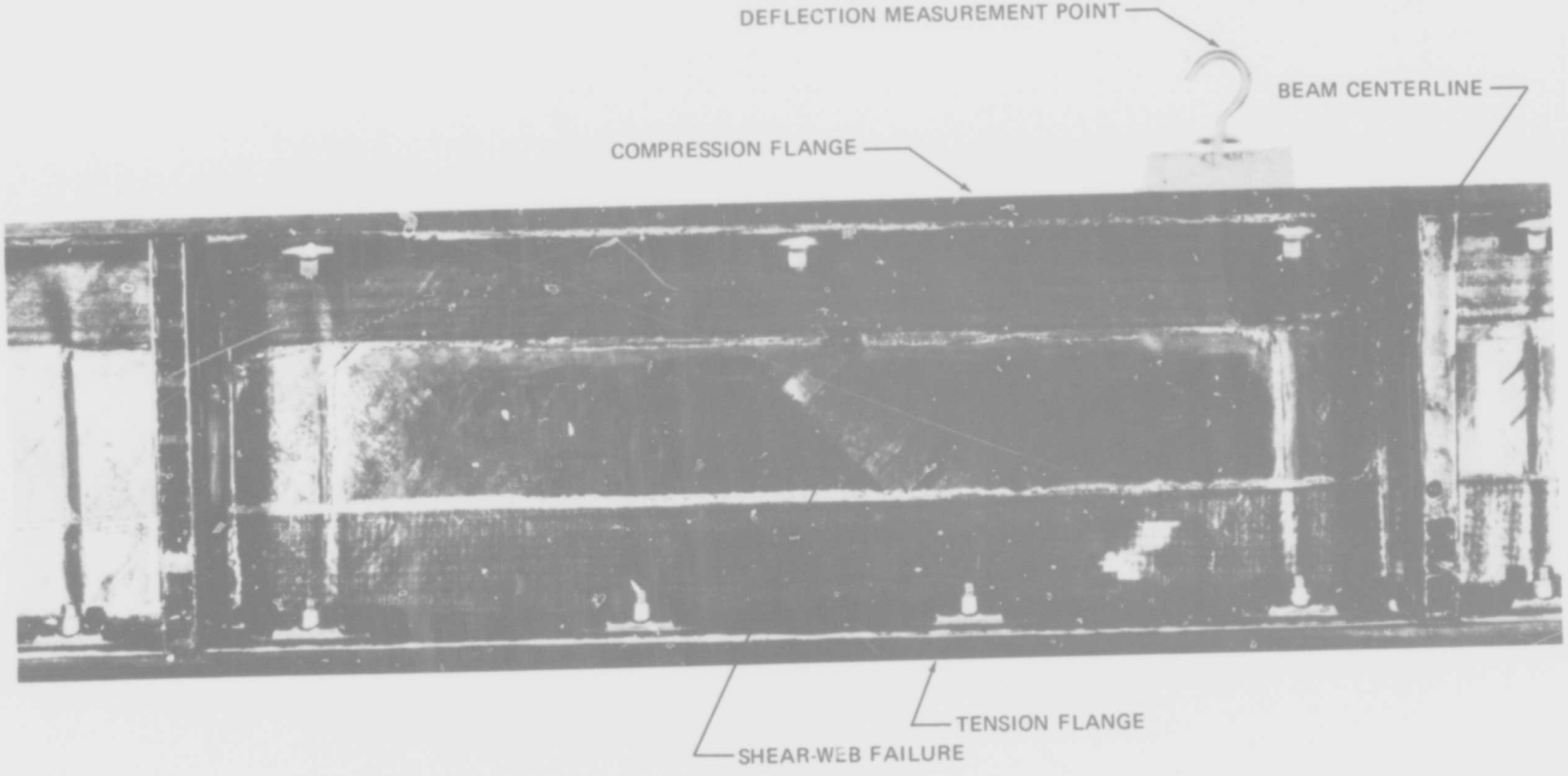

FIGURE 1. I-BEAM SHEAR WEB FAILURE

Prior to rework, the I-beams sustained static loads of 150%, 154%, and 164% DLL and a constant amplitude fatigue loading of 18,262 cycles at design limit load (7000 pounds). Thus, the reworked I-beams were superior to the original design in both static and fatigue load performance.

Structural Weight Summary

At the conclusion of the I-beam and box-beam intermediate component tests, a design decision was made to assemble the stabilizer structure using the combination bolted and bonded joint at the skin panel to substructure interface (see Reference 1). The preliminary weight projection for the bolted-bonded stabilizer design was 172 pounds. The actual weight of the first stabilizer unit exceeded the weight projection by approximately six pounds. The weight difference was attributed primarily to the cured ply thicknesses of the skin panels and attach angles of 6 mils rather than the expected 5.5 to 5.8 mils, a thicker than anticipated adhesive layer at the upper panel bond surface, and the use of steel rather than titanium bolts for attachment of the pivot and actuator fittings. The bolt substitution was made to avoid a procurement delay and resulted in approximately a one pound weight penalty to the finished structure.

A detailed weight and material utilization summary for the first stabilizer assembly is presented in Table I. The finished structure weight was comprised of approximately 62 percent graphite/epoxy, 11 percent fiberglass/epoxy, 10, 8, and 5 percent respectively of aluminum, steel, and titanium alloys, and 4 percent adhesive and epoxy fillets. The overall weight saving for the first unit was 28.2 percent by comparison to the equivalent metal structure. The redesigned structure (excluding the pivot and actuator fittings common to both graphite and metal stabilizers) was 30.3 percent lighter than the corresponding metal structure. Considering only the components in which the graphite/epoxy laminates were used (excluding all fittings, fasteners, and the fiberglass/epoxy leading edge assembly), a weight saving of 36.4 percent was attained by comparison with the analogous metal components.

STRUCTURAL ANALYSIS

The previously reported discrete element analyses of the structure (References 2 and 3) were completely revised and updated during the reporting period. The analysis model was improved to include the leading edge installation and both halves of the symmetrical stabilizer structure for the treatment of asymmetric load cases. Element geometries, thicknesses, and elastic properties were also updated to the current design configuration of the stabilizer. The procedures and results of the discrete element analysis are presented in this section together with revised buckling curves and the margins-of-safety calculated for critical points in the structure.

TABLE I
A-4 GRAPHITE STABILIZER
WEIGHT AND MATERIAL UTILIZATION SUMMARY – UNIT NO. 1
(WEIGHTS IN POUNDS)

ITEM	ELEMENT	GRAPHITE	FIBERGLASS	ALUMINUM	STEEL	TITANIUM	ADHESIVE AND EPOXY FILLETS	TOTAL WEIGHT (LB)
SUBSTRUCTURE	FRONT SPAR	2.68						2.68
	HONEYCOMB PANEL FACINGS	4.76						4.76
	CORE		1.00					1.00
	ADHESIVE						1.30	1.30
	CORNER ATTACH ANGLES	1.53						1.53
	ADHESIVE						0.50	0.50
	REAR SPAR	9.20						9.20
	CANT RIB BLANKS	4.68						4.68
	ATTACH TEES			0.20		1.12		1.32
	STA 58 HINGE BRACKETS				3.84			3.84
	ATTACH ANGLES	10.30						10.30
	ADHESIVE						3.90	3.90
	EPOXY FILLETS						2.00	2.00
	SUBTOTAL							(47.01)
SKIN PANELS	UPPER PANEL AND TI DBLRS	35.96				1.04		37.00
	LWR PANEL AND TI DBLRS	41.16				1.04		42.20
	SUBTOTAL							(79.20)
MISC FTGS	PIVOT			13.00				13.00
	ACTUATOR			4.00				4.00
	STA 20 HINGES				2.40			2.40
	STA 40 HINGES				2.10			2.10
	SUBTOTAL							(21.50)
LEADING EDGE	INBD AND OUTBD ASSYS		17.47					(17.47)
MISC FASTENERS	UPPER PANEL			0.40	1.16	2.61		4.17
	LOWER PANEL			0.42	1.16	2.99		4.57
	FITTING ATTACH			0.40	3.04	0.54		3.98
	SUBTOTAL							(12.72)
	TOTAL (LB)	110.27	18.47	18.42	13.70	9.34	7.70	177.90

Discrete Element Analysis

Discrete Element Model

The analysis procedure was based on the matrix displacement approach. As with other matric structural analysis methods, the solution was based on a specific discrete element model of the actual structure. This model was obtained by first creating a basic subdivision grid in which the partitions and boundaries were designed to match the actual structure as closely as possible. The basic grid was then subdivided into structural elements which required a node (or joint) at each end of a bar element or at each vertex of a plate element. The basic element types are illustrated in Figure 2. Details of the complete discrete element model are shown in Appendix A.

The origin and orientation for the local element coordinate systems α, β, were established by the locations of the element vertices which are identified by the letters P, Q, R and S. For the bar elements, the axial direction was specified by the letters P and Q. The principal directions of elasticity were similarly oriented with the quantity E_{11} parallel to the α direction and E_{22} parallel to the β direction. The PQ side of the element was artibrarily directed parallel to the α axis. This established the relationships between the orientation of the element geometry, the local coordinate axes, and the principal directions of elasticity.

Unless the specific material is either isotropic or transversely isotropic, it is necessary to arrange the element subdivision grid so that the local coordinate axes for each element are parallel to the principal directions of elasticity for the material. It is preferable to arrange the element subdivision grid so that the local coordinate axes are parallel to the principal directions of elasticity and so that at least one of the axes, α, β, be parallel to a base coordinate direction. When this practice is followed a coordinate transformation for the natural principal directions of elasticity is not necessary.

The orientation of the local systems α, β, relative to the base coordinate x, y, z was established by the specific arrangement selected for the element subdivision grid. The desired node identification numbers were entered in the element data columns marked P, Q, R and S on the element data sheet. Whenever possible, the PQ side of any element was located parallel to one of the base coordinate directions. This practice facilitated interpretation and application of the stress data produced by the computer program and aided in maintaining the correct orientation for the principal directions of elasticity. The analysis system calculated and printed stress values for each element and each load condition. The print-out consisted of axial stresses for bar elements and normal and shear stresses for plate elements. The stresses for the plate elements were computed in two orthogonal directions relative to the local coordinate directions of each element (established by the PQ side of the element). The orientation of the principal stresses was determined by the angle between the maximum stress direction and the PQ side.

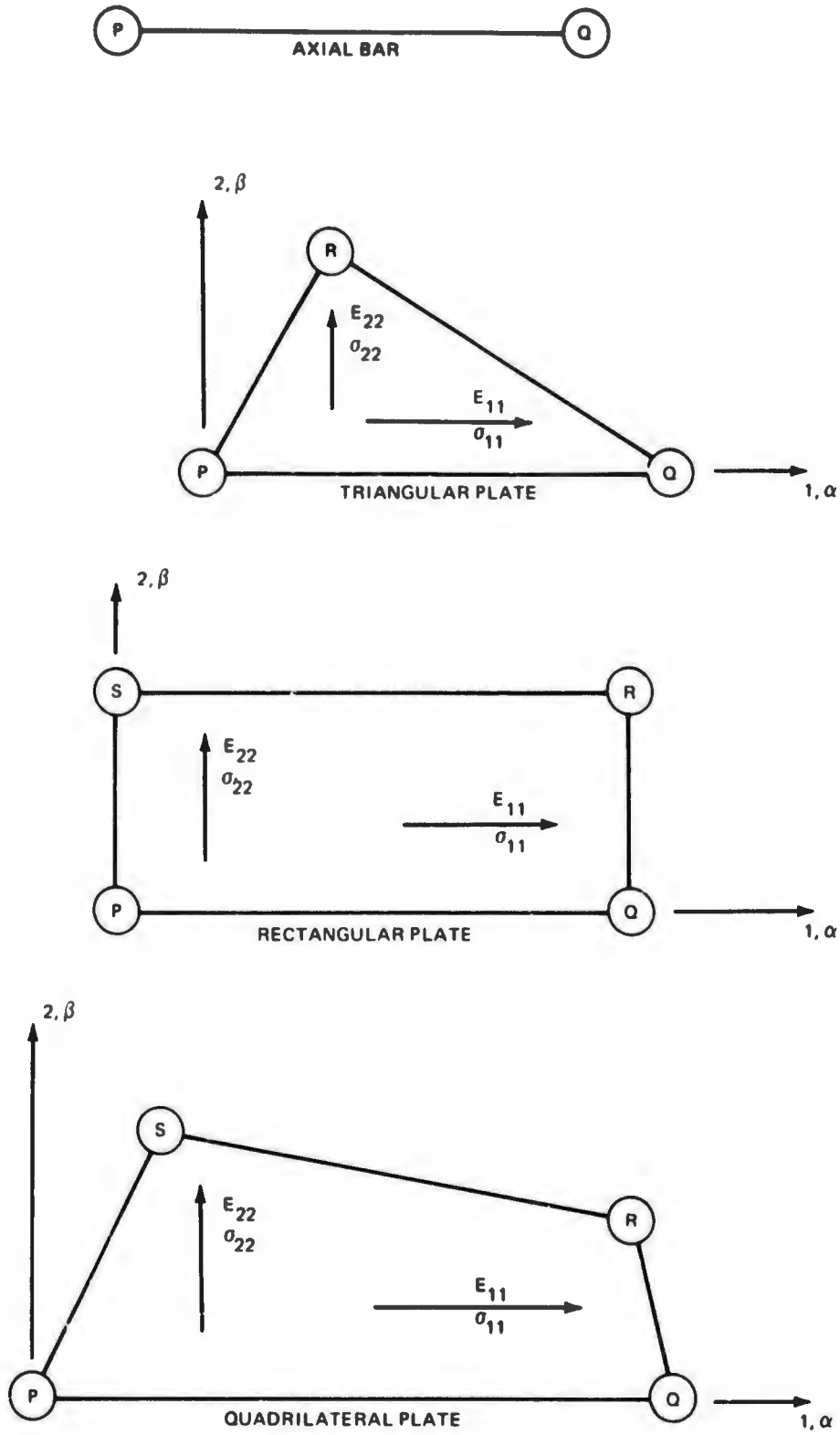

FIGURE 2. ELEMENT GEOMETRY AND ORIENTATION

The fittings were represented by various arrangements of nodes and elements according to the specific design of each fitting with consideration of the effect of adjacent structure. These fittings were not modeled with sufficent detail to compute accurate stresses within the parts. The additional degrees-of-freedom required would greatly increase the dimensions of the overall problem. The idealized representations of these fittings were primarily intended duplicate rigidities and the modes of attachment to the structure.

The location of each node was specified by the x, y, and z distances from the origin of the base coordinate system. The length and width dimensions for each element were thus determined by specifying the identification number of the node at each end for bars or at each vertex for plate elements. The thickness dimension (in inches) was specified separately in the element input data. The elastic constants for the material represented by each element was also included in the element input data along with any other special processing instructions required by the computer program. No elastic properties data were included in input for most of the elements. A special data bank routine was included in the program which permitted the storage of mechanical and physical property data for a number of materials. Specific property values were retrieved on command and automatically assigned to the proper elements according to the specific material and laminate pattern used in each. The material type, orientation of principal elastic axes, and other necessary data were contained in two code numbers which were included in the element data input.

Numerical values for the mechanical properties specified for metallic materials were obtained from Reference 4. Elastic properties for the fiberglass laminate were obtained from Reference 5. The elastic properties specified for the composite laminates were obtained from Reference 6. These values were modified on the basis of the I-beam and box-beam tests which indicated that the tension values were more indicative of the specimen behavior than the compression values. The usual practice in discrete element analysis is to specify either the tensile values or the average of the tensile and compressive values for each component. This is done because otherwise, tensile or compressive elastic property values would have to be specified for each element according to the expected directions of the normal stresses. In situations with pronounced biaxial loading, it is difficult to predict the directions of the normal stress components. Also, the signs of the normal stresses change according to the directions and magnitudes of the external loads.

Since the (0°/±45°/90°) ply pattern used in the skin panels is transversely isotropic, the shear modulus was modified in accordance with the relationship between E, υ, and G commonly accepted for isotropic materials which is given by

$$G = \frac{E}{2(1 + \upsilon)}$$

The elastic properties used in the discrete element analysis are shown in Table II.

TABLE II
MODIFIED ELASTIC CONSTANTS
USED IN ANALYSIS

PLY PATTERN	DESCRIPTION OF ELASTIC CONSTANT	SYMBOL	NUMERICAL VALUES		
			TENSION	COMPRESSION	SHEAR
±45	ELASTIC (YOUNG'S) MODULUS (MSI)	E_{11}, E_{22}	2.52	2.52	
	SHEAR MODULUS (MSI)	G_{12}			4.36
	POISSON'S RATIO	ν_{12}	0.818	0.818	
$0/\pm45^{o}/90^{o}$	ELASTIC (YOUNG'S) MODULUS (MSI)	E_{11}, E_{22}	7.19	7.19	
	SHEAR MODULUS (MSI)	G_{12}			2.75
	POISSON'S RATIO	ν_{12}	0.305	0.305	
0/±45	ELASTIC (YOUNG'S) MODULUS (MSI)	E_{11}	7.88	7.88	
	ELASTIC (YOUNG'S) MODULUS (MSI)	E_{22}	3.54	3.54	
	SHEAR MODULUS (MSI)	G_{12}			3.83
	POISSON'S RATIO	ν_{12}	0.731	0.731	

The total thicknesses of the graphite laminates were calculated on the basis of 0.0058 inch per ply. This value was derived from measurements of the design allowable test specimens, the I-beams, and the box-beam parts.

The thickness of the skin panel attach angles was added to the shear web thickness where the total depth of the web was small enough to permit the angles to overlap. This condition was present along a portion of the leading edge spar and at the aft end of the rib at station Y = 40.000. In addition, a filler-block replaced the portion of the core between station X = 100.000 and X = 106.750 at station Y = 40.000. This filler-block reduced the shear stress in the web face sheets.

The pivot and actuator fittings were idealized primarily to duplicate the stiffnesses of the components. However, the elements of the idealizations were designed to duplicate the physical dimensions of the structure wherever possible. Therefore, useful stress data for portions of fittings were obtained from the analysis.

Fictitious bulkheads were added at the outboard ends of the spars at stations 112.637 and 118.125. These elements were intended to replace the bending and torsional rigidity of the section which was lost due to idealizing the nose section as a triangular box. This step was deemed necessary only in the area near the outboard end because of the reduced overall thickness and consequent reduction in cross sectional area in this region. Therefore, such bulkheads were not added forward of station 118.125.

Analysis Procedure

An element stiffness matrix $\bar{K}^i$ was generated for each element in the structure after which all the element stiffness matrices were arranged in proper locations in the general stiffness matrix $\bar{K}$. The superior bar indicates that the quantities were referenced to the base coordinate system. The external forces for all load conditions were contained in a loads matrix $\bar{P}$. Thermal forces $\bar{Q}^i$ (if present) may be computed for each element and load condition and added to the loads matrix to form the complete matrix of applied forces $(\bar{P}-\bar{Q})$. The solution to the problem required that the matrix equation

$$(\bar{P}-\bar{Q}) = \bar{K}\bar{U} \qquad (1)$$

be solved for the displacements $\bar{U}$.

To solve Equation (1), the singular matrix $\bar{K}$ was rendered non-singular by elimination of the rows and columns which represented displacements in the directions of six rigid body degrees-of-freedom. The rows and columns for additional degrees-of-freedom which were fixed to represent physical restraints of the structure were similarly treated. The affected rows and columns were set equal to zero and a value of 1.0 was given the corresponding main diagonal

locations to create the reduced stiffness matrix $\bar{K}_r$ having the same dimensions as $\bar{K}$. The displacements were therefore obtained using the equation

$$(\bar{P}-\bar{Q}) = \bar{K}_r\bar{U} \tag{2}$$

The computer program utilized banded matrices for $\bar{K}$ and $\bar{K}_r$ so that computer core storage requirements were held to a minimum, thus permitting consideration of larger problems. All matrix operations were done in core which resulted in reduced processing time on the computer. The solution of Equation (2) for the displacements $\bar{U}$ was done in one operation by means of the Cholesky decomposition procedure. The application of this method to a banded matrix is described in Reference 7.

The primary structural elements consisted of axial bars, triangular plates and rectangular plates (see Figure 2). The quadrilateral elements were formed from two triangular plates to form an element pair. These element pairs were then treated as single, homogeneous bodies. Linearly varying boundary displacements were assumed for the plate elements, resulting in constant stress fields in the triangular and quadrilateral elements. For rectangular elements the assumption of linearly varying boundary displacements lead to a distribution of strain where the extensional components were constant along the reference coordinate direction but varied linearly in the perpendicular direction. The shearing strains varied linearly along both coordinate directions. A state of plane stress was assumed to exist in the plate elements. The properties of the primary elements are more completely described in Reference 8.

Data input consisted of Young's moduli E_{11} and E_{22}, Poisson's ratio υ_{12} (or υ_{21}) and a shear modulus G_{12}. Where thermal effects are required the thermal coefficients $\alpha_1 T$ and $\alpha_2 T$ must also be included. The program computed displacements at each node for each coordinate direction, the stresses σ_{11}, σ_{22}, and τ_{12} for each plate element and the reactions at nodal points were fixed degrees-of-freedom were imposed. Principal stresses and the direction of the maximum principal stresses relative to the local element coordinates were computed for all plate elements.

The reactions at fixed degrees-of-freedom together with the previously defined external loads were obtained from the matrix equation

$$\begin{bmatrix} (\bar{P}_r - \bar{Q}_r) \\ \bar{R}_w \end{bmatrix} = \begin{bmatrix} \bar{K}_{rr} & \bar{K}_{rw} \\ \bar{K}_{wr} & \bar{K}_{ww} \end{bmatrix} \begin{bmatrix} \bar{U} \\ 0 \end{bmatrix} \tag{3}$$

where $\bar{K}$ was partitioned into $\bar{K}_r$ and $\bar{K}_w$. As before, the subscript r refers to the reduced stiffness matrix and the corresponding applied loads. The subscript w refers to the restrained degrees-of-freedom for which the displacements $\bar{U}_r$ are zero.

The stresses (σ^i) were obtained from the displacements u by use of the relationships

$$\sigma = A\varepsilon + \alpha T\, B \quad \text{(stress-strain relationship)} \tag{4}$$

and

$$\varepsilon = bu \quad \text{(strain-displacement relationship)} \tag{5}$$

The matrix u defines displacements for a single element which are given relative to the local element coordinates. Therefore, the stress-displacement relationship was obtained by the substitution of (5) into (4) which yielded

$$\sigma = Abu + \alpha TB \tag{6}$$

where A and B are the matrix expressions for Hooke's law for elastic and thermal strains, respectively. Since the stresses were calculated relative to the local coordinates for each element, the displacement $\bar{U}^i$ obtained from Equation (2) were transformed by means of a rotation matrix λ which consisted of the direction cosines for the angles between the local coordinates for each element and the base system. This rotation of coordinates is symbolically expressed by the matrix equation

$$u = \lambda \bar{u} \tag{7}$$

where $\bar{u}$ is the displacement matrix for a specific element relative to the base system. The matrix $\bar{u}$ was generated by extracting the proper rows from $\bar{U}$ to form $\bar{U}^i$ which was then rearranged to yield $\bar{u}$.

The displacements were computed relative to the fixed supports and printed out for each degree-of-freedom referenced to the base coordinate system. The applied loads were regenerated by performing the matrix operation defined by Equation (3) which also yielded the reactions at fixed degrees-of-freedom. These quantities were also printed using the procedure described previously for the displacements.

External Loads

Critical load conditions for the stabilizer are summarized in Table III. Critical load conditions C, D and F were analyzed in detail. Condition D had the maximum total tail down-load (maximum stabilizer load). Condition F caused the maximum up-load on the horizontal surface. Condition C had the maximum elevator down-load combined with a near maximum total tail down-load and was critical for most of the structure. Condition E was critical at the leading edge but was not included in the discrete element analysis. This latter condition was analyzed in detail in Reference 6.

Condition B was listed in previous reports as critical for the horizontal stabilizer incidence actuator. This condition produced the maximum compression load in the actuator and was, therefore, critical for that part as a column. However, the maximum tension load (which is more than three times as much) occured during condition C and is critical for the actuator attachment to the stabilizer. Quantitative data on each of the load conditions considered in this analysis (C, D and F) may be found in Reference 6.

TABLE III
CRITICAL LOAD CONDITIONS

COND	ATTITUDE	MACH NO.	ALTITUDE (FT)	V_E (KTS)	n_z	$\dot{\omega}$ RAD SEC^2	C.G.	i_H (DEG)	α_H (DEG)	δ_E (DEG)	TOTAL TAIL LD (LB)	ELEVATOR LOAD (LB)	STABILIZER LOAD (LB)
B	+LAA	1.25	20,000	560	7.0	0	FWD	−4.01	−3.12	−25.0	−21,282	−13,740	−7,600
C	+LAA	1.10	10,000	603	7.0	C	FWD	−1.57	−1.55	−25.0	−21,230	−14,690	−6,300
D	+LAA	1.10	10,000	603	7.0	0	FWD	−12.75	−12.73	+10.25	−23,668	+1,653	−25,321
E	+HAA	0.95	0	628	7.0	0	FWD	−11.67	−10.42	+15.0	+10,778	+2,424	+8,354
F	+HAA	0.352	0	233	7.0	−6	AFT	+4.0	19.16	+12.35	+10,804	+2,437	+8,367

NOMENCLATURE:

+LAA = POSITIVE LOW ANGLE OF ATTACK

+HAA = POSITIVE HIGH ANGLE OF ATTACK

V_E = EQUIVALENT AIRSPEED (POSITIVE LEADING EDGE UP).

α_H = HORIZONTAL TAIL ANGLE OF ATTACK (POSITIVE LEADING EDGE UP).

δ_E = ELEVATOR DEFLECTION (POSITIVE TRAILING EDGE UP).

$\dot{\omega}$ = AIRPLANE PITCHING ACCELERATION (POSITIVE AIRCRAFT NOSE UP)

C.G. = AIRPLANE CENTER OF GRAVITY POSITION

FWD MAXIMUM FORWARD; AFT – MAXIMUM AFT.

n_z = AIRPLANE NORMAL LOAD FACTOR.

i_H = HORIZONTAL TAIL INCIDENCE ANGLE (POSITIVE LEADING EDGE UP).

TAIL LOADS POSITIVE UP.

The computer program required that external loads be applied to the analysis model in the form of concentrated force vectors. These force vectors were applied at node points parallel to one of the base coordinate directions. Distributed loads such as aerodynamic pressures were replaced by a statically equivalent system of concentrated forces which were represented by force vectors acting at the nodes.

Externally applied concentrated forces were also represented by force vectors. Since all force vectors acted on nodes, external concentrated forces were provided by placing nodes at the proper locations in the analysis model. All such force vectors were statically equivalent to the corresponding external forces.

The location, direction, and identification numbers for each load vector are shown in appropriate views and cross-sections of the analysis model in Appendix A. The numerical magnitude of each load vector for each load condition was printed out with the analysis results.

Element Stresses

Stresses were computed for all critical elements in the structure using the analysis model and procedure described previously for load conditions C, D, and F. For condition C, limit stresses are plotted in Figures 3 through 6 for the upper and lower skin panels, in Figures 7 through 11 for the rib and spar elements, and in Figures 12 and 13, respectively, for the pivot and actuator fittings. Similar figures for critical structural elements under load conditions D and F are included in Appendix B.

The signs for the normal stresses are based on the usual convention. Positive stresses indicate tension and negative stresses indicate compression. For the shear stresses the sign convention is as follows: positive shear causes a decrease in the 90° angle between the α and β element coordinates when oriented in their positive directions.

Because of the curvature of the skin panels, the upper and lower cover skins are not parallel to the base coordinate plane except at a few locations. The angular deviation of the cover skin elements from the x-y plane is small and (except for the leading-edge section) was neglected. In the stress diagrams (Figures 3 through 13) the cover skin stress components are designated as σ_x, σ_y, and τ_{xy}. The stress field components for the leading edge section are directed parallel and normal to the leading edge spar in the plane of each element. For leading edge section components, the orientation is defined by the y direction which is parallel to the front spar plane.

Structural Deflections

In the stress analysis of the metal surface, structural deflections were considered only in Condition C which had high elevator down-loads and high stabilizer torque. The following effects of flexibility were considered:

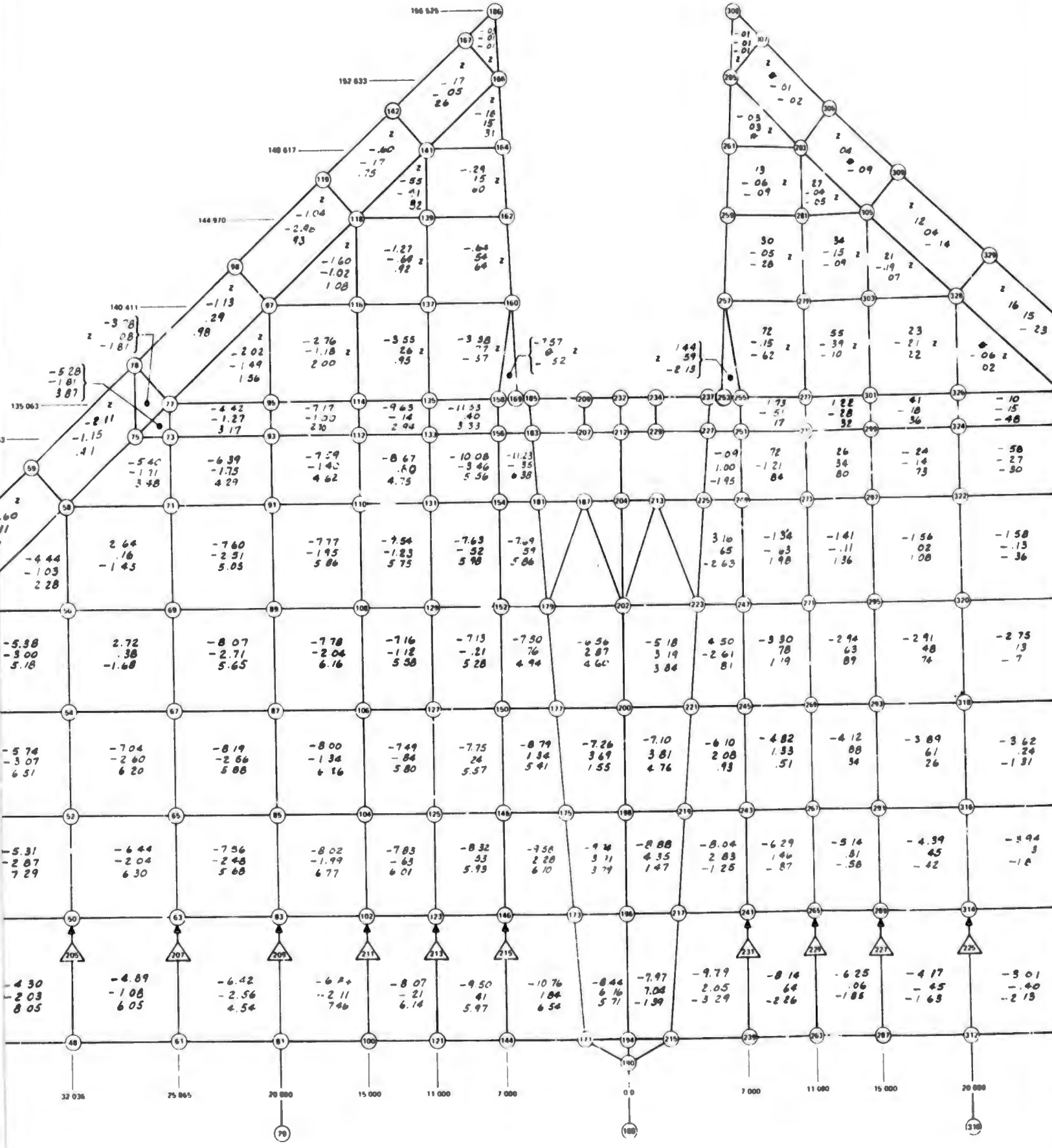

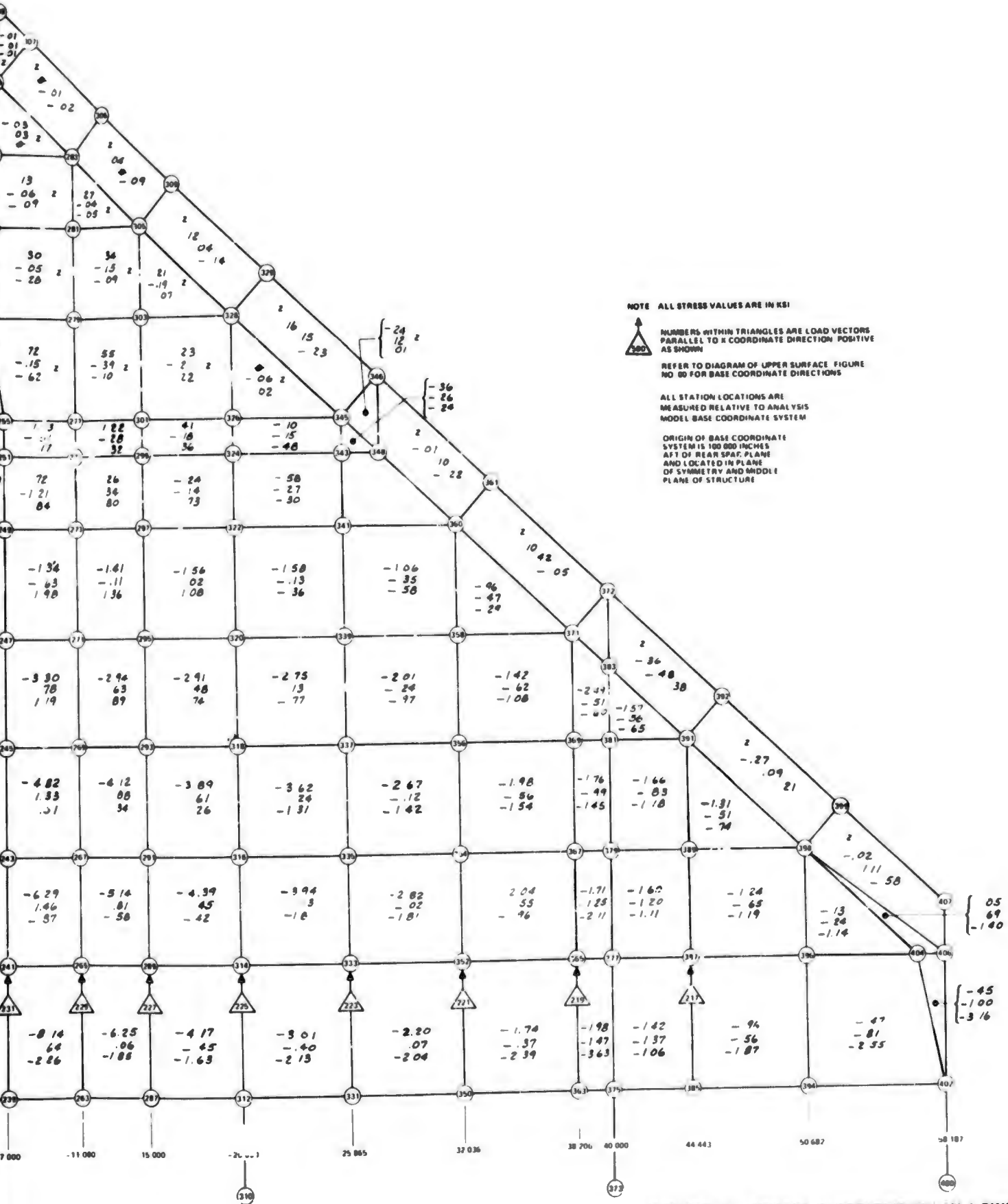

FIGURE 3. STRESS DISTRIBUTION IN LOWER PANEL AND LEADING EDGE – LOAD CONDITION C

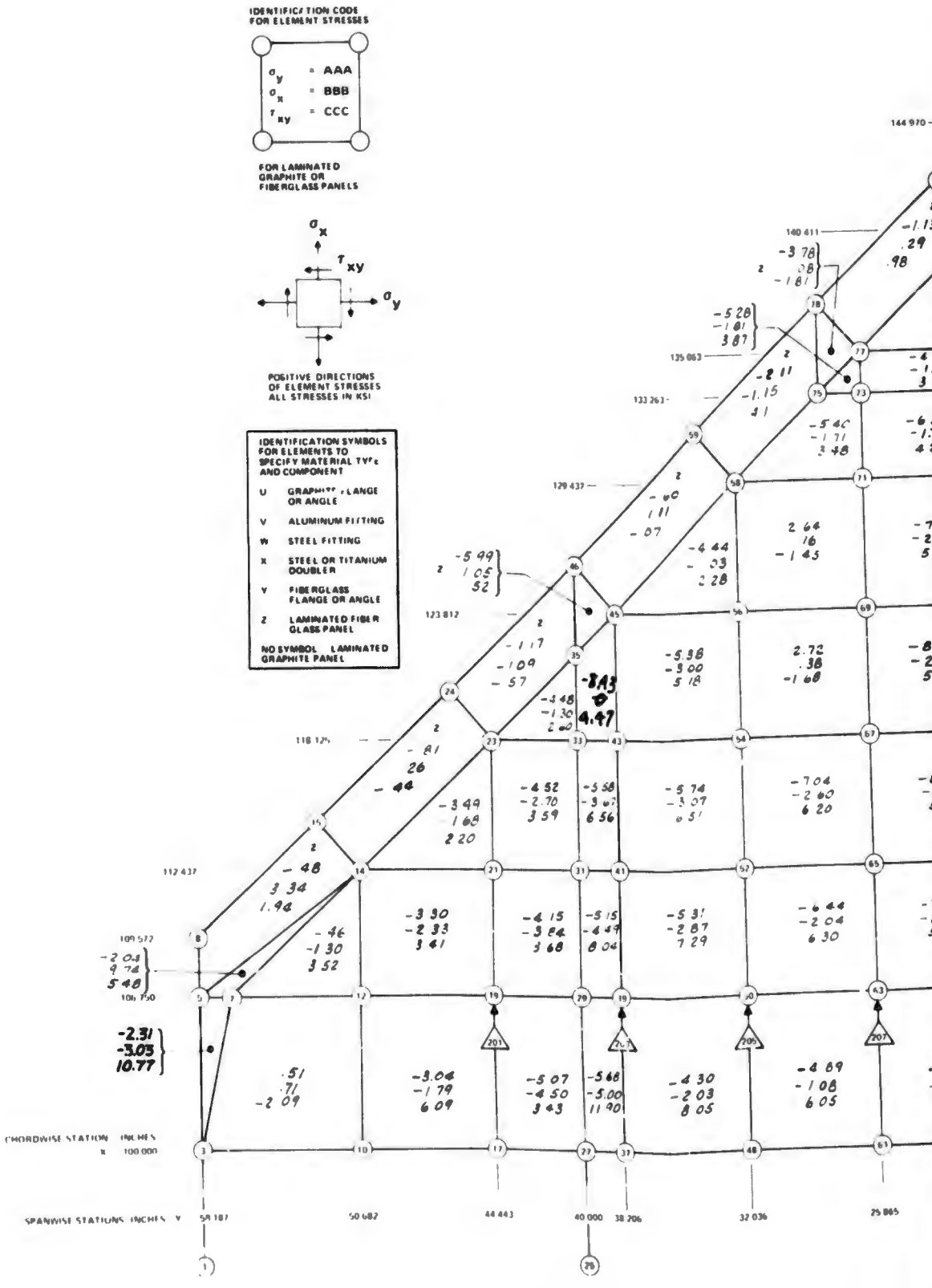
IDENTIFICATION CODE FOR ELEMENT STRESSES
σy = AAA
σx = BBB
τxy = CCC
FOR LAMINATED GRAPHITE OR FIBERGLASS PANELS
σx
τxy
σy
POSITIVE DIRECTIONS OF ELEMENT STRESSES ALL STRESSES IN KSI
IDENTIFICATION SYMBOLS FOR ELEMENTS TO SPECIFY MATERIAL TYPE AND COMPONENT
U GRAPHITE FLANGE OR ANGLE
V ALUMINUM FITTING
W STEEL FITTING
X STEEL OR TITANIUM DOUBLER
Y FIBERGLASS FLANGE OR ANGLE
Z LAMINATED FIBER GLASS PANEL
NO SYMBOL LAMINATED GRAPHITE PANEL
CHORDWISE STATION INCHES X
SPANWISE STATIONS INCHES Y
144 970
140 411
135 063
133 263
129 437
123 812
118 125
112 437
109 572
106 750
100 000
50 682
44 443
40 000
38 206
32 036
25 865

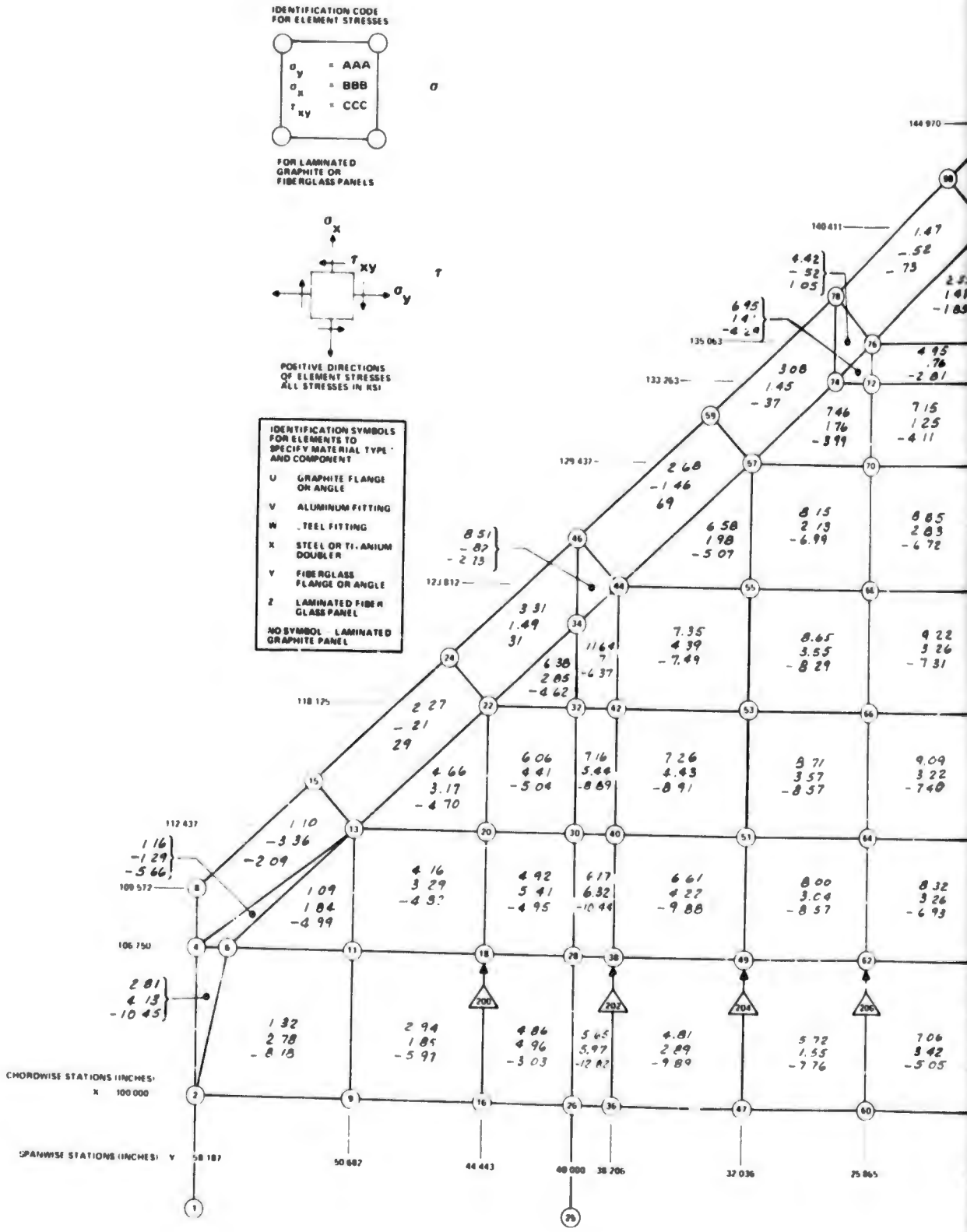
IDENTIFICATION CODE FOR ELEMENT STRESSES
σy = AAA
σx = BBB
τxy = CCC
σ
FOR LAMINATED GRAPHITE OR FIBERGLASS PANELS
σx
τxy
σy
τ
POSITIVE DIRECTIONS OF ELEMENT STRESSES ALL STRESSES IN KSI
IDENTIFICATION SYMBOLS FOR ELEMENTS TO SPECIFY MATERIAL TYPE AND COMPONENT
U GRAPHITE FLANGE OR ANGLE
V ALUMINUM FITTING
W STEEL FITTING
X STEEL OR TITANIUM DOUBLER
Y FIBERGLASS FLANGE OR ANGLE
Z LAMINATED FIBER GLASS PANEL
NO SYMBOL LAMINATED GRAPHITE PANEL
CHORDWISE STATIONS (INCHES) X
SPANWISE STATIONS (INCHES) Y
100 000
58 187
50 687
44 443
40 000
38 206
32 036
25 865
144 970
140 411
135 063
133 263
129 437
123 812
118 125
112 437
109 572
106 750

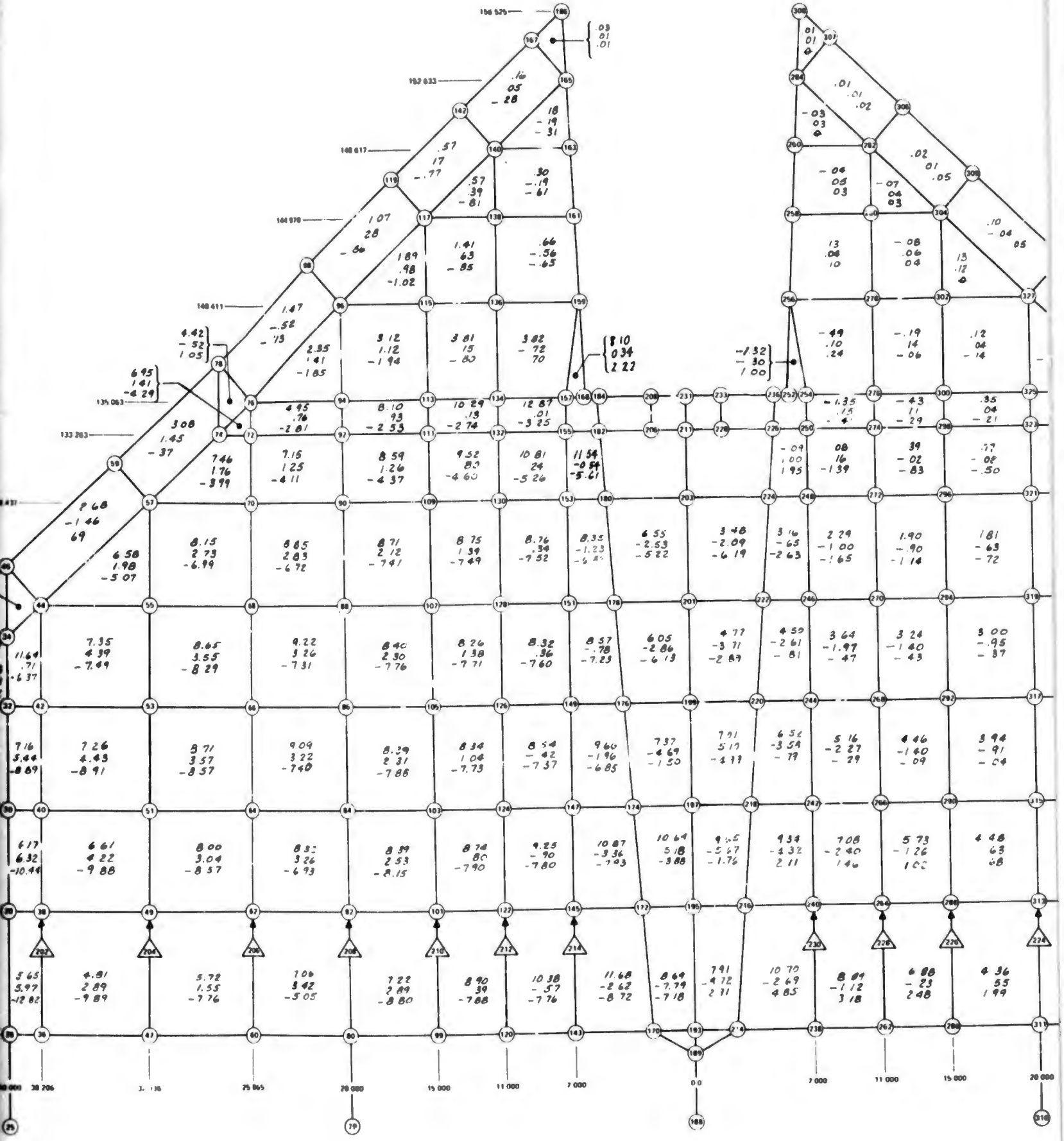
30 000
38 206
25 865
20 000
15 000
11 000
7 000
0 0
7 000
11 000
15 000
20 000

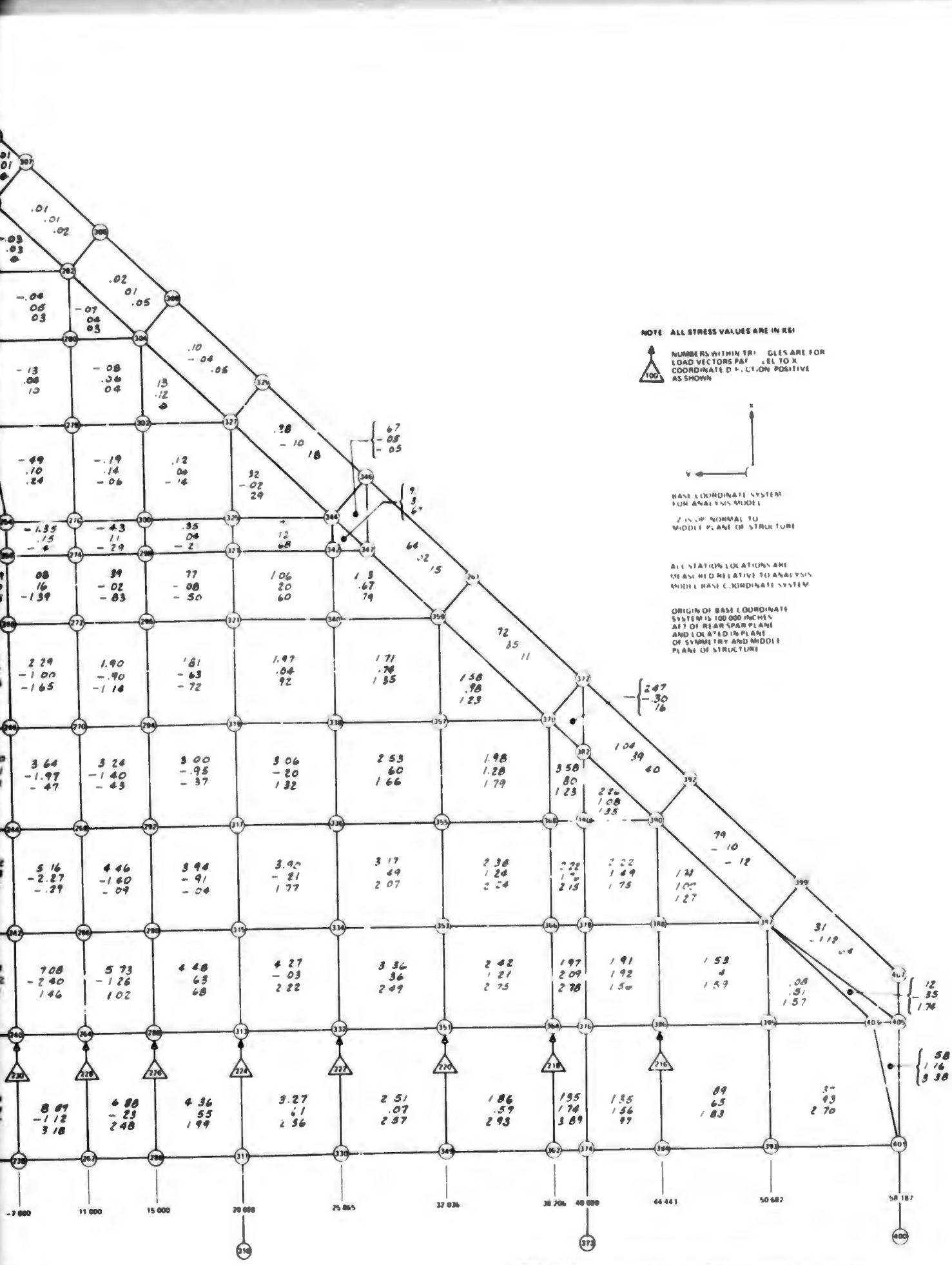

FIGURE 4. STRESS DISTRIBUTION IN UPPER PANEL AND LEADING EDGE – LOAD CONDITION C

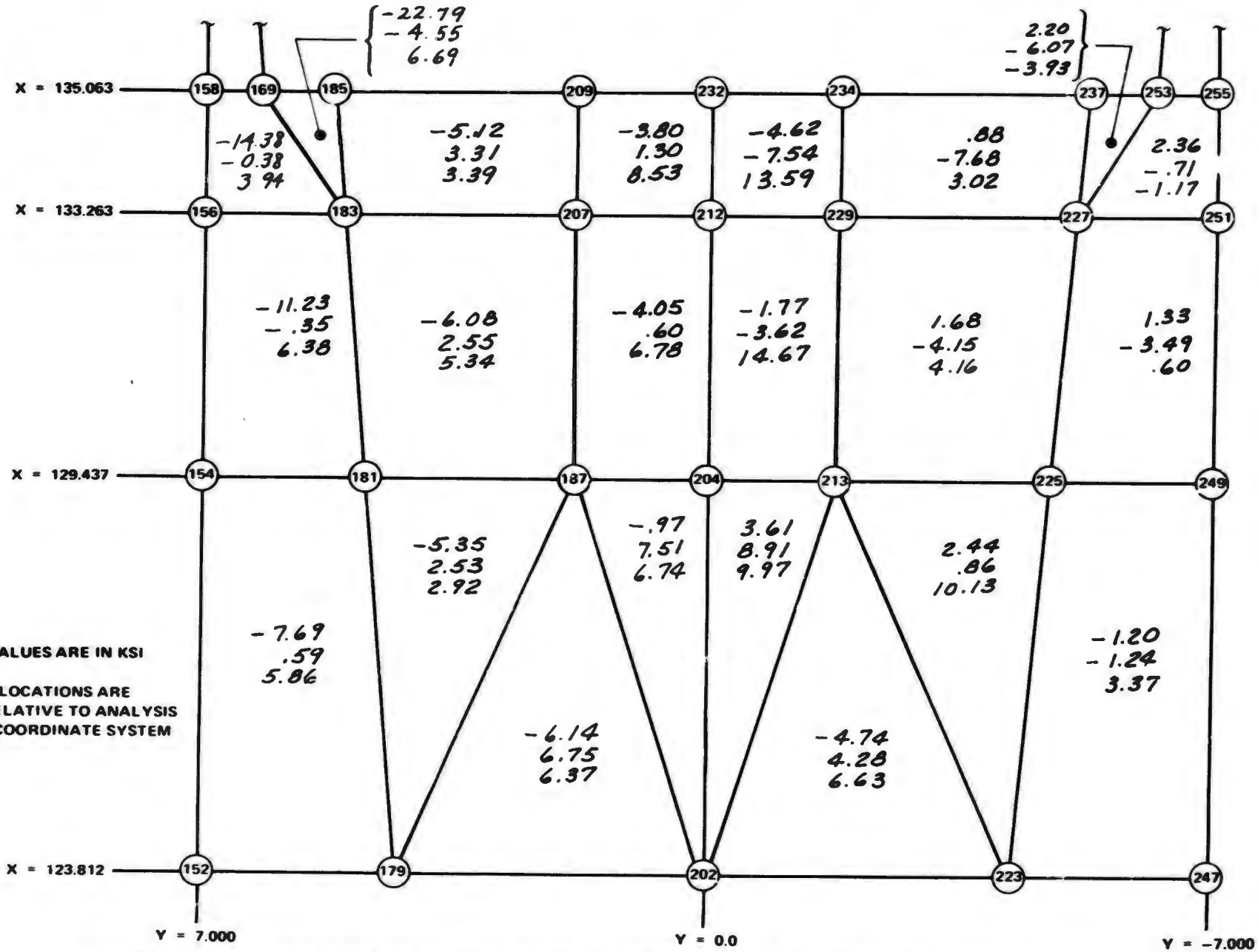

NOTE:
ALL STRESS VALUES ARE IN KSI

ALL STATION LOCATIONS ARE MEASURED RELATIVE TO ANALYSIS MODEL BASE COORDINATE SYSTEM

FIGURE 5. STRESS DISTRIBUTION IN LOWER PANEL ADJACENT TO PIVOT FITTING – LOAD CONDITION C

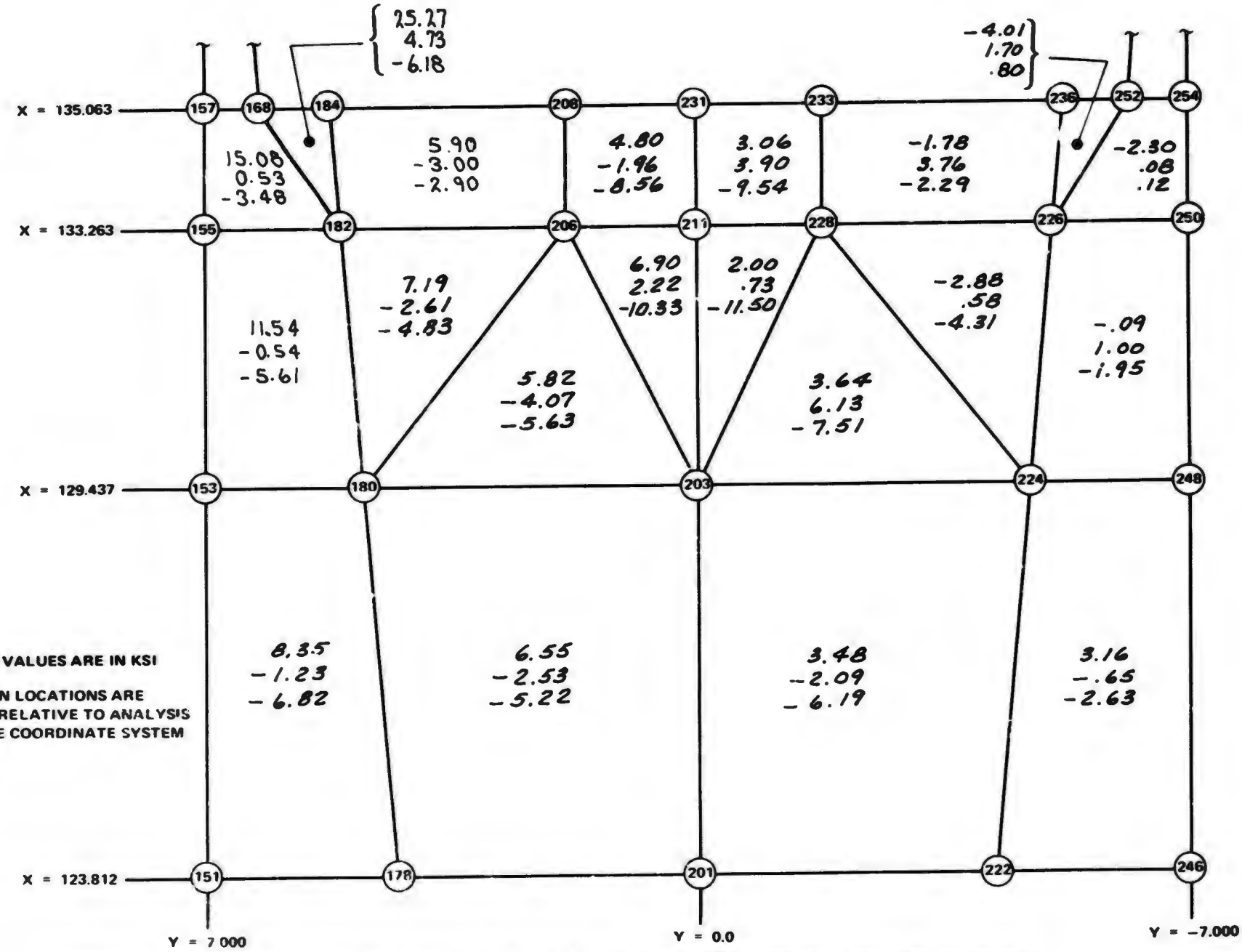

NOTE:
ALL STRESS VALUES ARE IN KSI

ALL STATION LOCATIONS ARE MEASURED RELATIVE TO ANALYSIS MODEL BASE COORDINATE SYSTEM

FIGURE 6. STRESS DISTRIBUTION IN UPPER PANEL ADJACENT TO PIVOT FITTING – LOAD CONDITION C

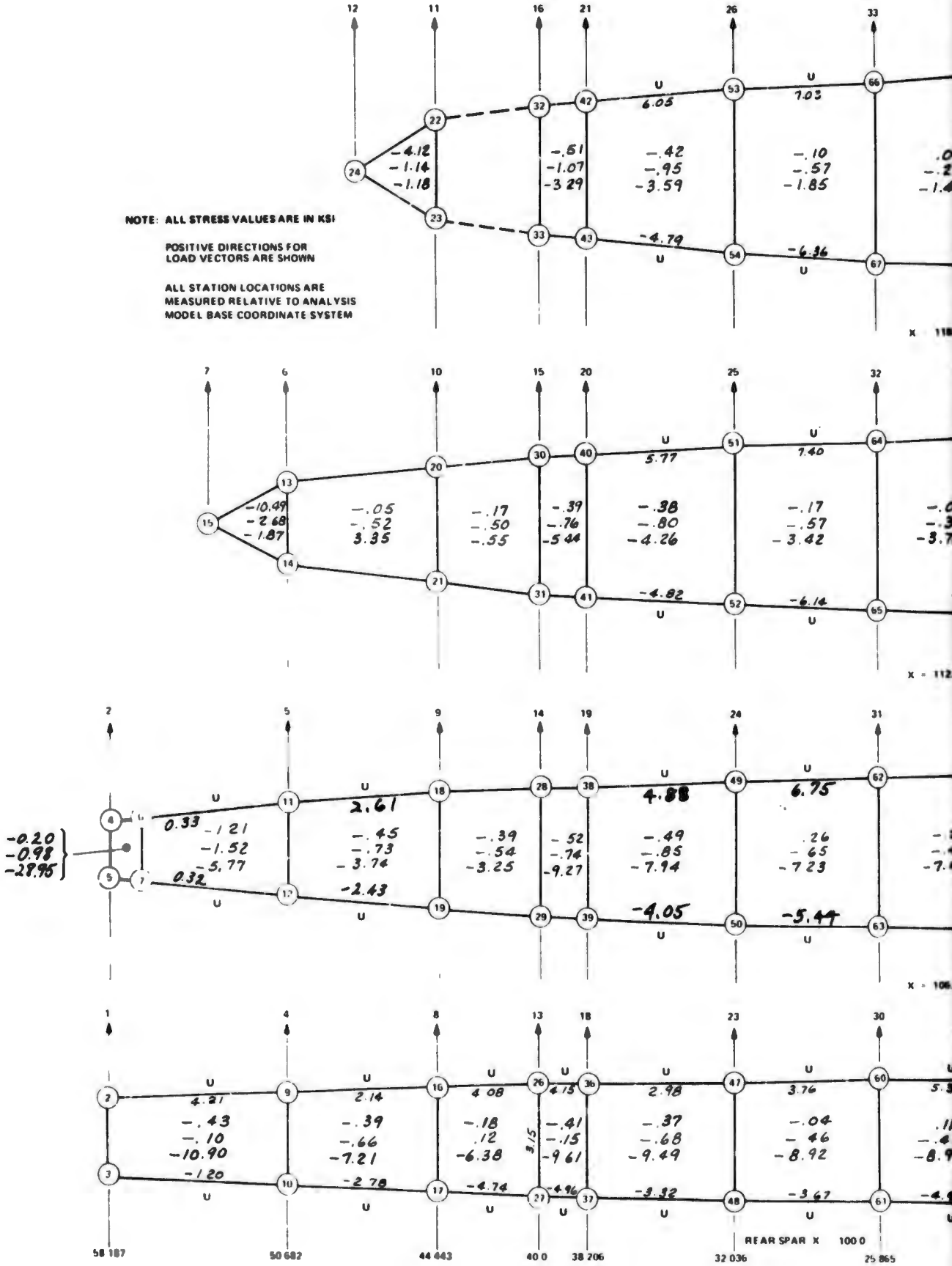
NOTE: ALL STRESS VALUES ARE IN KSI
POSITIVE DIRECTIONS FOR LOAD VECTORS ARE SHOWN
ALL STATION LOCATIONS ARE MEASURED RELATIVE TO ANALYSIS MODEL BASE COORDINATE SYSTEM
-4.12
-1.14
-1.18
-.51
-1.07
-3.29
-.42
-.95
-3.59
-.10
-.57
-1.85
6.05
7.03
-4.79
-6.36
-10.49
-2.68
-1.87
-.05
-.52
3.35
-.17
-.50
-.55
-.39
-.76
-5.44
-.38
-.80
-4.26
-.17
-.57
-3.42
5.77
7.40
-4.82
-6.14
-0.20
-0.98
-28.95
0.33
-1.21
-1.52
-5.77
0.32
2.61
-.45
-.73
-3.74
-2.43
-.39
-.54
-3.25
-.52
-.74
-9.27
-.49
-.85
-7.94
.26
-.65
-7.23
4.88
6.75
-4.05
-5.44
4.21
-.43
-.10
-10.90
-1.20
2.14
-.39
-.66
-7.21
-2.78
4.08
-.18
.12
-6.38
-4.74
4.15
3.15
-.41
-.15
-9.61
-4.96
2.98
-.37
-.68
-9.49
-3.32
3.76
-.04
-.46
-8.92
-3.67
REAR SPAR X 100.0
58.187
50.682
44.443
40.0
38.206
32.036
25.865

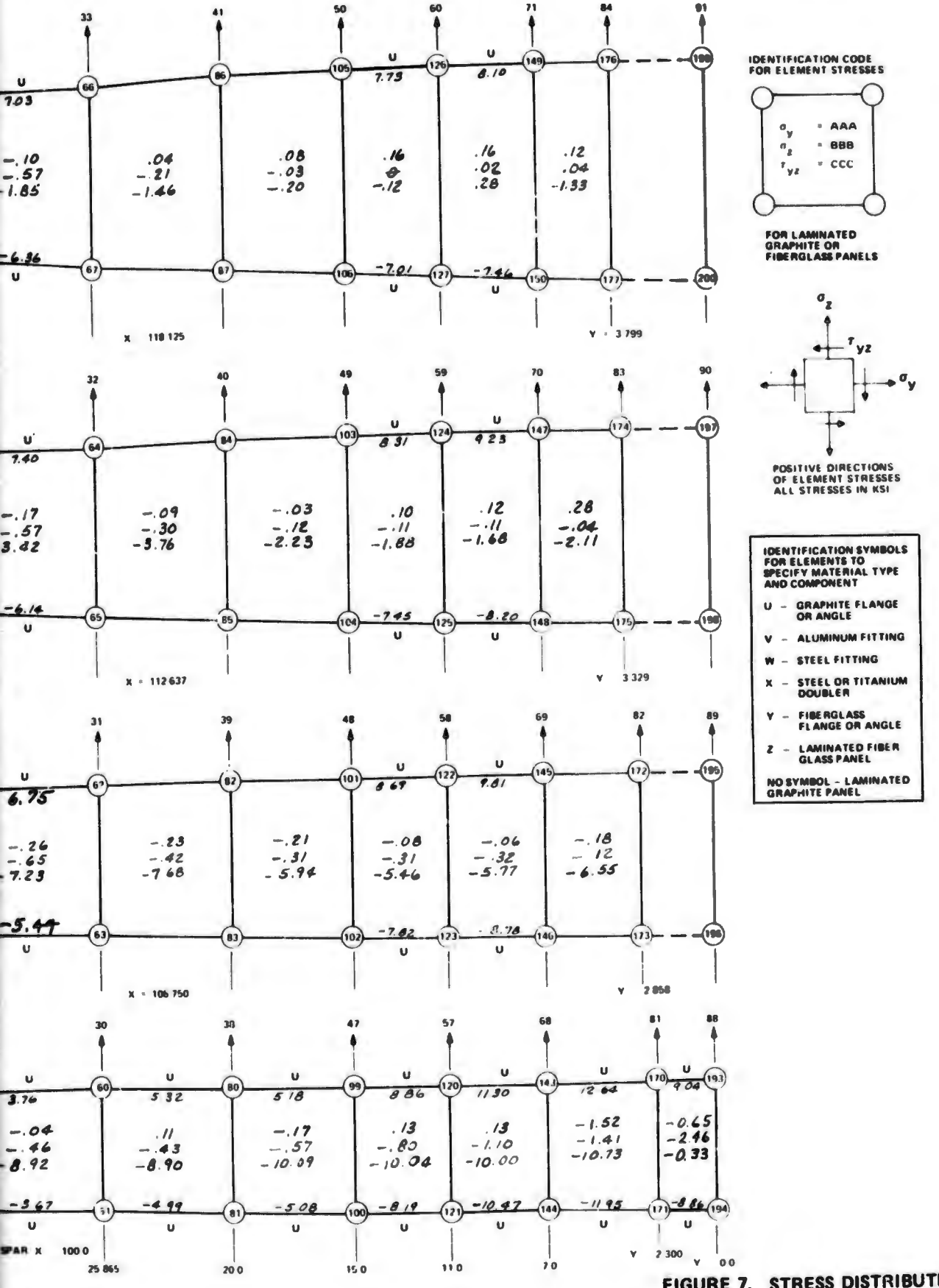

FIGURE 7. STRESS DISTRIBUTION IN SPANWISE SPARS – LOAD CONDITION C

IDENTIFICATION SYMBOLS FOR ELEMENTS TO SPECIFY MATERIAL TYPE AND COMPONENT:

- **U – GRAPHITE FLANGE OR ANGLE**
- **V – ALUMINUM FITTING**
- **W – STEEL FITTING**
- **X – STEEL OR TITANIUM DOUBLER**
- **Y – FIBERGLASS FLANGE OR ANGLE**
- **Z – LAMINATED FIBER-GLASS PANEL**

NO SYMBOL – LAMINATED GRAPHITE PANEL

IDENTIFICATION CODE FOR ELEMENT STRESSES

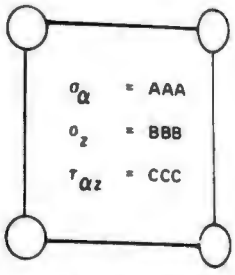

FOR LAMINATED GRAPHITE OR FIBERGLASS PANELS

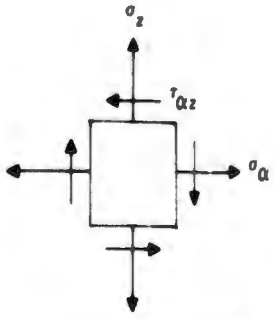

POSITIVE DIRECTIONS OF ELEMENT STRESSES
ALL STRESSES IN KSI
FOR CANTED RIB ONLY
α IS COORDINATE DIRECTION NORMAL TO Z DIRECTION AND ≈ PA

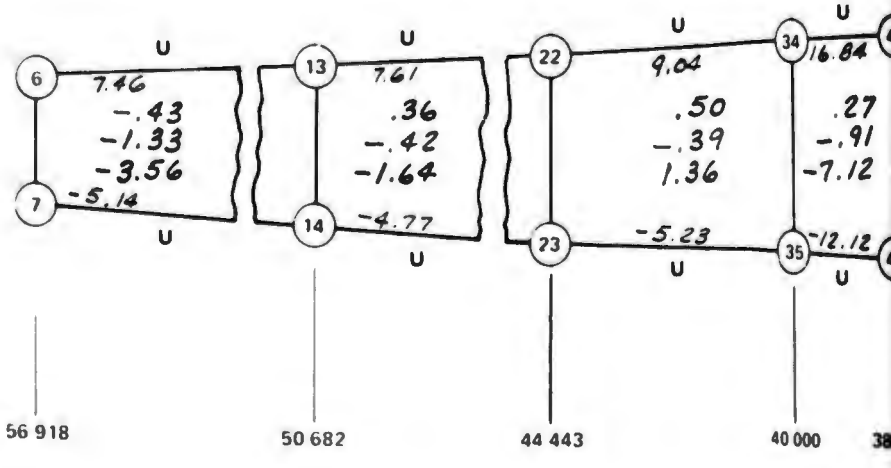

ALL STATION LOCATIONS ARE MEASURED RELATIVE TO ANALYSIS MODEL BASE COORDINATE SYSTEM

ION CODE
IT STRESSES

AAA
BBB
CCC

IATED
OR
S PANELS

$\tau_{\alpha z}$

σ_α

IRECTIONS
IT STRESSES
SES IN KSI
D RIB ONLY
INATE DIRECTION
Z DIRECTION AND ≈ PARALLEL TO X

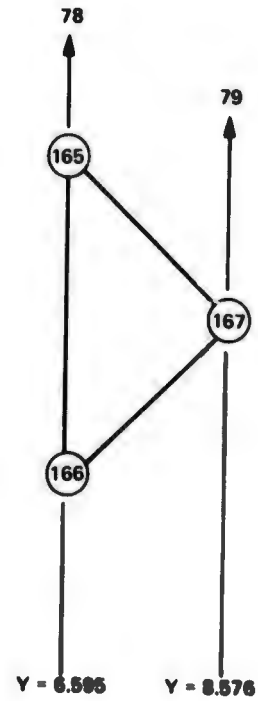

CROSS SECTION THROUGH LEADING EDGE STRUCTURE (CANTED)

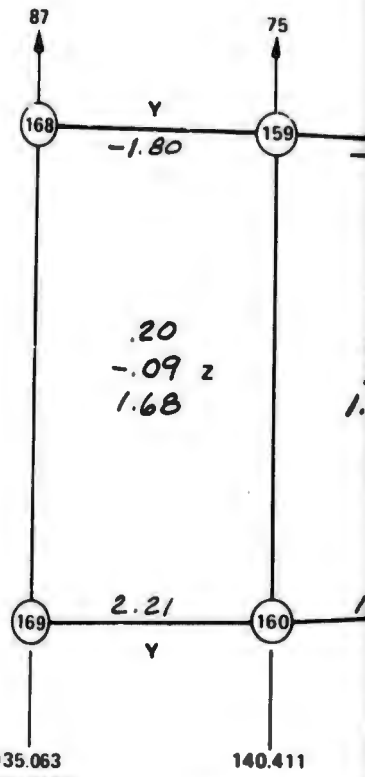

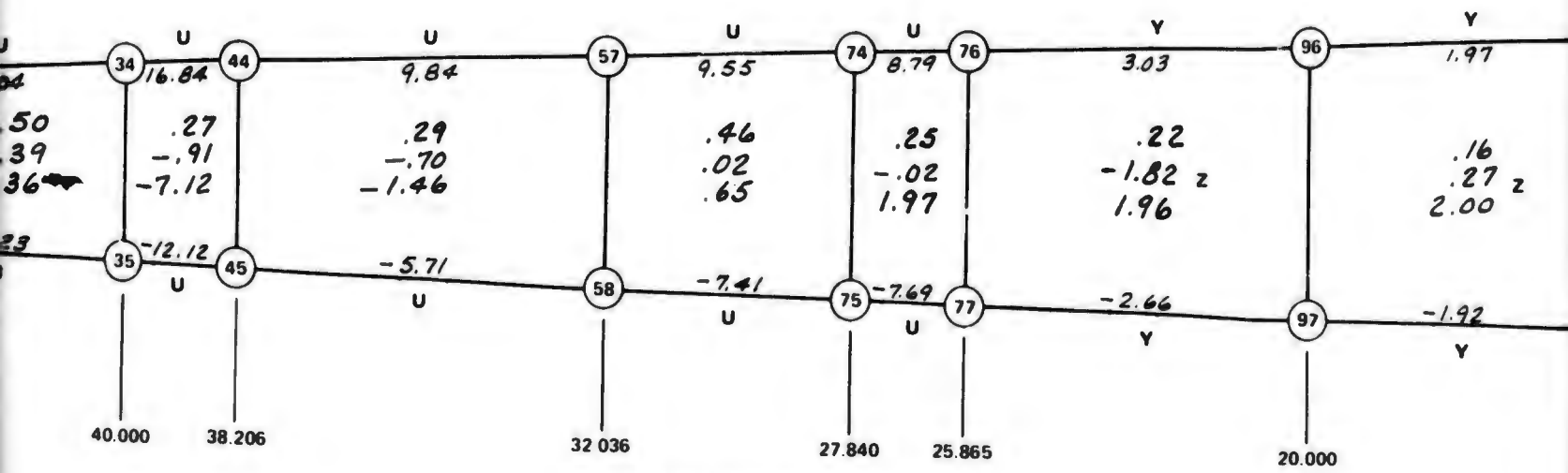

LEADING EDGE SPAR MEMBER (CANTED)

LYSIS
TEM

POSITIVE DIRECTIONS FOR
LOAD VECTORS ARE SHOWN

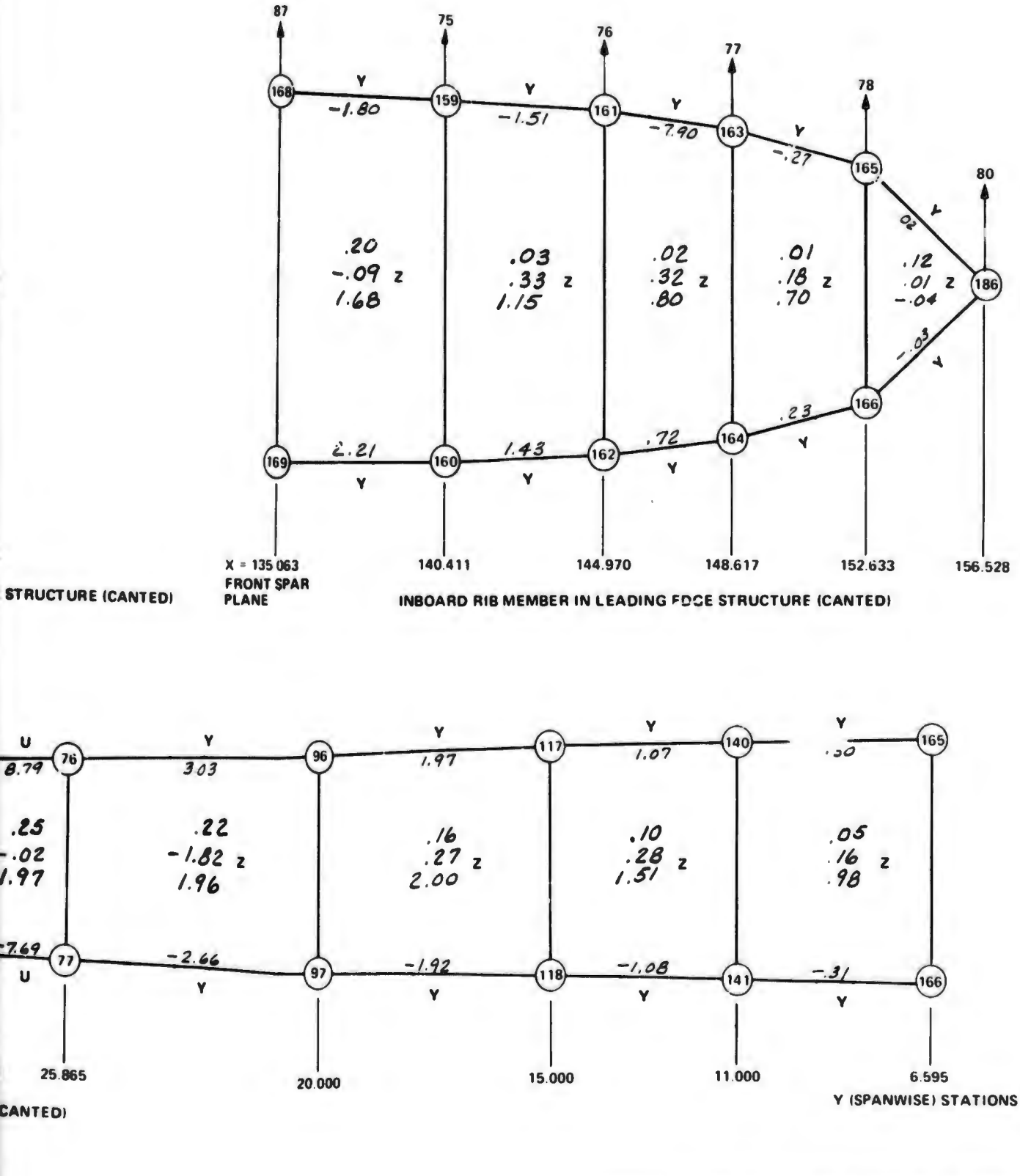

FIGURE 8. STRESS DISTRIBUTION IN LEADING EDGE SPAR AND INBOARD RIB – LOAD CONDITION C

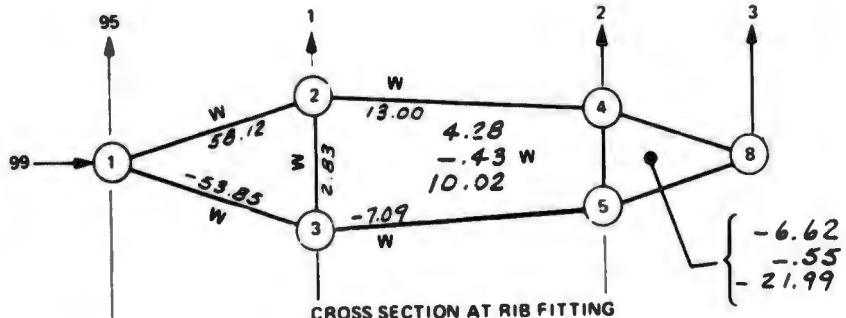

CROSS SECTION AT RIB FITTING
LOCATED AT Y = 58.187

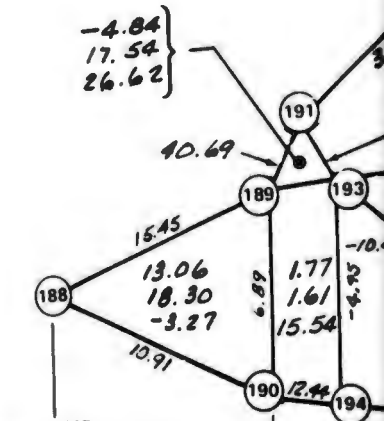

X = 94.625
ELEV HINGE
LINE

X = 98.500

X = 100.0
REAR SP
PLANE

ALL STATION LOCATIONS ARE
MEASURED RELATIVE TO ANALYSIS
MODEL BASE COORDINATE SYSTEM

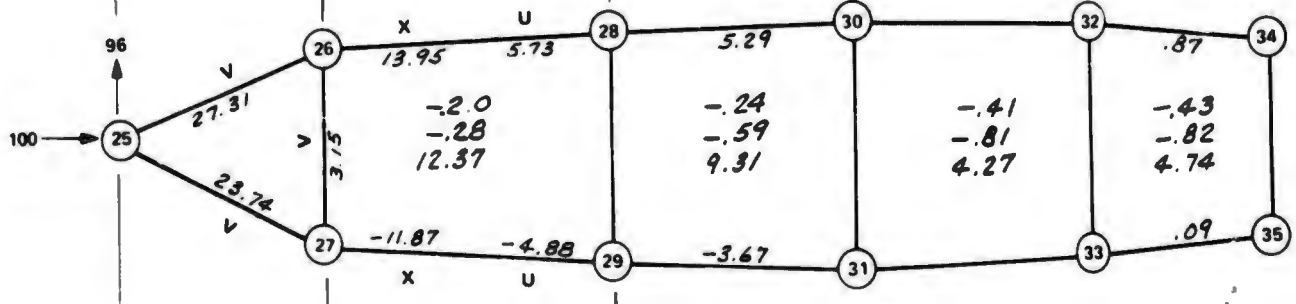

CROSS SECTION AT Y = 40.000 RIB

X = 94.625
ELEV HINGE
LINE

X = 100.00
REAR SPAR
PLANE

106.750

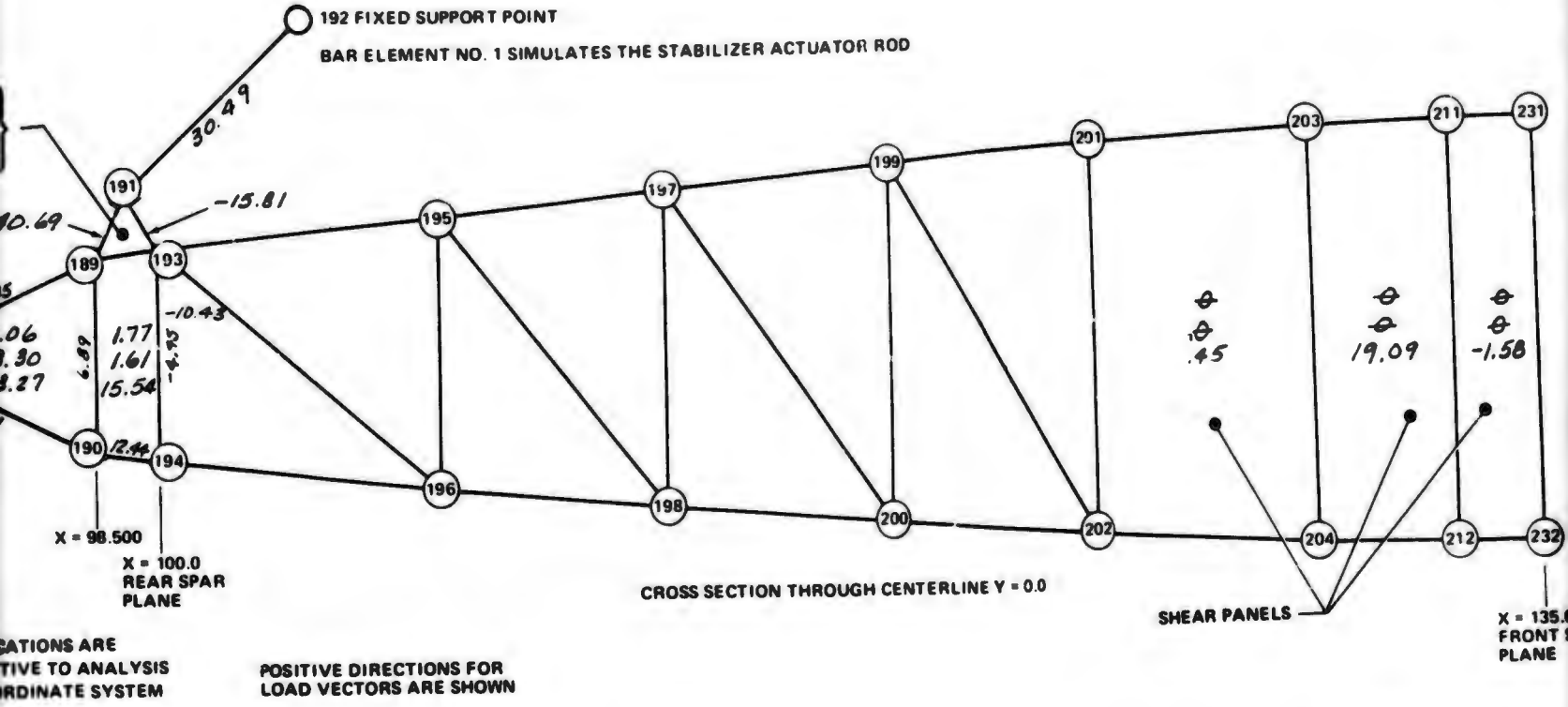
192 FIXED SUPPORT POINT
BAR ELEMENT NO. 1 SIMULATES THE STABILIZER ACTUATOR ROD
30.49
-15.81
10.69
191
189
193
195
197
199
201
203
211
231
190
194
196
198
200
202
204
212
232
-10.43
1.77
1.61
15.54
-4.35
6.89
12.44
.45
19.09
-1.58
X = 98.500
X = 100.0
REAR SPAR
PLANE
CROSS SECTION THROUGH CENTERLINE Y = 0.0
SHEAR PANELS
FRONT
PLANE
CATIONS ARE
TIVE TO ANALYSIS
RDINATE SYSTEM
POSITIVE DIRECTIONS FOR
LOAD VECTORS ARE SHOWN

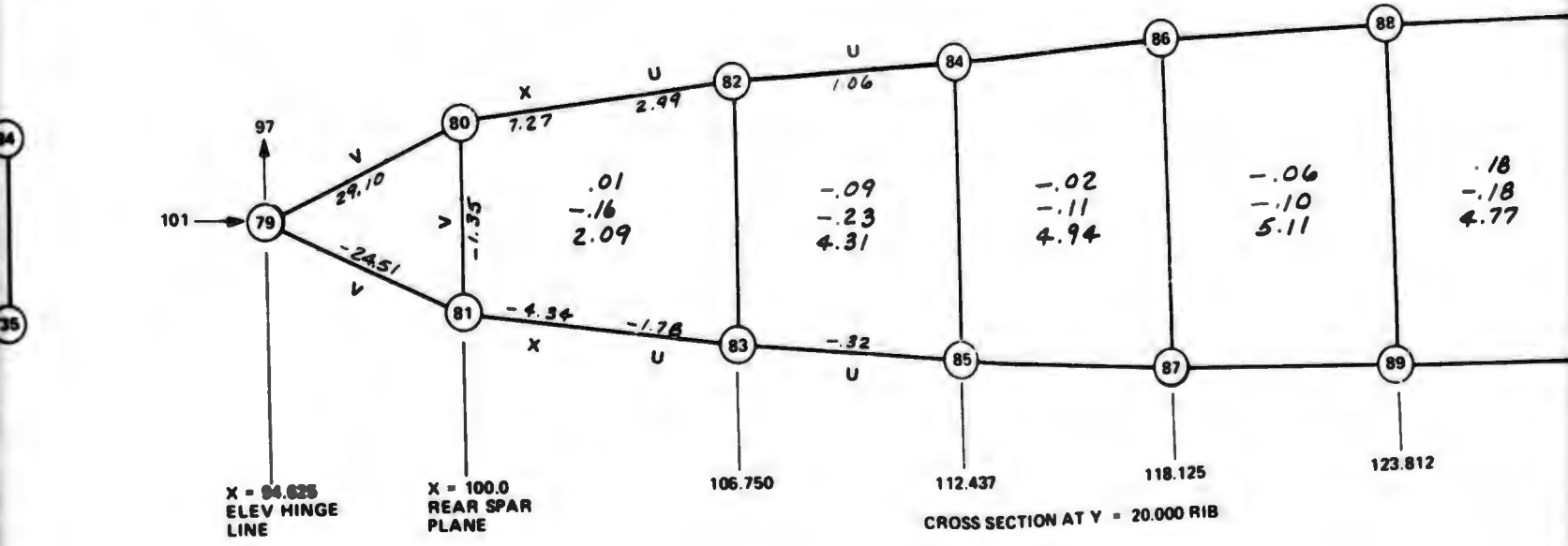
97
101
79
80
81
82
83
84
85
86
87
88
89
V
29.10
-24.51
V
X
7.27
U
2.49
U
1.06
X
-4.34
U
-1.78
U
-.32
-1.35
.01
-.16
2.09
-.09
-.23
4.31
-.02
-.11
4.94
-.06
-.10
5.11
.18
-.18
4.77
X = 94.625
ELEV HINGE
LINE
X = 100.0
REAR SPAR
PLANE
106.750
112.437
118.125
123.812
CROSS SECTION AT Y = 20.000 RIB

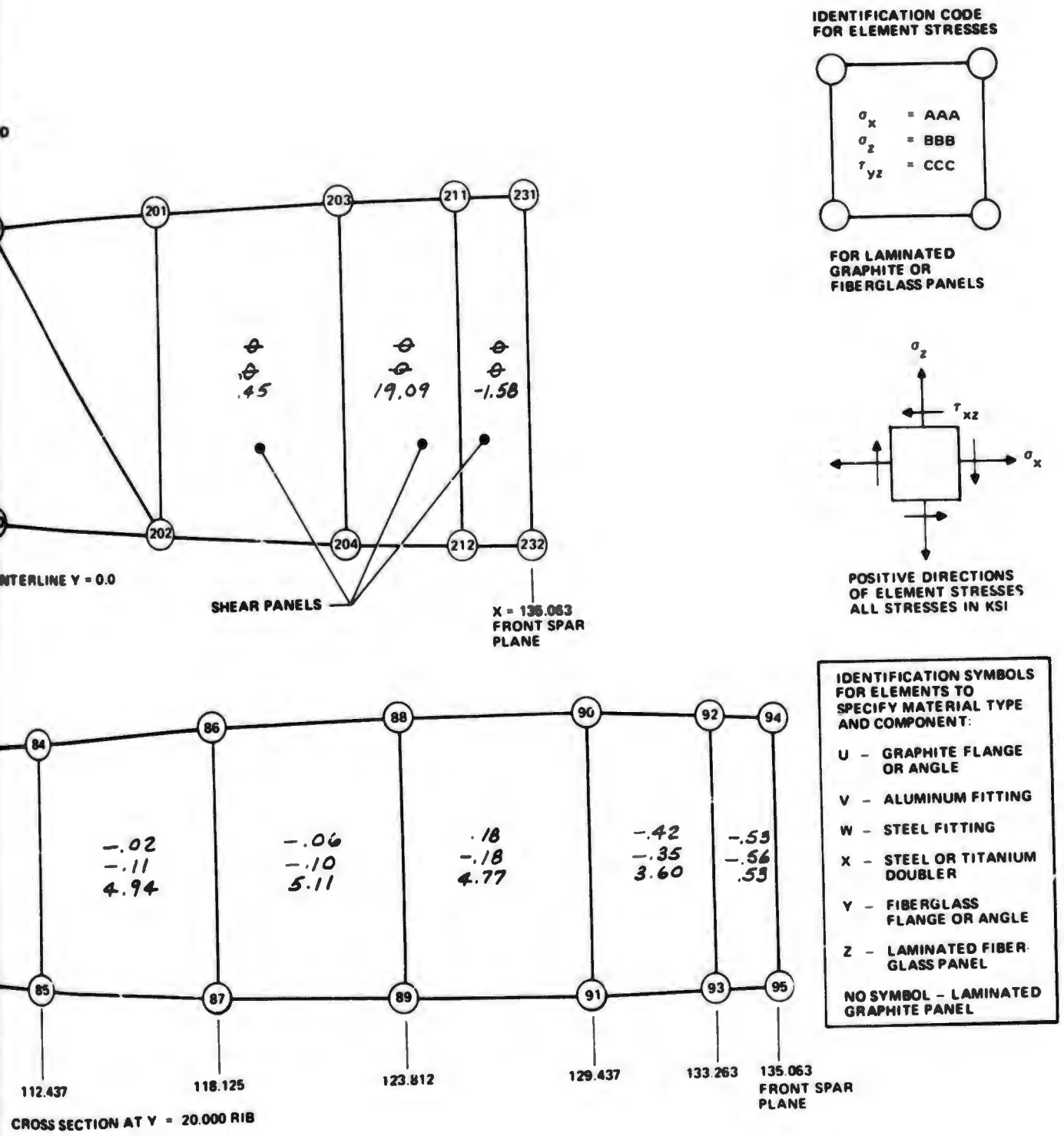

FIGURE 9. STRESS DISTRIBUTION IN CHORDWISE RIBS – LOAD CONDITION C

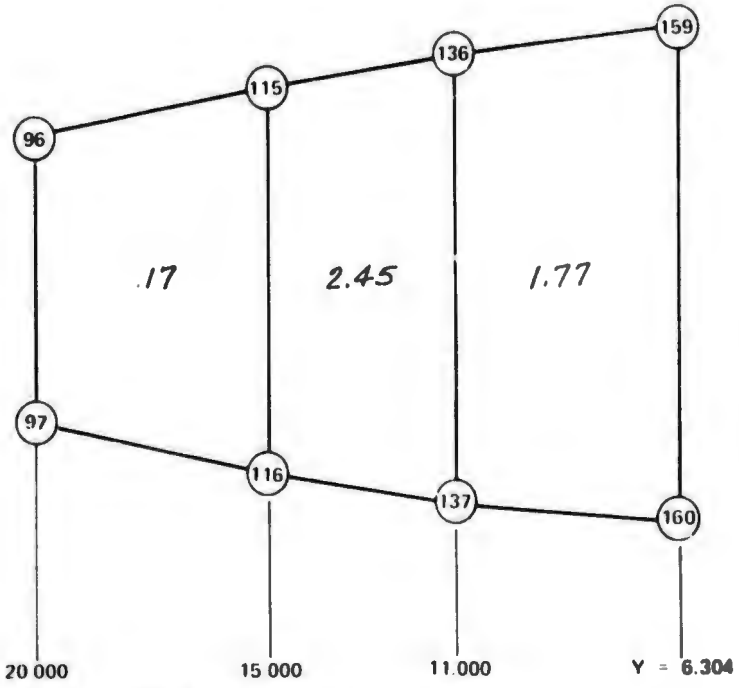

CROSS SECTION THRU X = 140.411
LEADING EDGE STRUCTURE – SHEAR PANELS

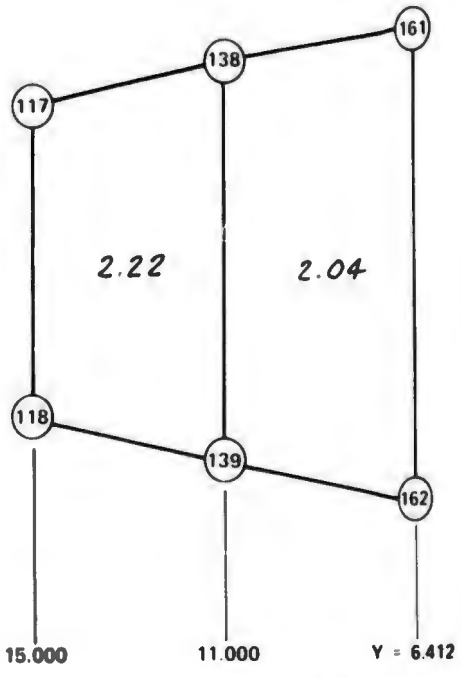

CROSS SECTION THRU X = 144.970
LEADING EDGE STRUCTURE – SHEAR PANELS

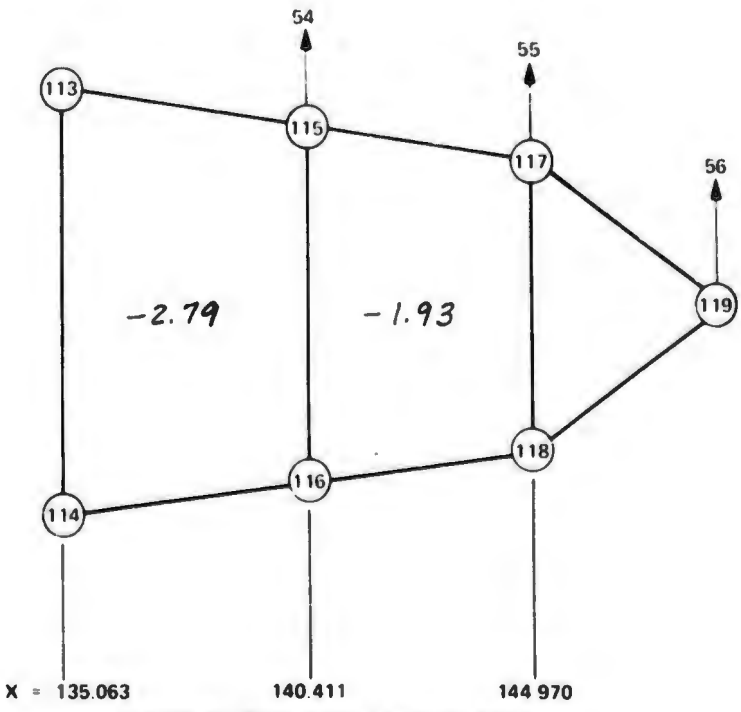

CROSS SECTION THRU LEADING EDGE
STRUCTURE AT Y = 15 000 – SHEAR PANELS

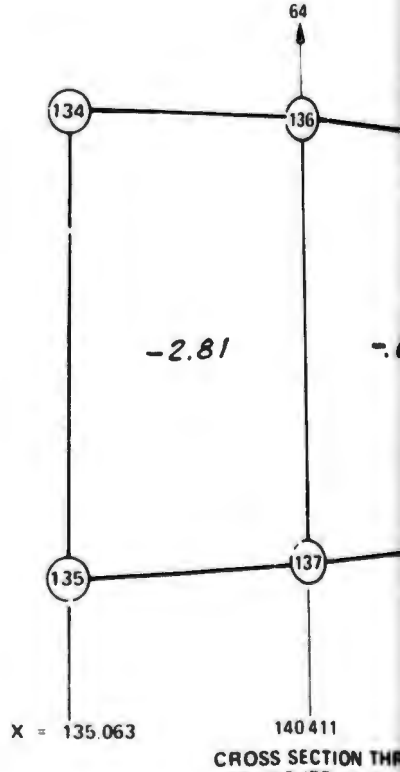

CROSS SECTION THR
STRUCTURE AT Y =

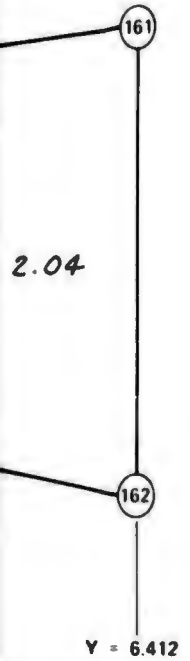

144.970
F – SHEAR PANELS

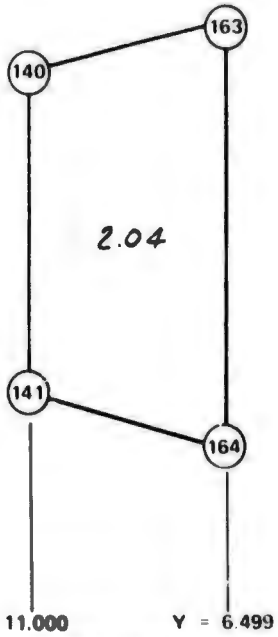

CROSS SECTION THRU X = 148.617 LEADING EDGE STRUCTURE – SHEAR PANELS

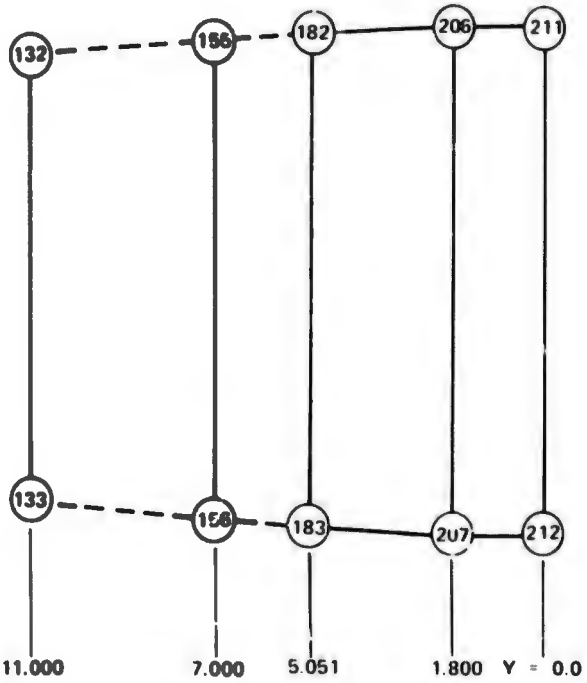

CROSS SECTION THRU X = 133.263 – SHEAR PANELS

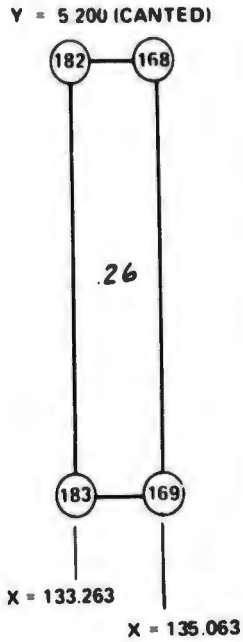

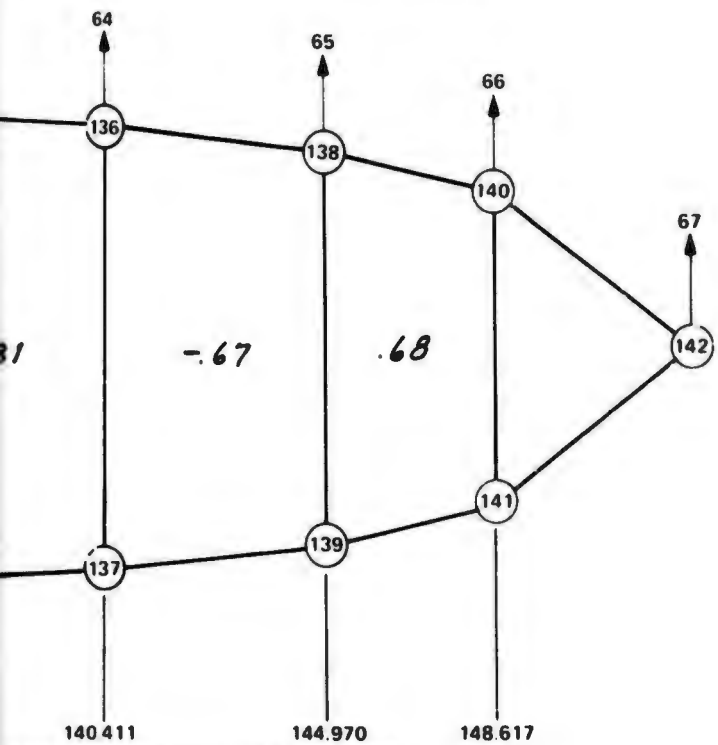

CROSS SECTION THRU LEADING EDGE STRUCTURE AT Y = 11.000 – SHEAR PANELS

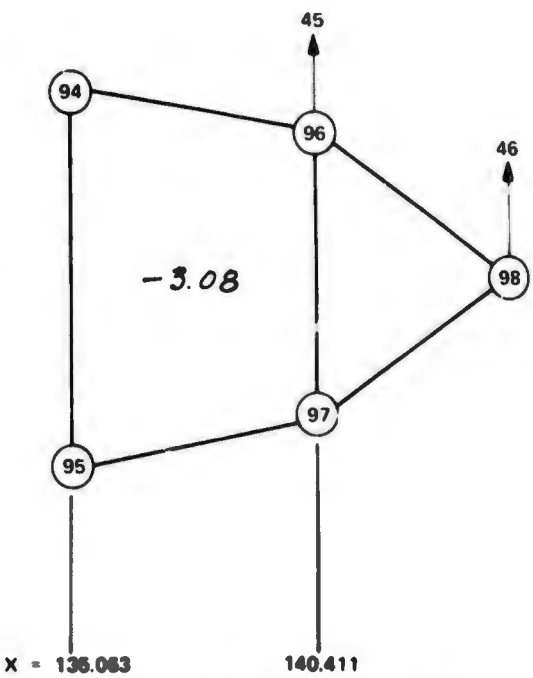

CROSS SECTION THRU LEADING EDGE STRUCTURE AT Y = 20.000 – SHEAR PANELS

NOTE: ALL

POS
LOA

ALL
MEA
MOD

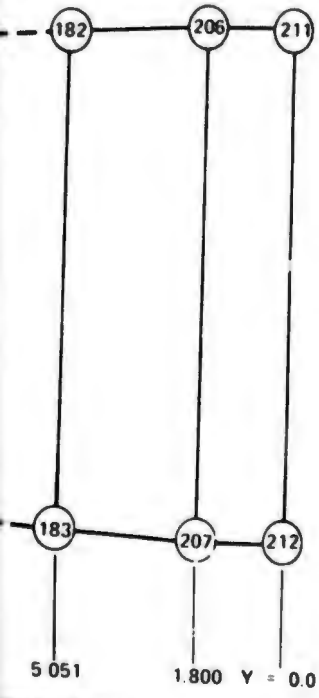

CTION THRU X = 133.263 –
NELS

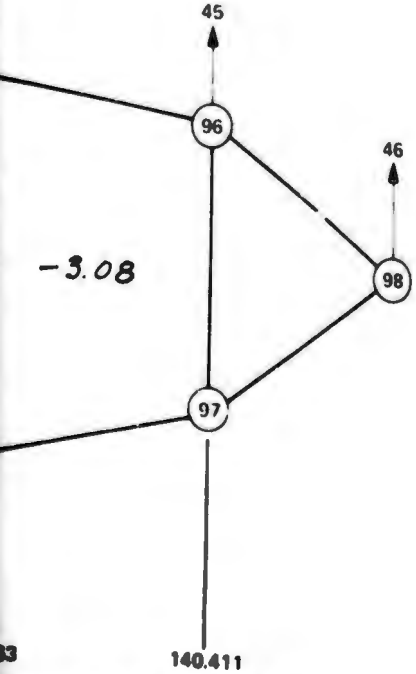

3
ECTION THRU LEADING EDGE
URE AT Y = 20.000 – SHEAR PANELS

CHORDWISE SHEAR PANELS ADJACENT TO FRONT SPAR

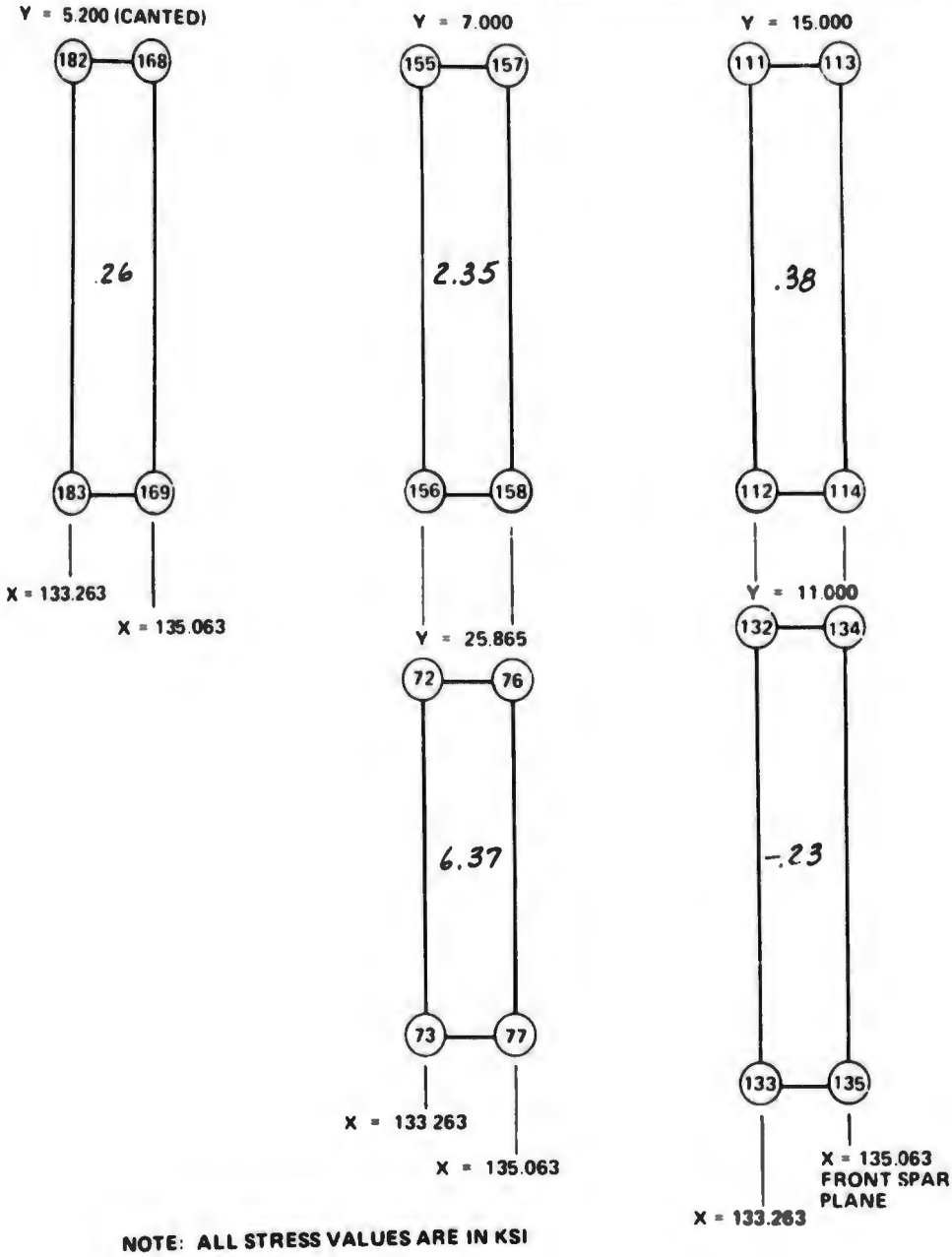

NOTE: ALL STRESS VALUES ARE IN KSI

POSITIVE DIRECTIONS FOR
LOAD VECTORS ARE SHOWN

ALL STATION LOCATIONS ARE
MEASURED RELATIVE TO ANALYSIS
MODEL BASE COORDINATE SYSTEM

FIGURE 10. IN-PLANE SHEAR STRESSES IN SHEAR PANELS – LOAD CONDITION C

IDENTIFICATION CODE
FOR ELEMENT STRESSES

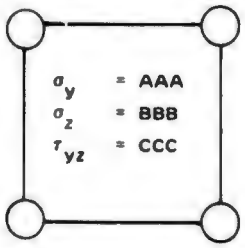

FOR LAMINATED
GRAPHITE OR
FIBERGLASS PANELS

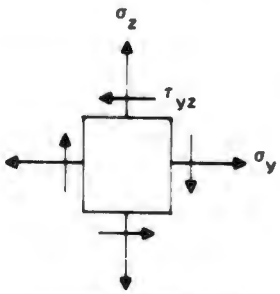

POSITIVE DIRECTIONS
OF ELEMENT STRESSES
ALL STRESSES IN KSI
(NOT APPLICABLE TO
CANTED RIB)

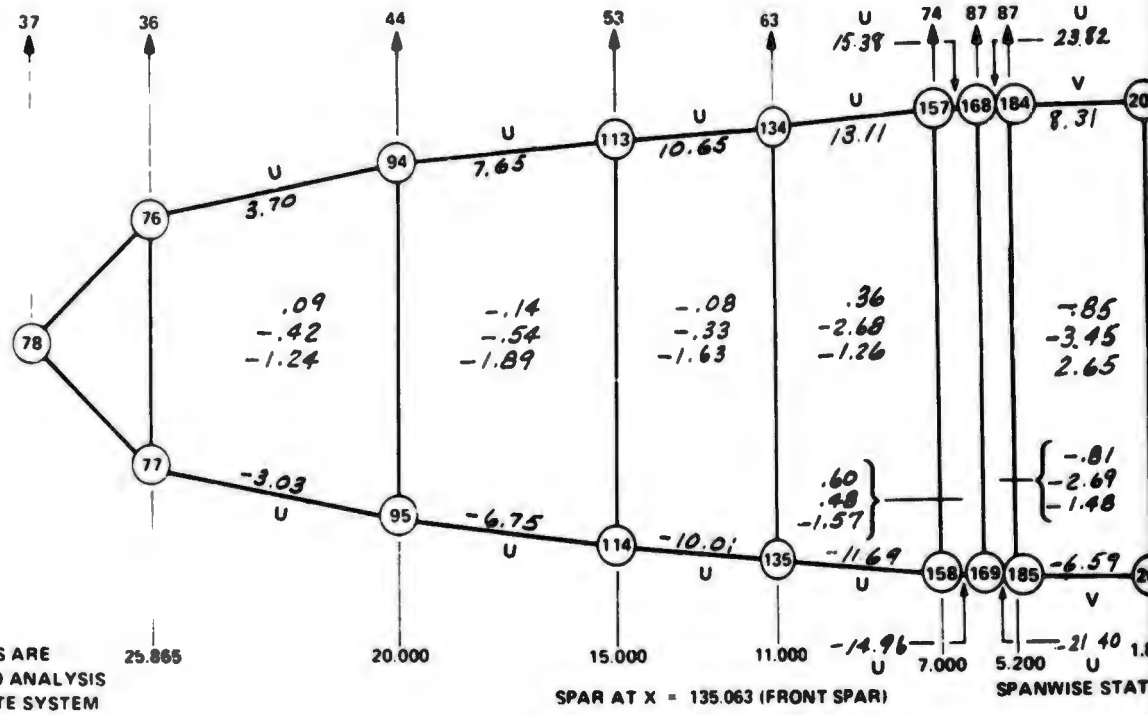

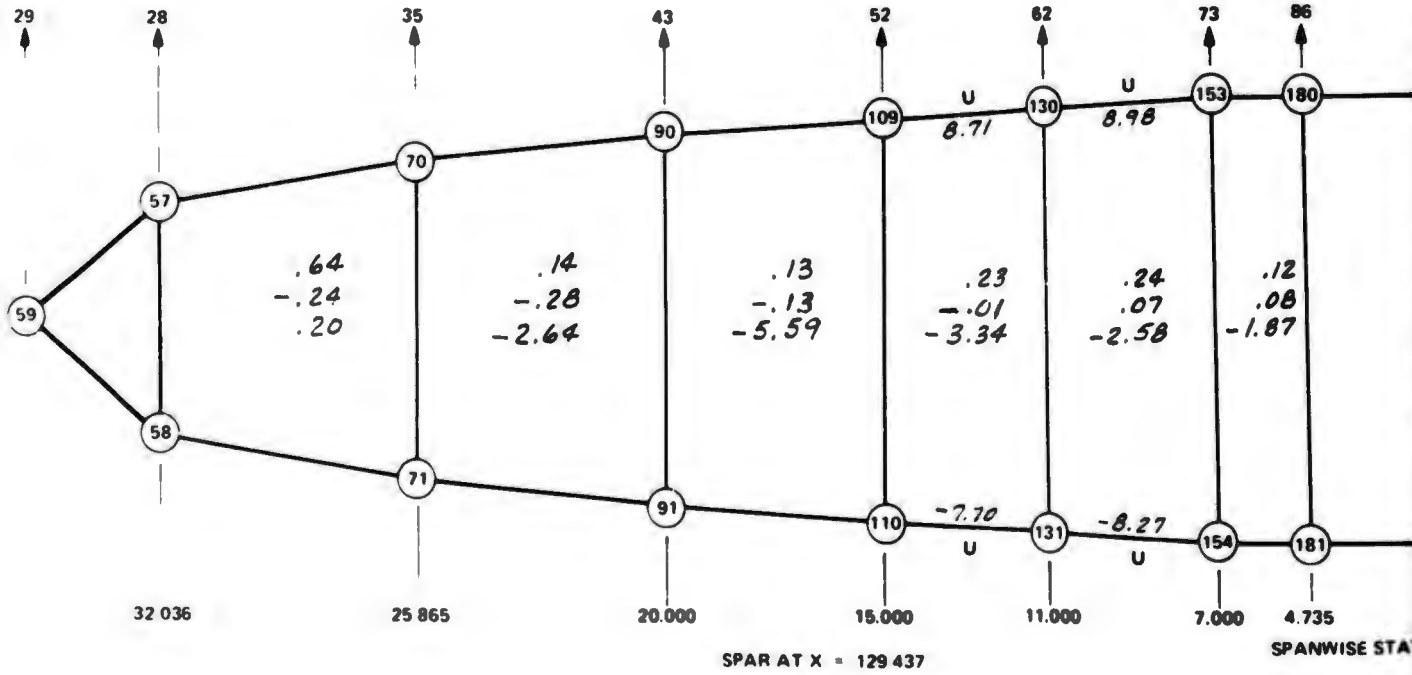

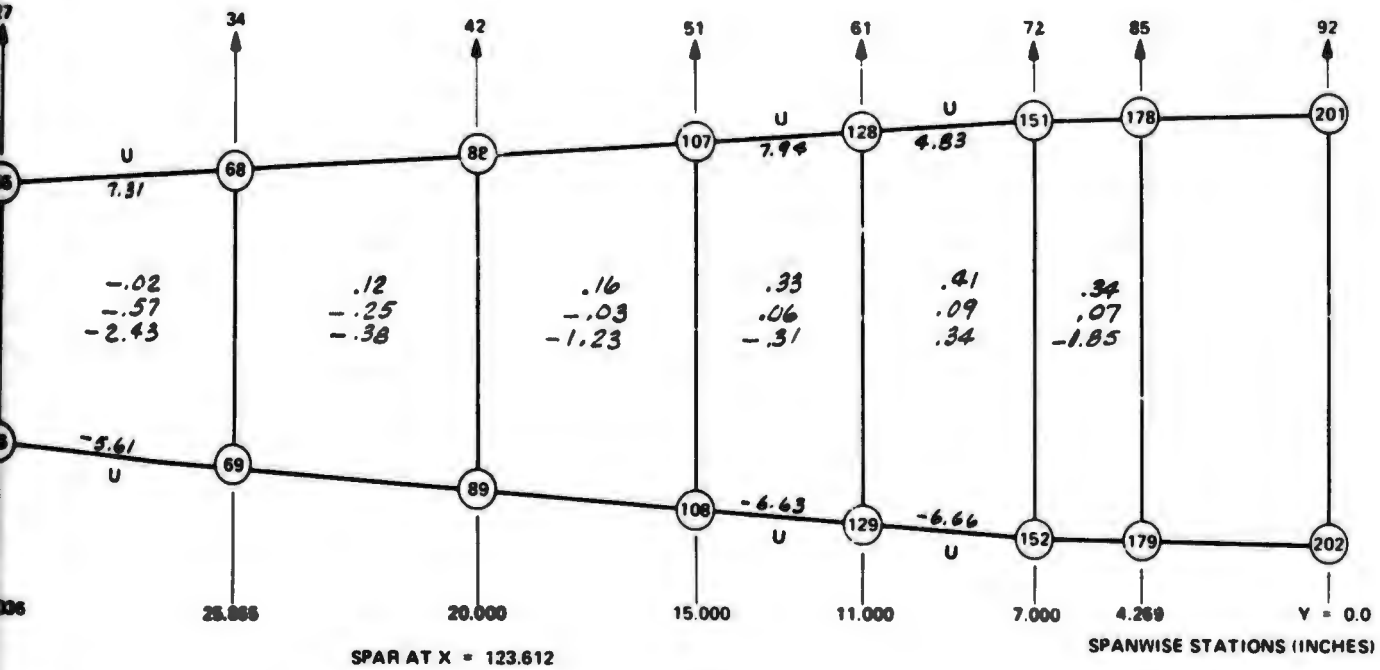

NTED RIB ONLY
ORDINATE DIRECTION
L TO Z DIRECTION AND ≈ PARALLEL TO X

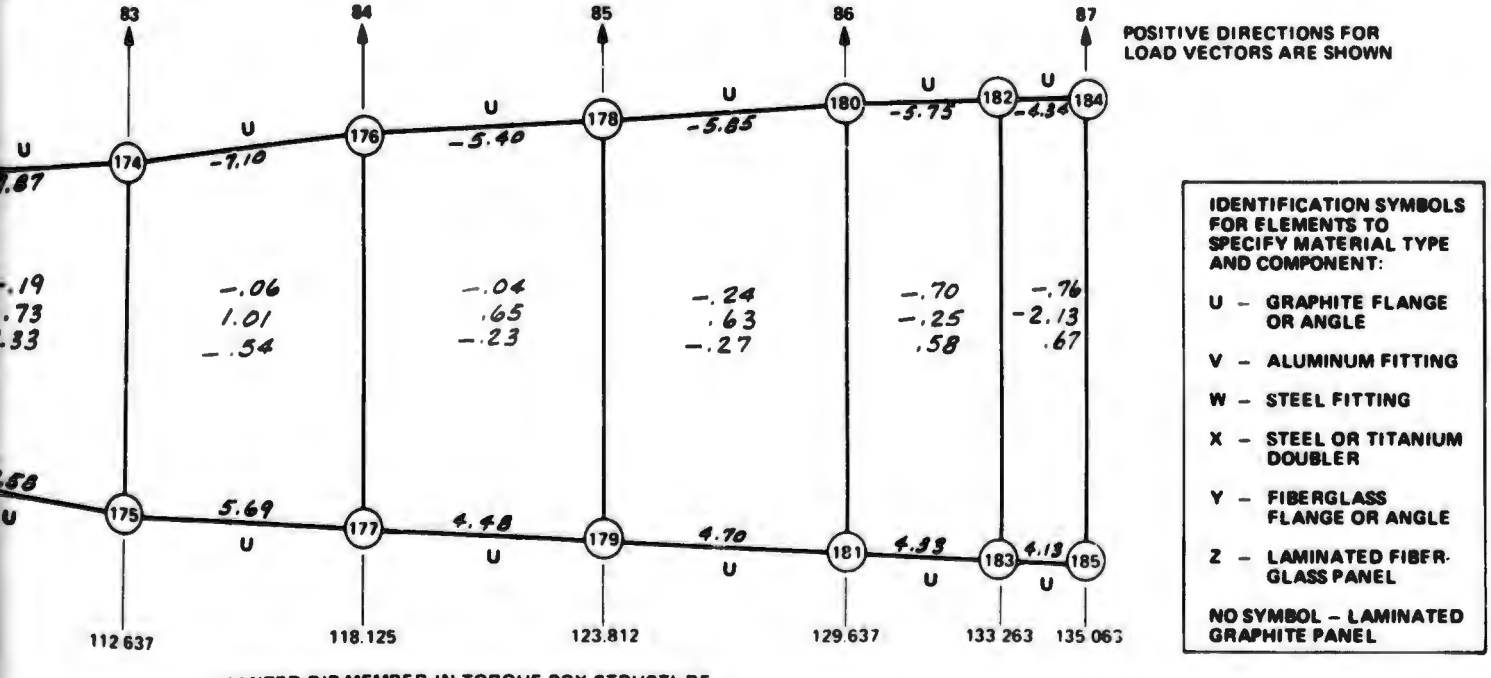

FIGURE 11. STRESS DISTRIBUTION IN RIBS AND SPARS – LOAD CONDITION C

BOTTOM VIEW

NOTE ALL STRESS VALUES ARE IN KSI

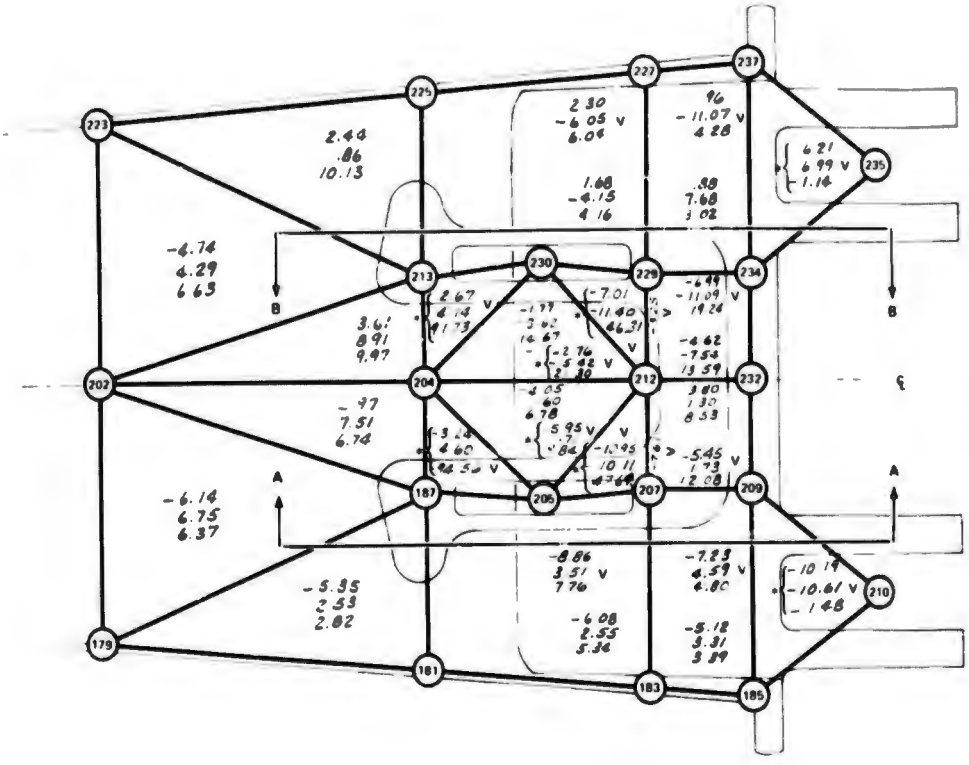

IDENTIFICATION SYMBOLS FOR ELEMENTS TO SPECIFY MATERIAL TYPE AND COMPONENT

U	GRAPHITE FLANGE OR ANGLE
V	ALUMINUM FITTING
W	STEEL FITTING
X	STEEL OR TITANIUM DOUBLER
Y	FIBERGLASS FLANGE OR ANGLE
Z	LAMINATED FIBER GLASS PANEL

NO SYMBOL LAMINATED GRAPHITE PANEL

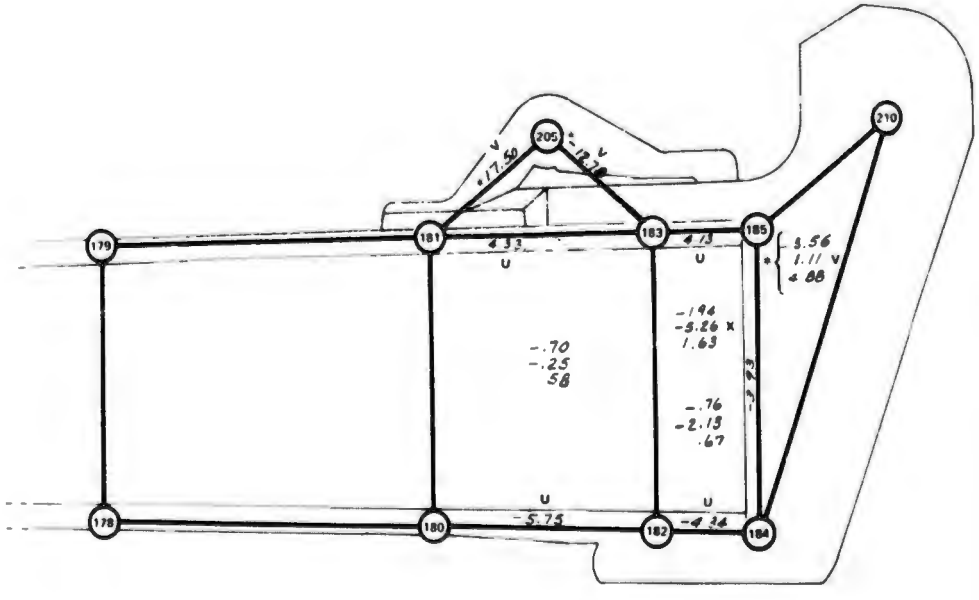

TOP VIEW

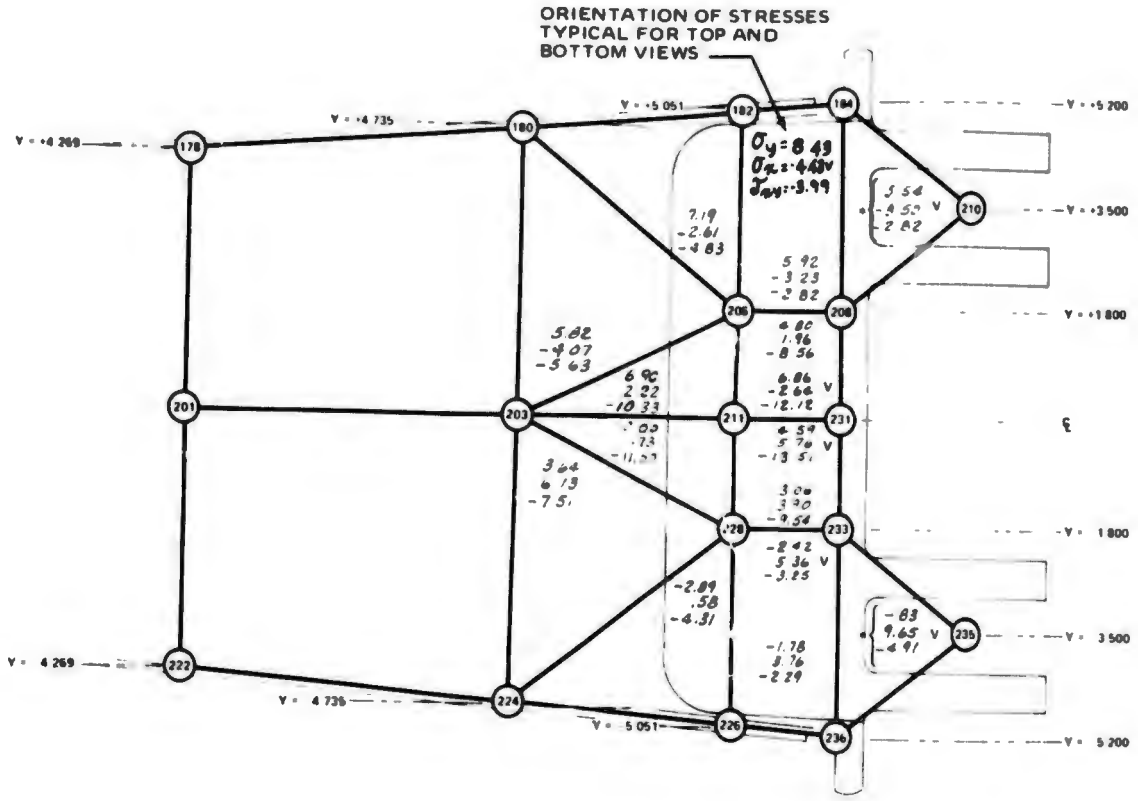

TYPICAL FOR LEFT
AND RIGHT VIEWS
α IS COORDINATE-DIRECTION
IN PLANE OF ELEMENT AND
NORMAL TO z COORDINATE

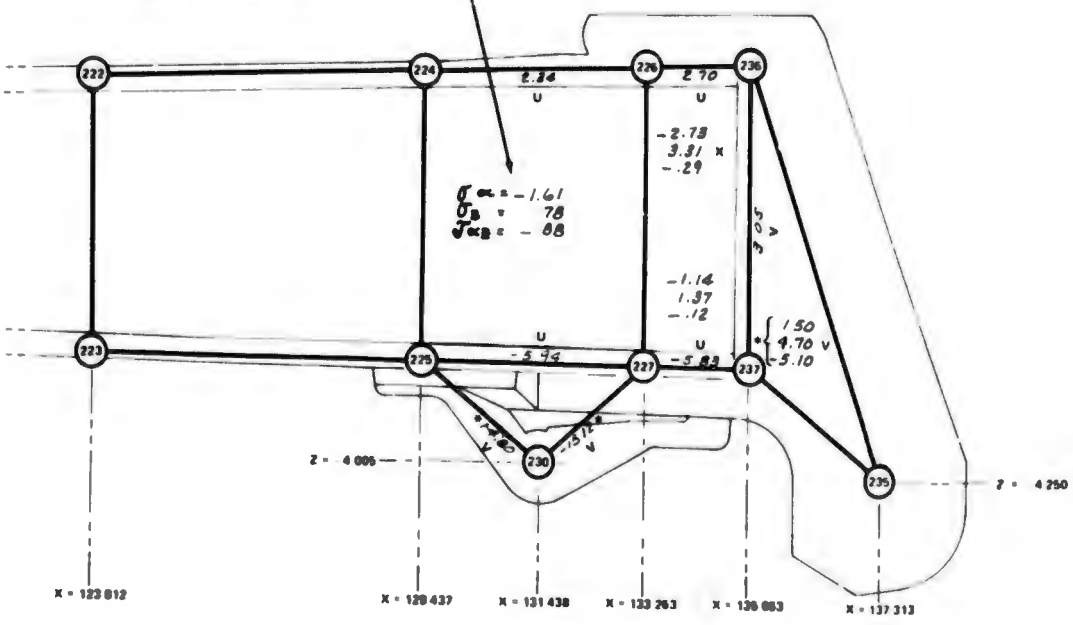

TOP VIEW

NTATION OF STRESSES
CAL FOR TOP AND
OM VIEWS

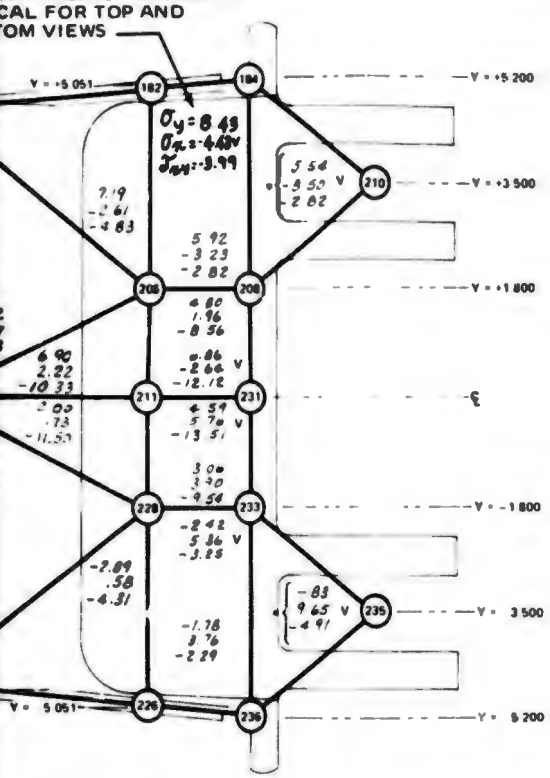

NOTES

QUANTITIES MARKED * REPRESENT STRESSES IN THE LUG AREA OF THE PIVOT POINT FITTING AND THE ELEVATOR MECHANISM ATTACH FITTING

SINCE THESE AREAS ARE HIGHLY IDEALIZED, THESE VALUES ARE NOT REPRESENTATIVE OF THE ACTUAL STRESS FIELD IN THE FITTINGS AND ARE LISTED FOR REFERENCE ONLY

NODES NO 210 AND 235 ARE FIXED SUPPORT POINTS

ALL STATION LOCATIONS ARE MEASURED RELATIVE TO ANALYSIS MODEL BASE COORDINATE SYSTEM

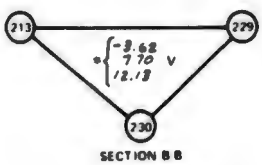

SECTION B B

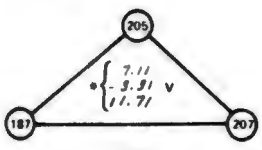

SECTION A A

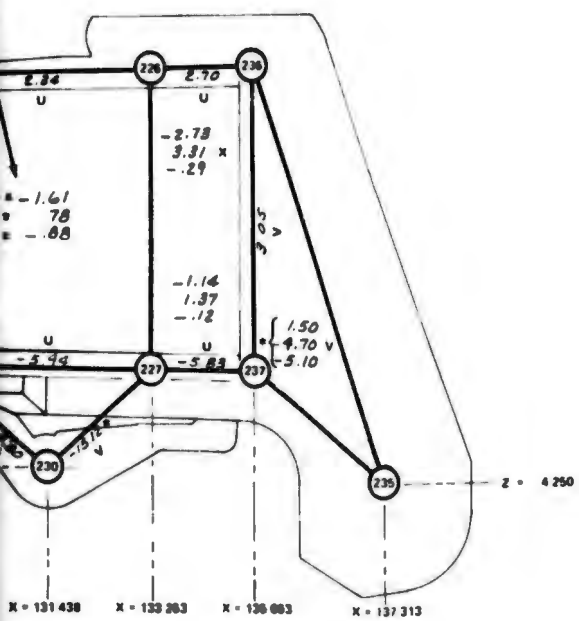

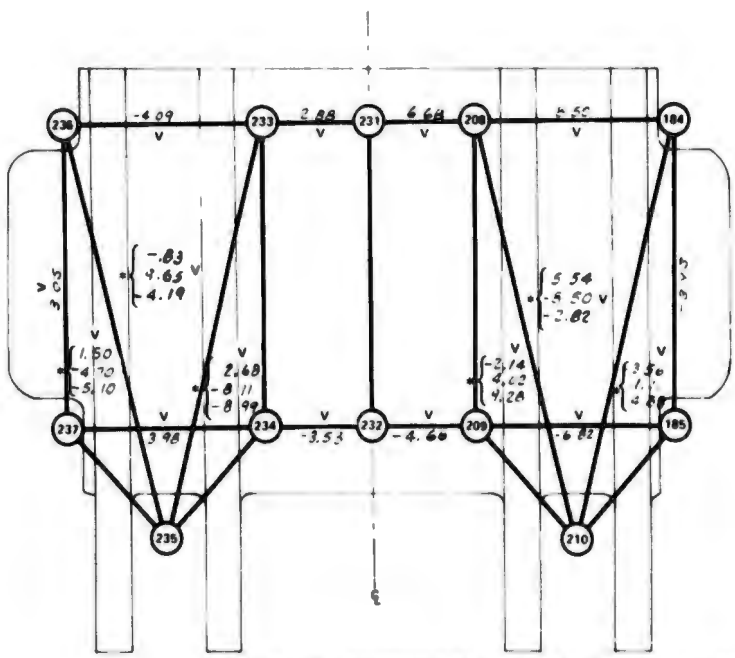

FIGURE 12. STRESSES IN IDEALIZED PIVOT FITTING AND ADJACENT STRUCTURE – LOAD CONDITION C

NOTE ALL STRESS VALUES ARE IN KSI

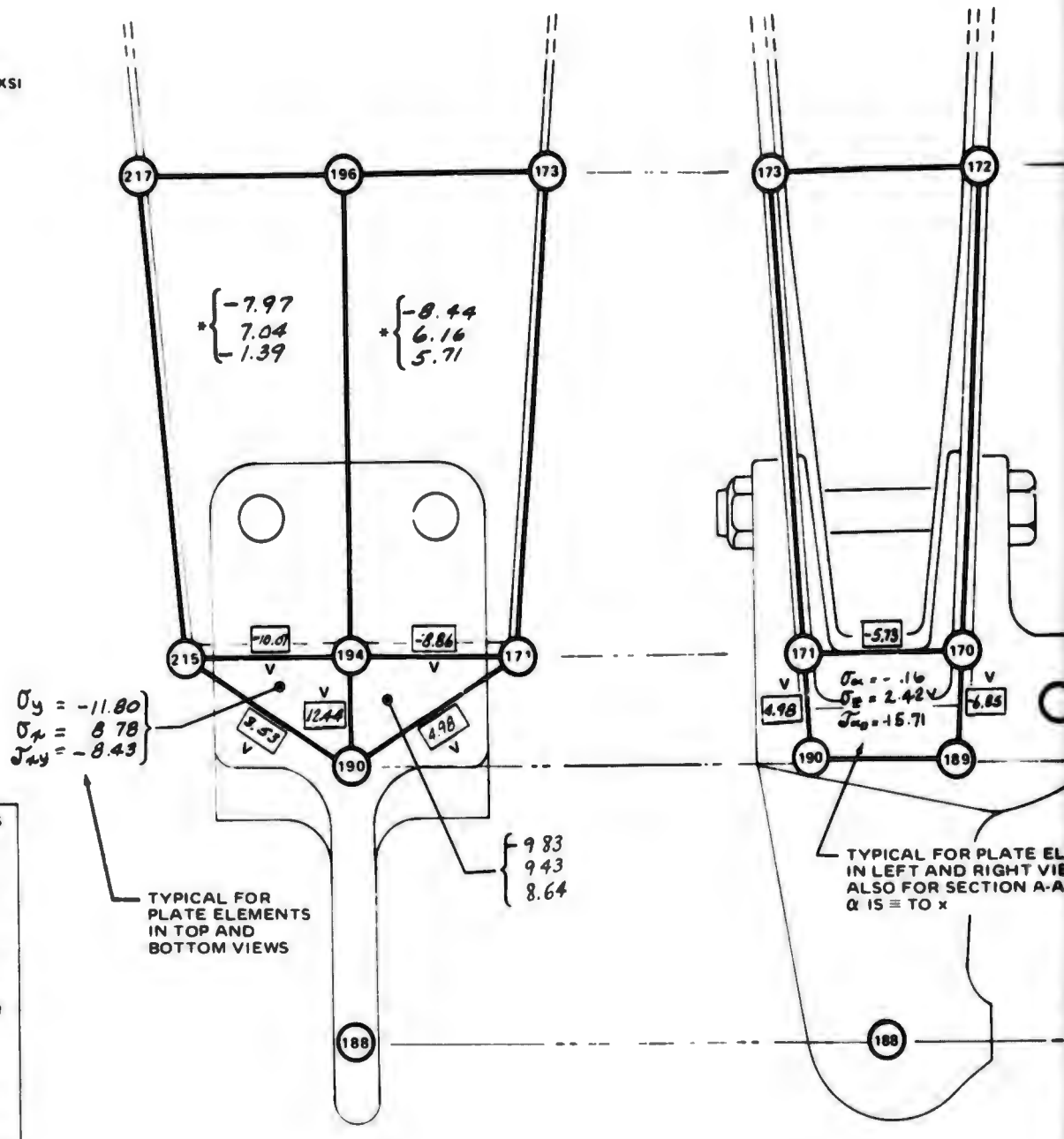

IDENTIFICATION SYMBOLS FOR ELEMENTS TO SPECIFY MATERIAL TYPE AND COMPONENT

U	GRAPHITE FLANGE OR ANGLE
V	ALUMINUM FITTING
W	STEEL FITTING
X	STEEL OR TITANIUM DOUBLER
Y	FIBERGLASS FLANGE OR ANGLE
Z	LAMINATED FIBER GLASS PANEL
NO SYMBOL	LAMINATED GRAPHITE PANEL

BOTTOM VIEW

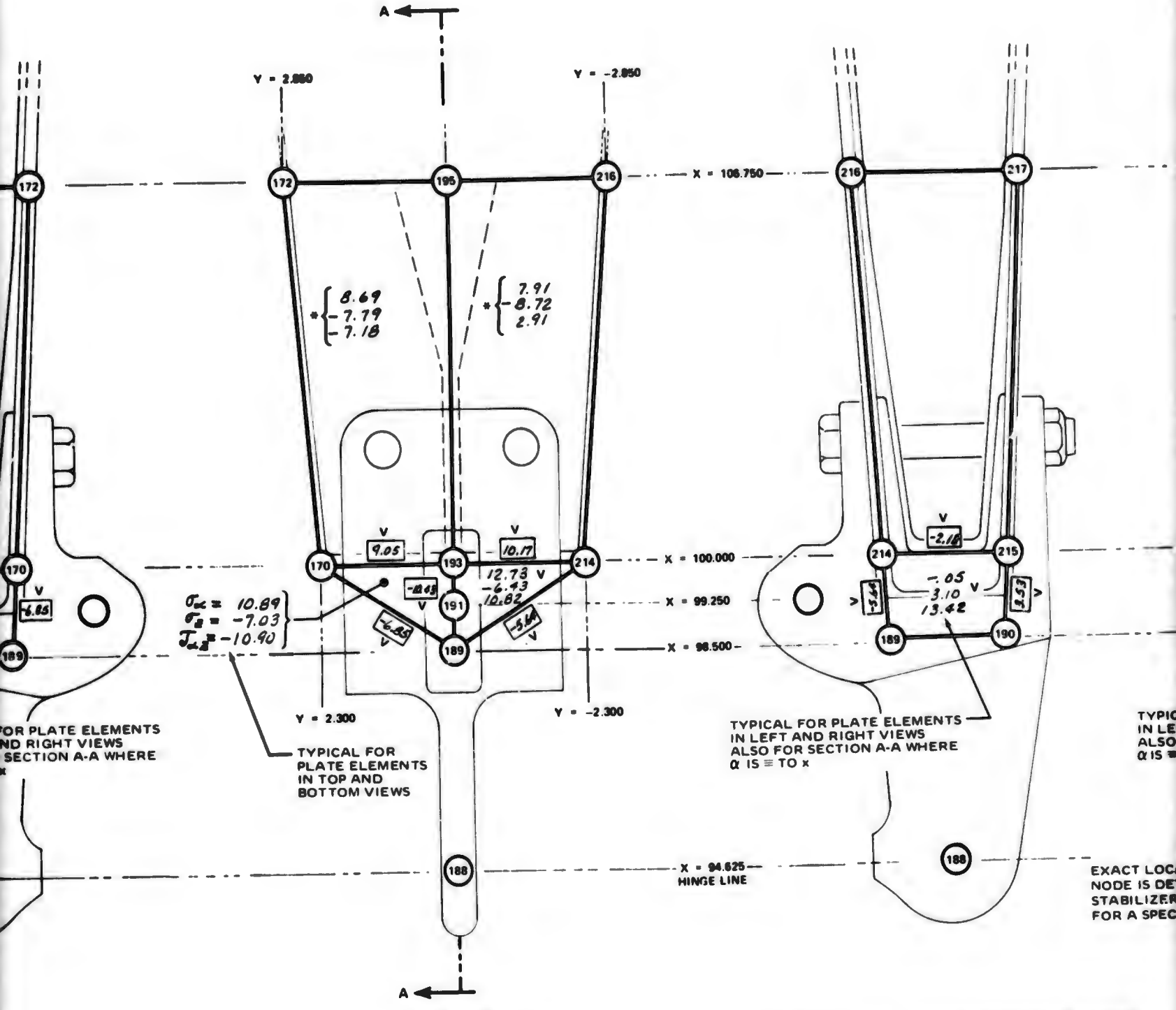

TOP VIEW

*THESE QUANTITIES ARE STRESSES IN THE CANT RIB FLANGES.

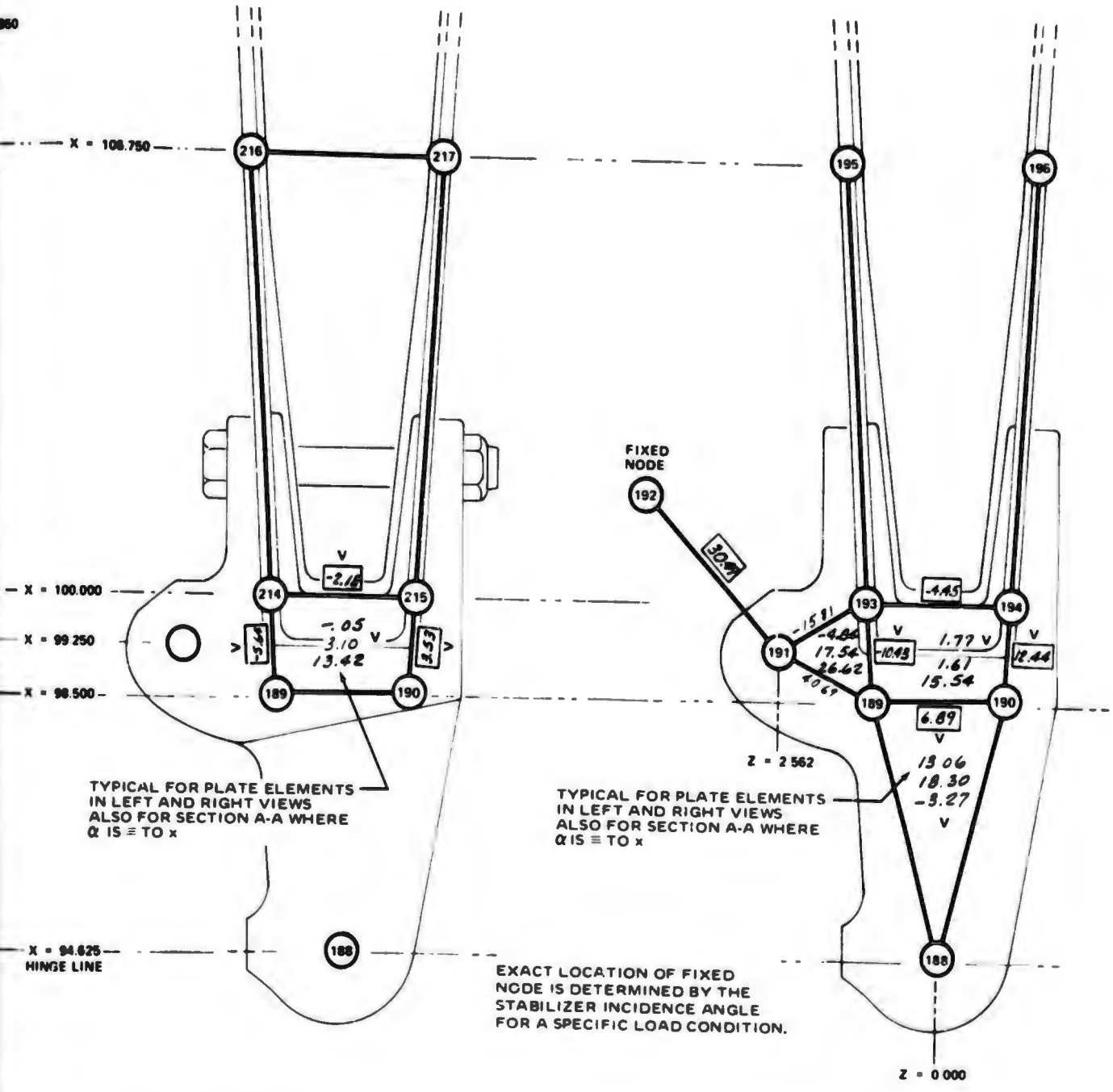

*THESE QUANTITIES ARE STRESSES IN THE CANT RIB FLANGES.

SECTION A-A

ALL STATION LOCATIONS ARE MEASURED RELATIVE TO ANALYSIS MODEL BASE COORDINATE SYSTEM

FIGURE 13. STRESSES IN IDEALIZED ACTUATOR FITTING AND ADJACENT STRUCTURE – LOAD CONDITION C

1. Elevator twist was taken into account in determining the effective elevator setting. In condition C, full 25° up elevator angle was required by the design condition. This angle was achieved at the airplane centerline where the system stops prevented greater deflection. Elevator torsion reduced the average angle to 19.2° (Reference 9, Vol. III, Pg. 214).

2. Stabilizer and elevator twist in condition C shifted the spanwise center of total load from station 33.8 to station 32.2 (Ibid, pg. 214, 216, and 217).

3. Stabilizer bending was considered in determining the elevator hinge reactions. Examination of the deflection terms in the hinge reaction equations showed that they were relatively small and affected the hinge reactions by less than 10 percent.

The general effect of the structural deflections was to produce a small reduction in structural loads, except for the hinge loads where some were increased and some were reduced.

Graphs of experimental deflections at the front and rear-spars as obtained from tests on the metal stabilizer and from calculated data for the graphite stabilizer are shown in Figure 14 for load condition C. Calculated deflections for condition D at the rear-spar are also included.

The deflection curve for the metal stabilizer at the rear-spar as given in Reference 2 has been revised for the present report. When this data (from Reference 10) was first examined, it was determined that the deflections for the front and rear-spars for load conditions C and D contained a spurious increment, most of which was caused by deformations in the support fixture. The deflection curve shown in Reference 2 was derived by subtracting the estimated increment due to fixture deformation. A subsequent study of this data revealed that not all of this deformation was accounted for in this correction. Therefore, a further modification for fixture deformation was made when deriving the deflection data shown in Figure 14. The data given in Figure 14 for load condition C is a reasonable accurate representation of the actual load deflection curve for the metal stabilizer. The comparable deflection data for load condition D found in Reference 10 contained a greater error than the data for condition C. This latter deflection data was therefore not used as a basis for comparison in Figure 14.

A direct comparison of the calculated deflections for the graphite stabilizer with those of the metal structure is difficult since the elevator was not included in the discrete element analysis, and the metal stabilizer tests were made with the elevator attached. The elevator was placed in the proper flight attitude as defined by the angle of elevator deflection (δ_e) which for condition C was 25.0 degrees nose-down. The elevator caused an increase in the apparent stiffness of the stabilizer structure since each elevator is attached to the stabilizer through a statically indeterminate (four hinge point) system. However, it was possible to draw some conclusions from the test data by comparing the effect of the elevator on the deflections measured at the rear-spar with the comparable effect on front-spar deflections.

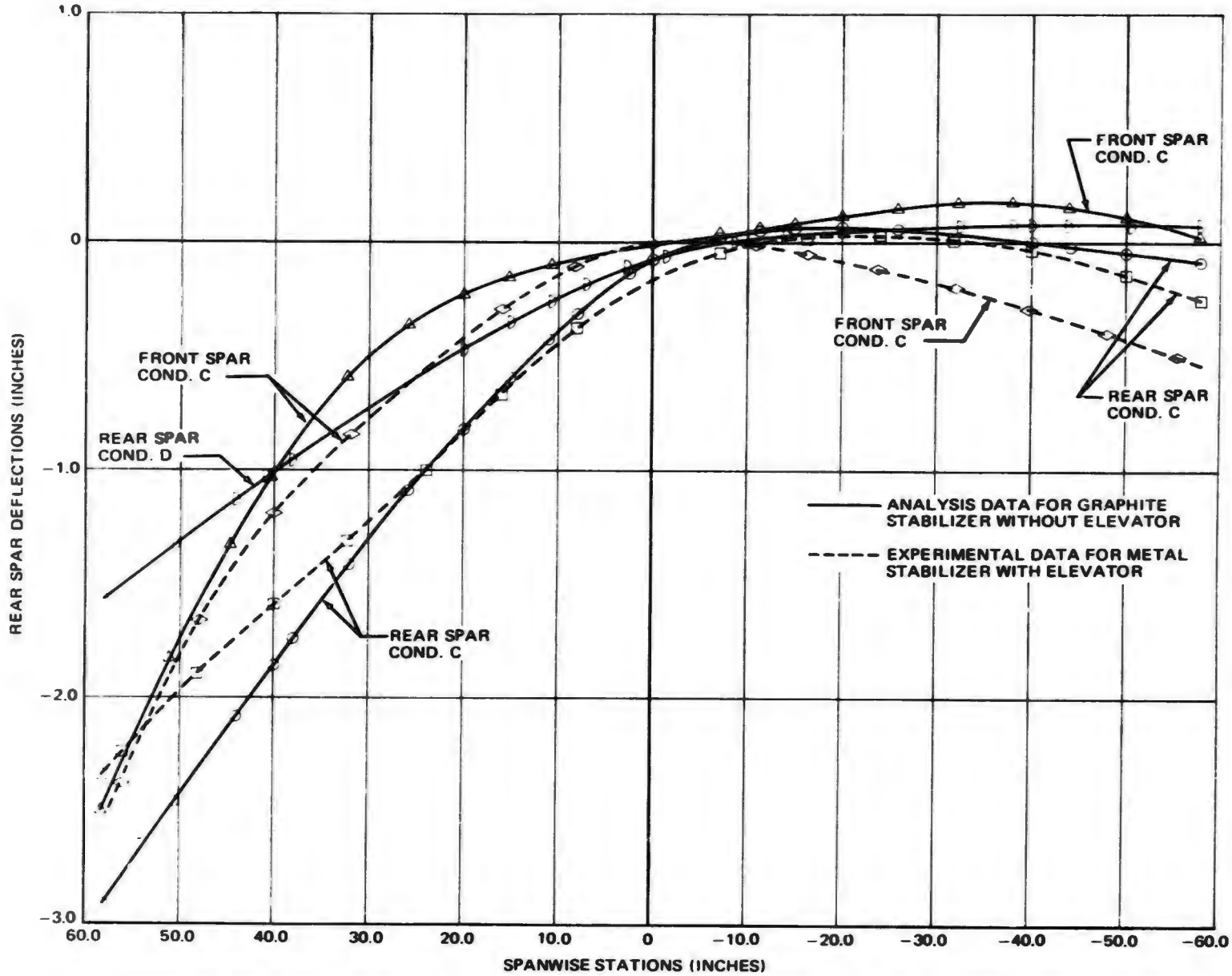

FIGURE 14. COMPARISON OF CALCULATED AND EXPERIMENTAL DEFLECTIONS AT FRONT AND REAR SPARS

Figure 14 indicates the experimental front-spar deflections are greater than the calculated deflections for both the left and right sides. In contrast, the calculated rear-spar deflection is greater outboard of spanwise station 20.0 but follows the experimental curve quite closely to station -40.0 at which point the two curves began to deviate again. The rather large difference in the deflections noted at the rear-spar outboard of station 20.0 can be caused by the presence of the elevator as previously discussed. The stiffening effect of the deflected elevator would also influence the deflection at the front-spar in the region adjacent to the outboard hinge fitting. This effect is verified by the relationship of analytical and experimental deflections at the front-spar. The two curves diverge with increasing distance to the left of the centerline up to about station 30.0 or 35.0 after which they began to approach each other again. Near the outboard hinge fitting they are nearly parallel. It appears that the spanwise bending rigidities of the metal and graphite structures are approximately equal. In view of the generally small effect of the structural deflections on loads, the differences in the rigidity of the two structures is not considered significant. Since a production metal elevator will be used with the composite structure, the elevator twist will be identical to that previously computed.

Allowable Buckling Stresses

Critical buckling stresses for the cover skins were recomputed using the 5.8 mil per ply thickness and the elastic properties given in Table II. For this analysis, the degree of edge fixity was accounted for by assuming pin-jointed panels with dimensions equal to those between the bolt centerlines. Buckling allowable curves obtained in this manner are presented in Figures 15 through 19 for combined biaxial compression and shear loadings. A graph of critical buckling stress versus thickness for pure shear and for uniaxial compression is shown in Figure 20. This figure illustrates the correlation between the maximum compressive stress obtained in the box-beam test and the critical buckling stress for uniaxial compression. Since the box-beam skin did not buckle in this test, it was concluded that the PANBUCK program and the assumed panel dimensions gave a satisfactory solution.

The $(0°, \pm 45°, 90°)$ pattern is quasi-isotropic. Consequently, isotropic stability equations should give nearly the same critical stresses as the PANBUCK solution. Table IV compares the buckling stresses obtained from PANBUCK with the buckling stresses obtained from commonly used isotropic formulas for uniaxial compression and for shear.

The isotropic relationships are in fair agreement with the PANBUCK solutions. Interpolation or extrapolation of buckling allowables from PANBUCK is, therefore, considered permissible on the basis of F_{cr} proportional to Et^2/b^2.

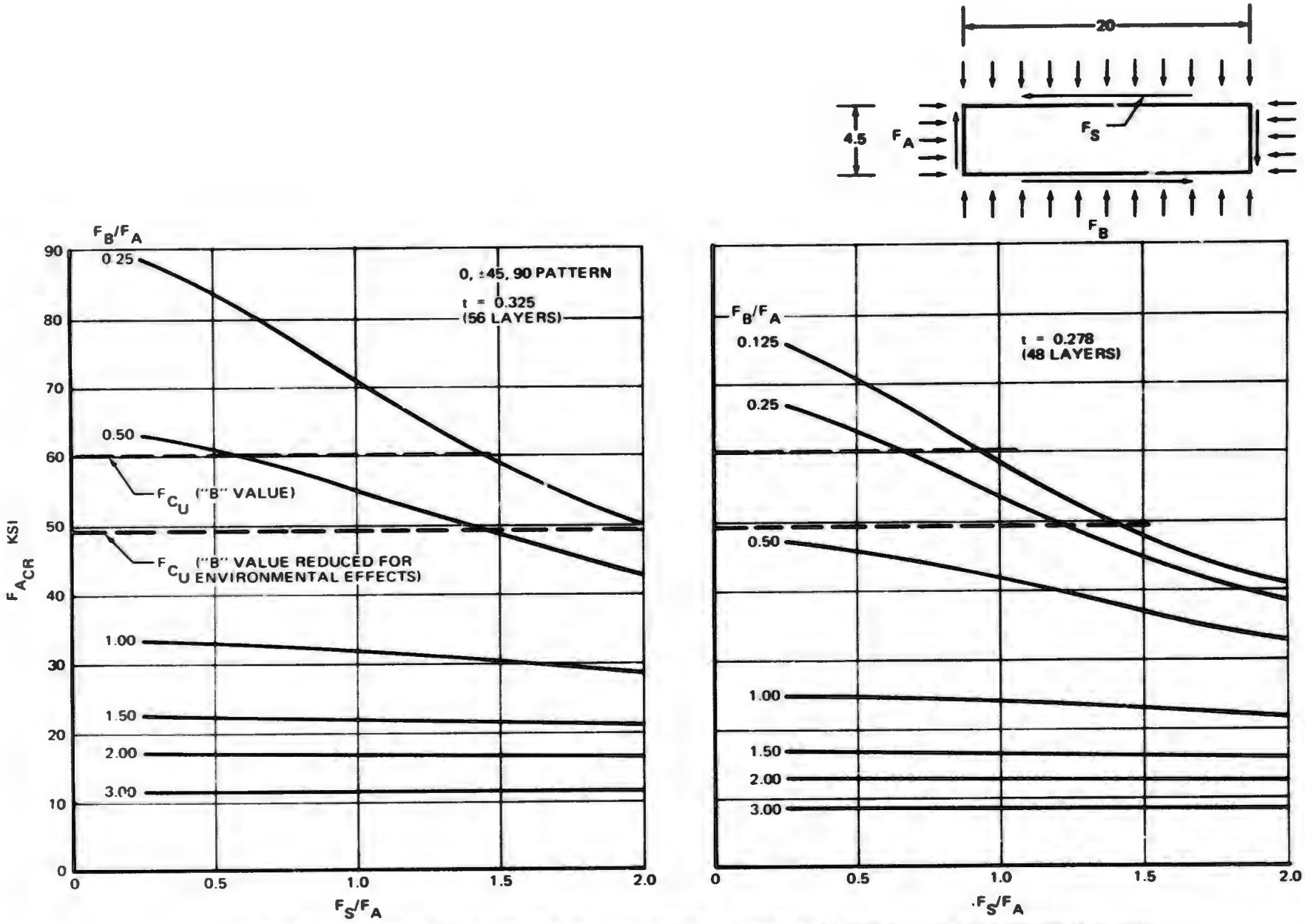

FIGURE 15. ALLOWABLE BUCKLING STRESSES FOR 56 AND 48 LAYER LAMINATES (20-INCH PANEL)

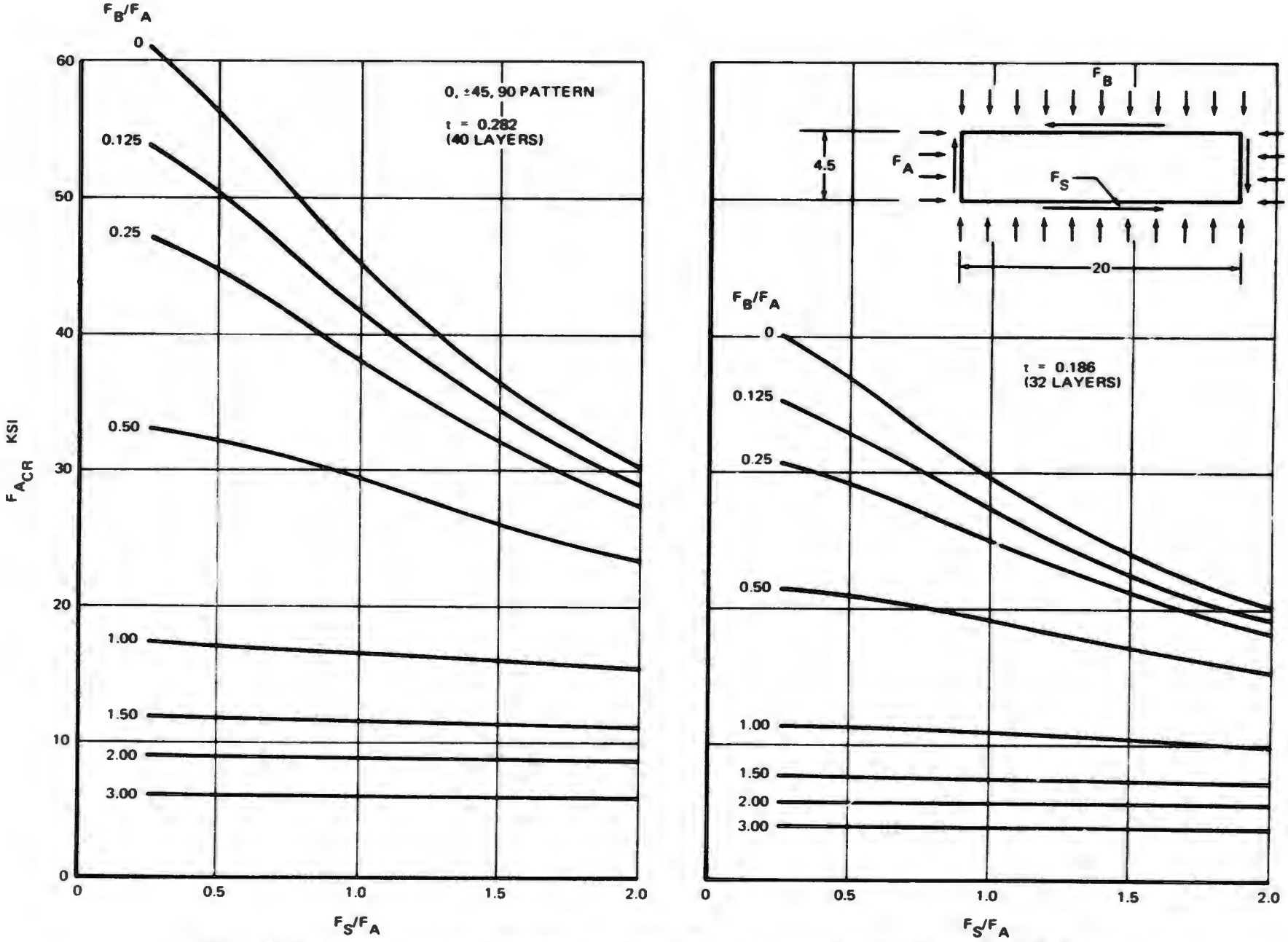

FIGURE 16. ALLOWABLE BUCKLING STRESSES FOR 40 AND 32 LAYER LAMINATES (20-INCH PANEL)

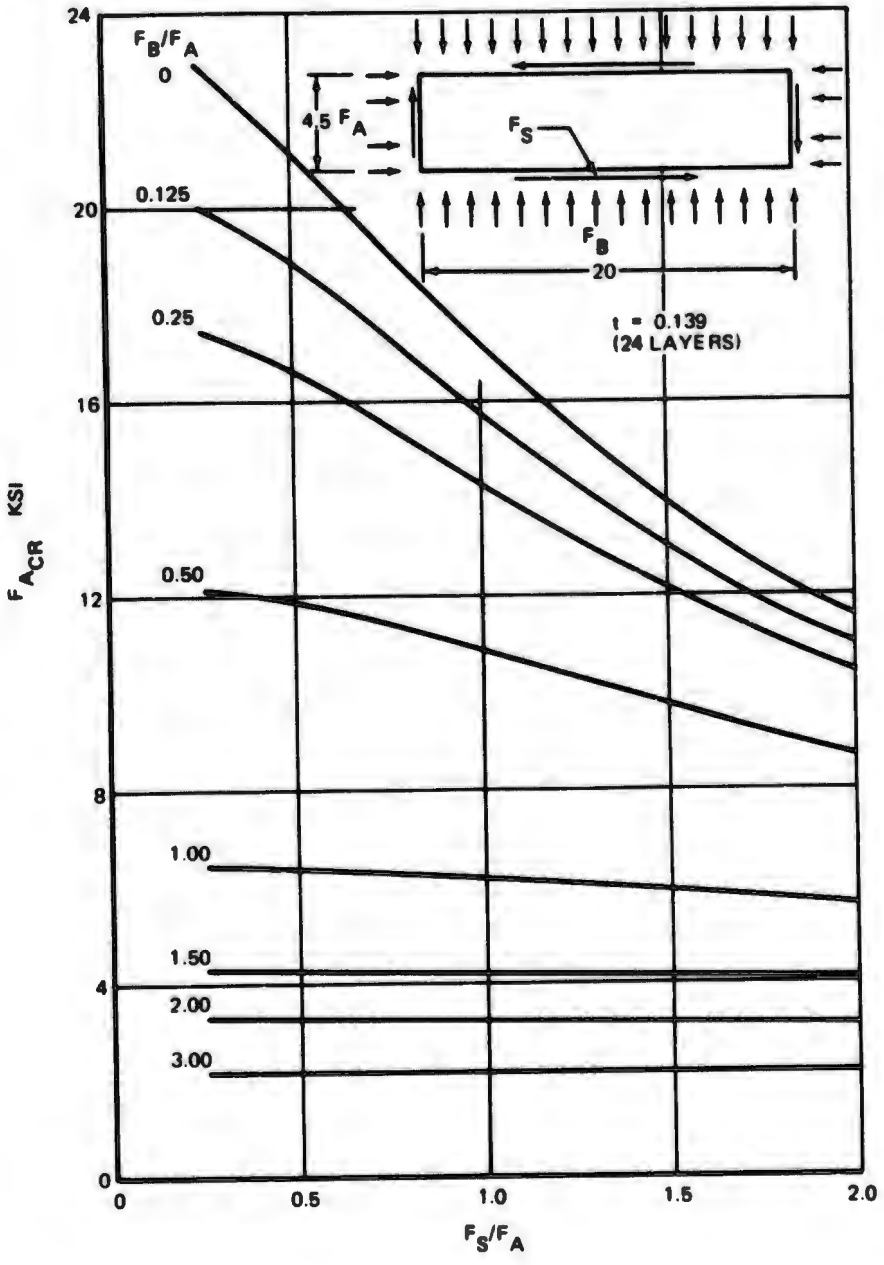

FIGURE 17. ALLOWABLE BUCKLING STRESSES FOR 24 LAYER LAMINATES (20-INCH PANEL)

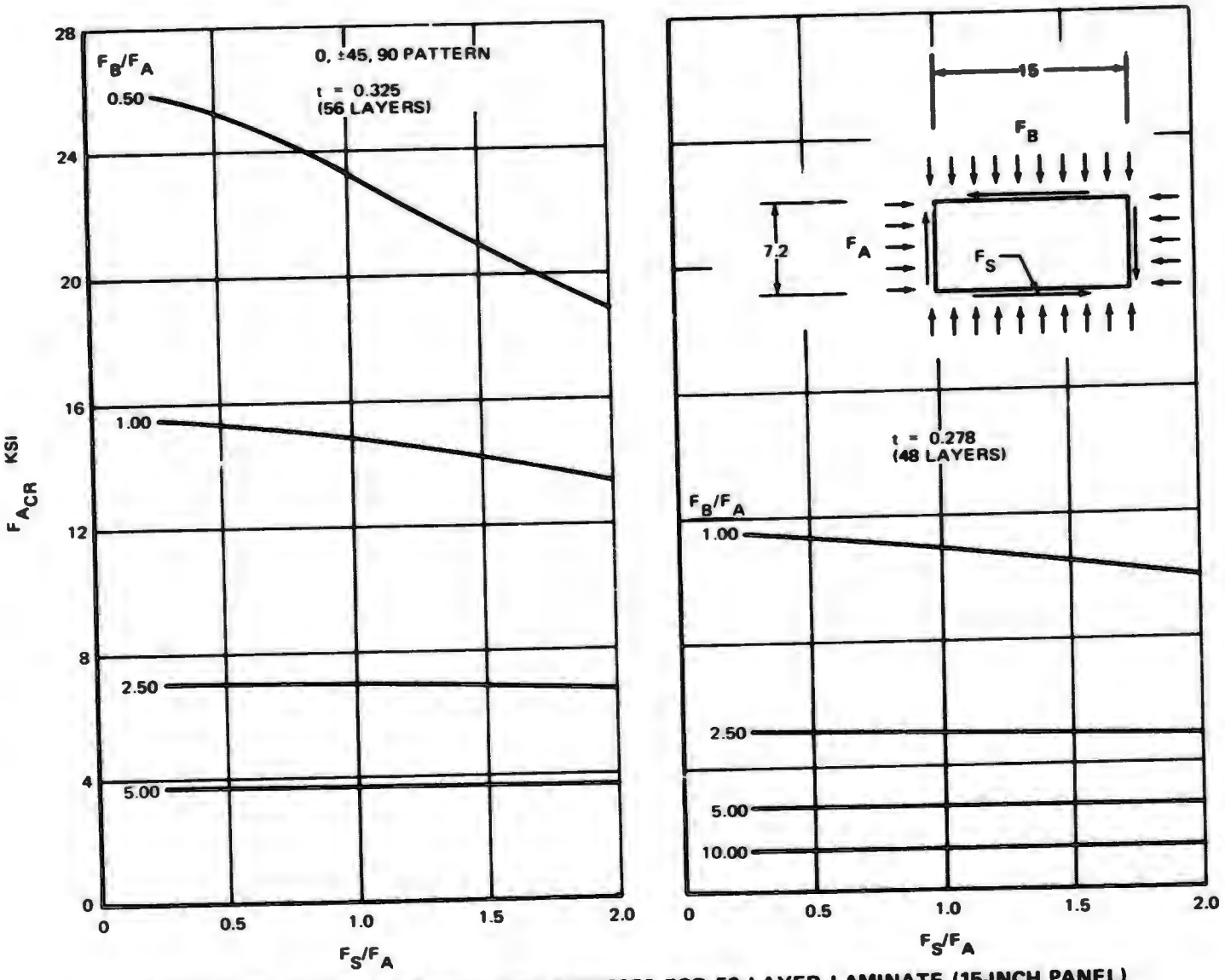

FIGURE 18. ALLOWABLE BUCKLING STRESSES FOR 56 LAYER LAMINATE (15-INCH PANEL)

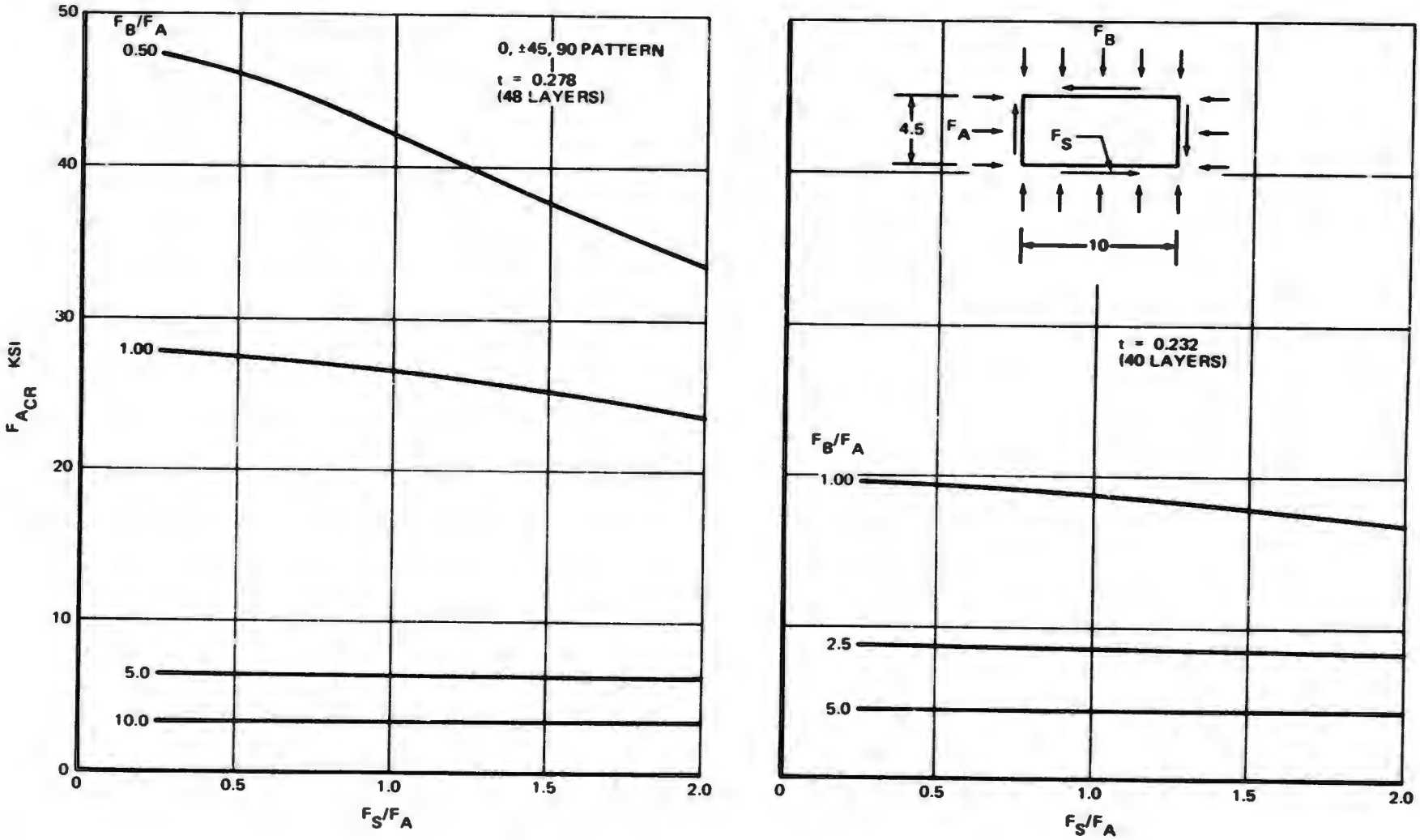

FIGURE 19. ALLOWABLE BUCKLING STRESSES FOR 48 AND 40 LAYER LAMINATES (10-INCH PANEL)

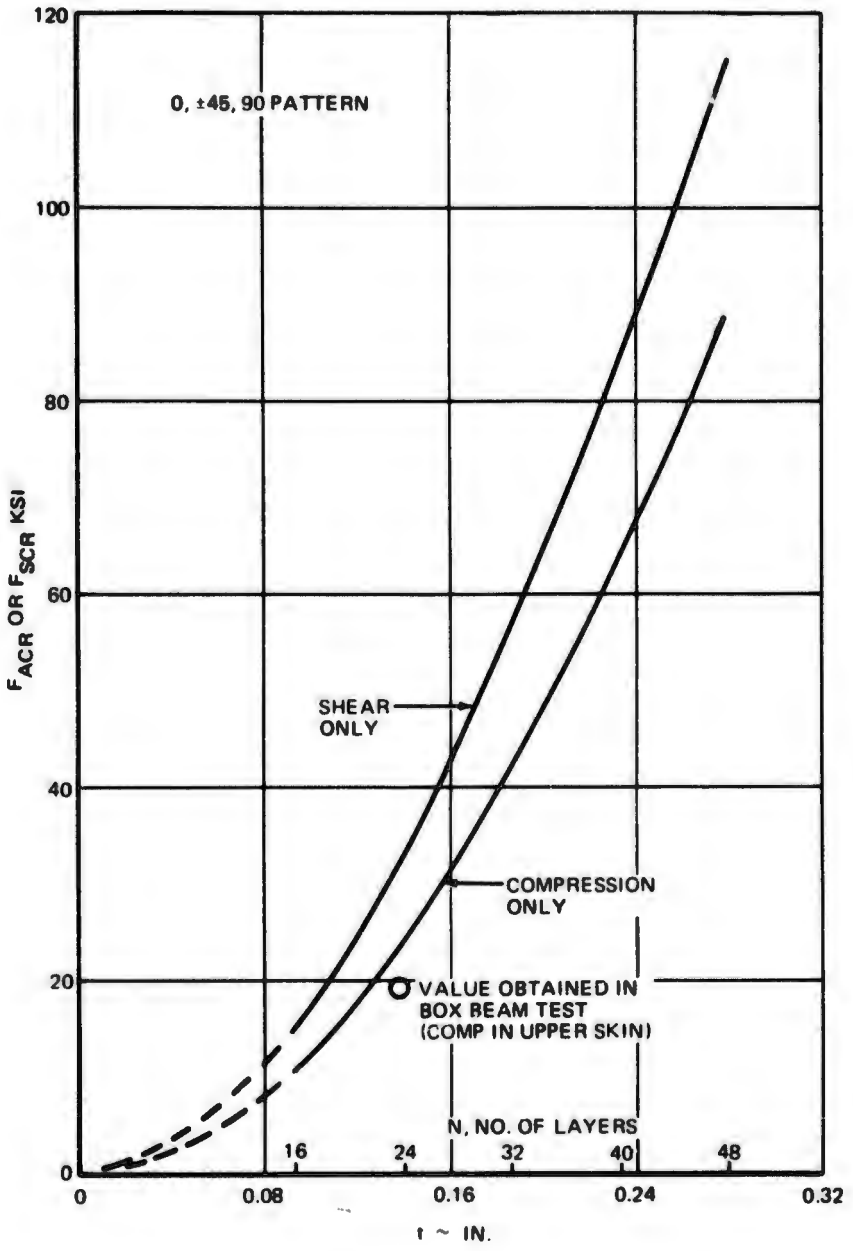

FIGURE 20. ALLOWABLE BUCKLING STRESS VERSUS PANEL THICKNESS

TABLE IV

COMPARISON OF BUCKLING STRESSES

NO. OF LAYERS	t	PANBUCK		ISOTROPIC	
		COMP.	SHEAR	COMP.	SHEAR
16	0.0928	10,644	14,760	11,000	14,700
24	0.139	23,690	32,430	24,000	33,100
32	0.186	41,400	55,800	44,000	58,800

Margins-of-Safety

A general stress analysis of all load resisting components and details in the stabilizer structure was completed during the current reporting period. The detailed calculations may be found in Reference 6. Significant results from this effort are sumarized in the list of critical margins-of-safety presented in Table V. Attention is directed to the margin-of-safety value for load condition F as given in the table. This margin is based on buckling of the upper panel which could result from the up-load associated with condition F. This load is opposite to conditions C and D where the down-load induces tension in the upper panel. The prevailing stress levels for condition F are less than one-half of the corresponding values for conditions C and D. Since the above referenced margin-of-safety is greater than 2, there is no possibility of a structural failure resulting from condition F and experimental verification is therefore considered unnecessary.

TABLE V
SUMMARY OF CRITICAL MARGINS OF SAFETY FOR GRAPHITE STABILIZER STRUCTURE

COORDINATE LOCATION (IN) x	COORDINATE LOCATION (IN) y	DRAWING NO.	DESCRIPTION	LOAD COND	TYPE OF STRESS	NET MARGIN OF SAFETY
94	20	Z3569978	ELEVATOR HINGE BRACKET	C	SHEAROUT	0.63
94	20	Z3569978	ELEVATOR HINGE BRACKET	C	BOLT SHEAR	0.24
94	20	Z3569978	ELEVATOR HINGE BRACKET	C	BEARING	0.53
100	20	Z3569978	REAR SPAR WEB	C	BEARING	0.77
100	20		REAR SPAR WEB	C	TENSION THROUGH HOLES	0.64
100	20		REAR SPAR WEB	C	SHEAR IN WEB	0.13
99	20		REAR SPAR FLANGE	C	SHEAR	0.41
99	20	Z3569976	TI DOUBLER	C	BEARING	0.49
99	20	Z3569978	ELEVATOR HINGE BRACKET	C	TENSION IN FLANGE	0.43
99	20	Z3569976	TI DOUBLER	C	TENSION	0.20
99	20	Z3569976	TI DOUBLER	C	BOND BETWEEN DBLR AND SKINS	0.87
94	40	Z2547222	BEARING ASSY-ELEV HINGE	C	BEARING STRENGTH	0.28
94	40	Z3569979	ELEVATOR HINGE BRACKET	C	BENDING AT SECTION A-A	0.16
94	40	Z3569979	ELEVATOR HINGE BRACKET	C	BOLT SHEAR	0.06
94	40	Z3569979	ELEVATOR HINGE BRACKET	C	BEARING	0.82
94	40	Z3569979	ELEVATOR HINGE BRACKET	C	SHEAROUT	0.38
100	40	Z3569979	ELEVATOR HINGE BRACKET	C	BOLT SHEAR	0.57
100	40	Z3569979	ELEVATOR HINGE BRACKET	C	BEARING	0.93
100	40	Z3569979	REAR SPAR WEB	C	BEARING	0.34
100	40	Z3569979	ELEVATOR HINGE BRACKET	C	TENSION THROUGH HOLES	0.25
100	40	Z3569979	REAR SPAR WEB	C	WEB SHEAR	0.21
101	40	Z3569979	ELEVATOR HINGE BRACKET	C	BOLT SHEAR	0.44
101	40	Z3569979	ELEVATOR HINGE BRACKET	C	TENSION AT HOLES	0.46
101	40	Z3569976	TI DOUBLER	C	TENSION AT HOLES	0.22
101	40	Z3569976	SHEAR ATTACH. BETWEEN RIB AND SPAR WEB	C	BOND SHEAR AT WEB	0.71
101	40	Z3569976	SHEAR ATTACH. BETWEEN RIB AND SPAR WEB	C	BOLT STRENGTH (FAIL SAFE)	0.59
101	40	Z3569976	SHEAR ATTACH. BETWEEN RIB AND SPAR WEB	C	BOND SHEAR AT RIB	0.32
101	40	Z3569976	SHEAR ATTACH. BETWEEN RIB AND SPAR WEB	C	STRENGTH OF CLIP	0.36
100	58	Z3569971	ELEVATOR HINGE BRACKET AND RIB	C	BOLT SHEAR	0.30
107	58	Z3569971	ELEVATOR HINGE BRACKET AND RIB	C	BEARING IN SKIN	0.16
94	58	Z3569971	ELEVATOR HINGE BRACKET AND RIB	C	BEARING IN LUG	0.40
96	58	Z3569971	ELEVATOR HINGE BRACKET AND RIB	C	TORSION INH SECT OF BRKT	0.18
96	58	Z3569971	ELEVATOR HINGE BRACKET AND RIB	C	WEB SHEAR (IN BRACKET)	0.40

TABLE V
SUMMARY OF CRITICAL MARGINS OF SAFETY FOR GRAPHITE STABILIZER STRUCTURE (CONT)

COORDINATE LOCATION (IN)		DRAWING NO.	DESCRIPTION	LOAD COND	TYPE OF STRESS	NET MARGIN OF SAFETY
x	y					
134	0-5	Z5569966	PIVOT POINT FITTING	C	BOLT SHEAR	0.37
134	5-(-5)	Z5569966	PIVOT POINT FITTING	C	BEARING IN SKIN AND CANT RIB	0.60
134	5-(-5)	Z5569973	UPPER SKIN PANEL	C	STRESS FIELD IN SKIN PANEL	0.10
134	5-(-5)	Z5569973	UPPER SKIN PANEL	C	SHEAROUT AT HOLES	0.43
99	0	5547524	ACTUATOR FITTING	C	BOLT SHEAR	0.15
101	0	Z5569973	UPPER SKIN PANEL AND RIB	C	BEARING AT BOLTS	0.28
101	0	Z5569973	UPPER SKIN PANEL AND RIB	C	TENSION AT HOLES	0.49
101	0	Z5547524	ACTUATOR FITTING RIB	C	BOLT SHEAR	0.18
135-152	7-25	Z5569975-13,-14	SKIN PANEL	E	BUCKLING OF SKIN	0.18
135-152	7-25	Z5569975-33,-35	L.E. SPAR WEB	E	BUCKLING OF WEB	0.37
135-152	7-25	Z5569975-33,-35	L.E. SPAR WEB	C	WEB RIVETS	0.20
135-152	7-25	Z5569975-33,-35	L.E. SPAR WEB	E	SHEAR IN WEB BOND	0.68
152	7	Z5569975-35	L.E. SPAR WEB	E	SHEAR IN BOND AT ATTACHMENT TO RIB	0.18
135	25	Z5569975-33	L.E SPAR WEB	E	LOAD IN BOLTS	0.39
135	25	Z5569975-33	L.E. SPAR WEB	E	BEARING IN –33	0.47
135	6	Z5569975-17,-19	STA 5 RIB	E	SHEAROUT AT BOLT	0.10
135	5-15	Z5569973	UPPER SKIN PANEL	E	TENSION IN SKIN	0.67
135	6	Z5569975-17,-19	STA 5 RIB CAPS	E	TENSION AND COMP	0.43
135-140	6	Z5569975-17,-19	STA 5 RIB	E	BUCKLING OF WEB	0.14
135	6	Z5569975-17,-19	STA 5 RIB	E	BEARING IN –17 AND –19	0.72
135-152	7-22	Z5569975-13,-14	SKIN PANELS	E	BENDING	0.22
135-152	8	Z5569975-13,-14	SKIN PANELS	E	BENDING	0.27
136	7-22	Z5569975-13,-14	SKIN PANELS	E	BENDING	0.18
100-107	32-40	Z5569974	SKIN PANELS	C	BUCKLING	0.30
112-118	20-26	Z5569974	SKIN PANELS	C	BUCKLING	1.04
133-135	7-11	Z5569974	SKIN PANELS	D	BUCKLING	1.53
118-124	20-26	Z5569973	SKIN PANELS	F	BUCKLING	2.24
135	15-20	Z5569970	SPAR WEB	D	BUCKLING	0.31
133-135	-6	Z5569973	SKIN PANEL	D	TENSION	0.10
133-135	5-6	Z5569974	SKIN PANEL	D	COMPRESSION	0.38
135	5-6	Z5569970	ATTACH ANGLE	D	TENSION	0.02
133-135	5-6	Z5569973	SKIN PANEL	C	TENSION	0.19
133-135	5-6	Z5569973	SKIN PANEL	C	BOLT BEARING	0.25
100-102	–3	Z5569973	SKIN PANEL	C	BOLT BEARING	0.09
119-123	38-40	Z5569973	SKIN PANEL	C	TENSION	0.19
119-123	38-40	Z5569973	SKIN PANEL	C	BOLT BEARING	0.18
110	38-40	Z5569973	SKIN PANEL	C	BOLT BEARING	0.42

SECTION 3

MANUFACTURING DEVELOPMENT

All fabrication and assembly tools for the stabilizer and leading edge structures were completed during the reporting period. The stabilizer laminated details were laid-up and cured against high temperature plastic laminating molds (PLMs) which were supported on welded steel reinforcing structures. Although care was exercised during tool design to match expansion characteristics of the tool components, some difficulty was encountered due to mold distortions under curing conditions of 350°F temperature and 100 psi pressure. Mold surface porosity was also a problem during the high-pressure cure cycles. Corrective actions for these problems are described in the following discussions.

Stabilizer unit one was completed and sent to NADC for vibration and static tests. The substructure for stabilizer unit two was completed at Rohr and sent to Douglas for inclusion in the fatigue test article. The second substructure was completed using essentially the same techniques described previously (Reference 1) for stabilizer unit one. The fabrication and assembly of the stabilizers are discussed in this section. Detailed fabrication procedures for substructure machining, attach-angle bonding, and final assembly are included in Appendix D.

STABILIZER UNIT ONE

Detail fabrication and final assembly for stabilizer unit one were completed during the reporting period. After the skin panels were laminated and cured, the substructure was machined to precise contour to match the inner profiles of the skin panels. The skin panels were then located and bonded to the substructure. The fittings, leading-edge assemblies, and attaching hardware were installed in an assembly jig to complete the structure.

Skin Panels

Both upper and lower skin panels were laid-up and cured on the same tool since the aerodynamic contours of both upper and lower surfaces are identical. The plastic laminating mold Z5569973-1PLM1 female layup and bond tool, Figure 21, was completed using high temperature epoxy laminates in the mold surface. The reinforcing structure was fabricated of welded steel framework which was attached to the under surface of the epoxy laminate for rigidity. After several test bond-cycles (both heat and pressure) it was noted that the steel reinforcing structure developed a permanent set that distorted the tool surface. The reinforcing structure was cut free in several locations and the tool surface returned to original contour. The tool was reworked using welded clips clamped to the mold surface and allowed lateral motion of the surface relative to the support frame without distortion of the contour.

The skin panels were laminated using mylar templates as cutting patterns for the graphite prepreg plies. The completed layups were double bagged with one bag over the tool surface to eliminate tool porosity and the other

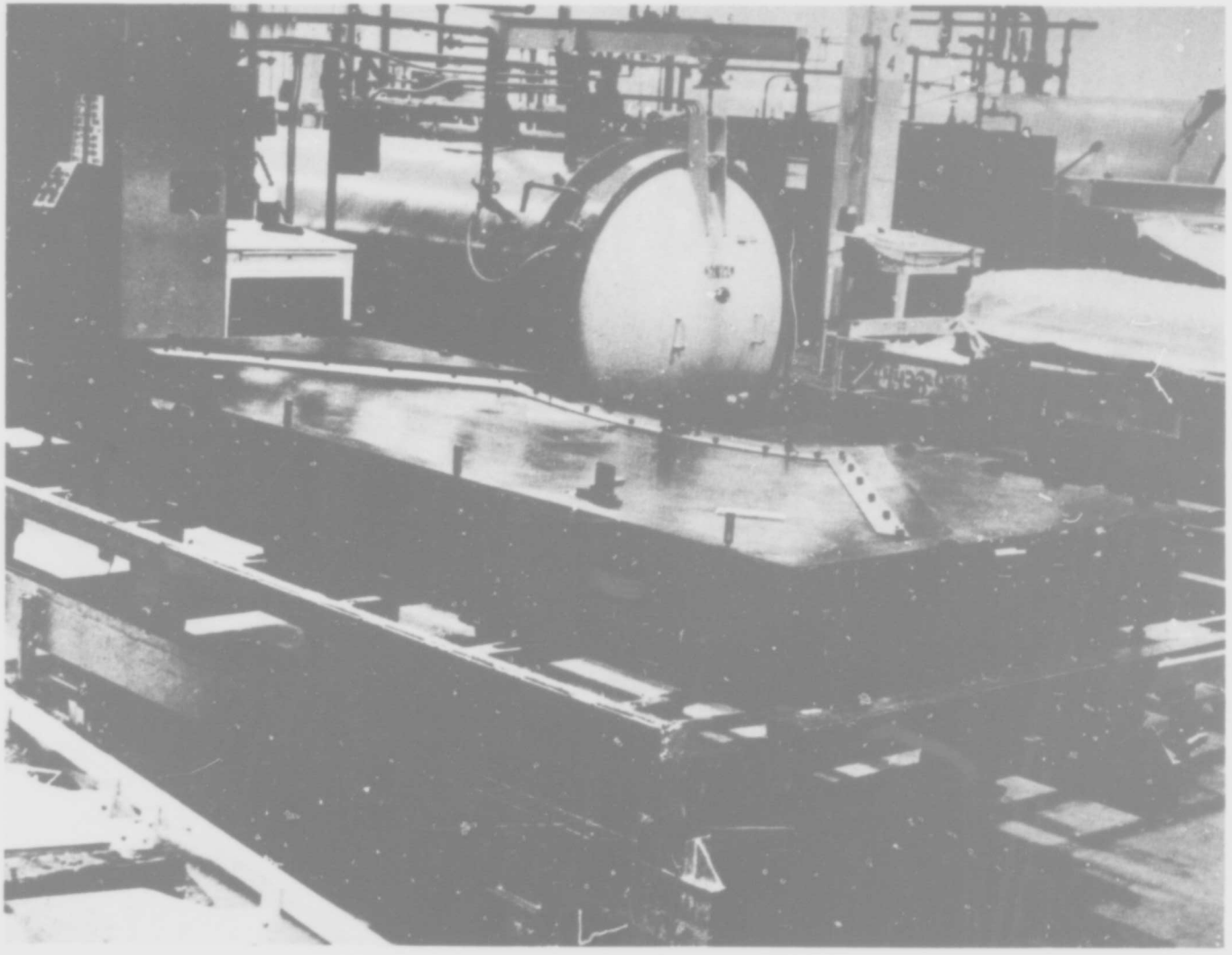

FIGURE 21. PLASTIC LAMINATING MOLD FOR GRAPHITE SKIN PANELS

bag over the layup. The cure cycle required the release of vacuum when the pressure reached 100 psi but the vacuum at the mold surface was maintained to keep the part pressed against the tool. After curing, the graphite skin laminates were trimmed using air routers and 0.25 inch diameter medium diamond pattern carbide bits running at approximately 12,000 rpm. Dry cutting was accomplished in one pass at a feed rate of 6 to 7 inches per minute through laminate varying in thickness from 0.144 to 0.288 inch. Trim locations were established by router templates which were indexed to the laminates by means of coordinated tooling holes.

After the trim operation, the skin panels were examined using ultrasonic, C-scan and X-ray nondestructive test (NDT) techniques. The NDT indicated several areas of porous or low-resin laminates near the elevator hinge doublers and along the built-up area near the aircraft centerline. The NDT techniques and results are discussed in Appendix C.

Substructure Machining

The upper and lower edges of the substructure assembly, including the flanges of the rear-spar and cant-ribs, were machined to contour using a profiling setup, Figure 22. The plaster profile templates were cast directly against the inner surfaces of the graphite skin panels. The manufacturing plan originally called for obtaining the plaster templates from the skin panels while the latter were installed in the PLM. However, the PLM was not deemed suitable after the previously mentioned contour checks, so the plaster templates were made using an exact cast taken from the master tooling. The skin panels and plaster templates were held against the cast using vacuum pressure so that minor distortions of the skin panels were removed. The plaster templates were reinforced with standard metal tubular base structures.

The substructure, holding fixture, and the plaster templates were optically aligned at three master tooling points and clamped to the bed of the Rockford machine as shown in Figure 22. The machine operator traced the contour of the plaster template with the machine stylus as shown in Figure 23. The substructure attach-angles and honeycomb webs were machined at a rate of 6 to 12 inches per minute with a 1/4 inch diameter diamond-stem router rotating at 3600 rpm. The honeycomb panel faces were machined individually as shown in Figure 24 without the use of a cutting fluid. A 1/2 inch diameter, two-flute carbide end-mill was used to machine the solid laminate front-spar web, the rear-spar flanges, and the cant-rib flanges. Critical flange thickness dimensions were monitored during machining to limit the depth of cuts. The machine cutter accurately reproduced the inner contour of the skin panel at the mating surface of the substructure. After machining, the total indicated dimensional variation across the length of the cant-ribs was within 0.020 inch.

The substructure was removed from the holding fixture, inverted, and relocated in the holding fixture on the Rockford machine with the lower surface up. The same setup and machining operations were performed on the substructure lower surfaces. The machined substructure was inspected and certified, then removed from the Rockford and prepared for attach angle bonding.

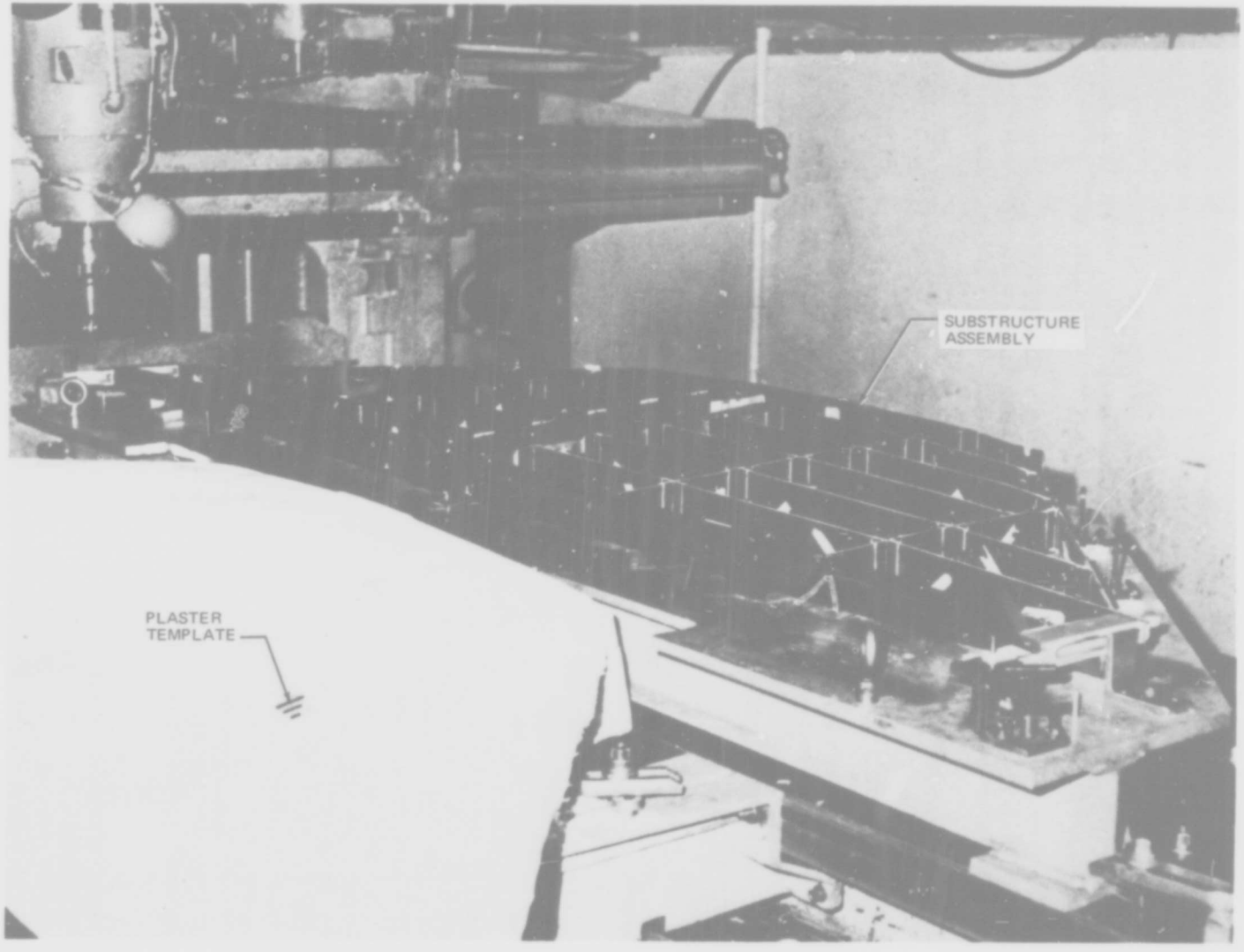

FIGURE 22. CONTOUR MACHINING SETUP FOR SUBSTRUCTURE ASSEMBLY

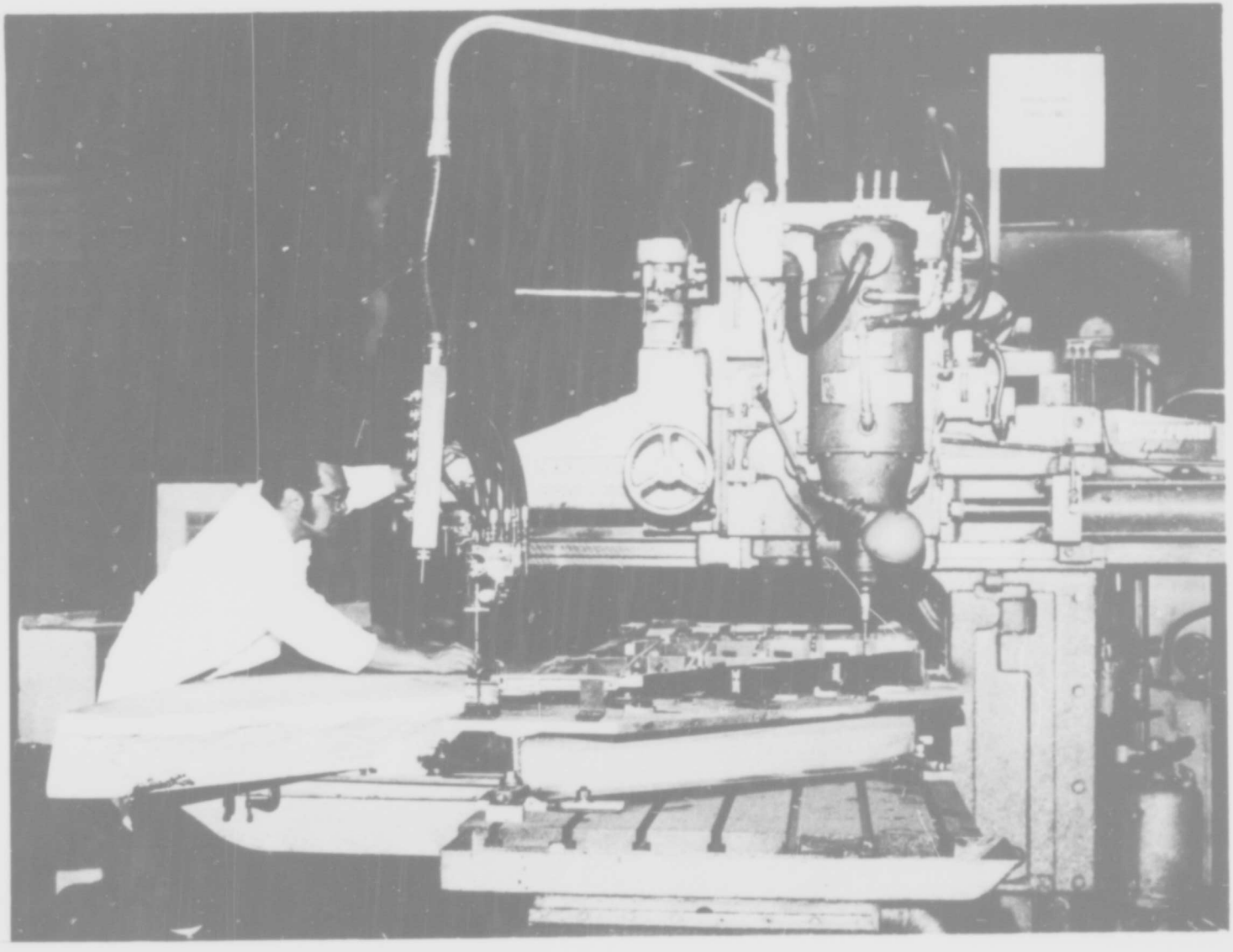

FIGURE 23. SUBSTRUCTURE MACHINING OPERATION

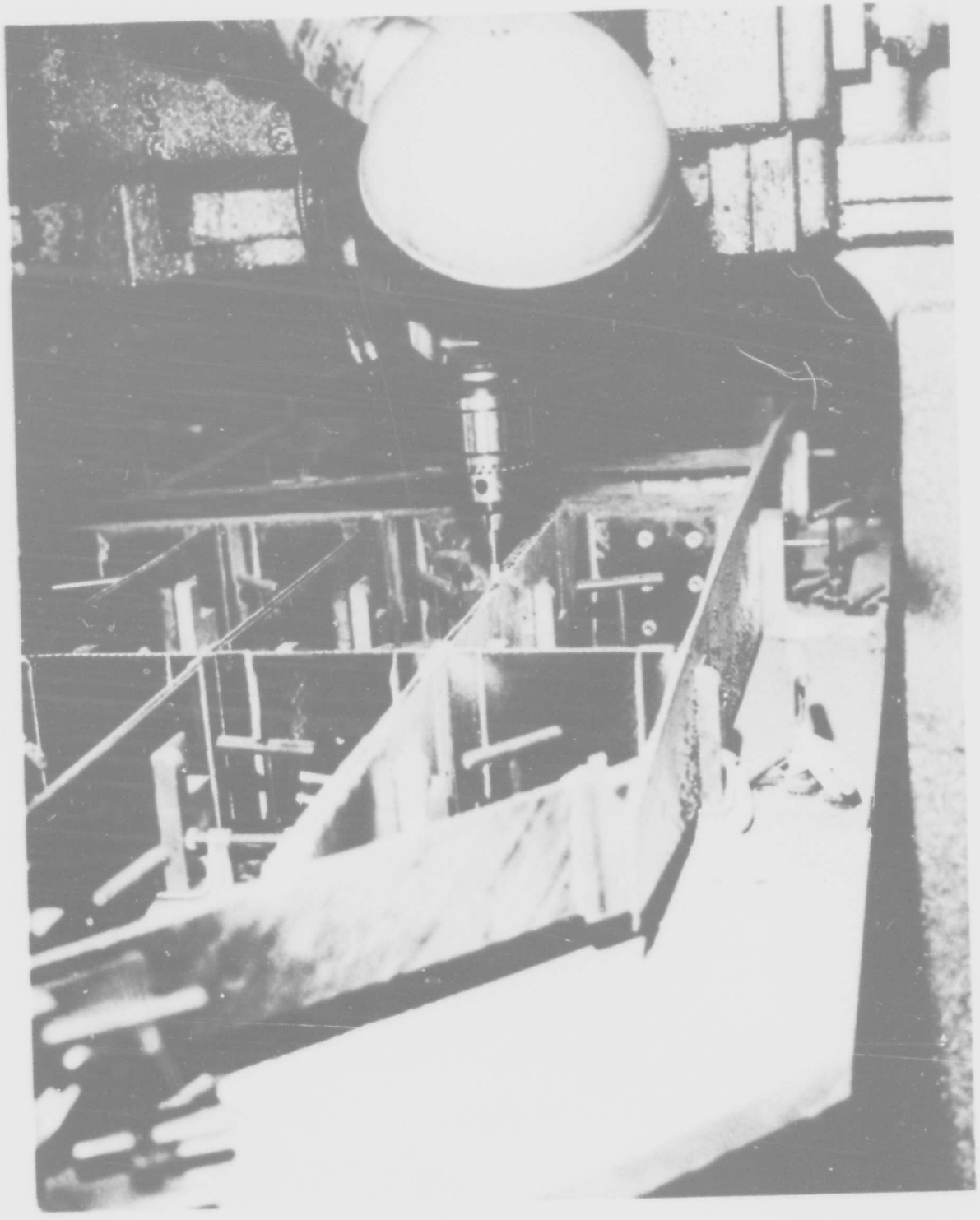

FIGURE 24. SUBSTRUCTURE HONEYCOMB PANEL MACHINING WITH DIAMOND STEM-ROUTER

Assembly Bonding

After the upper and lower skin panels were cured, extensive rework of the PLM was accomplished to insure that proper contour was maintained while curing the substructure attach-angles to match skin contour. The PLM was re-laminated with a continuous reinforcing flange around the edges and an extensive backup structure of fiberglass laminate rather than steel. Some improvement was also noted in the surface porosity of the tool.

The attach-angles for the bond of the upper skin panel to the substructure were laminated and densified in preparation for the co-cure and bond operation. After densification, the angles were cut to length and stored under refrigeration until used. The substructure was cleaned by hand-sanding and located on the upper skin panel in the PLM. A layer of 5 mil teflon film was placed between the skin panel and the substructure to preclude bonding to the skin during the attach-angle cure and bond cycle. An epoxy fillet to control the bend-radius of the attach-angles was swept into the corners at the junctions between the substructure and skin panels as shown in Figure 25. The upper attach-angles were then applied to the substructure/skin bond assembly in accordance with the fabrication procedure (Appendix D). The attach-angles, edge-dams, glass stripper ply, Armalon and Mockburg bleeder paper were applied as shown in Figure 26. A teflon film seal was also applied to the layup before the silicone-rubber pressure bag was installed and sealed.

At a critical point in the cure cycle (280°F and 50 psi) the silicone rubber pressure bag failed at a bonded seam and autoclave pressure was lost. At that time, the resin was about to gel and there was insufficient time to open the autoclave and reseal the bag. Thus, the cure cycled was continued to completion without pressure. The resulting angles were low-density, high-void laminates with approximately half the required strength properties and were therefore rejected.

The rejected attach-angles were removed from the substructure using a trim, disk-sand, and final hand-sand technique developed during rework of the I-beam specimens (see Section 1). All the defective graphite was removed, but most of the Narmco 329 adhesive layer was left on the substructure. This adhesive layer was properly cured and of excellent quality. The thickness of this adhesive layer (about 0.007 inch) minimized sanding damage to the substructure sandwich facings during the salvage operation.

After repair of the silicone rubber bag, the replacement attach-angles were laid-up and vacuum bagged. Just prior to positioning the silicone rubber bag, all interior corners of the substructure assembly were filled with leather fillets with a one-half inch concave-radius as shown in Figure 27. The fillets eliminated the deep corners in the substructure cavities and reduced the amount of elongation required from the silicone rubber. The bagged assembly was placed in the autoclave and cured under the standard heat and pressure cycle. The resultant angles and bond were of acceptable quality as shown by the in-process quality control tests, Appendix C. The silicone rubber bag developed leaks four times during the early part of the cure cycle (prior to the gel-point) and each time the autoclave was opened and the bag repaired. It became apparent that the failures occurred in the

FIGURE 25. EPOXY FILLET AT JUNCTIONS OF SUBSTRUCTURE AND SKIN PANEL

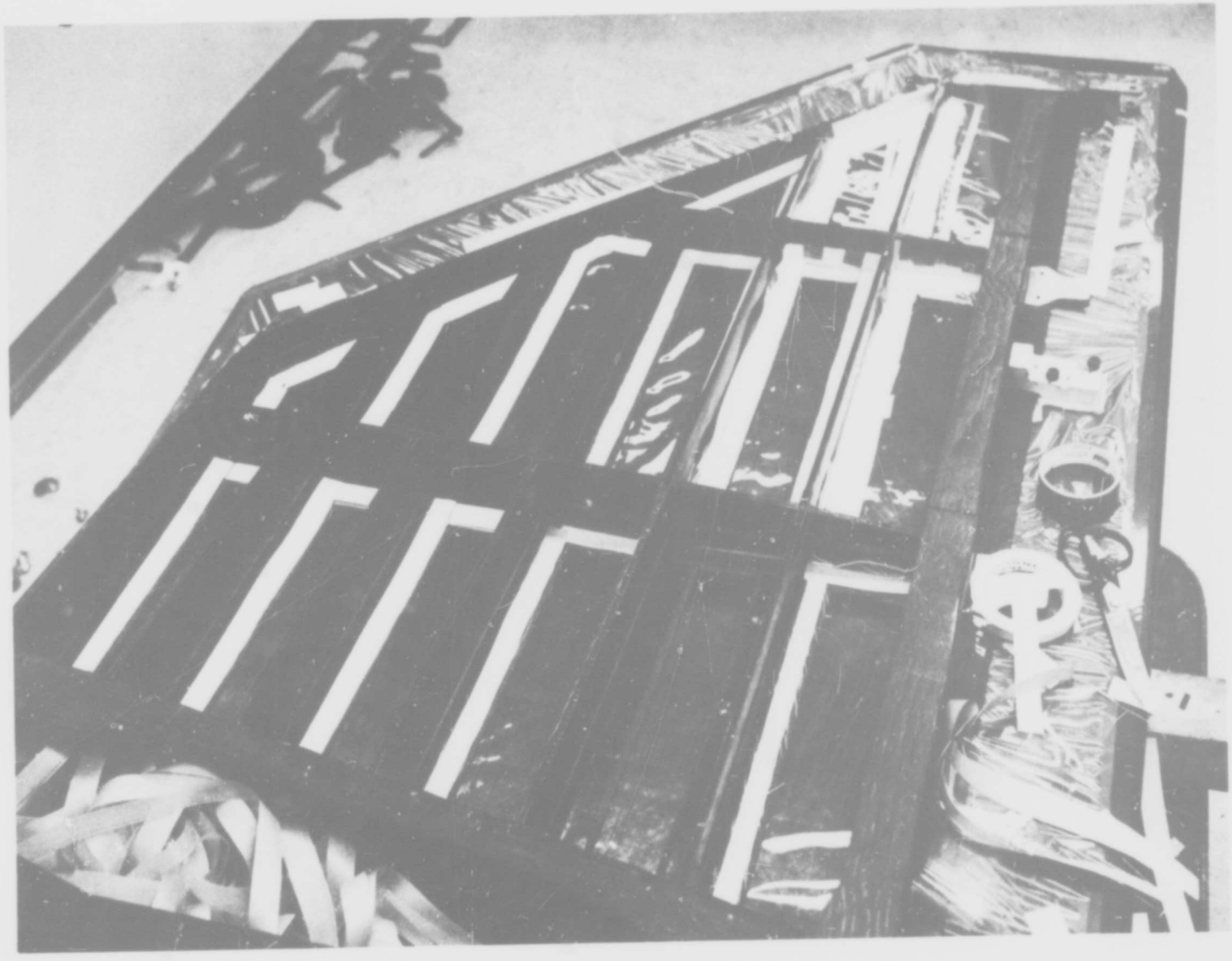

FIGURE 26. PREPARATIONS FOR ATTACH-ANGLE BOND CYCLE

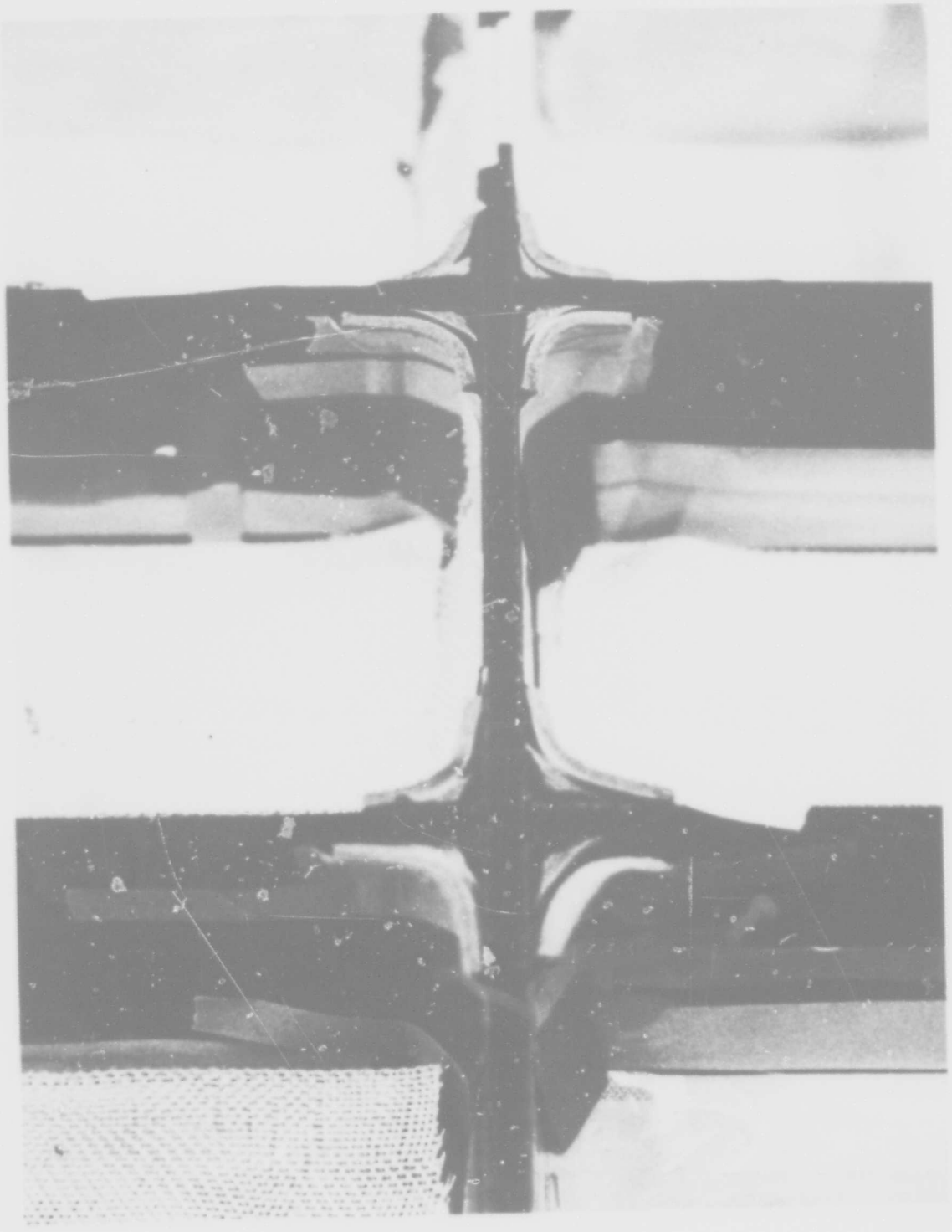

FIGURE 27. CORNER FILLETS FOR SILICONE RUBBER PRESSURE BAG

cavities where excessive stretch (about 3/4 inch) was designed into the bag to prevent wrinkling of the attach-angles.

The lay-up and vacuum-bagging of the lower attach-angles were accomplished using the same procedure as the upper attach-angles except the bond to the lower skin panel was included and the silicone rubber pressure bag was replaced by a large sheet of conventional nylon bag material. The nylon was carefully hand formed into each cavity. The nylon bag developed leaks three times early in the cure cycle but was easily repaired and the cycle was successfully completed.

After completion of the attach-angle bond cycles, 34 strain-gages were bonded to the structure in accordance with the test-plan (31 three-channel rosettes and three single-channel axial gages), Reference 1. Wiring from the internal gages (37 channels) was fed through the tooling holes to terminal strips aft of the rear spar.

Hole Preparation

After completion of the strain-gage installation, the structure was installed in the assembly jig (AJ). Approximately 1500 holes were piloted, drilled, reamed, and countersunk in the upper and lower skin panels, attach-angles, brackets, fittings, and the rear-spar. The pivot, actuator, and elevator hinge bracket fittings were located on the stabilizer in the assembly jig, and all pilot holes were drilled through the fitting flanges and the corresponding composite parts.

After curing the upper and lower attach-angles, the Armalon separator film and the Mockburg bleeder plies were left in place on the cured attach-angles. These plies served as back-up members during the drilling operations and minimized splintering of the graphite laminates due to drill break-out. The inner surface of the upper skin panel and the inner surfaces of the cant-ribs and rear-spar were similarly protected with a layer of peel ply covered with a bleeder cloth impregnated with a room temperature curing epoxy resin. After the drilling operations, the peel plies and bleeder cloths were stripped-off and the excess resin was scraped from the inner surface of the skin panel using carbide deburring tools. The excess resin was completely removed without damage to the graphite-epoxy laminate.

The drilling, reaming, and countersinking operations were accomplished with the structural bond assembly installed in the AJ as shown in Figure 28. A drill-jig, Figure 29, was used to locate the lower surface fastener holes. The drill-jig was indexed to the skin panel using coordinated tooling holes and then "C" clamped in place as shown in Figure 29.

The position of the drill-jig was initially checked by drilling number 30 (0.128 inch diameter) pilot holes at selected locations and verifying the hole locations with respect to the attach-angles and substructure webs. A drill table was used to maintain the hole center-line normal to the skin contour. When the drill-jig was properly positioned, all hole locations were piloted with a number 30 drill at 2700 rpm. The holes were then enlarged with a 3/16 inch diameter carbide drill and finished to the required size with a piloted 0.1895 inch diameter reamer in a 450 to 600 rpm airmotor. An offset bushing was used to realign any pilot hole which was too close to the attach-

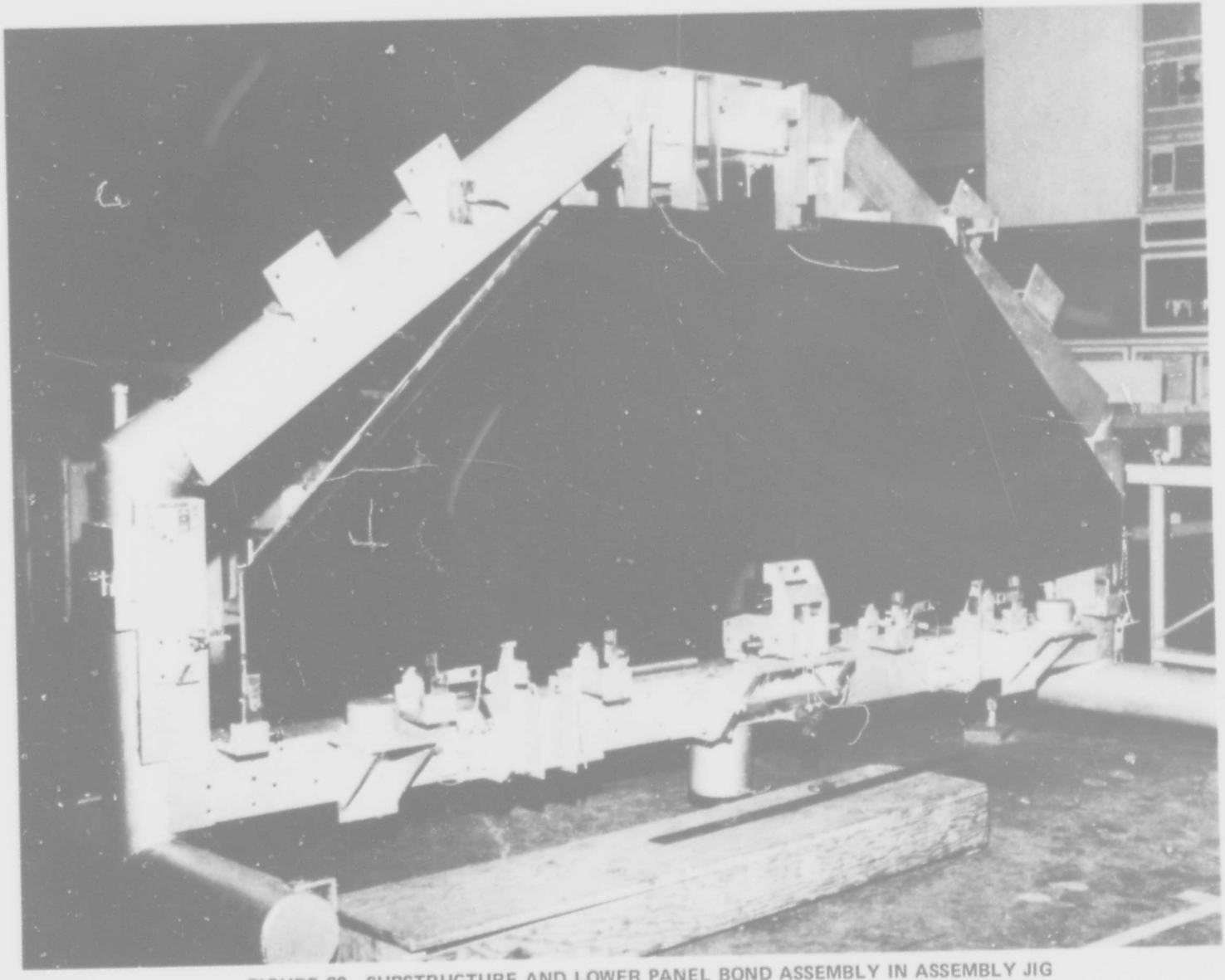

FIGURE 28. SUBSTRUCTURE AND LOWER PANEL BOND ASSEMBLY IN ASSEMBLY JIG

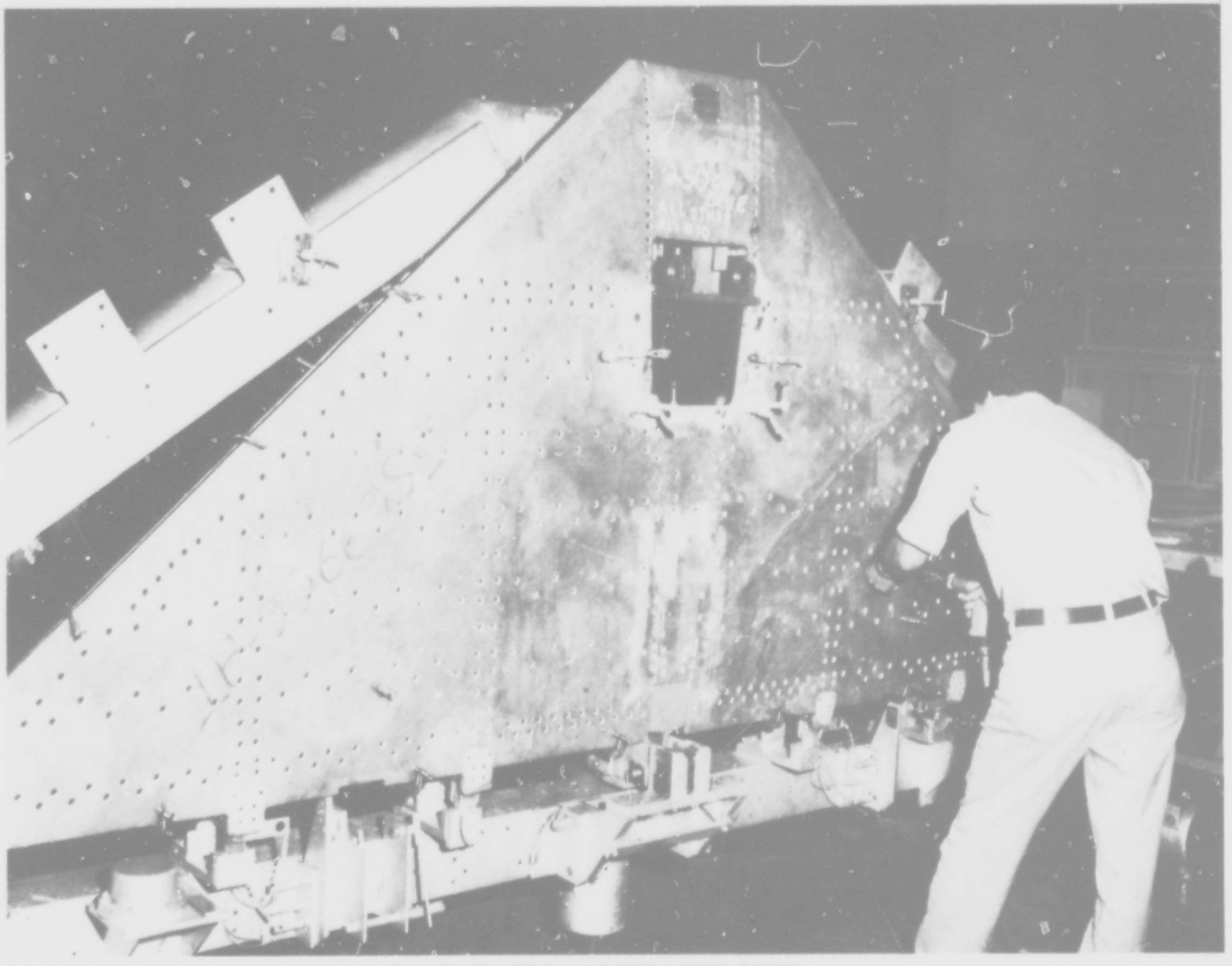

FIGURE 29. DRILL JIG FOR LOWER PANEL

angle corner radius or to the flange-edge. All hole drilling, reaming, and countersinking on the final assembly was performed without a cutting fluid.

The upper skin panel and attach-angles were drilled using a thin translucent fiberglass-epoxy hole template made from the master plaster pattern. The template was first checked against the attach-angles since the drilling operation was blind when the upper skin panel was in place. After verifying that the upper attach-angle hole pattern satisfied design requirements, the stabilizer was removed from the assembly jig and placed on a work bench. The skin panel was indexed to the template and clamped in place as shown in Figure 30. The upper surface holes were piloted, drilled, and reamed in the same manner as the lower surface holes.

All holes for flush fasteners were countersunk in a two-step operation. The countersinks were started with a piloted 3-flute high-speed steel cutter, and finished with a piloted 2-flute carbide cutter. The two-step operation was necessary because the outer surface of the graphite-epoxy skin chipped if the countersinking was started using a 2-flute cutter. The operation could be accomplished in one-step using a carbide cutter with 3 or more flutes.

The pivot fitting was jig located while the upper panel was properly indexed to the substructure bond assembly. A special pivot fitting drill plate was indexed to the drill-jig as shown in Figure 31. The pivot fitting flanges and the mating skin panels were piloted, drilled, and reamed to size using the drill plate to locate the holes. The stabilizer actuator fitting at the rear-spar centerline was also jig located. The attach holes were drilled and reamed full-size using pilot holes in the fitting to locate the holes.

Leading-Edge

The laminating molds for the leading edge skins also indicated some porosity during 100 psi cure cycles. The Z5569975-13 and -14 panels (see Reference 1) were fabricated using the double bagging technique to eliminate porosity. A unique method was used to seal the mold for the -27 skins since the double bagging technique could not be used because of the more severe contour. A male thix-fiber cast was made from the female mold and subsequently polished and prepared with a layer of release film. The female mold was sandblasted and liberally coated with a high temperature epoxy resin filler (Fiberesin 1445). The thix-fiber cast was then forced into position and the resin was cured on the female mold surface. The excess air and resin flowed out during the cure cycle and the resultant tool surface was smooth and free of porosity. Detail tools for the leading edge support structure (i.e., ribs and channels) were machined from aluminum alloy stock and therefore did not present a porosity problem.

The leading-edge honeycomb sandwich details (-13 and -14) were fabricated using Scotchply 1009-26s fiberglass epoxy skins. The outer skin was precured for aerodynamic smoothness and secondarily bonded to the honeycomb core. The inner skin was laminated in place over the honeycomb and co-cured and bonded in a single cure cycle. Two adhesive systems (Metlbond 329 and Hysol EA951) were considered for the honeycomb bonding. These adhesives were evaluated using small sandwich panel flexural and flatwise tension specimens fabricated using the same processes planned for the -13 and -14 panels. The

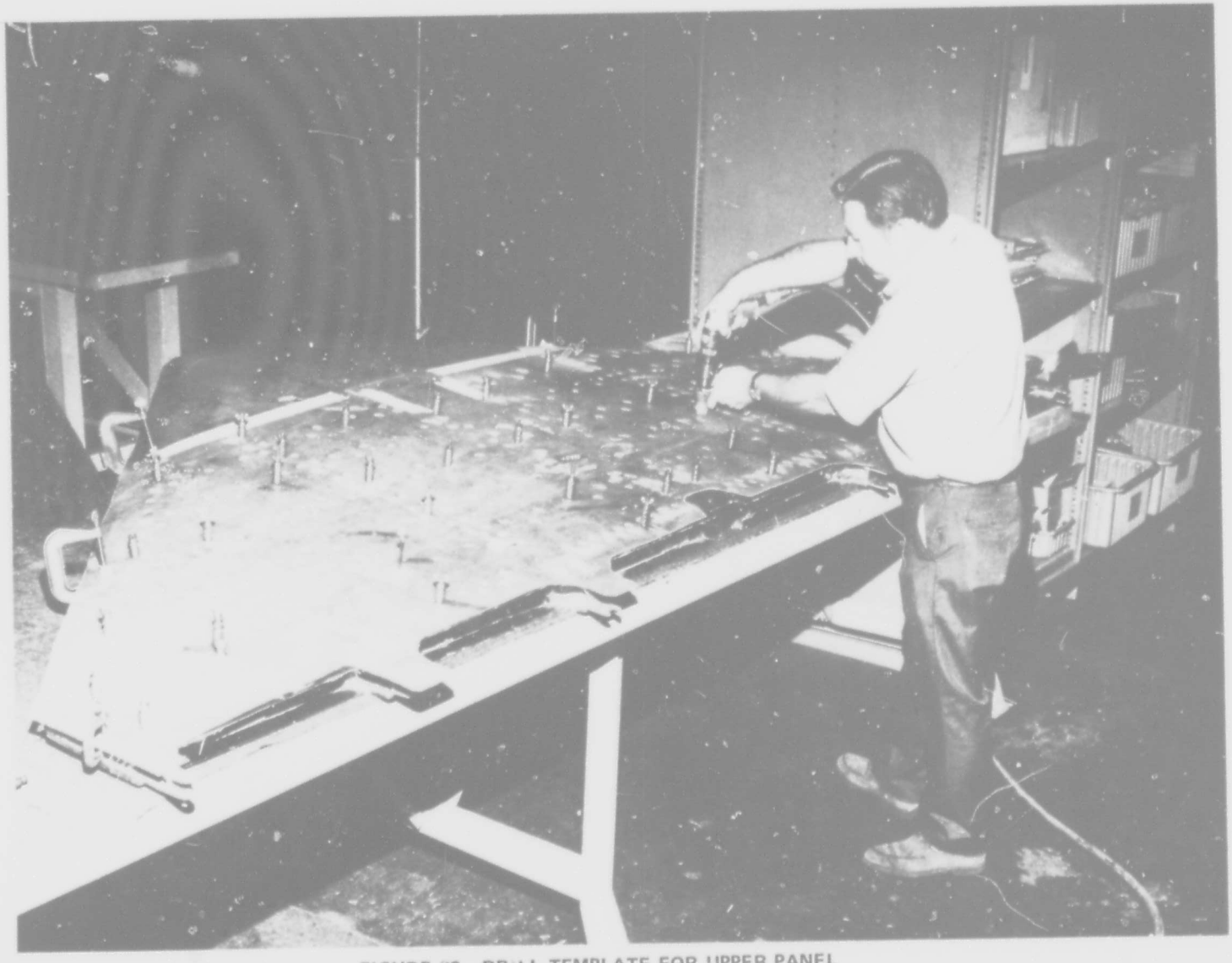

FIGURE 30. DRILL TEMPLATE FOR UPPER PANEL

FIGURE 31. DRILL PLATE FOR PIVOT FITTING

Metlbond 329 adhesive system was selected for this bonding operation. Although the skin to core tensile strength was slightly lower, the Metlbond 329 specimens were significantly stronger in flexural strength. The Metlbond 329 film also had excellent "tack" and therefore offered better handling properties for the sandwich construction. The balance of the laminated fiberglass details for the leading-edge installation were fabricated using the appropriate fabrication procedures (see Reference 1).

Final Assembly

The final assembly operations consisted of bonding the internal nutplates, installing and bonding the upper skin panel, attaching the pivot, actuator, and hinge bracket fittings, and locating and installing the leading-edge components.

The internal nutplates were bonded to the structure using EA951 adhesive film. After cleaning, the nutplates and adhesive were secured in position against the structure with spring-loaded Cleco-clamps. The structural bond assembly was then secured on the PLM and the nutplate adhesive was cured in a circulating air oven for two hours at 350°F.

On completion of the nutplate adhesive bond cycle, the Cleco-clamps were removed from the structural bond assembly and a fit-check was conducted to determine the gap between the inner profile of the upper skin panel and the mating attach-angles. The gap was determined by effecting a skin panel fit-up against a layer of room-temperature curing silicone rubber contained between two teflon films. After curing, the rubber layer was removed and carefully measured with a micrometer to determine the uniformity of the gap. The rubber thickness was constant within 0.015 inch in all but two regions of the planform area. These two regions were near the forward ends of the two cant-ribs. Special graphite-epoxy shims varying in thickness from zero to 0.030 inches were prepared for these two regions. The rest of the planform area was mapped to indicate regions where more than one layer of adhesive film was required during the skin panel bond-cycle.

The faying surfaces of the upper attach-angles, cant-ribs, and rear-spar and the inner surface of the upper skin were prepared for bonding and the surfaces were primed with Hysol ADX228 adhesive primer. The primer was dried in a circulating air oven for one hour at 250°F. A number of internal nutplates debonded during the fit check were also repaired during this oven cycle. These nutplates were cleaned and relocated using Cleco-clamps and Hysol EA9306, a 250°F curing adhesive. Hysol EA951 adhesive film was then applied to the faying surface of each upper surface attach flange for the rear-spar, cant-ribs, and attach-angles. Additional local layers were cut and fit in appropriate areas identified during the fit-check.

The upper skin was carefully located on the substructure to avoid displacing the adhesive film. The upper skin fasteners were then installed and torqued to the required value. During the fastener installation, several additional nutplates were unbonded. (The screws at these locations were subsequently replaced with Jo-Bolt blind fasteners after the skin bond was effected). The stabilizer assembly was located on the PLM and the tool and bond assembly were placed in a circulating air oven pre-set to 350°F. After 15 minutes the

stabilizer was removed from the oven and the fasteners were re-torqued. The stabilizer was then returned to the oven and the adhesive was cured for two hours at 350°F. After curing, the bond was tested nondestructively using a Fokker bond tester and ultrasonic testing techniques. The NDT results are discussed in Appendix C.

The structural bond assembly was returned to the AJ and the tooling pins were installed through the station 58.187 hinge brackets. The station 20.000 and 40.000 hinge bracket fittings and the pivot and actuator fittings were also jig located. The attaching hardware was installed in the previously prepared holes in accordance with the engineering drawing.

The leading-edge structure was also built-up in the AJ against contour boards which controlled the external dimensions. The Z5569975-13 and -14 panel assemblies were installed against the contour boards and the supporting members (e.g., the -17 and -19 rib assembly and the -33 and -35 channel assembly) were located. The latter members were designed as two piece assemblies for tolerance take-up at the lofted surfaces. Rivet hole patterns were drilled through the rib and channel details and the parts were subsequently bonded with a cold-set adhesive and riveted together (see Figure 32).

The -27 leading-edge caps were placed in a special drill and trim jig and pilot holes were drilled for attachment to the panel assemblies and the graphite-epoxy stabilizer skins. The outboard ends of the leading-edge caps were trimmed net, but the inboard edges were left oversize as shown in Figure 33 to allow final trimming on assembly.

The leading edge caps and panel assemblies were relocated on the stabilizer in the AJ as shown in Figure 33. A drill table and bushing were used to align and drill the -27 leading-edge cap pilot hole pattern through the -13 and -14 leading-edge and the graphite-epoxy stabilizer skins. The holes were drilled, reamed, and countersunk to design requirements. The inboard edges of the -27 leading-edge caps were measured and marked for final trim. The leading-edge cap and panel assemblies were removed from the AJ and prepared for final assembly by removing peel plies and cleaning. The leading-edge components were finally assembled into the Z5569975-3 and -4 inboard and the -5 and -6 outboard leading-edge assemblies which were installed on the structure to complete the stabilizer as shown in Figure 34.

STABILIZER UNIT TWO

The substructure assembly for stabilizer unit two was completed at the Rohr Corporation using essentially the same techniques employed for unit one. A drawing change was issued on completion of stabilizer unit one to correct minor dimensional errors and to facilitate bonding of acute and obtuse attach-angle pairs. The change required revisions to the detail planning paper and bonding tools for the affected parts. Fabrication and assembly of the second substructure are discussed in this section under the headings Detail Part Fabrication and Substructure Assembly.

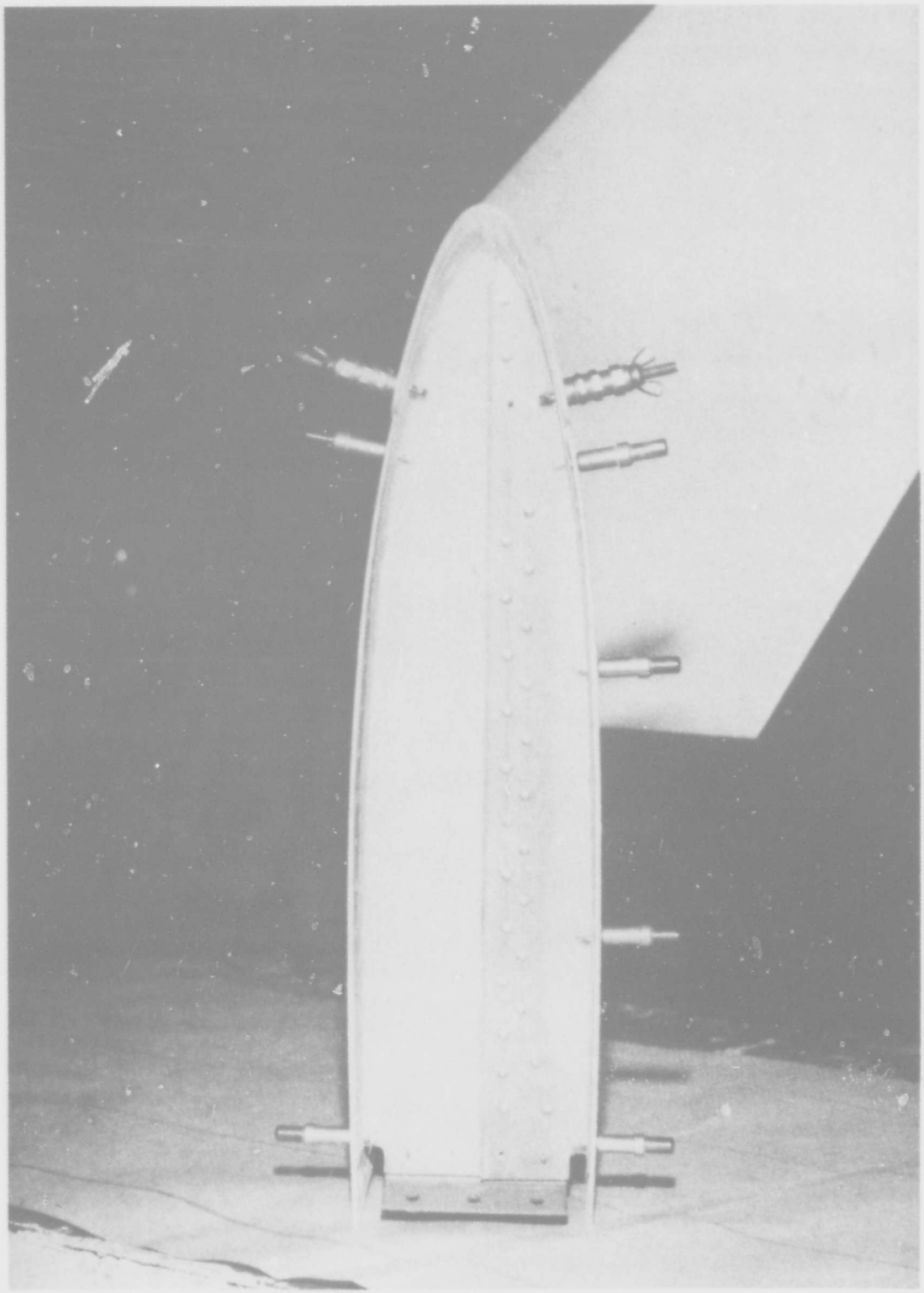

FIGURE 32. LEADING-EDGE TWO-PIECE RIB ASSEMBLY

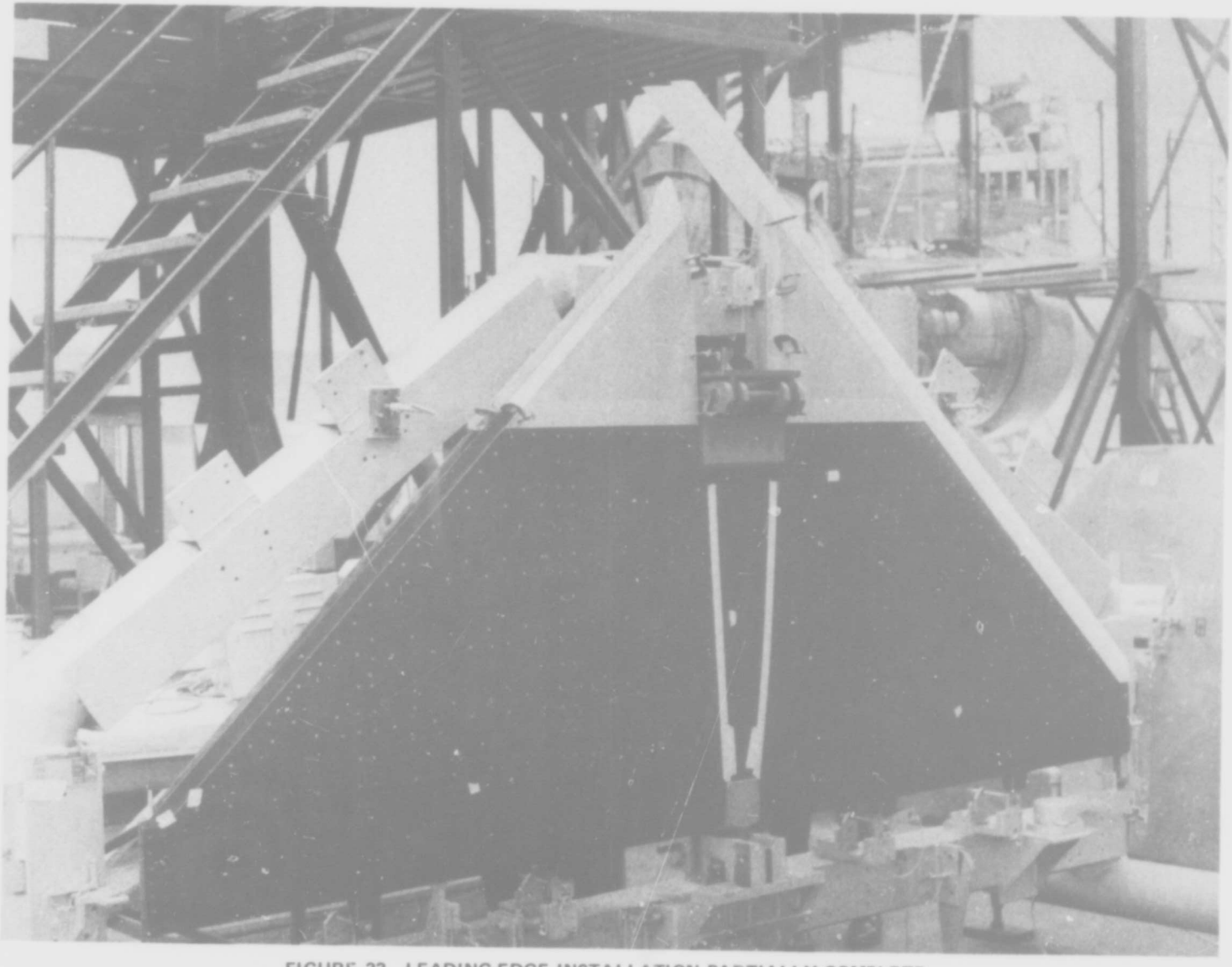

FIGURE 33. LEADING-EDGE INSTALLATION PARTIALLY COMPLETE

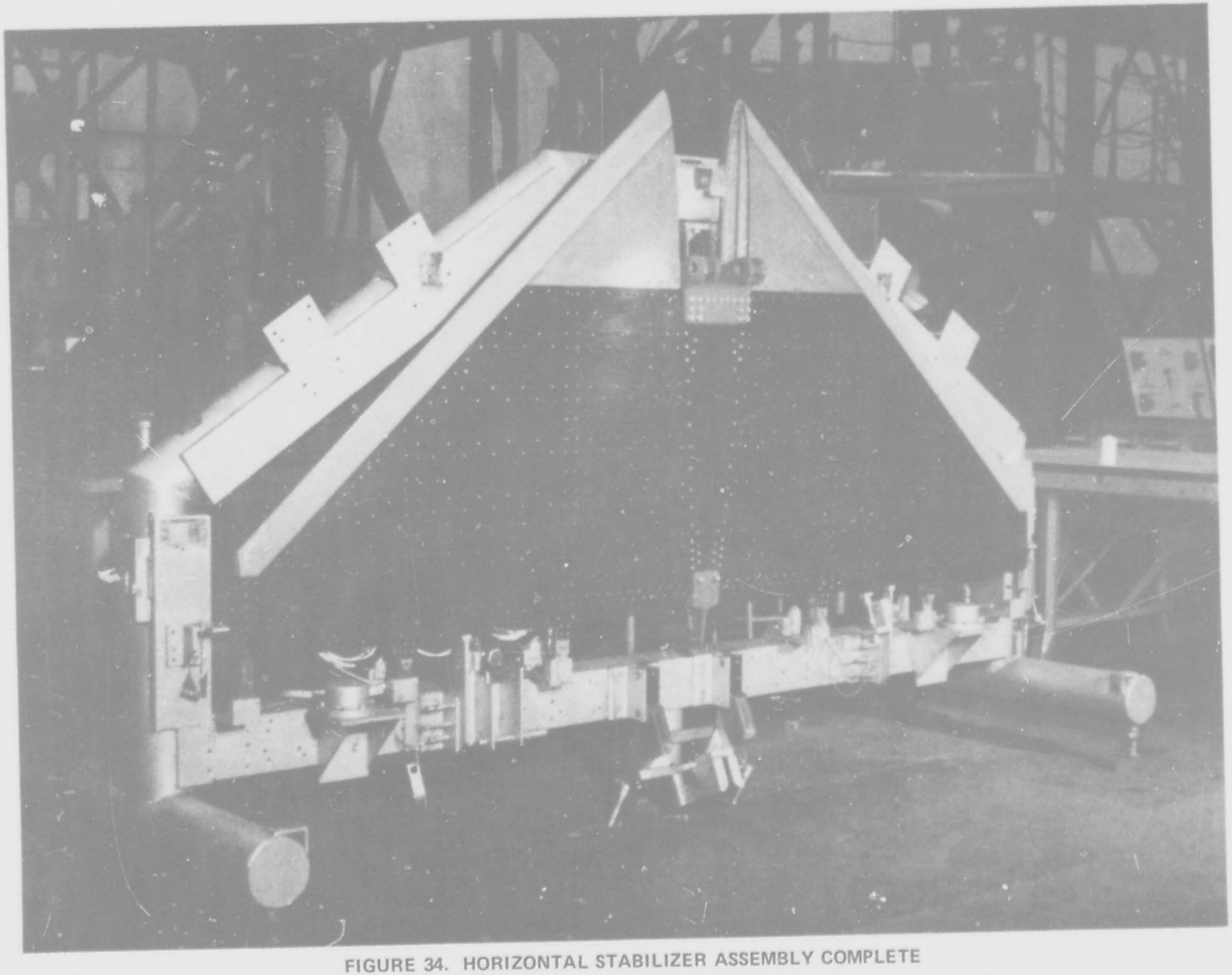

FIGURE 34. HORIZONTAL STABILIZER ASSEMBLY COMPLETE

Detail Part Fabrication

Modifications to parts and operations logs (POL) and detail tooling were necessitated by a drawing change issued on completion of the first substructure assembly. The flat pattern templates (FLTP) and the POL's for cutting the Z5569970-23, -25, and -33 sandwich webs were modified for revised dimensions. The bond-jigs (BONJ) for the -81, -85, and -91 obtuse angles were also changed. The latter changes also necessitated revisions of the heated clamps used for assembly bonding. The clamp for joining the -35 web to the -43 web (-79 and -81 angles) required rework of the obtuse angle ram. The clamp for bonding the -23 web (-83 and -85 angles), -25 web (-87 and -89 angles), and -33 web (-99 and -101 angles) to the -35 web were remade. The rear-spar to cant-rib bonding clamp (Figure 35) was also modified to conform to a change in the cant-rib flange thickness.

Three large, honeycomb sandwich panels were fabricated from which the substructure web details were subsequently cut. The honeycomb core and fiberglass inserts for the sandwich panels (see Reference 2) were cut to required sizes and the panels were bonded in a platen press. Flatwise tension specimens to check the bond quality were cut from the panels and tested with satisfactory results. The 20 required sandwich webs were rough-cut from the three panels. The 112 required corner attach-angles were laid-up, cured, quality tested, and trimmed to net dimensions.

Substructure Assembly

After the first substructure assembly was machined to contour at Douglas, the assembly bond-jig was returned to Rohr together with the rear-spar and cant-rib blanks and the necessary metal details. Using the bond-jig as a holding fixture, the ends of the rear-spar were machined to net requirements. The aft ends of the cant-ribs were also machined to the point where only hand finishing to net dimensions was required prior to bonding.

A fit check of the substructure details on the assembly bond-jig was conducted prior to actual bonding. As with unit one, the cant-ribs were first bonded to the rear-spar. Hand sanding of the cant-rib ends was required to obtain uniform bondline thickness. The heated bond clamp for this joint was shown in Figure 35. Note that springs, rather than clamps were used to retain the cant-ribs against the locators without restraining cant-rib movement in a fore and aft direction. This setup allowed the cant-ribs to move approximately 0.050 inch into the rear-spar as the adhesive softened and flowed.

The assembly bonding proceeded in stages similar to those used during assembly of unit one. Generally, two joints were bonded at one time as shown in Figure 36. During each cure cycle the joints to be bonded during the subsequent cure cycle were setup as shown in the figure. After completion of the assembly bonding, the joints were inspected ultrasonically as shown in Figure 37.

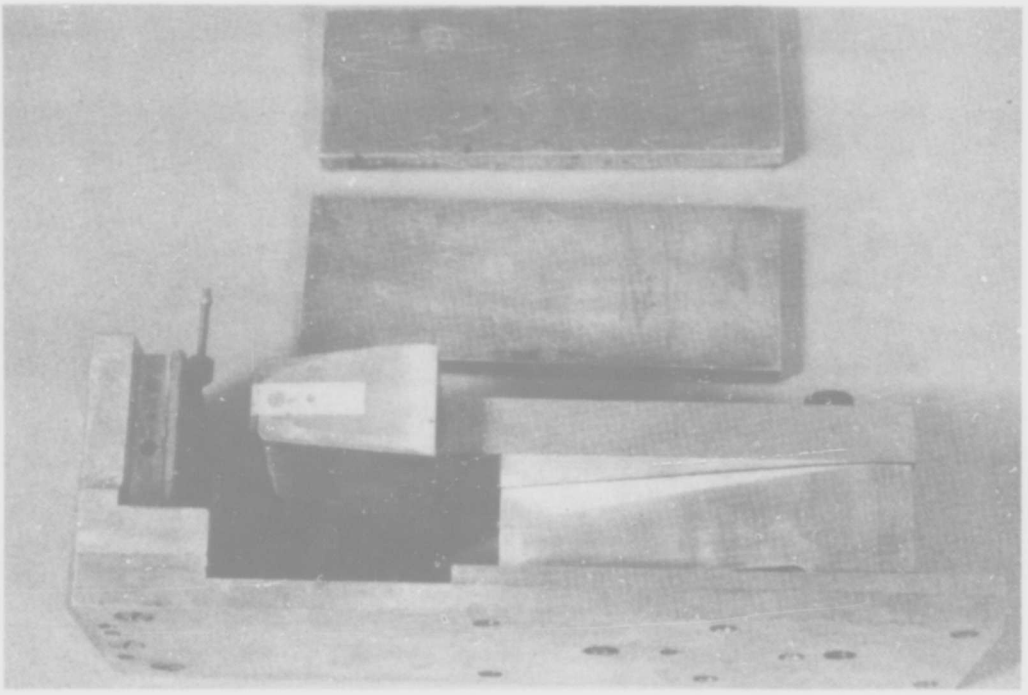

FIGURE 35 (a) CLAMP DETAILS

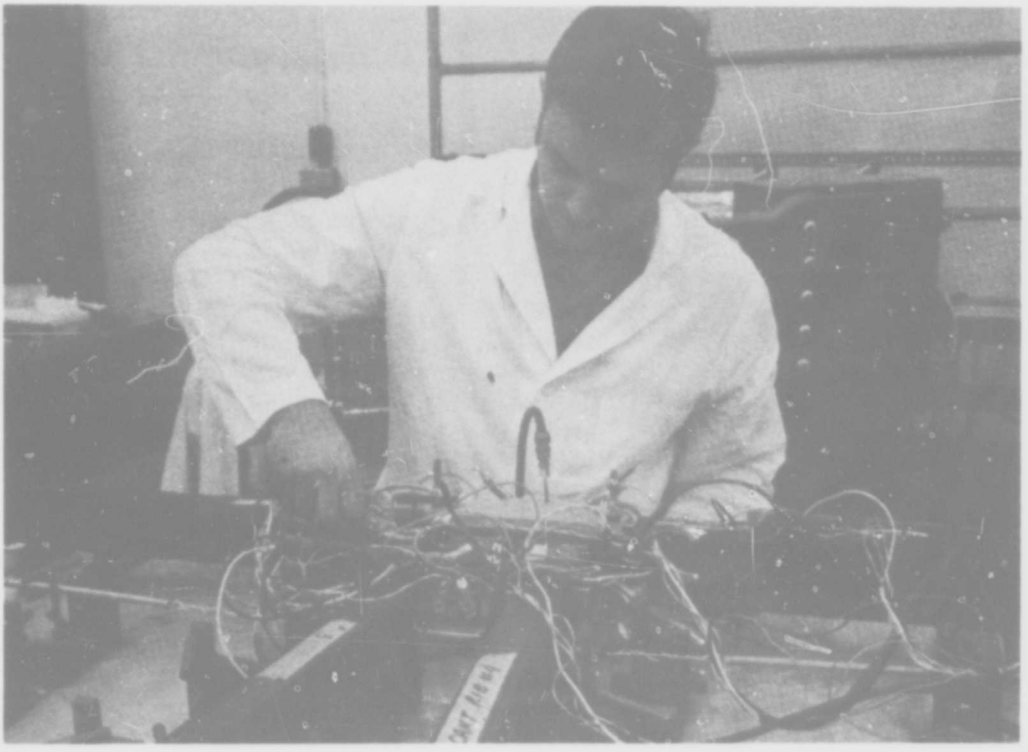

FIGURE 35 (b) BONDING SET-UP

FIGURE 35. CANT-RIB TO REAR-SPAR BONDING CLAMP

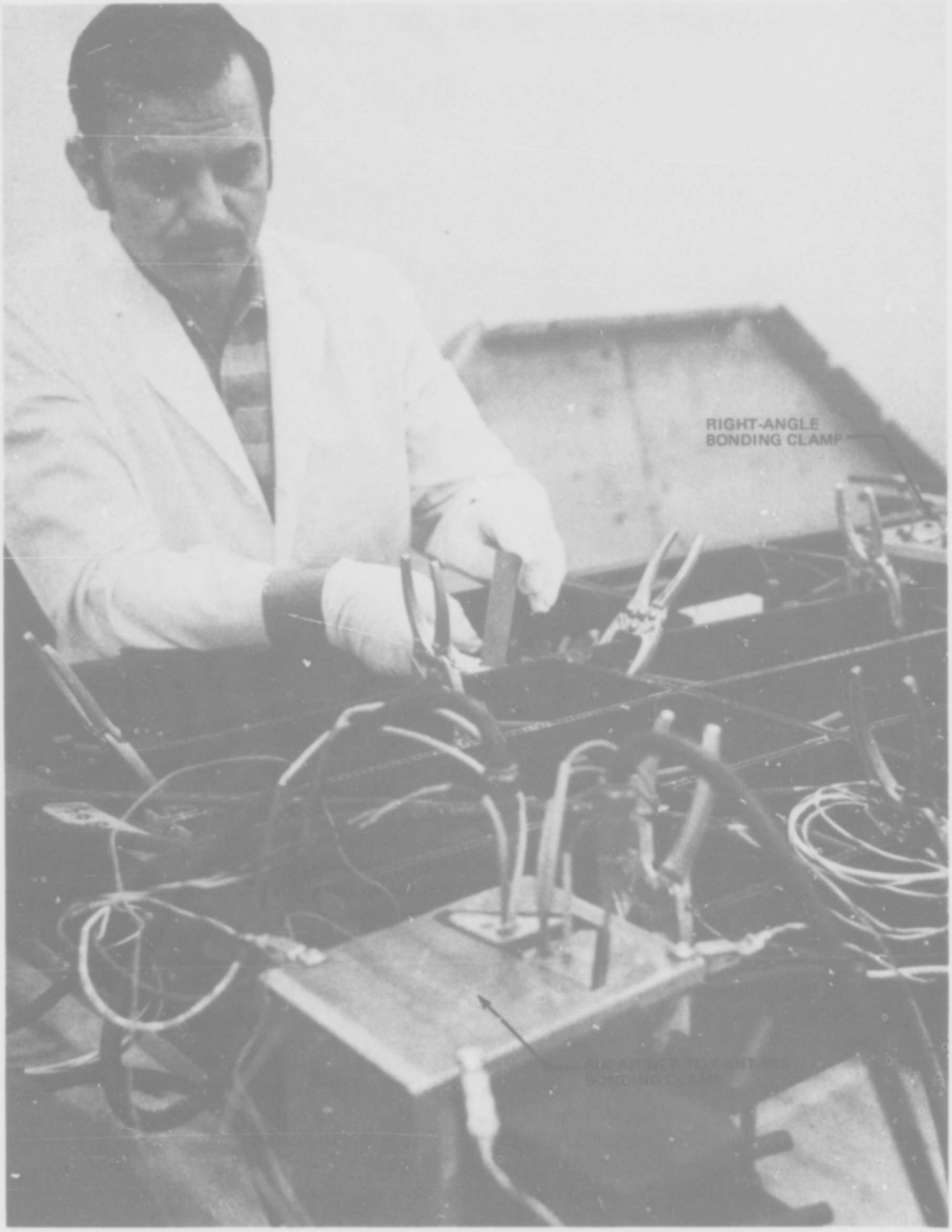

FIGURE 36. ASSEMBLY BONDING OF SUBSTRUCTURE UNIT TWO

FIGURE 37. ULTRASONIC INSPECTION OF SUBSTRUCTURE UNIT TWO

THIS PAGE LEFT BLANK INTENTIONALLY.

APPENDIX A

DISCRETE ELEMENT ANALYSIS MODEL

The discrete element model of the stabilizer structure was prepared according to the general procedure discussed in Section 2. The subdivision grid for the model was designed to correspond to the natural boundaries and subdivisions of the actual structure. The analysis model was subdivided at each spanwise spar between the rear-spar (at x = 100.000) and the front-spar (at x = 135.063). The coordinate distances and locations utilized in the analysis were referenced to the analysis model base coordinate system. The basic subdivision grid and element geometry for the upper and lower cover sheets is illustrated in Figures A1 and A2, respectively. Enlarged views of the upper and lower cover sheets in the area adjacent to the pivot fitting are shown in Figures A3 and A4 for the upper and lower panels, respectively. The origin and directions for the base coordinate system may be found on Figure A1.

Element details for interior portions of the stabilizer structure are shown as section cuts at the interior subdivisions. Only the left-hand portions of the idealization are shown because the model is symmetrical about the centerline of the airplane. The spars at station x = 106.750, 112.437, and 118.125 together with the rear-spar are shown in Figure A5. Except for the rear-spar and the two cant-ribs (which have continuous integral flanges), the bar elements represent the shear angles only and are present where the angles were considered continuous across one or more adjacent nodes. The spars at station x = 123.612, 129.437, and 135.063 (front-spar) and the cant-rib adjacent to the torque-box are illustrated in Figure A6. The ribs at stations y = 20.000, 40.000 and 58.187 together with the cross-section through the center plane of symmetry are shown in Figure A7. The leading edge spars and the inboard ribs for the leading edge structure (both of which are canted members) are shown in Figure A8.

Several shear panels were added to provide a connection between top and bottom nodes at the leading edge cover sheets and the region between stations x = 133.263 and 135.063 adjacent to the front-spar. These panels provided lateral stability to the cover sheets in these areas by simulating the bending stiffness of the individual cover sheets. The added panels are shown in Figure A9. The diagonal bars shown in Figure A7 perform a similar function for the upper and lower panel nodes located at the plane of symmetry.

The element subdivision arrangements used to represent the pivot and actuator fittings are illustrated in Figures A10 and A11, respectively, together with the adjacent structures.

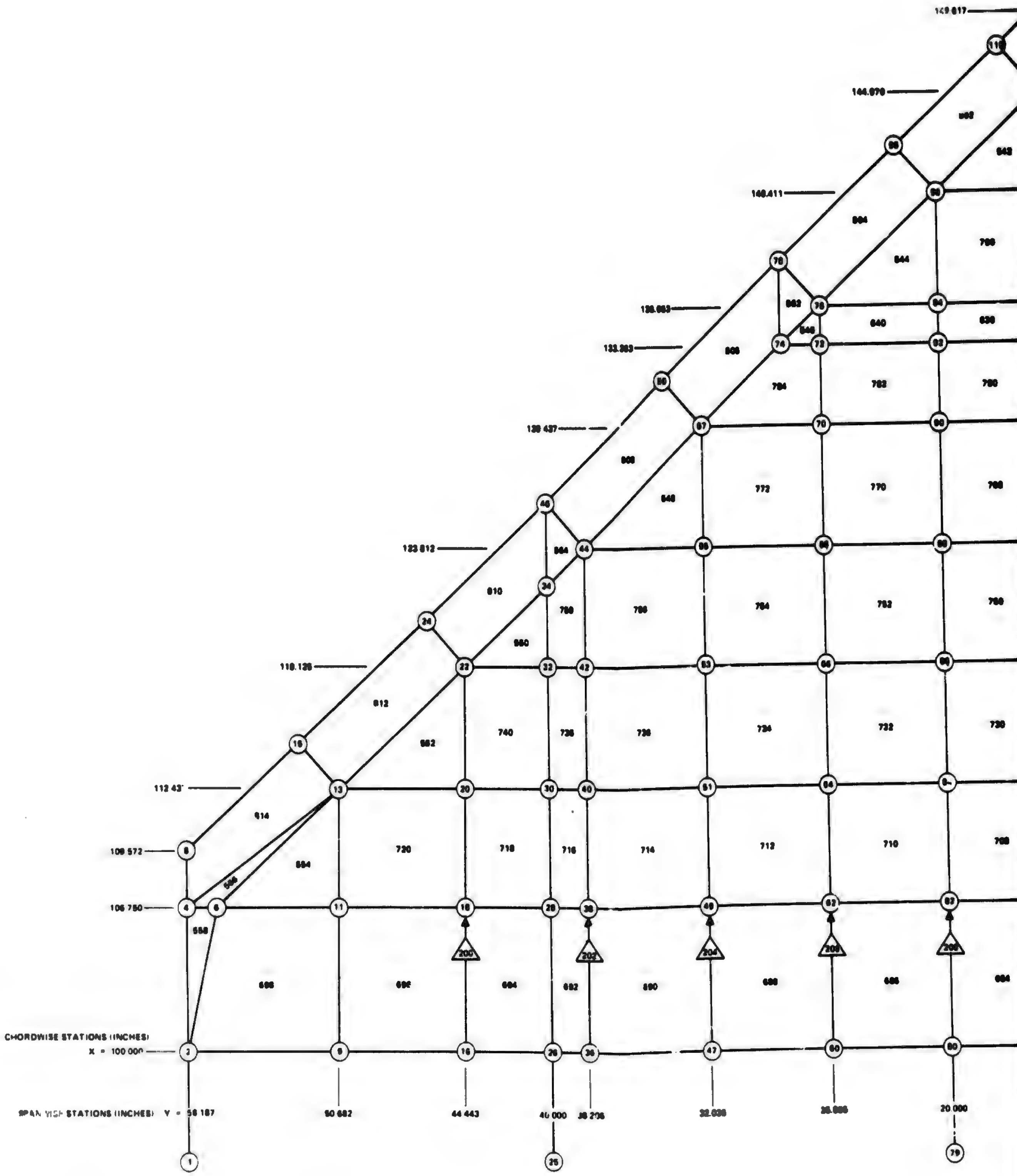
CHORDWISE STATIONS (INCHES)
X = 100.000
SPANWISE STATIONS (INCHES)

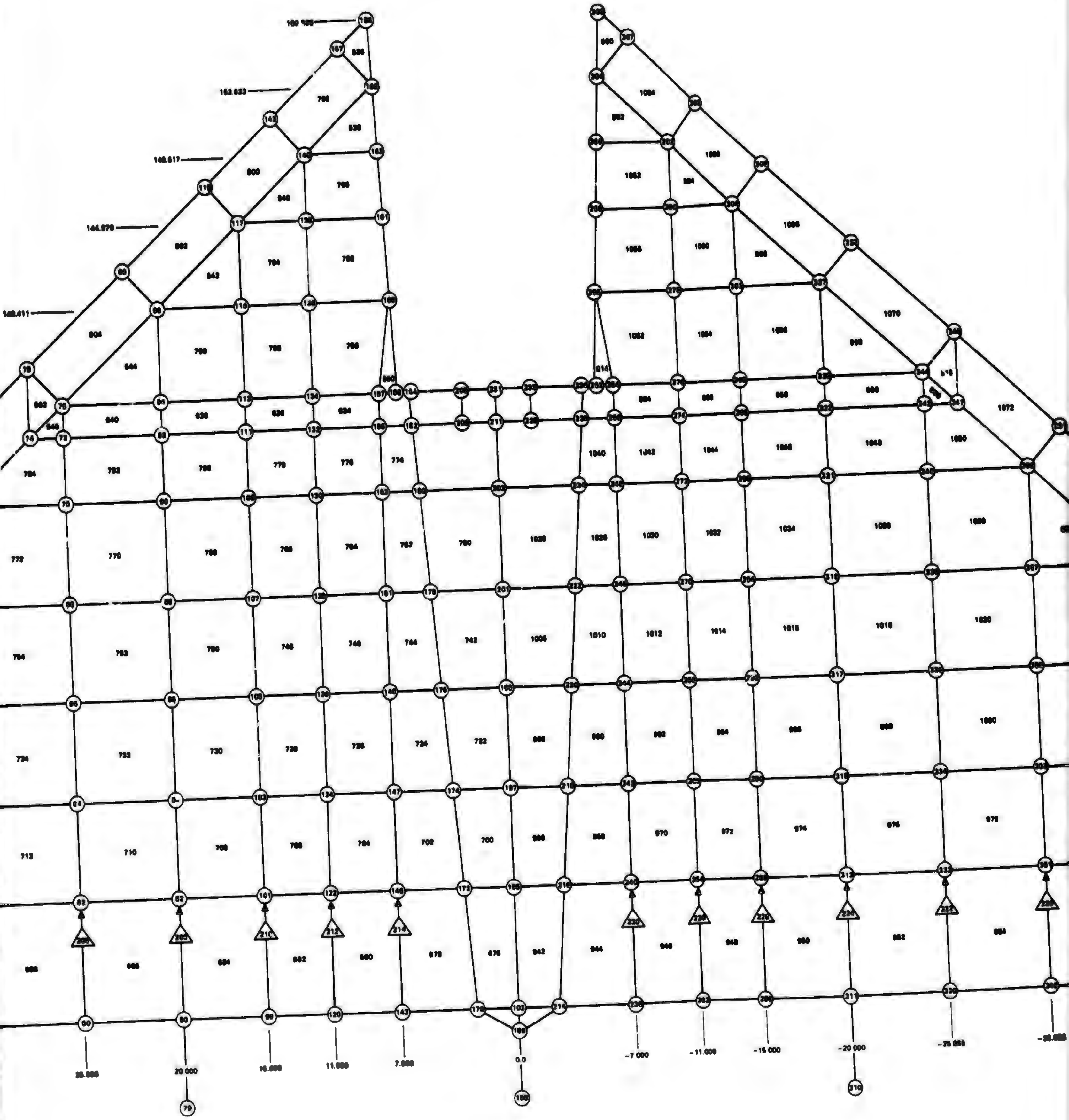
20.000
0.0
-7.000
-11.000
-15.000
-20.000

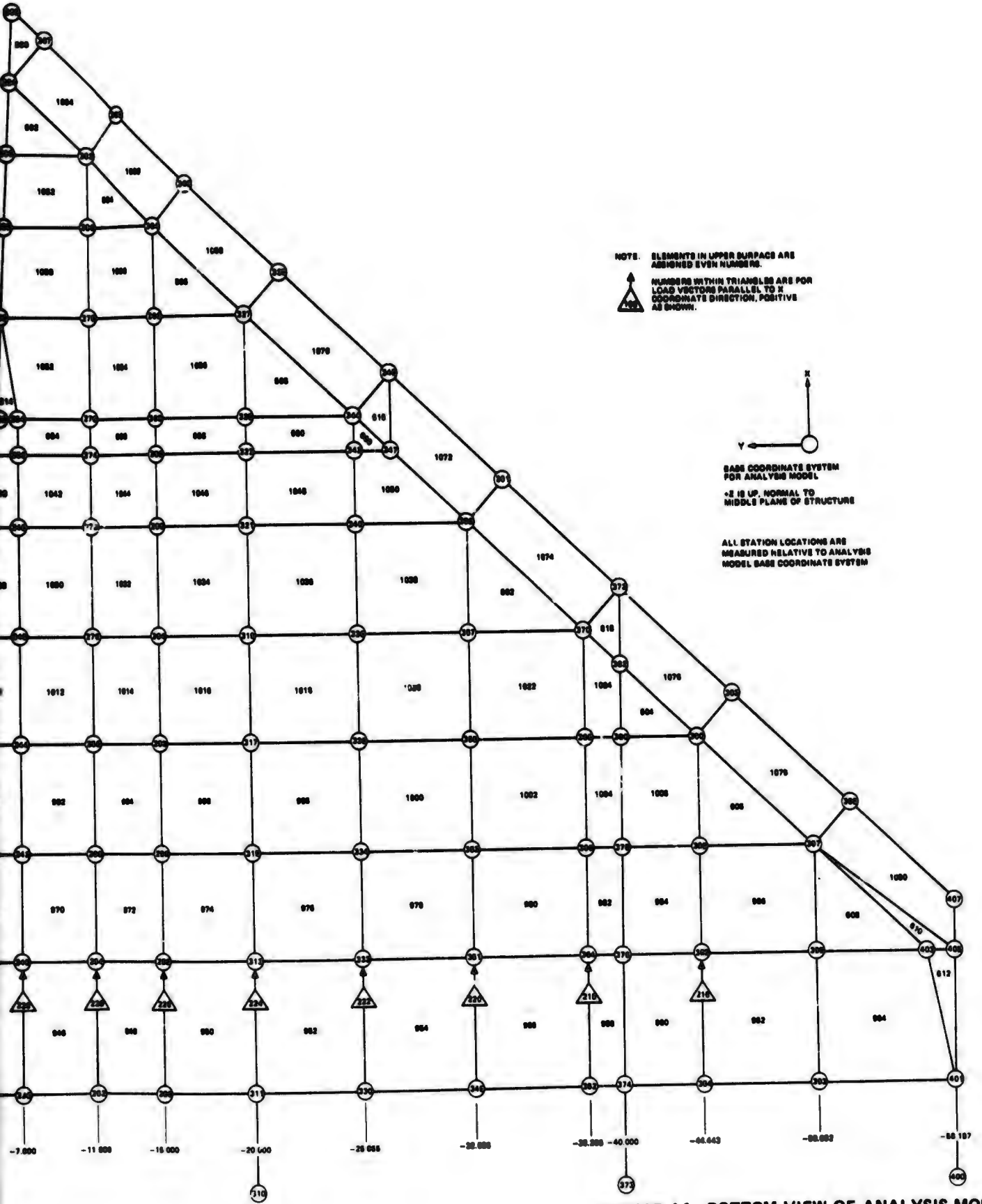

FIGURE A1. BOTTOM VIEW OF ANALYSIS MODEL

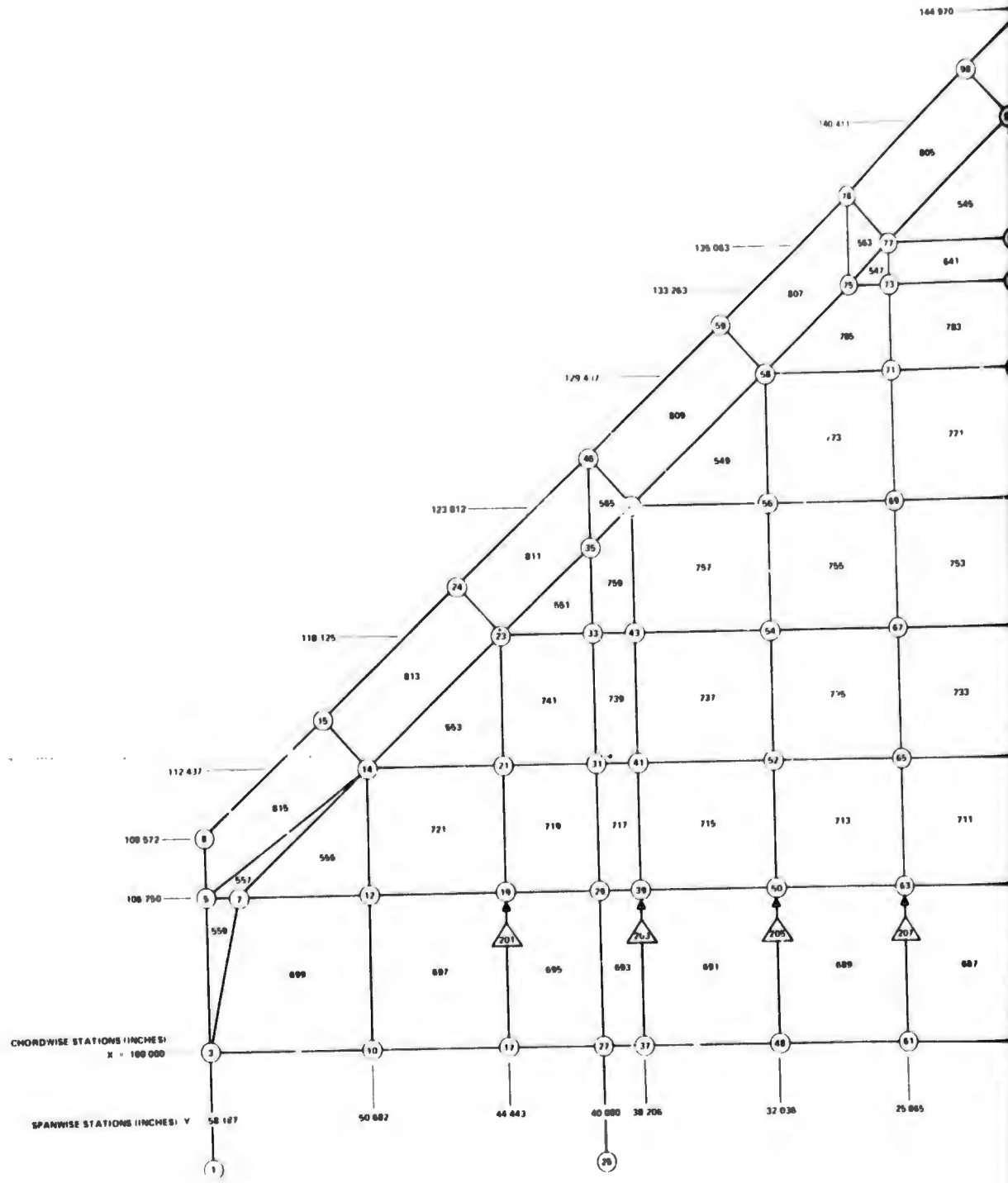
144 970
140 411
135 083
133 263
129 417
123 812
118 125
112 437
108 572
108 750
CHORDWISE STATIONS (INCHES)
X = 100 000
SPANWISE STATIONS (INCHES) Y
58 127
50 682
44 443
40 880
38 206
32 036
25 865

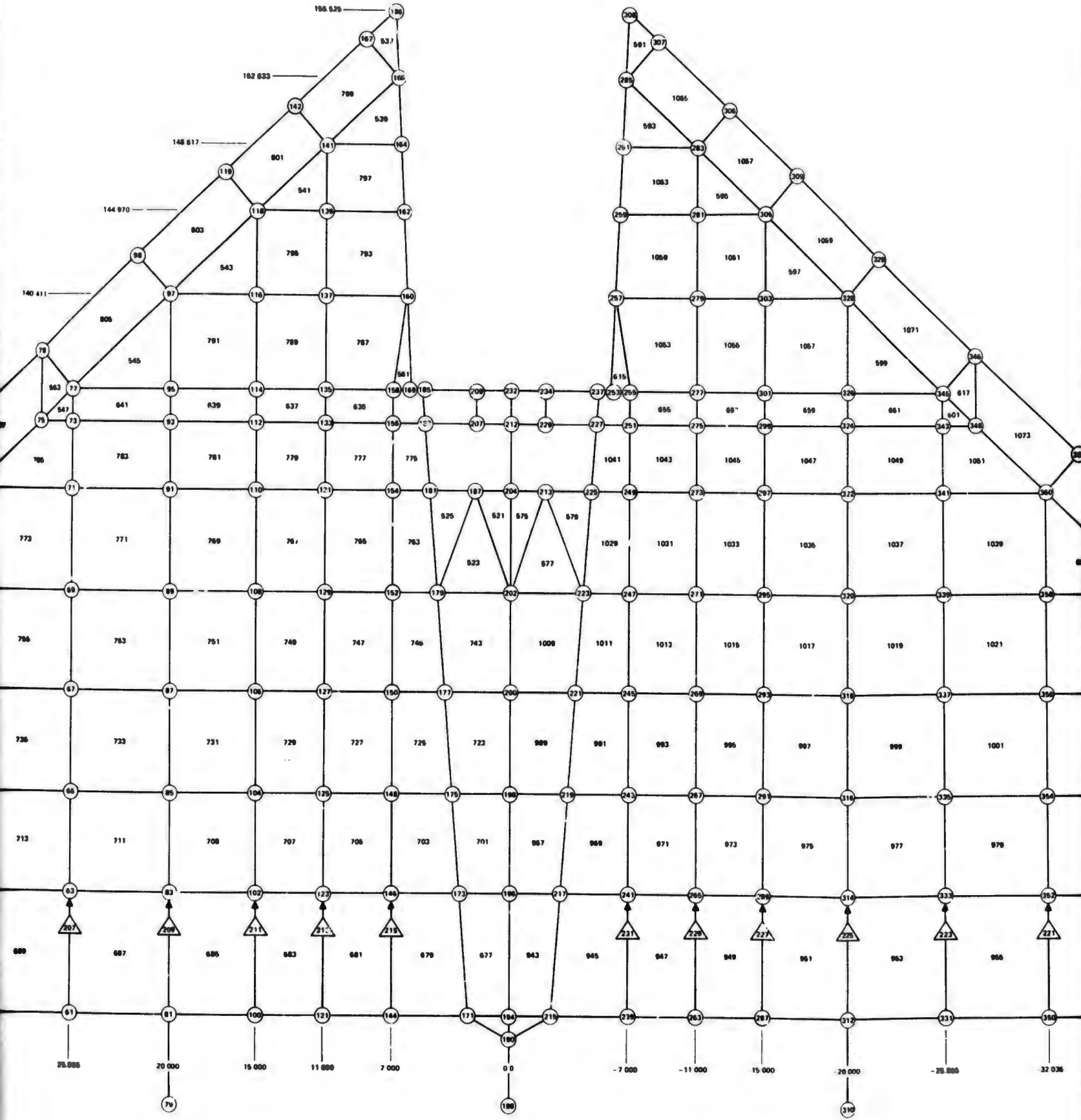
152 633
148 617
144 970
140 411
20 000
15 000
11 000
7 000
0 0
- 7 000
- 11 000
15 000
- 20 000
- 25 000
- 32 036

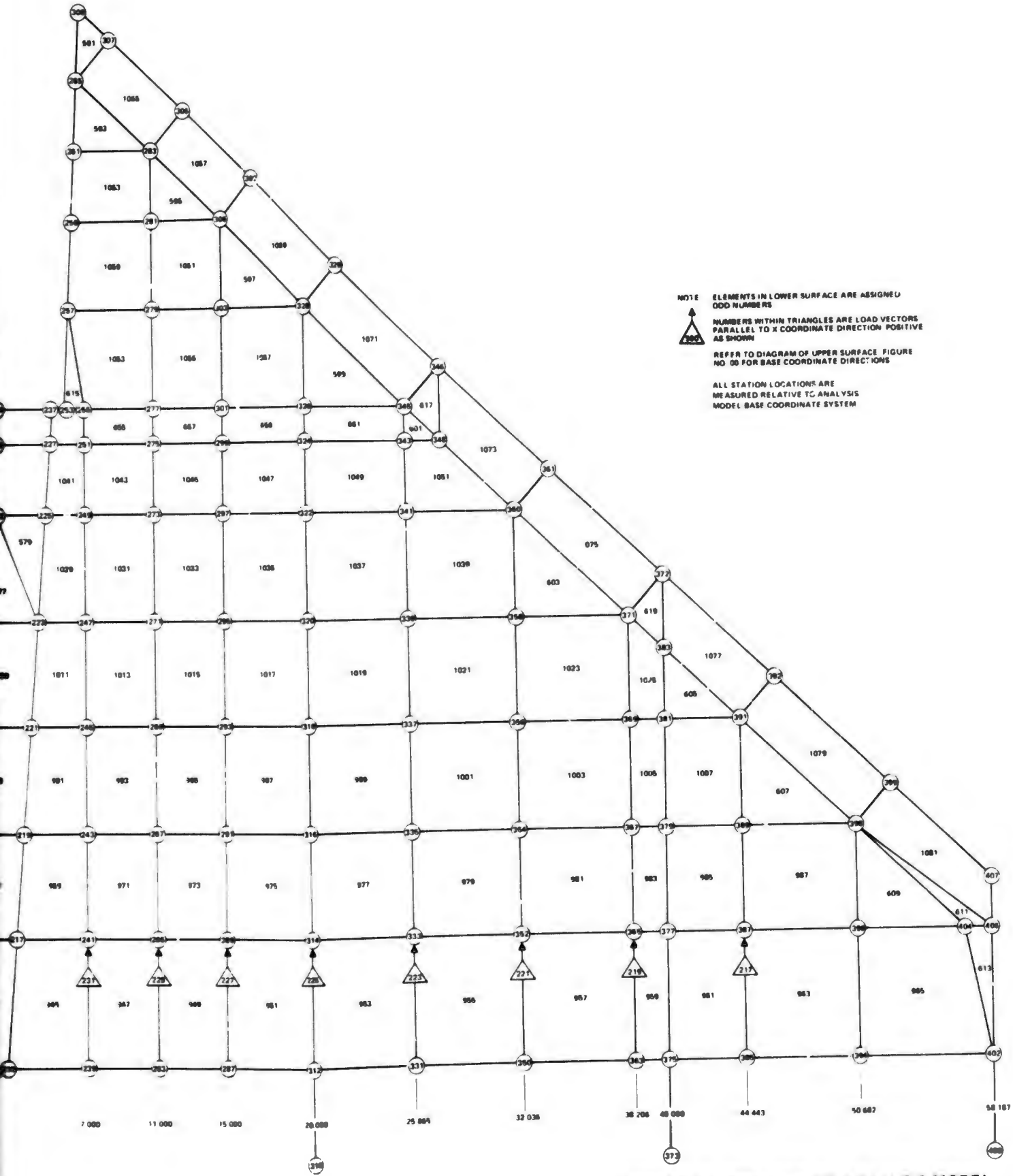

FIGURE A2. TOP VIEW OF ANALYSIS MODEL

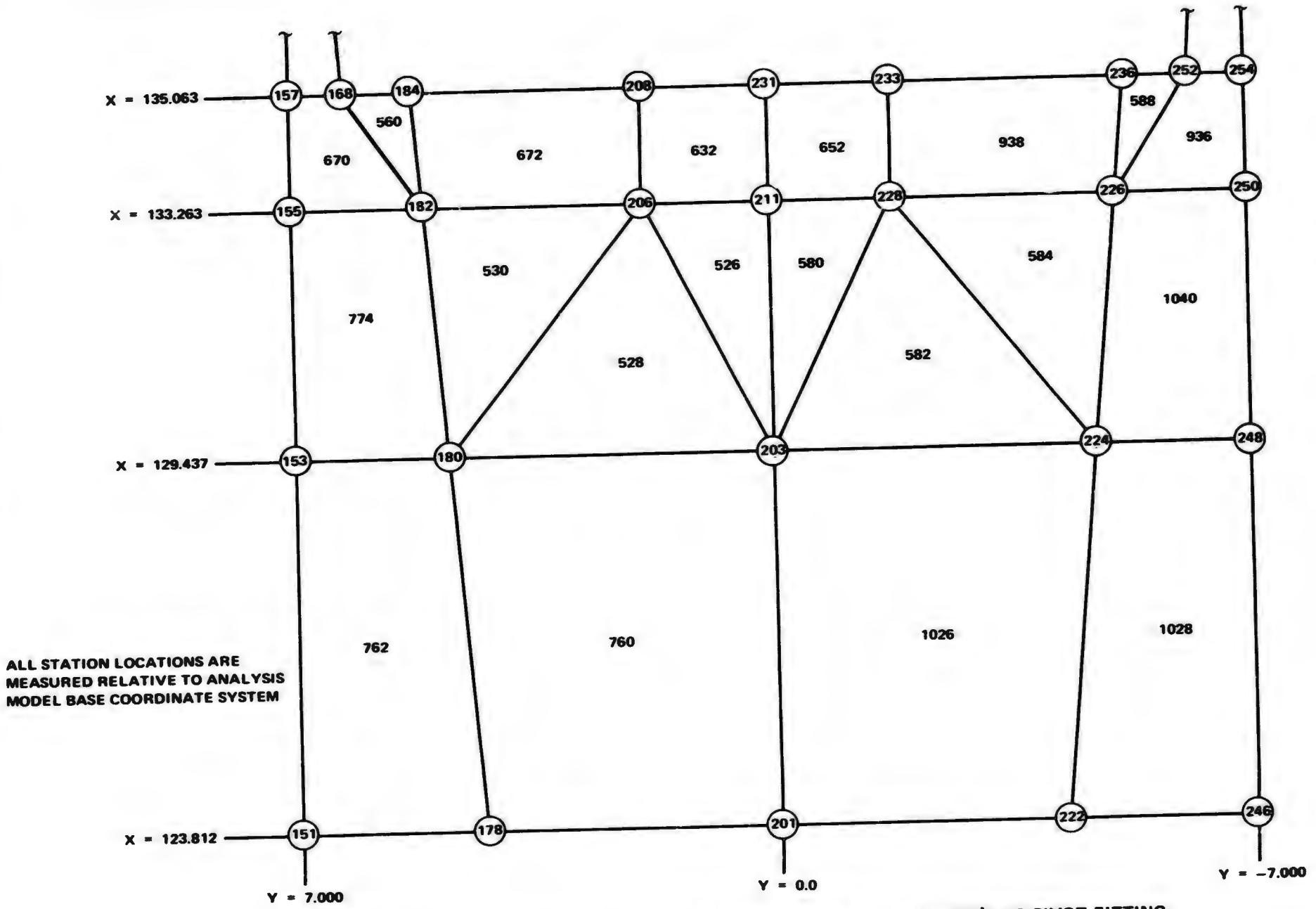

FIGURE A3. DISCRETE ELEMENT SUBDIVISION FOR LOWER PANEL ADJACENT TO PIVOT FITTING

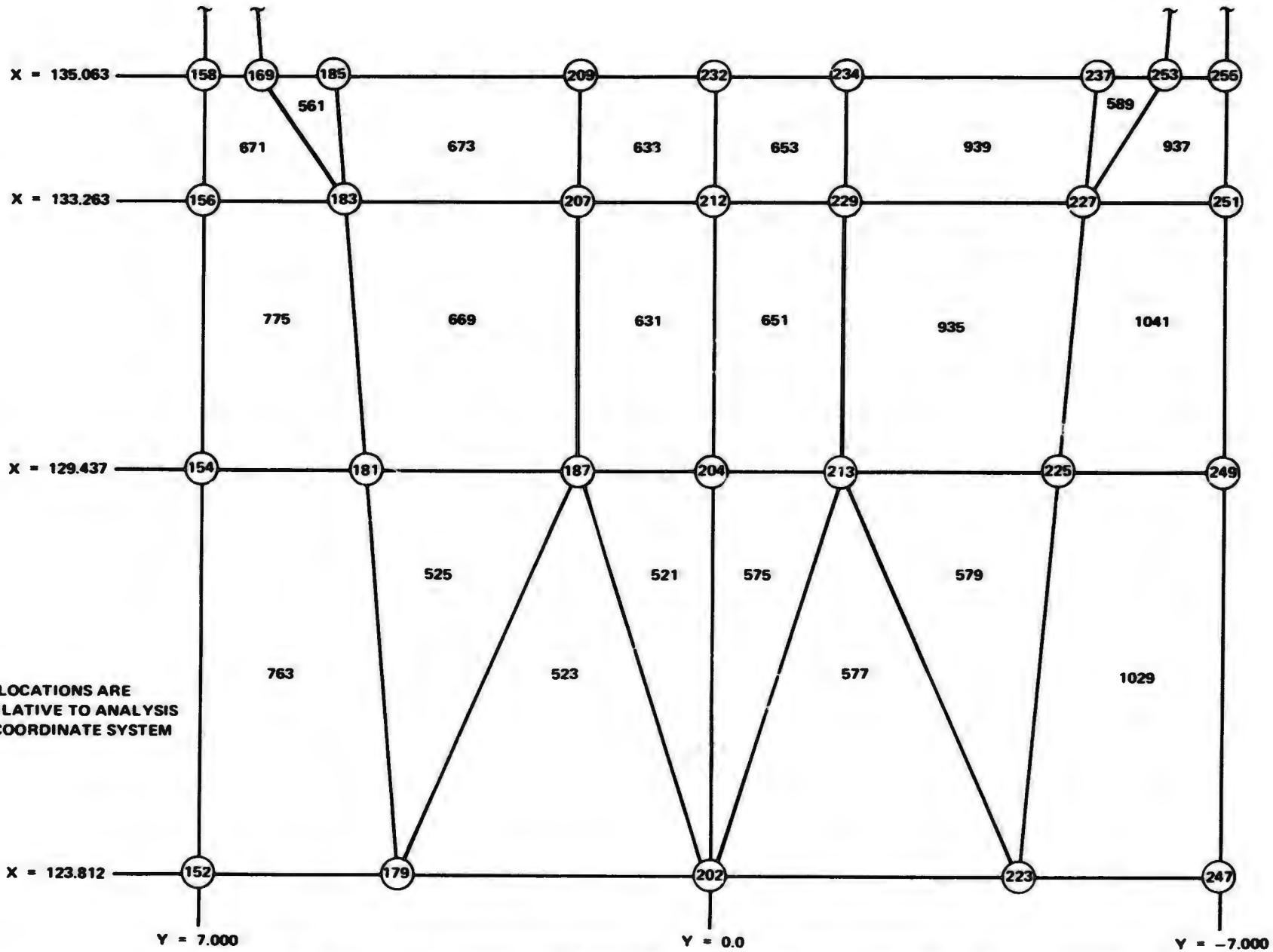

FIGURE A4. DISCRETE ELEMENT SUBDIVISION FOR UPPER PANEL ADJACENT TO PIVOT FITTING

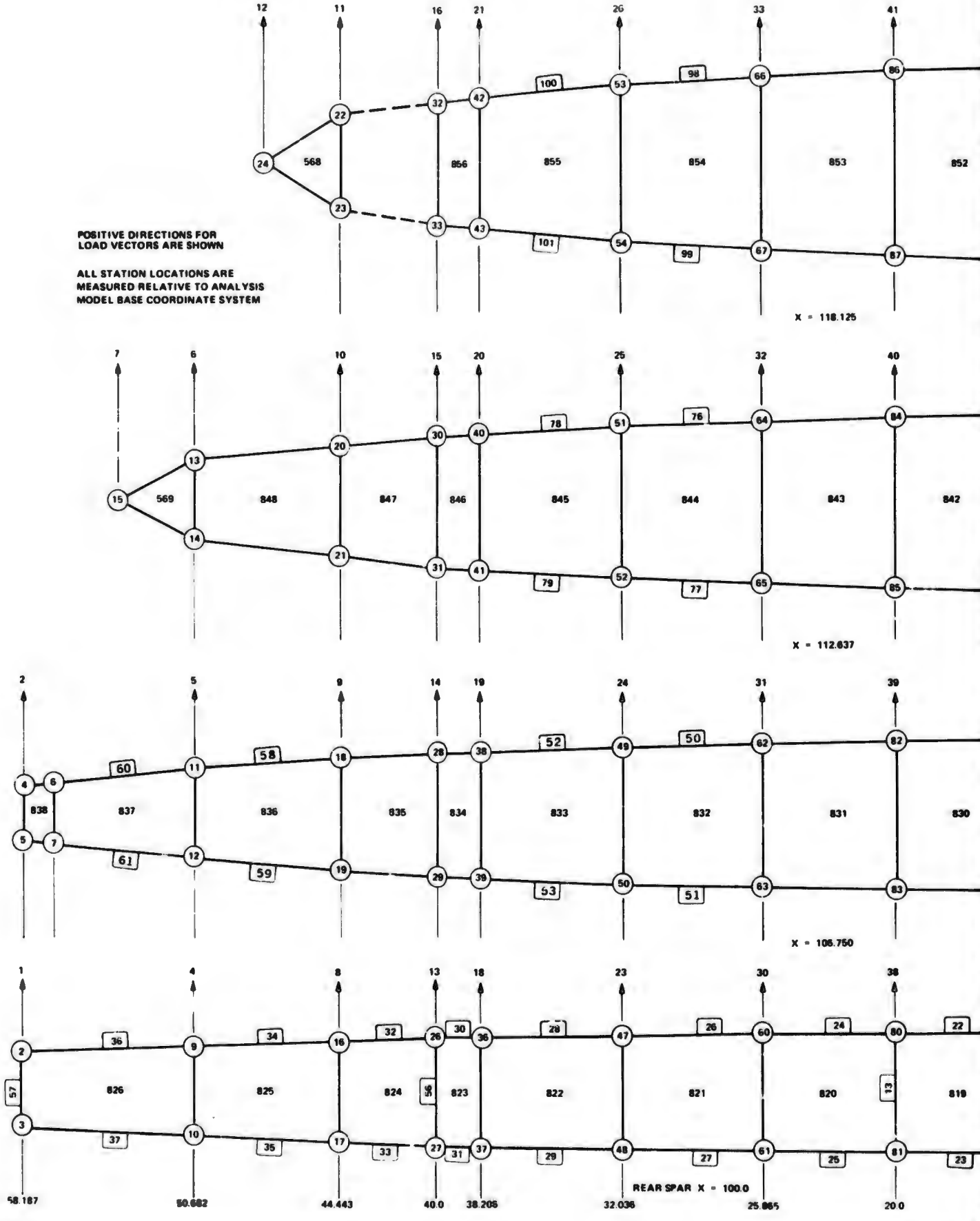
POSITIVE DIRECTIONS FOR LOAD VECTORS ARE SHOWN
ALL STATION LOCATIONS ARE MEASURED RELATIVE TO ANALYSIS MODEL BASE COORDINATE SYSTEM
X = 118.125
X = 112.637
X = 106.750
REAR SPAR X = 100.0
58.187
50.682
44.443
40.0
38.205
32.036
25.865
20.0

FIGURE A

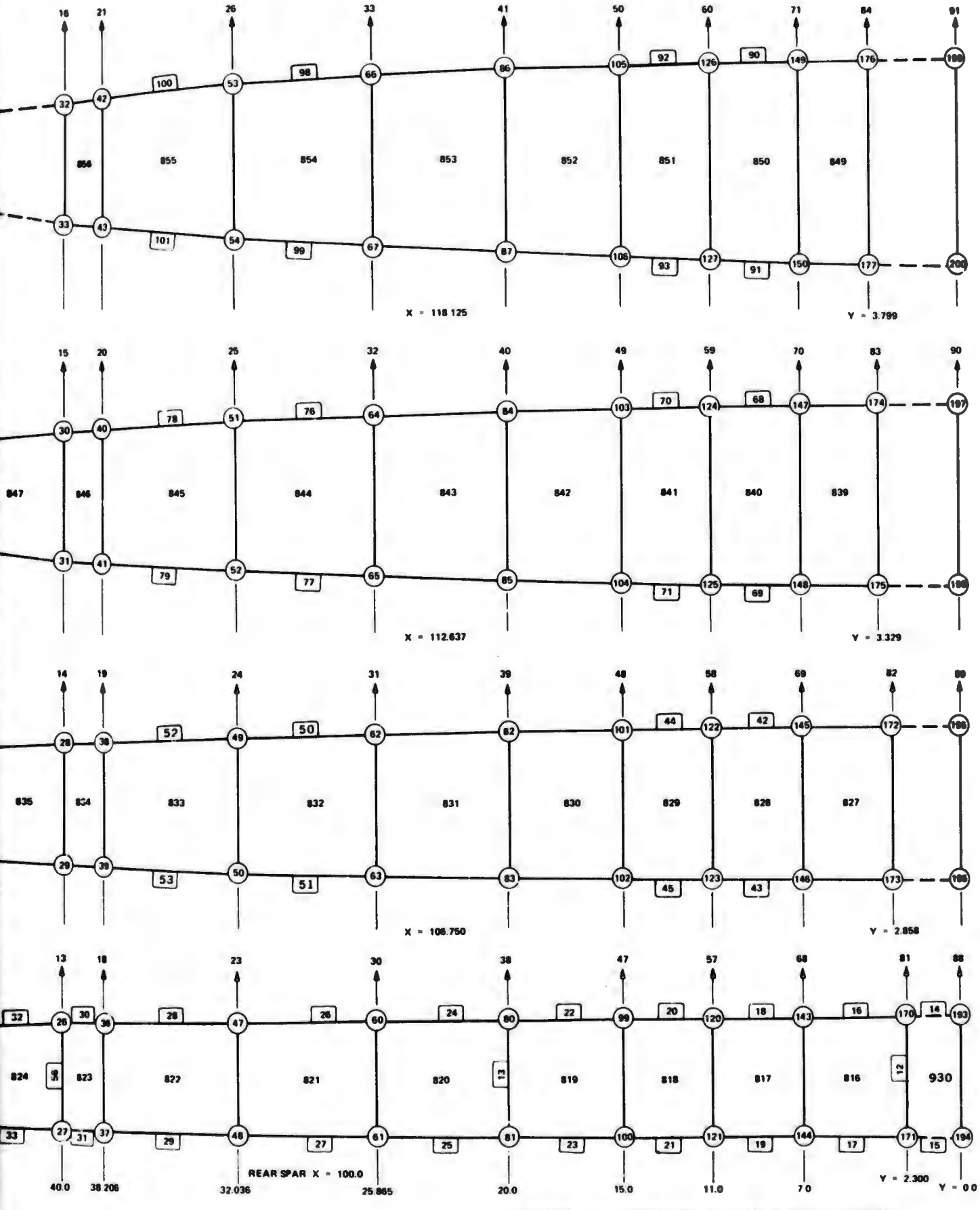

FIGURE A5. DISCRETE ELEMENT SUBDIVISION FOR SPANWISE SPARS

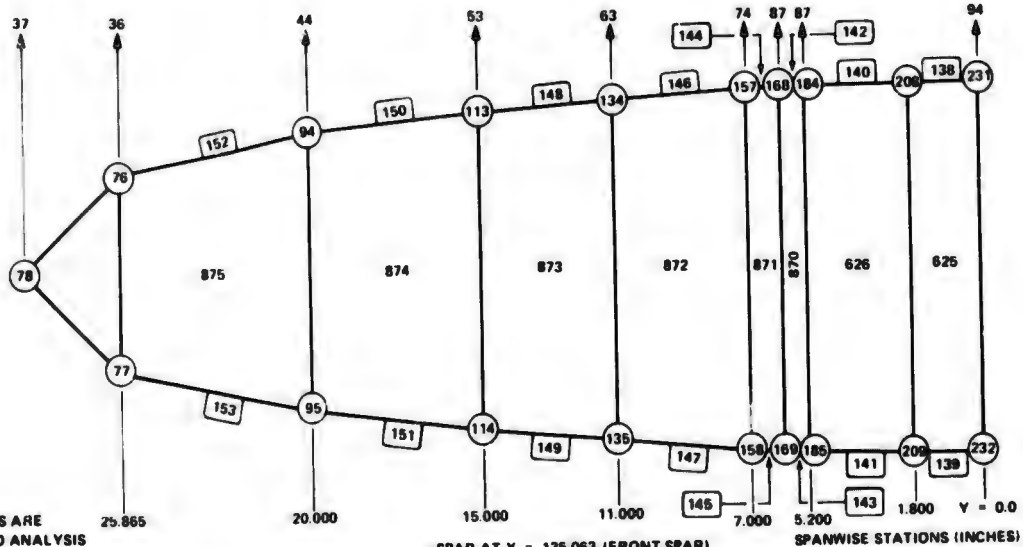

ALL STATION LOCATIONS ARE MEASURED RELATIVE TO ANALYSIS MODEL BASE COORDINATE SYSTEM

SPAR AT X = 135.063 (FRONT SPAR)

SPANWISE STATIONS (INCHES)

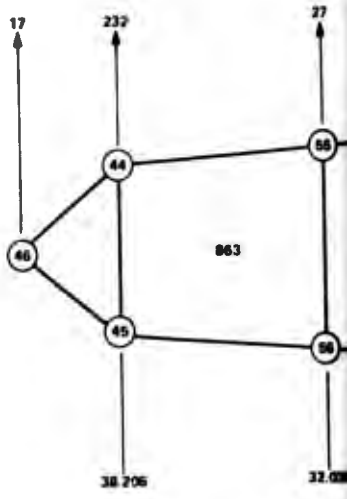

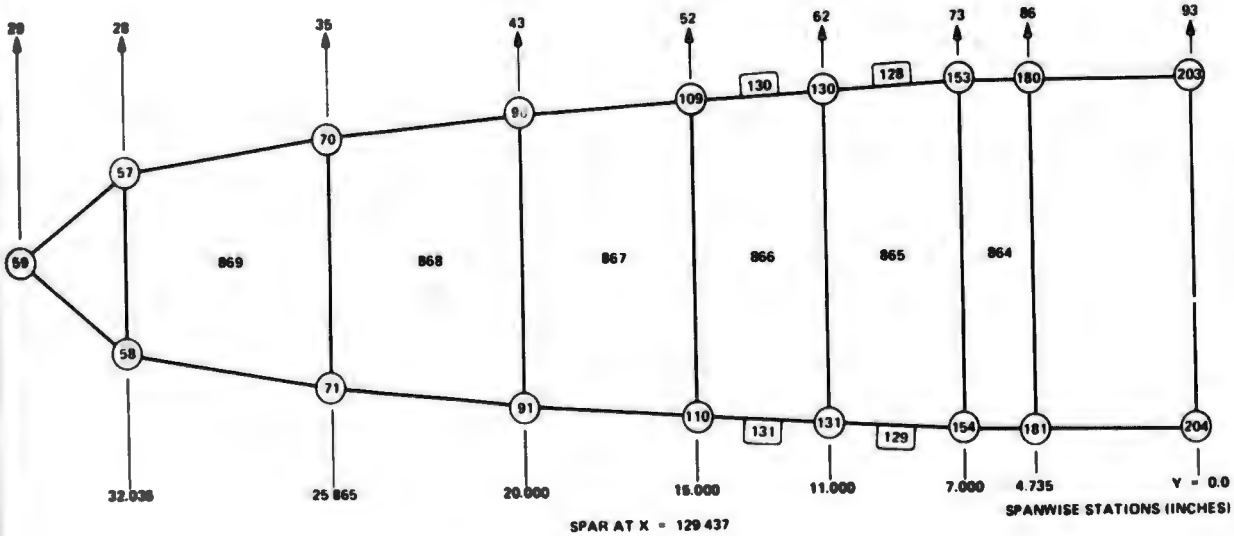

SPAR AT X = 129.437

SPANWISE STATIONS (INCHES)

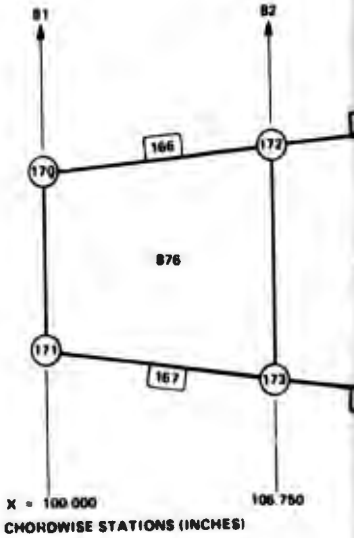

CHORDWISE STATIONS (INCHES)

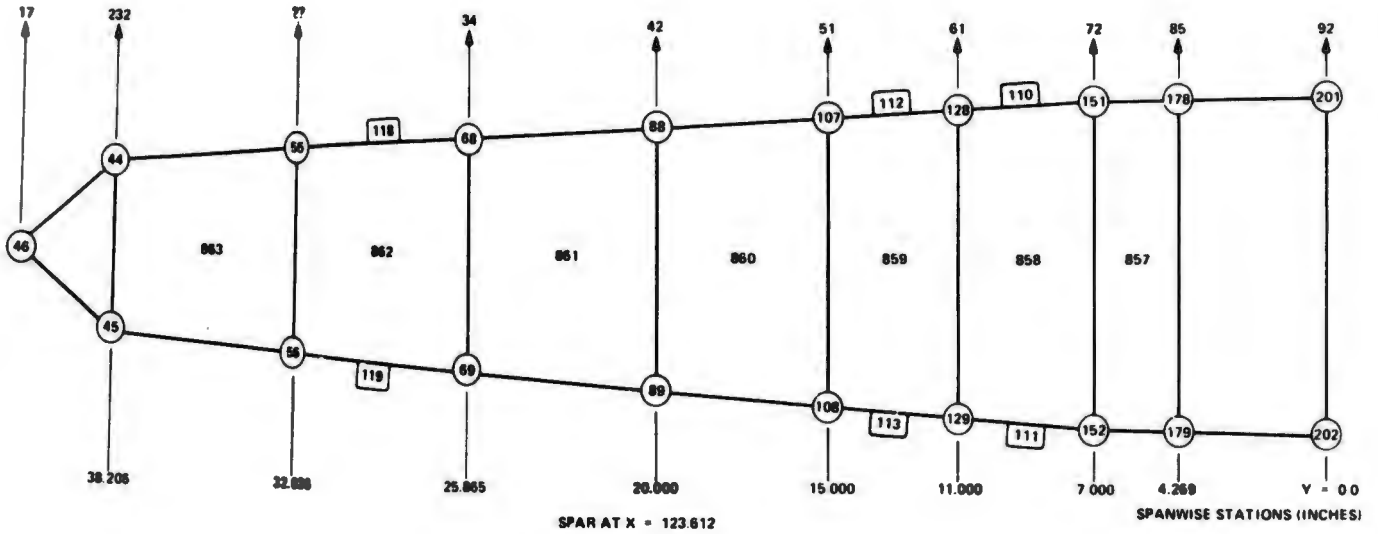

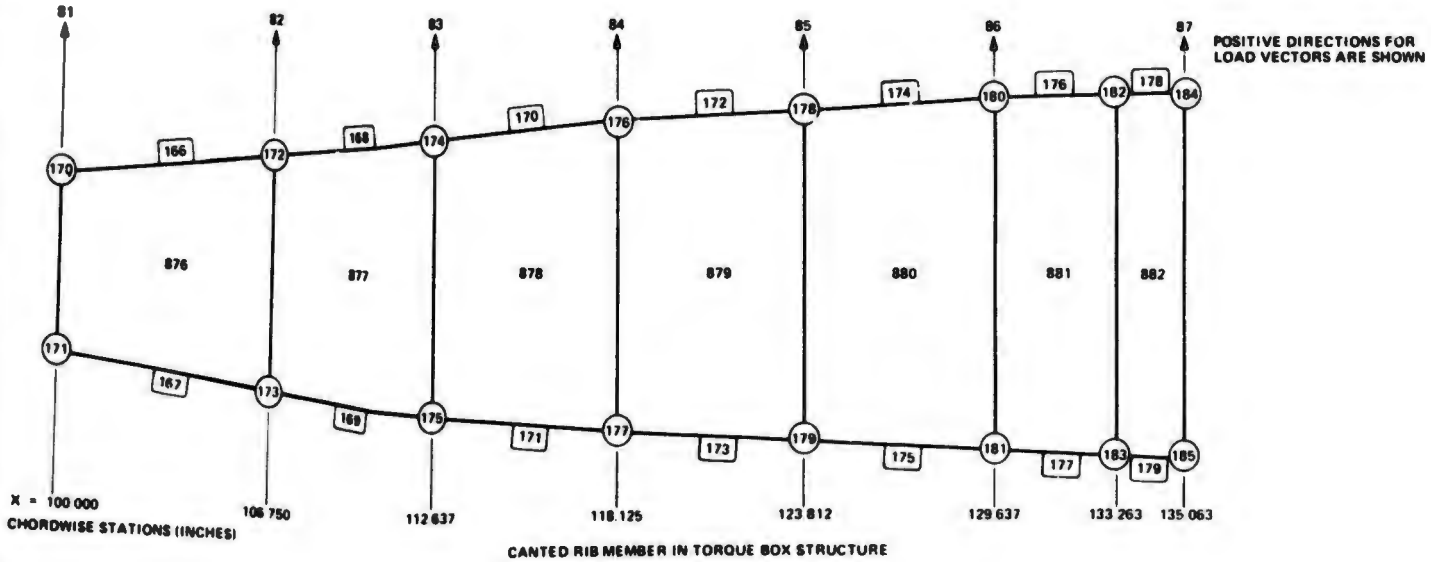

FIGURE A6. DISCRETE ELEMENT SUBDIVISION FOR SPANWISE SPARS AND CANT-RIB

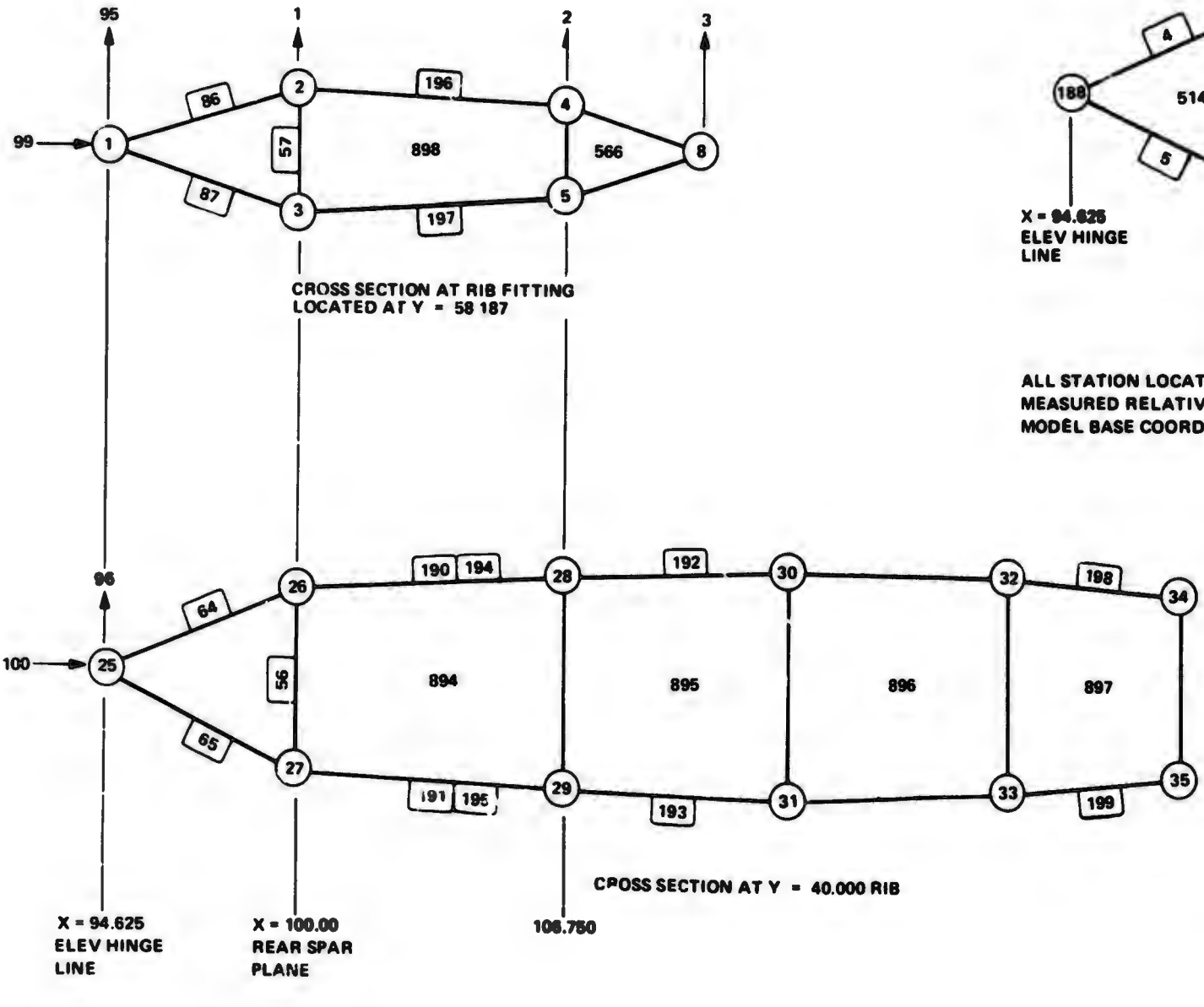
95
1
2
3
99
1
2
3
4
5
8
86
87
57
196
197
898
566
CROSS SECTION AT RIB FITTING
LOCATED AT Y = 58 187
188
514
4
5
6
X = 94.625
ELEV HINGE
LINE
ALL STATION LOCATIONS ARE
MEASURED RELATIVE TO ANAL
MODEL BASE COORDINATE SYST
96
100
25
26
27
28
29
30
31
32
33
34
35
64
65
56
190
194
191
195
192
193
198
199
894
895
896
897
CROSS SECTION AT Y = 40.000 RIB
X = 94.625
ELEV HINGE
LINE
X = 100.00
REAR SPAR
PLANE
106.750

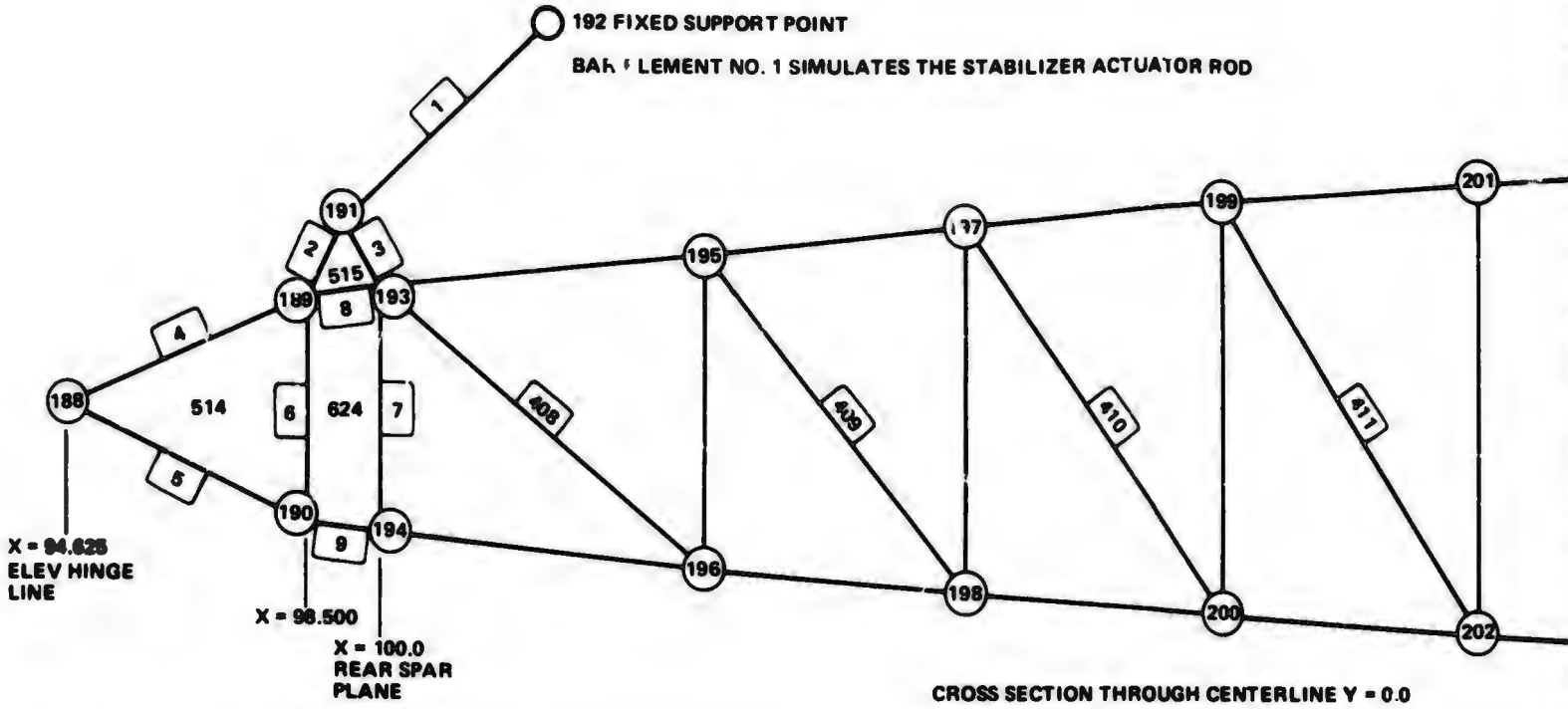

ALL STATION LOCATIONS ARE
MEASURED RELATIVE TO ANALYSIS
MODEL BASE COORDINATE SYSTEM

POSITIVE DIRECTIONS FOR
LOAD VECTORS ARE SHOWN

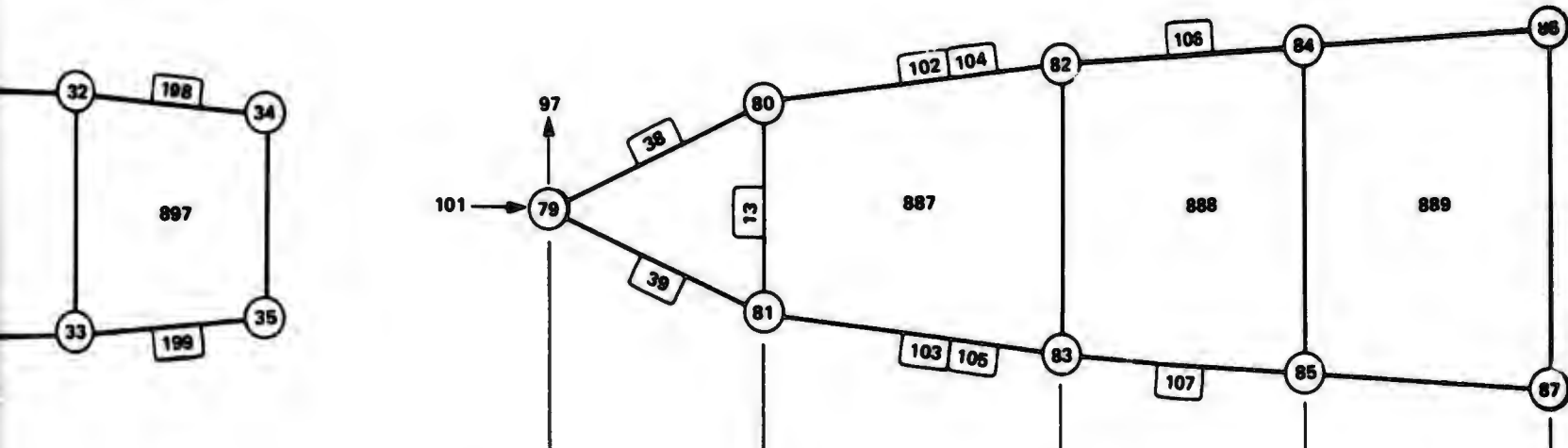

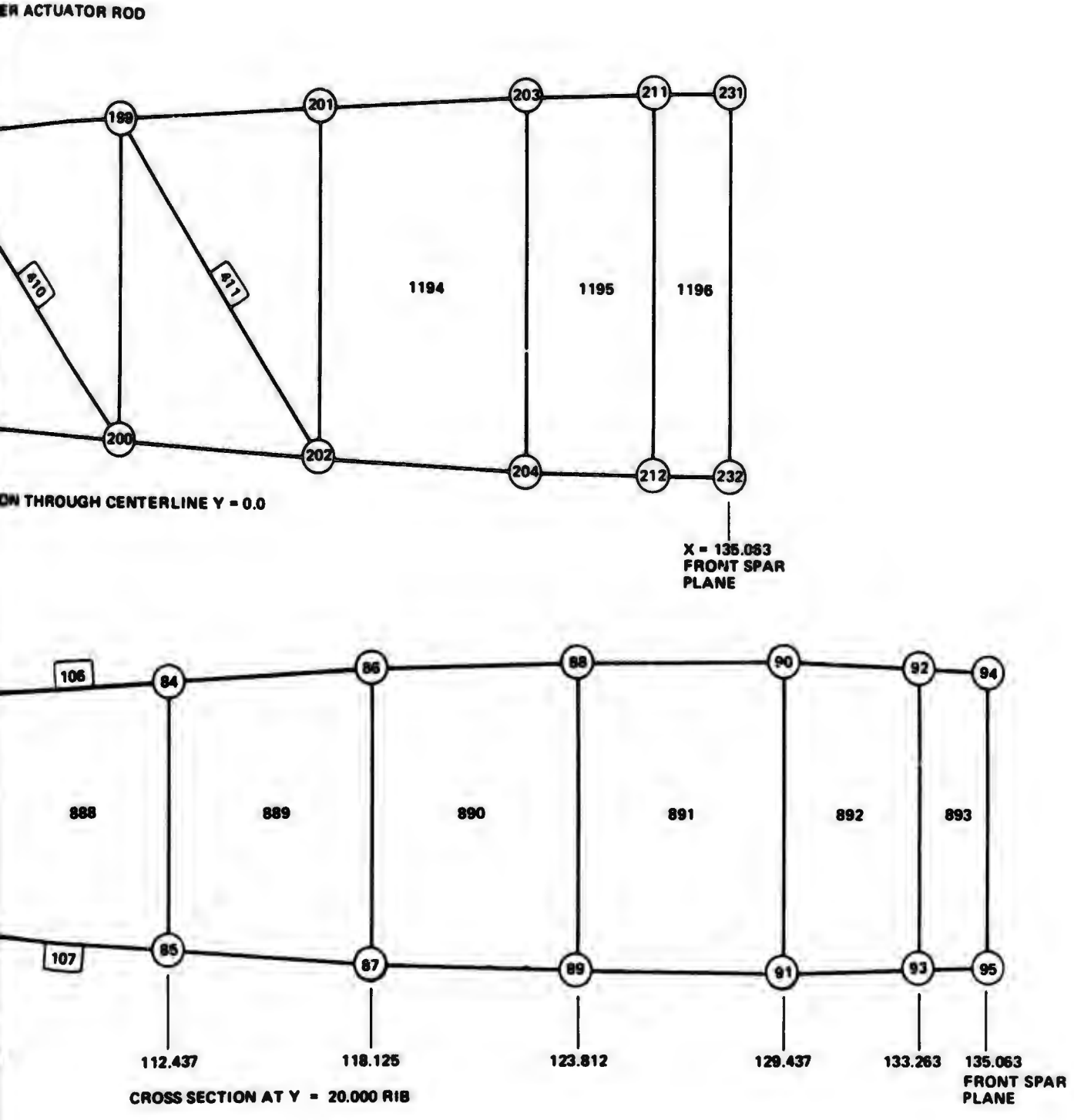

FIGURE A7. DISCRETE ELEMENT SUBDIVISION FOR CHORDWISE RIBS

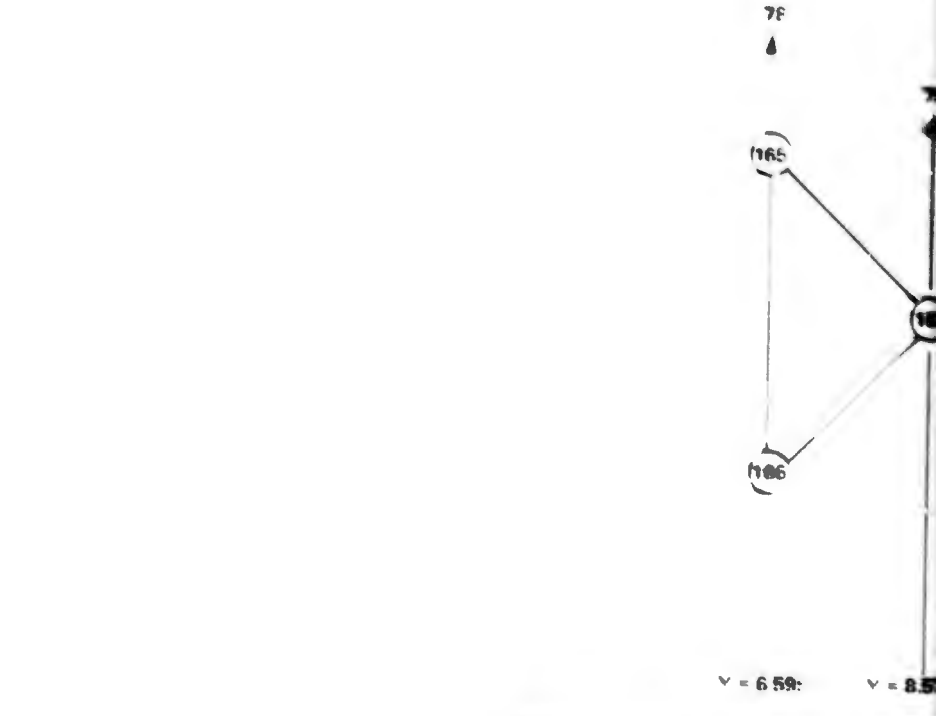

Y = 6.59: Y = 8.5

CROSS SECTION THROUGH LEADING ED

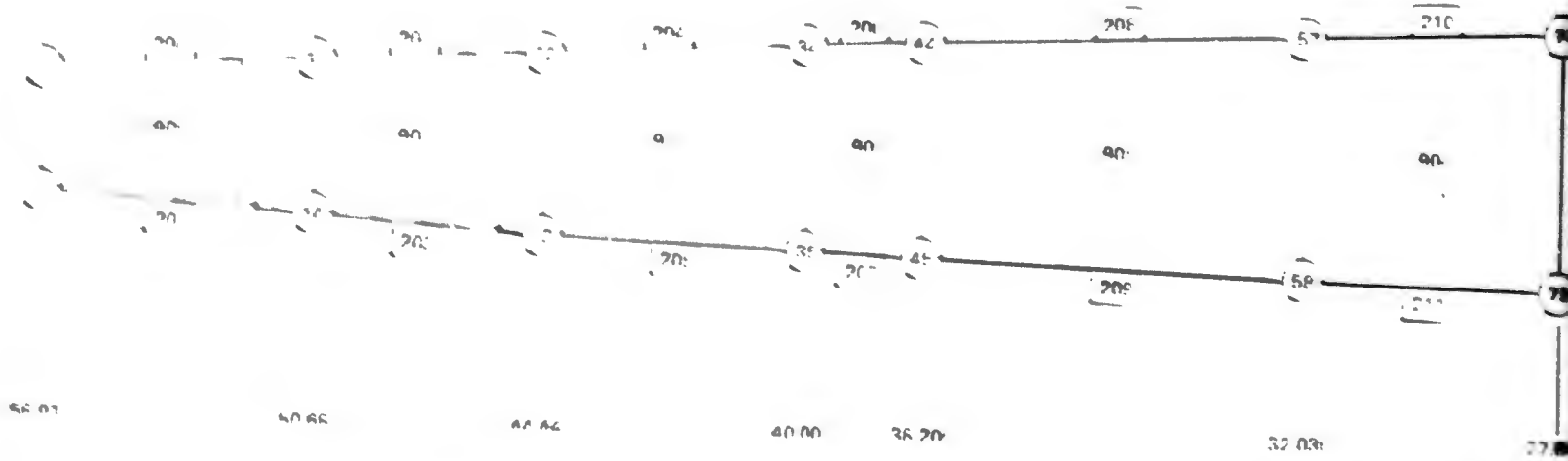

LEADING EDGE SPAR MEMBER

ALL STATION LOCATIONS AR
MEASURED RELATIVE TO AN A VS
MODEL BASE COORDINATE SYSTEM

POSITIVE DIRECTIONS FOR
LOAD VECTORS ARE SHOWN

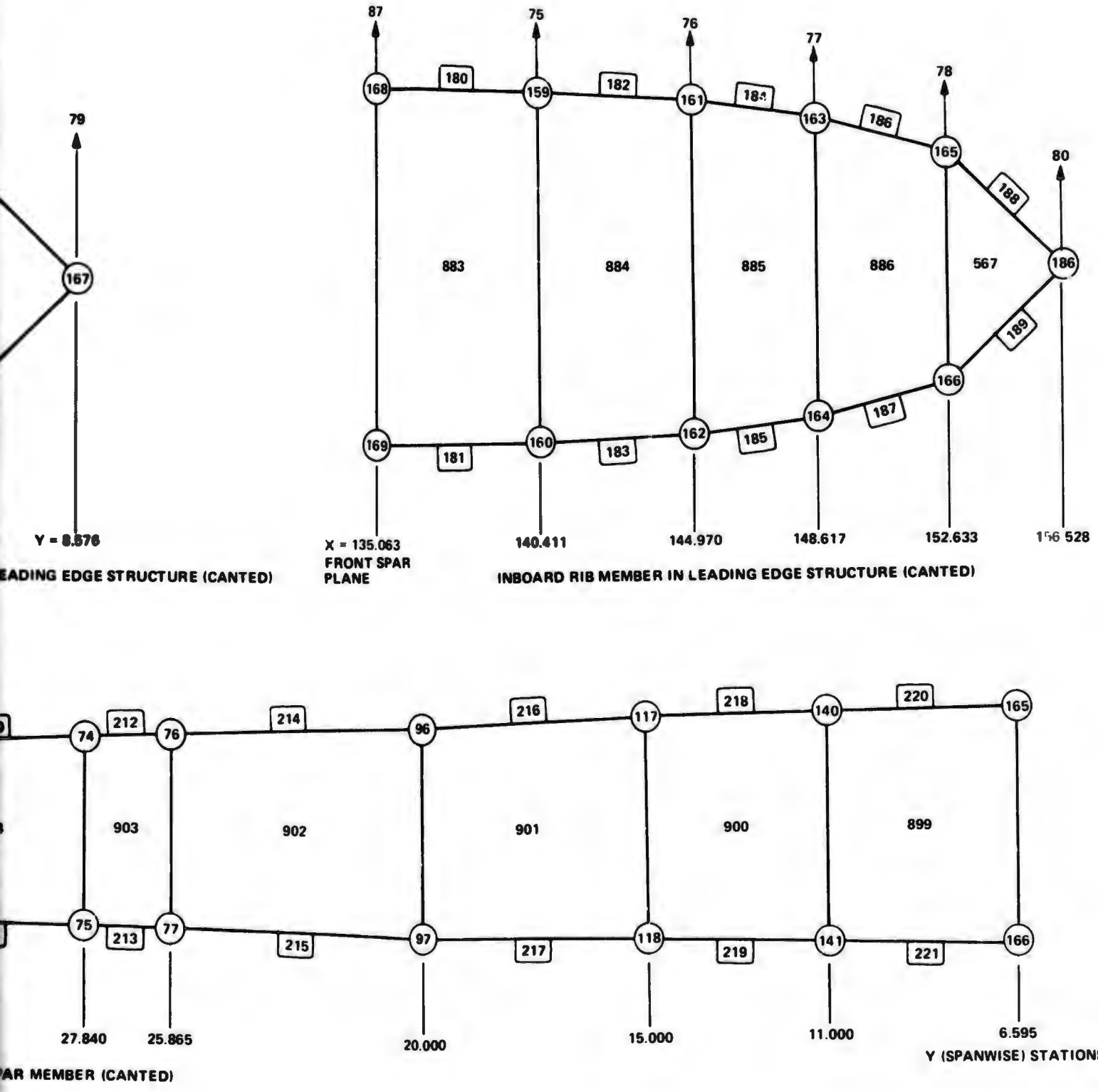

FIGURE A8. DISCRETE ELEMENT SUBDIVISION FOR LEADING EDGE SPAR AND INBOARD RIB

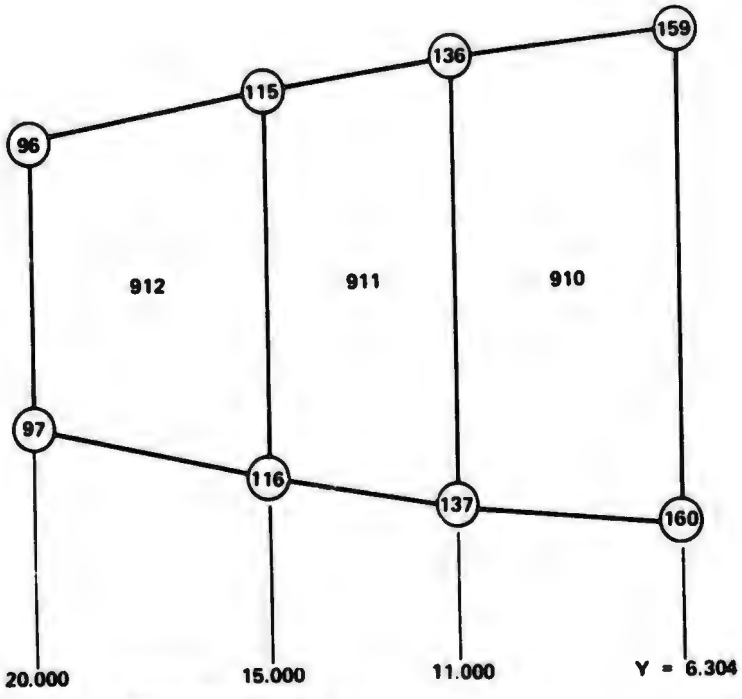

CROSS SECTION THRU X = 140.411
LEADING EDGE STRUCTURE – SHEAR PANELS

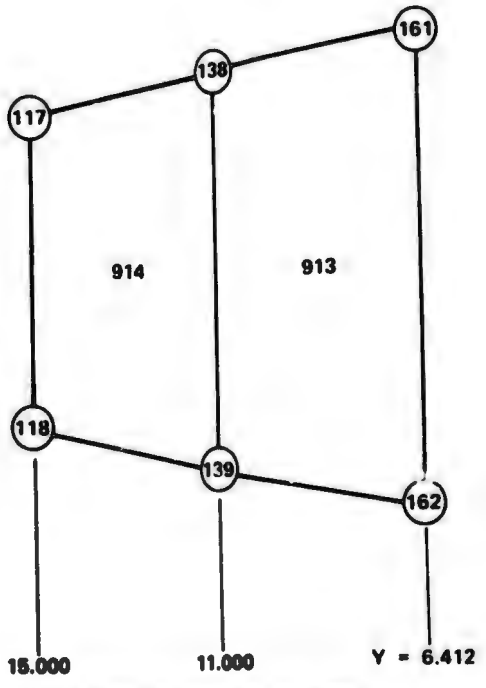

CROSS SECTION THRU X = 144.970
LEADING EDGE STRUCTURE – SHEAR PANELS

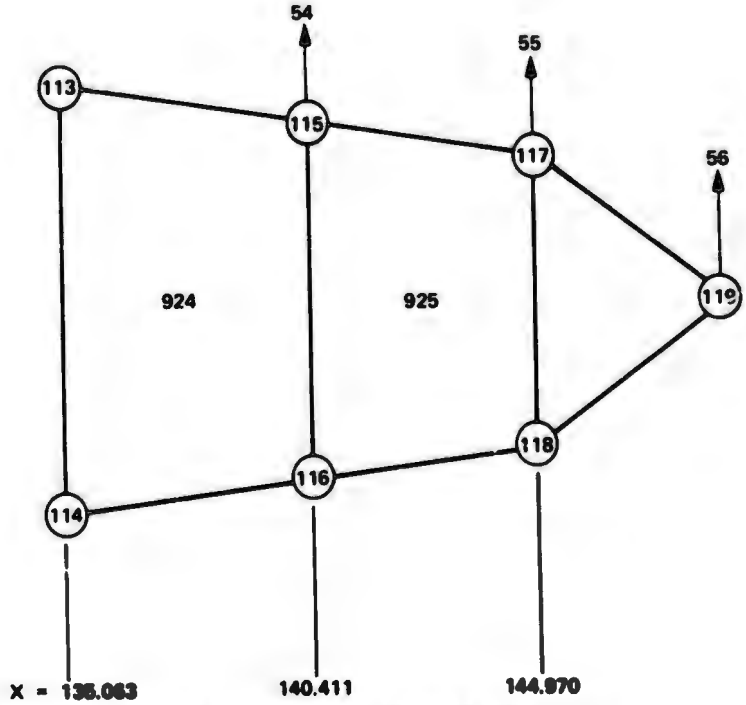

CROSS SECTION THRU LEADING EDGE
STRUCTURE AT Y = 15.000 – SHEAR PANELS

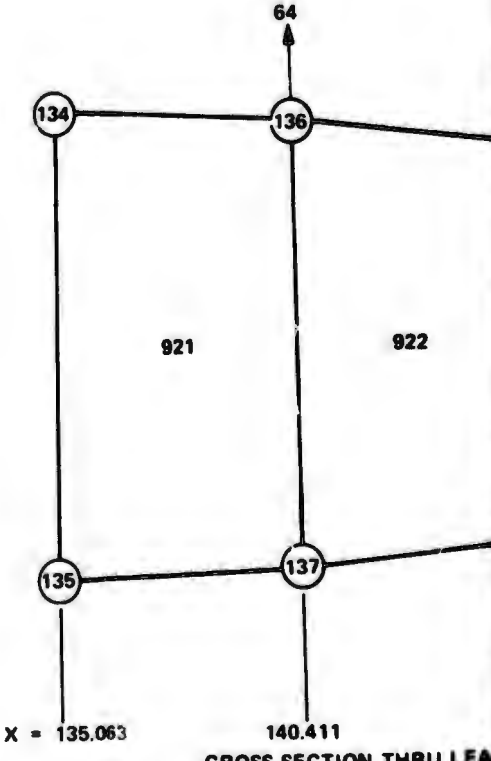

CROSS SECTION THRU LEA
STRUCTURE AT Y = 11.000

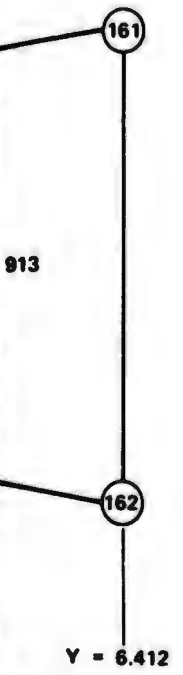

4.970
– SHEAR PANELS

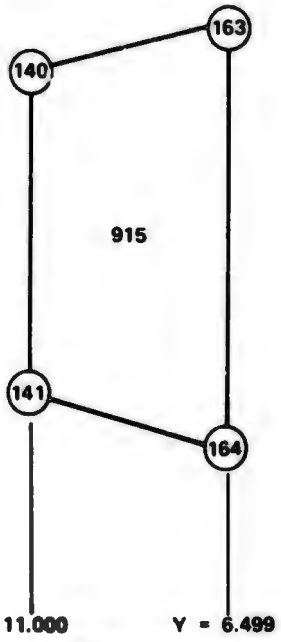

CROSS SECTION
THRU X = 148.617
LEADING EDGE
STRUCTURE –
SHEAR PANELS

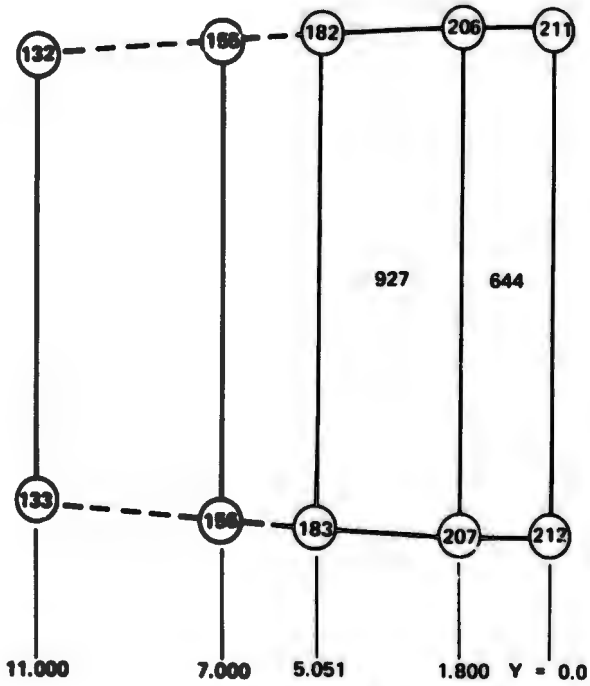

CROSS SECTION THRU X = 133.263 –
SHEAR PANELS

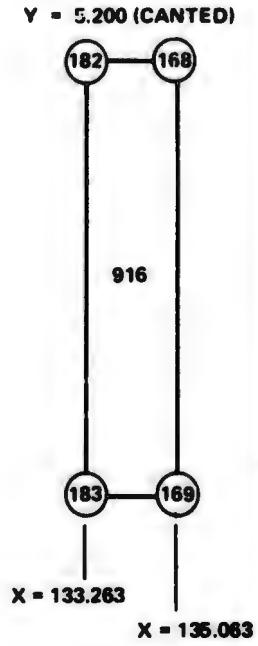

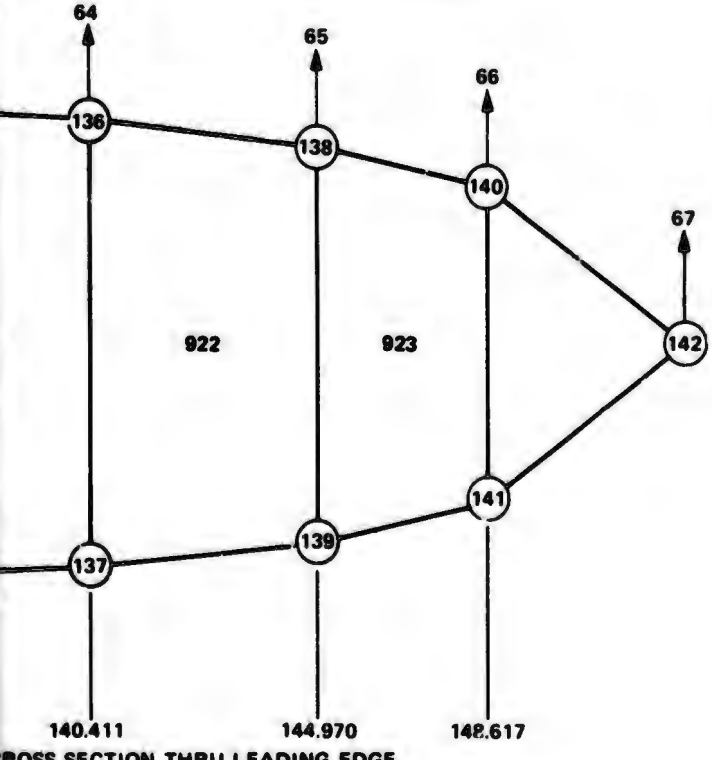

ROSS SECTION THRU LEADING EDGE
TRUCTURE AT Y = 11.000 – SHEAR PANELS

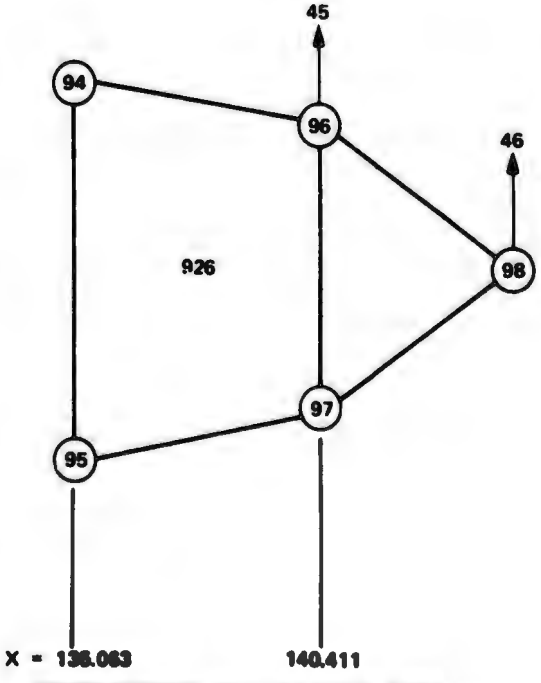

CROSS SECTION THRU LEADING EDGE
STRUCTURE AT Y = 20.000 – SHEAR PANELS

POS
LOA

ALL
MEA
MOD

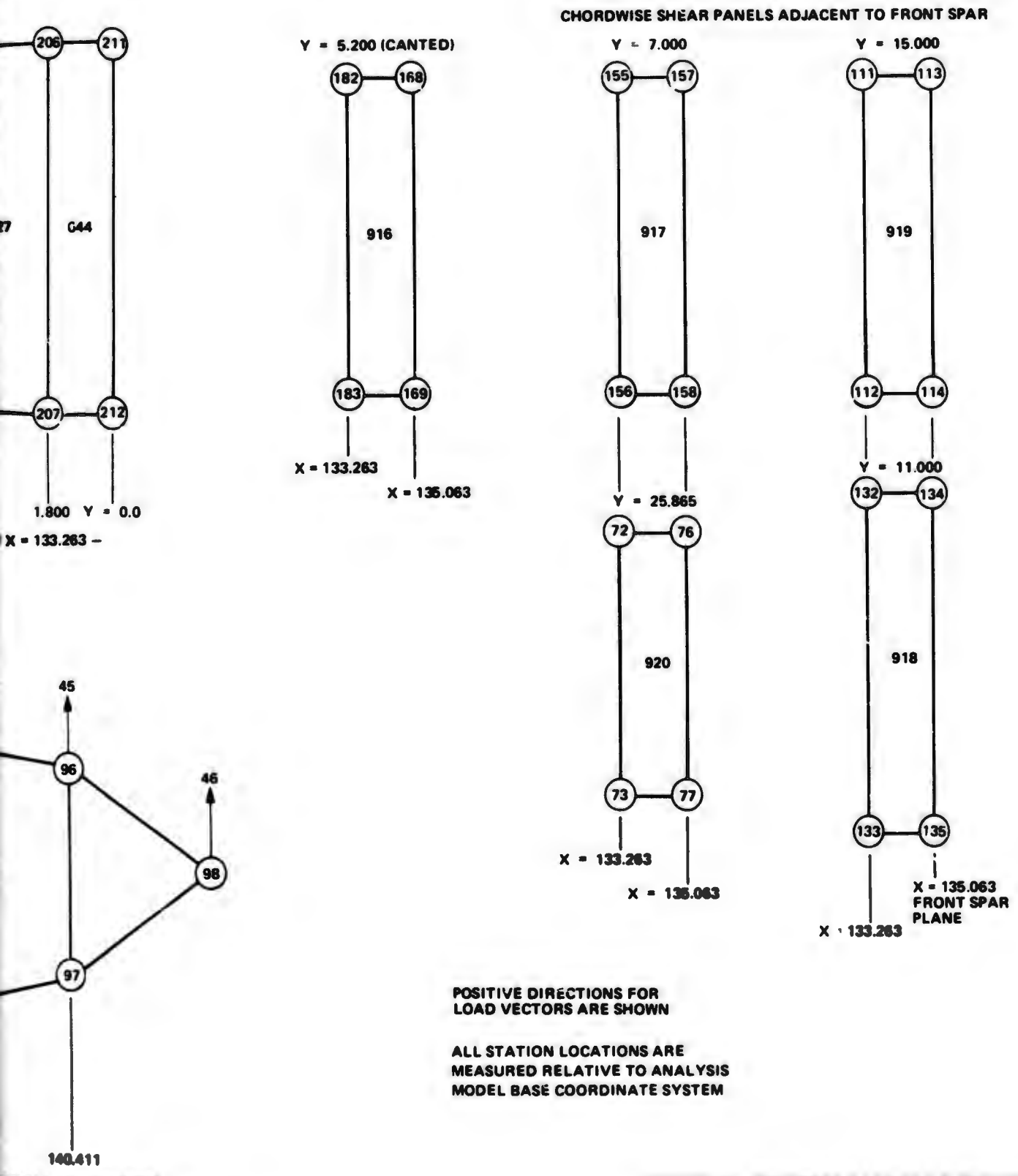

FIGURE A9. DISCRETE ELEMENT SUBDIVISION FOR LEADING EDGE SHEAR PANELS

BOTTOM VIEW

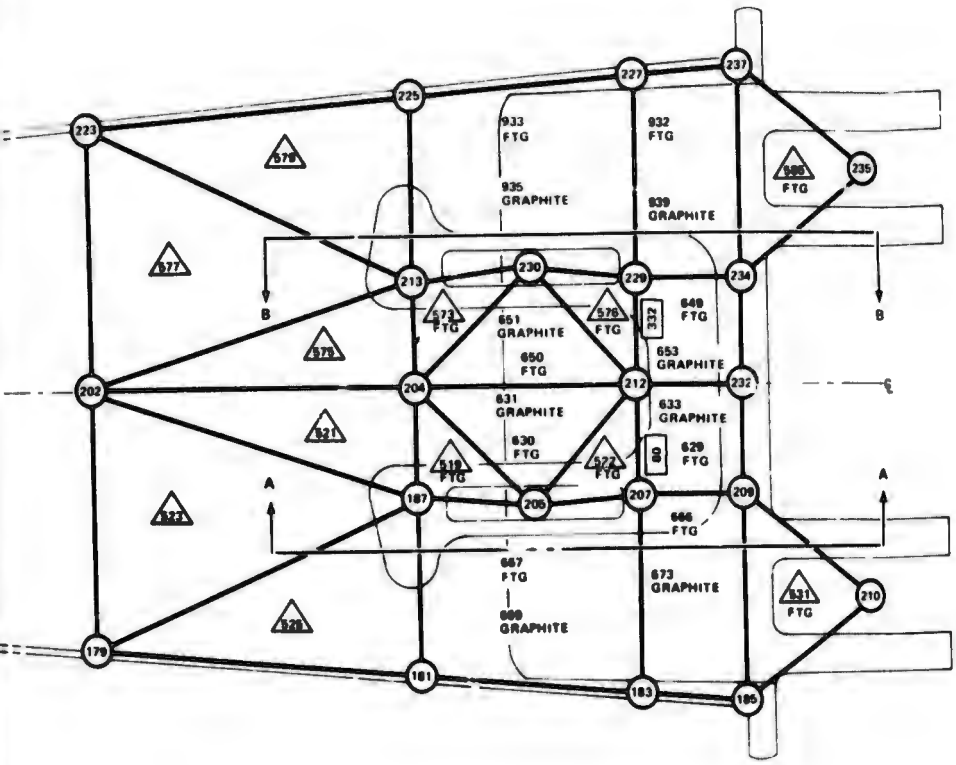
933 FTG
932 FTG
935 GRAPHITE
939 GRAPHITE
649 FTG
651 GRAPHITE
650 FTG
653 GRAPHITE
631 GRAPHITE
633 GRAPHITE
630 FTG
629 FTG
666 FTG
667 FTG
669 GRAPHITE
673 GRAPHITE
B
A
223
225
227
237
235
213
230
229
234
202
204
212
232
187
206
207
209
210
179
181
183
185

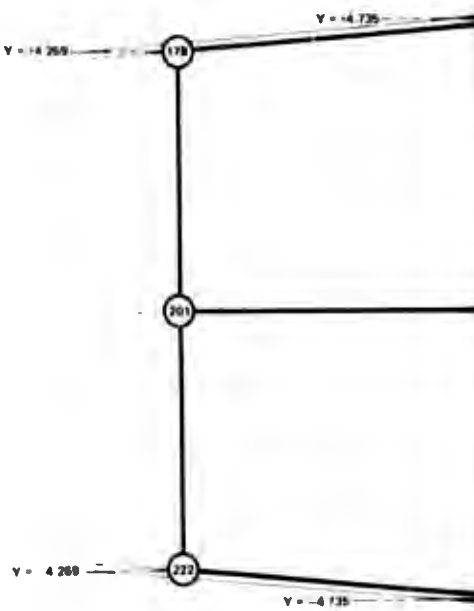
Y = 4 269
Y = 4 735
Y = -4 269
Y = -4 735
178
201
222

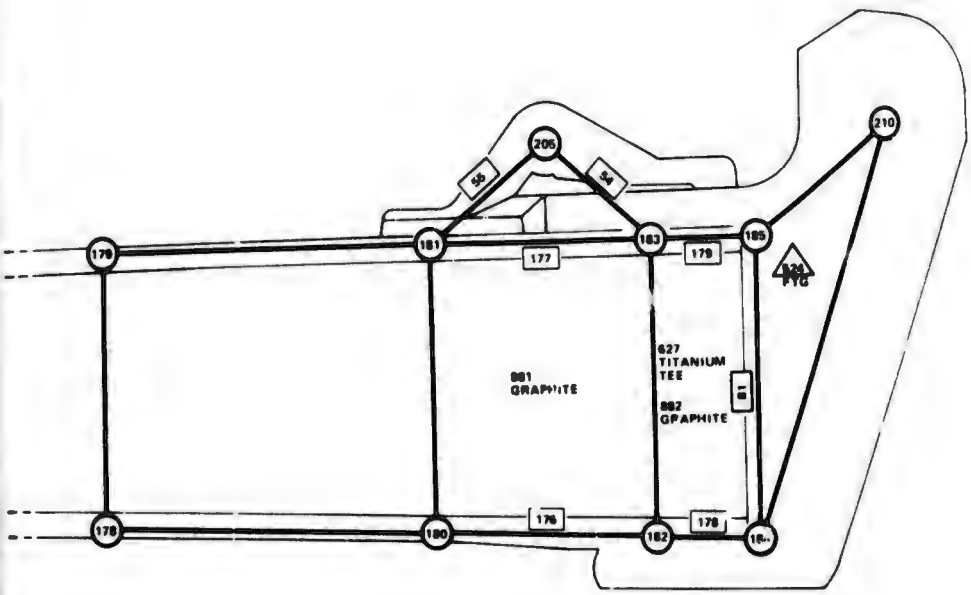
206
210
179
181
183
185
177
179
627 TITANIUM TEE
881 GRAPHITE
882 GRAPHITE
178
180
182
176
178

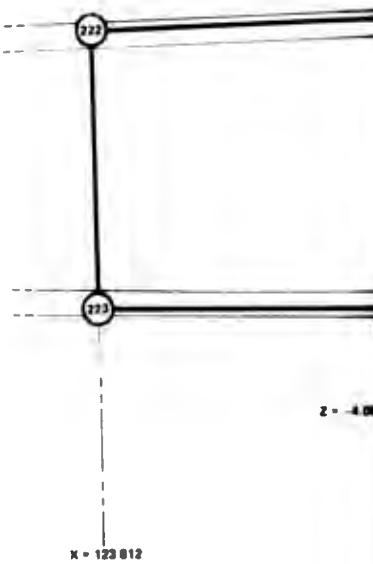
222
223
X = 123 812

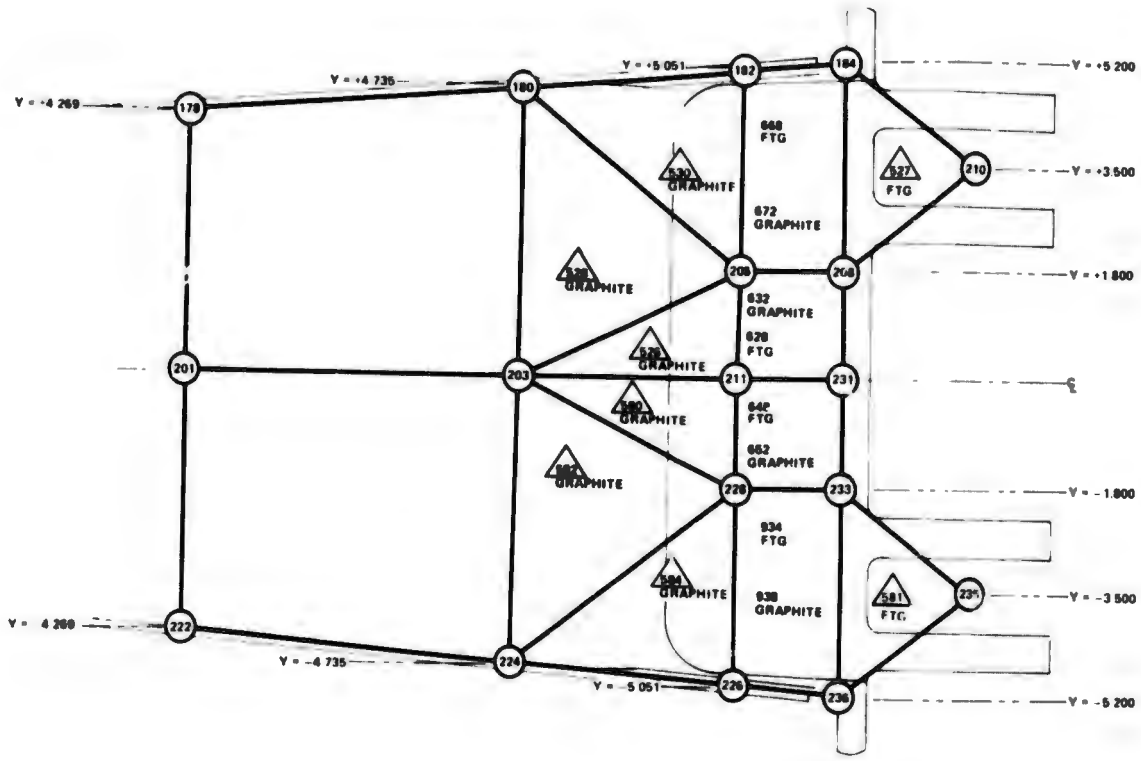

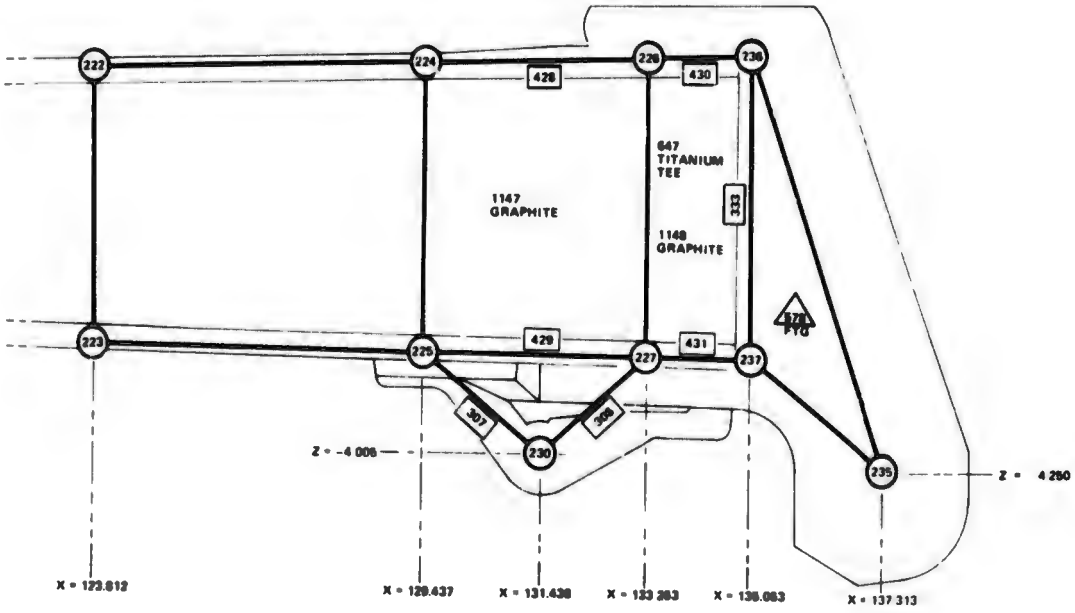

NOTES

NUMBERS ENCLO

NUMBERS ENCLO

BAR ELEMENTS, 573 AND 576 REP

TRIANGULAR EL PORTIONS OF TH

NODES NO 210 A

ALL STATION LO

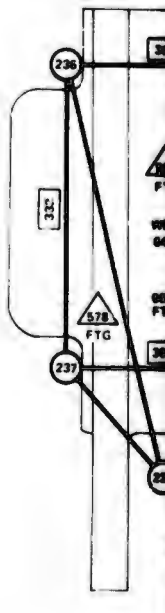

FIGURE A10

TOP VIEW

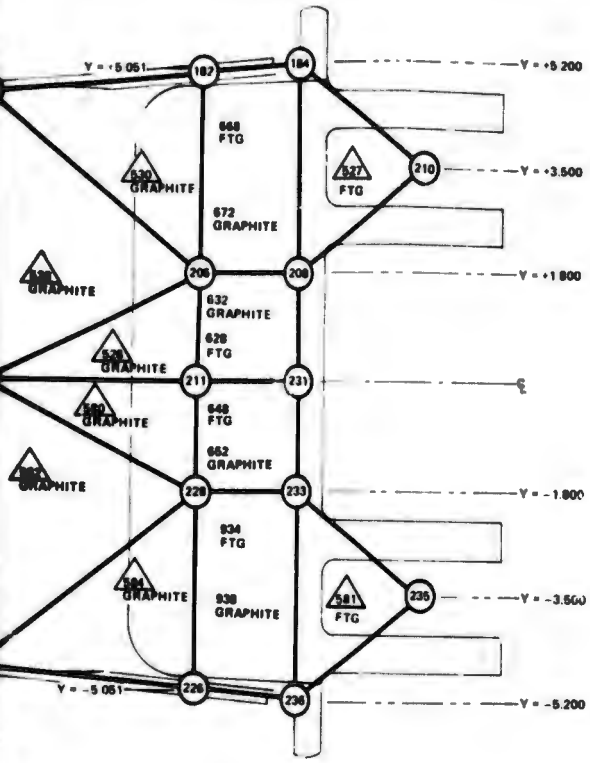

NOTES

NUMBERS ENCLOSED IN SQUARE IDENTIFY AXIAL BAR ELEMENTS THUS [XXX]

NUMBERS ENCLOSED IN TRIANGLES IDENTIFY TRIANGULAR PLATE ELEMENTS THUS, △XXX

BAR ELEMENTS, NUMBERS 54, 55, 306, 307 AND TRIANGULAR ELEMENTS, NUMBERS 519, 522, 573 AND 576 REPRESENT DIFFERENT PARTS OF THE 3553456 FITTING AS ILLUSTRATED

TRIANGULAR ELEMENTS, NUMBERS 524, 527, 529, 531, 578, 581, 583 AND 585 REPRESENT THE PORTIONS OF THE Z3569977 FITTING ASSEMBLY IN THE REGION FORWARD OF STATION 135.063

NODES NO 210 AND 235 ARE FIXED SUPPORT POINTS

ALL STATION LOCATIONS ARE MEASURED RELATIVE TO ANALYSIS MODEL BASE COORDINATE SYETEM

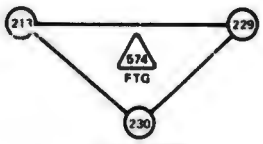

SECTION B B

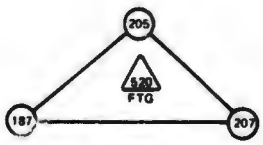

SECTION A A

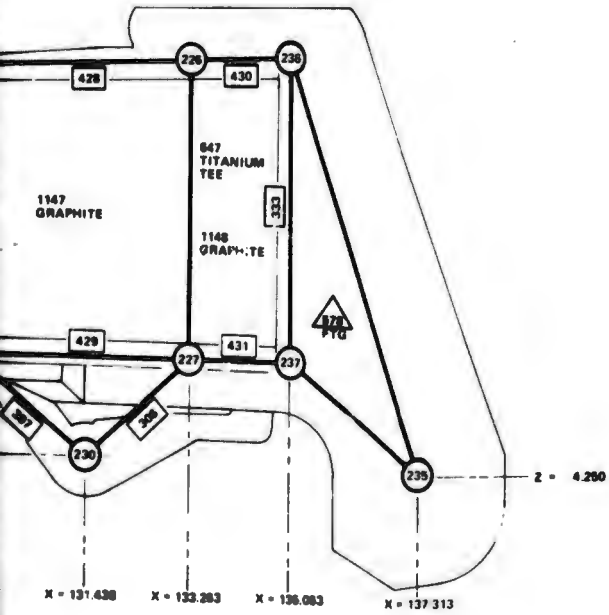

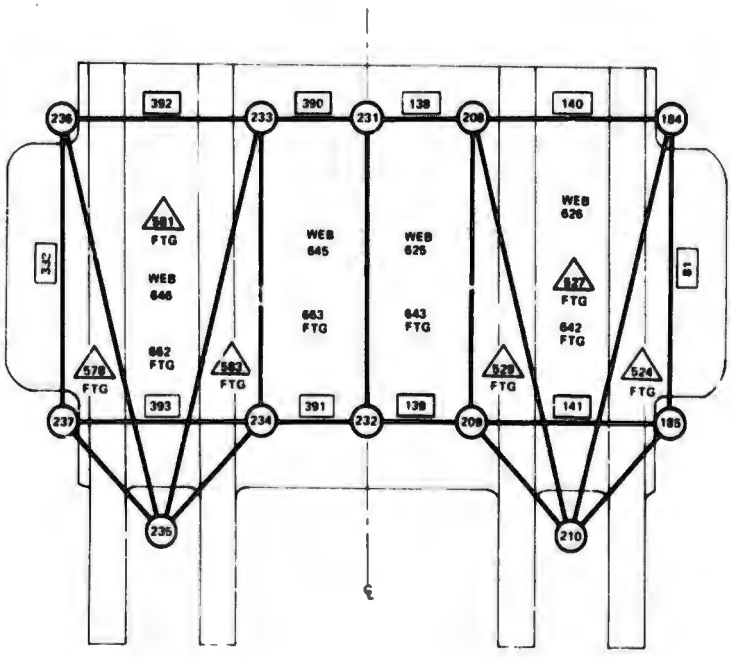

FIGURE A10. DISCRETE ELEMENT SUBDIVISION FOR IDEALIZED PIVOT FITTING AND ADJACENT STRUCTURE

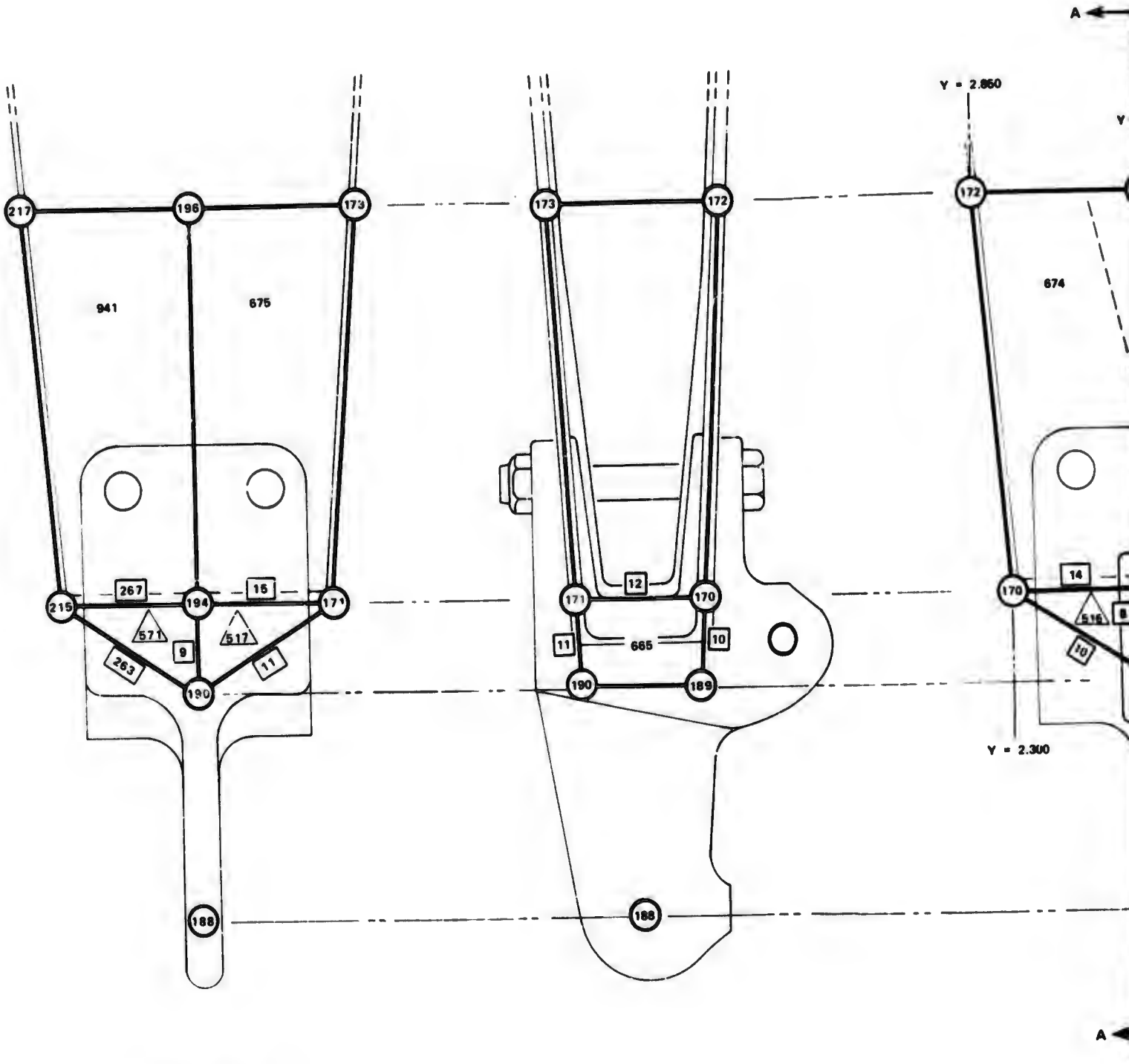
A
Y = 2.850
217
196
173
941
675
215
267
194
15
171
571
517
9
263
11
190
188
173
172
12
171
170
11
665
10
190
189
188
172
674
170
14
516
10
Y = 2.300
A

BOTTOM VIEW

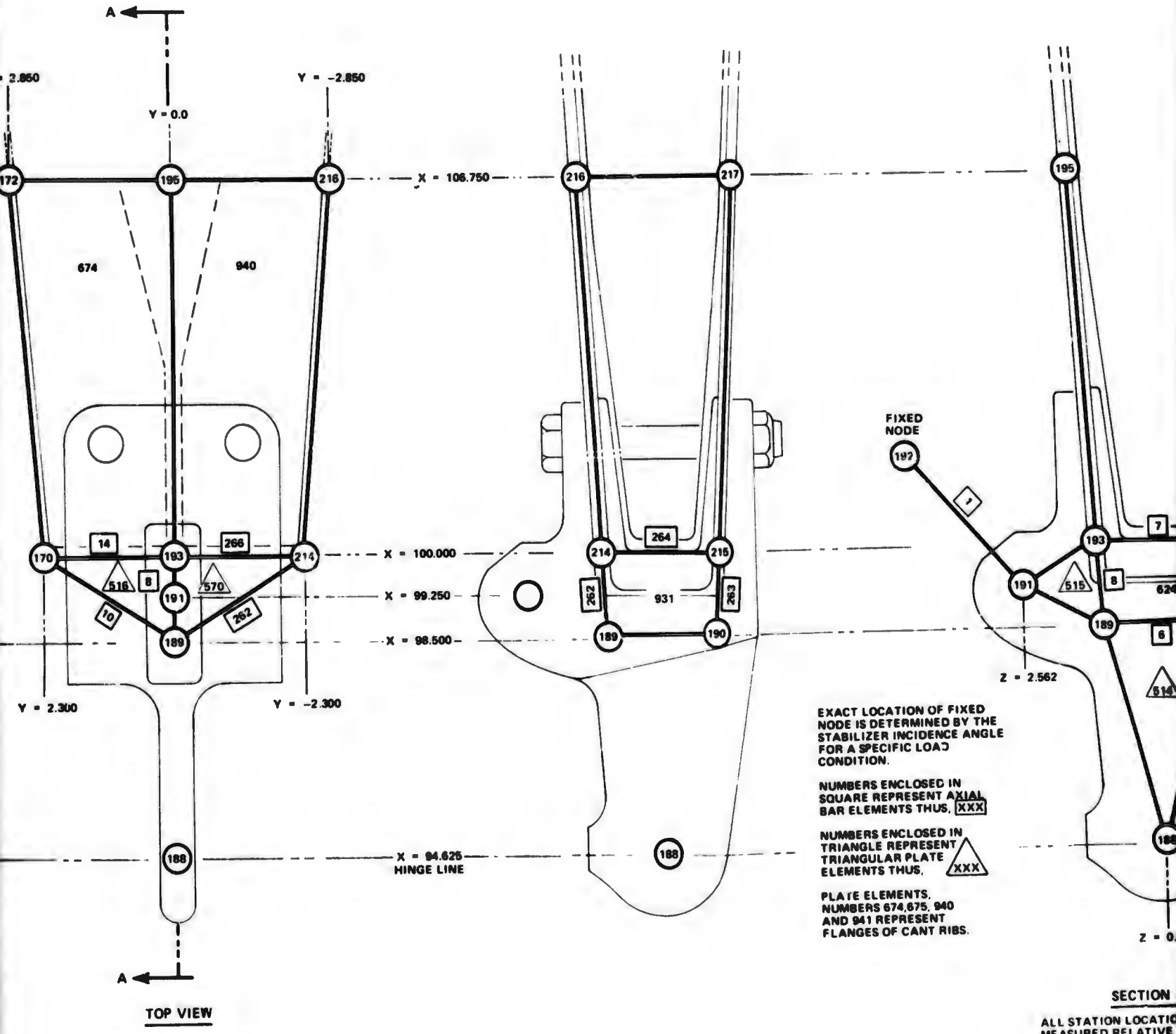

EXACT LOCATION OF FIXED NODE IS DETERMINED BY THE STABILIZER INCIDENCE ANGLE FOR A SPECIFIC LOAD CONDITION.

NUMBERS ENCLOSED IN SQUARE REPRESENT AXIAL BAR ELEMENTS THUS, [XXX]

NUMBERS ENCLOSED IN TRIANGLE REPRESENT TRIANGULAR PLATE ELEMENTS THUS, △XXX

PLATE ELEMENTS, NUMBERS 674,675, 940 AND 941 REPRESENT FLANGES OF CANT RIBS.

ALL STATION LOCATIO
MEASURED RELATIVE
MODEL BASE COORDIN

**FIGURE A11. DISCRETE ELEMENT
FOR IDEALIZED ACT
TING AND ADJACEN**

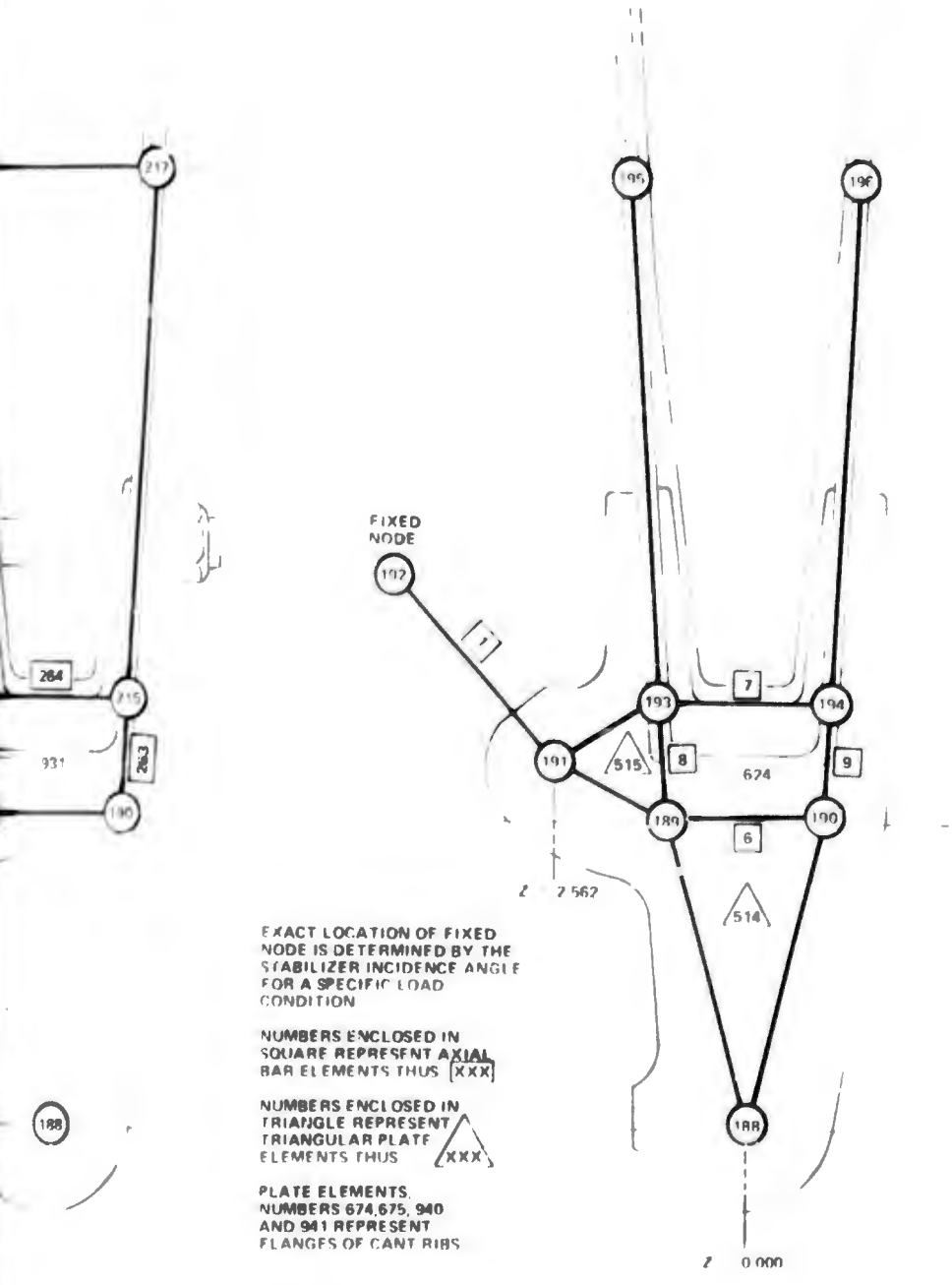

SECTION A A

ALL STATION LOCATIONS ARE MEASURED RELATIVE TO ANALYSIS MODEL BASE COORDINATE SYSTEM

FIGURE A11. DISCRETE ELEMENT SUBDIVISION FOR IDEALIZED ACTUATOR FITTING AND ADJACENT STRUCTURE

APPENDIX B

STRESS ANALYSIS RESULTS - LOAD CONDITIONS D and F

Limit stresses for load condition D determined by discrete element analysis (described in Section 2) are shown in Figure B1 through B10. The portions of the structure investigated for the critical up-load condition (load condition F) are shown in Figures B11 and B12.

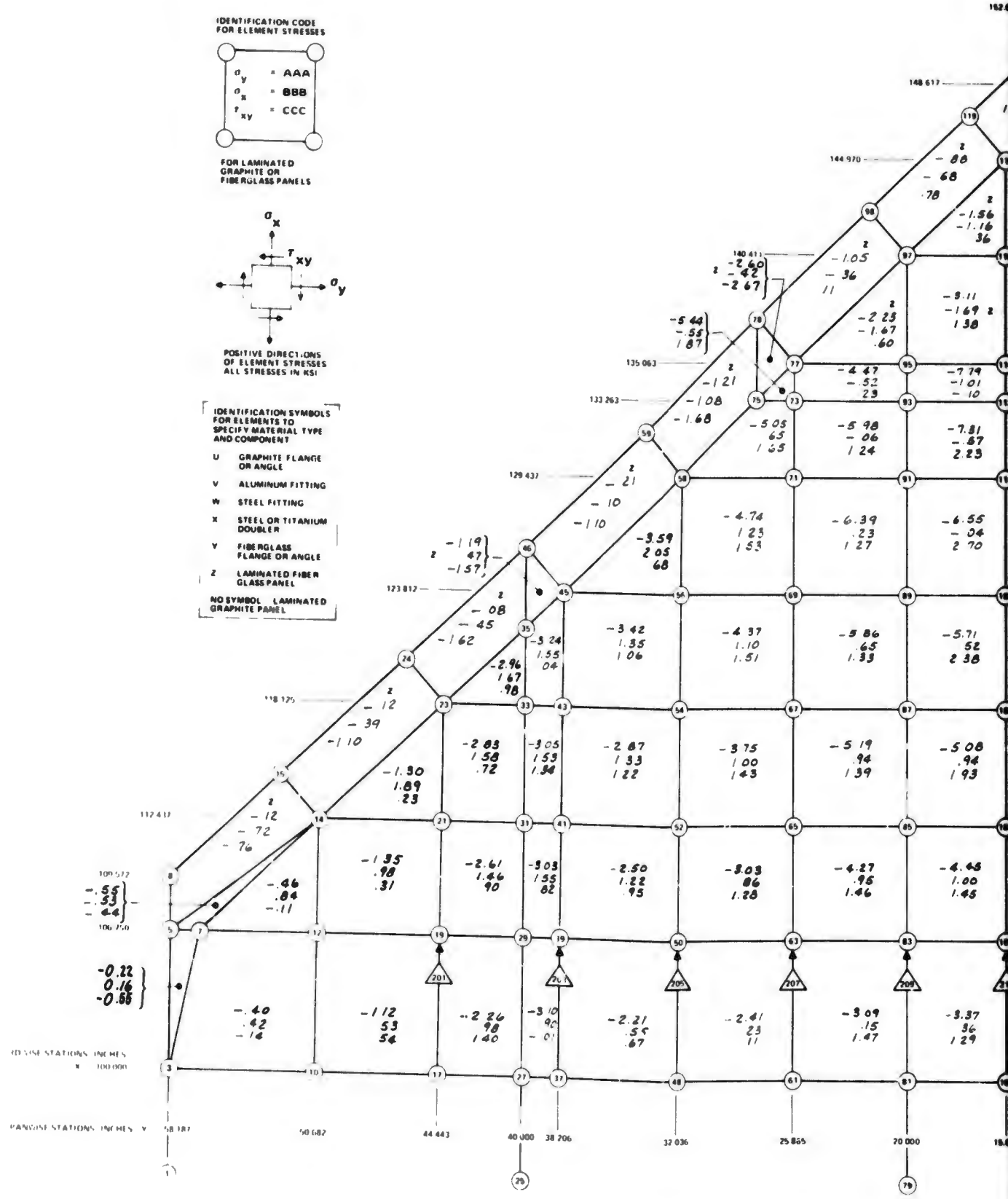
IDENTIFICATION CODE FOR ELEMENT STRESSES
σ_y = AAA
σ_x = BBB
τ_{xy} = CCC
FOR LAMINATED GRAPHITE OR FIBERGLASS PANELS
σ_x
τ_{xy}
σ_y
POSITIVE DIRECTIONS OF ELEMENT STRESSES ALL STRESSES IN KSI
IDENTIFICATION SYMBOLS FOR ELEMENTS TO SPECIFY MATERIAL TYPE AND COMPONENT
U GRAPHITE FLANGE OR ANGLE
V ALUMINUM FITTING
W STEEL FITTING
X STEEL OR TITANIUM DOUBLER
Y FIBERGLASS FLANGE OR ANGLE
Z LAMINATED FIBER GLASS PANEL
NO SYMBOL LAMINATED GRAPHITE PANEL
148 617
144 970
140 411
135 063
133 263
129 437
123 812
118 125
112 417
109 572
106 750
BUTTLINE STATIONS INCHES Y 58 187 50 682 44 443 40 000 38 206 32 036 25 865 20 000
STATIONS INCHES X 100 000

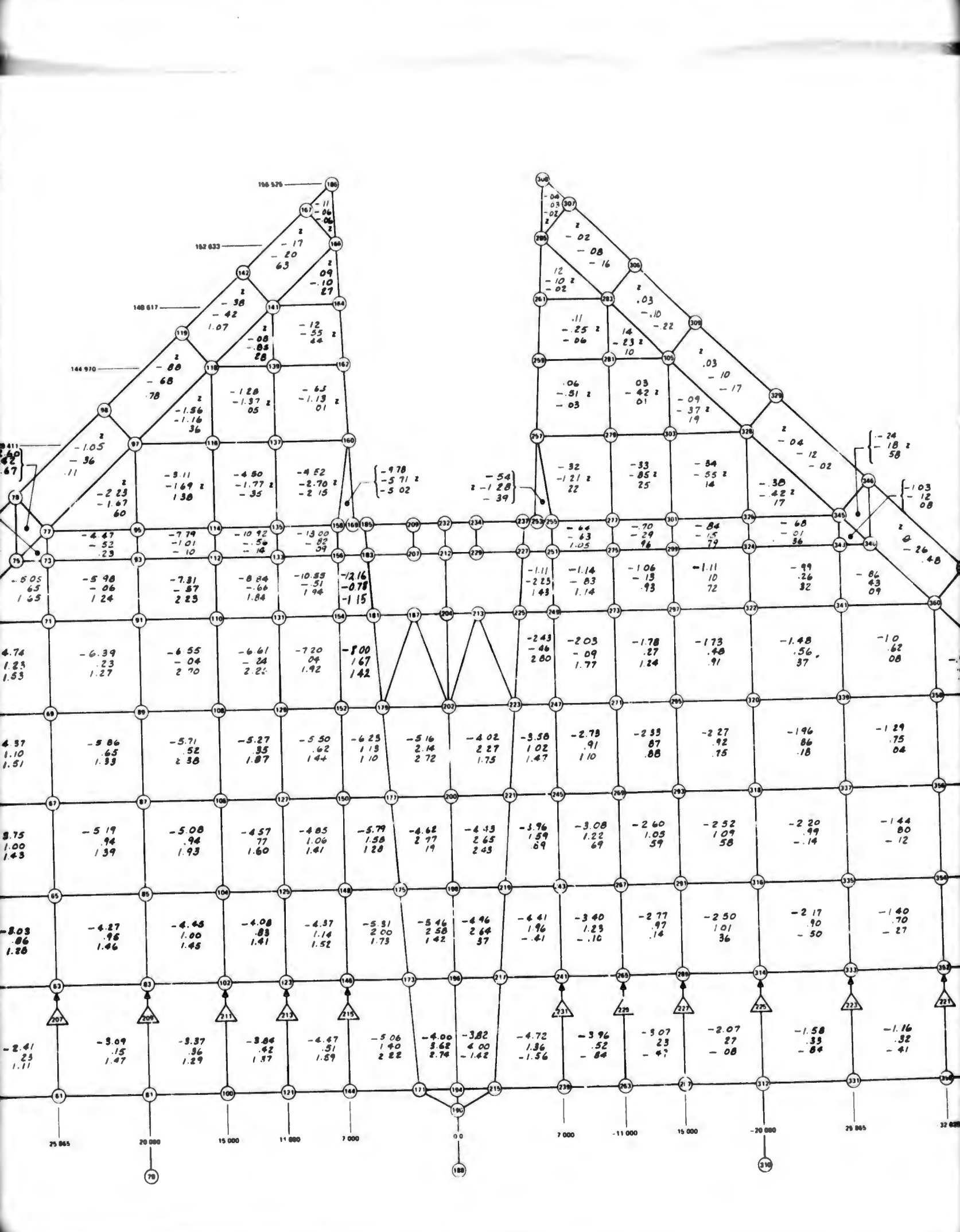

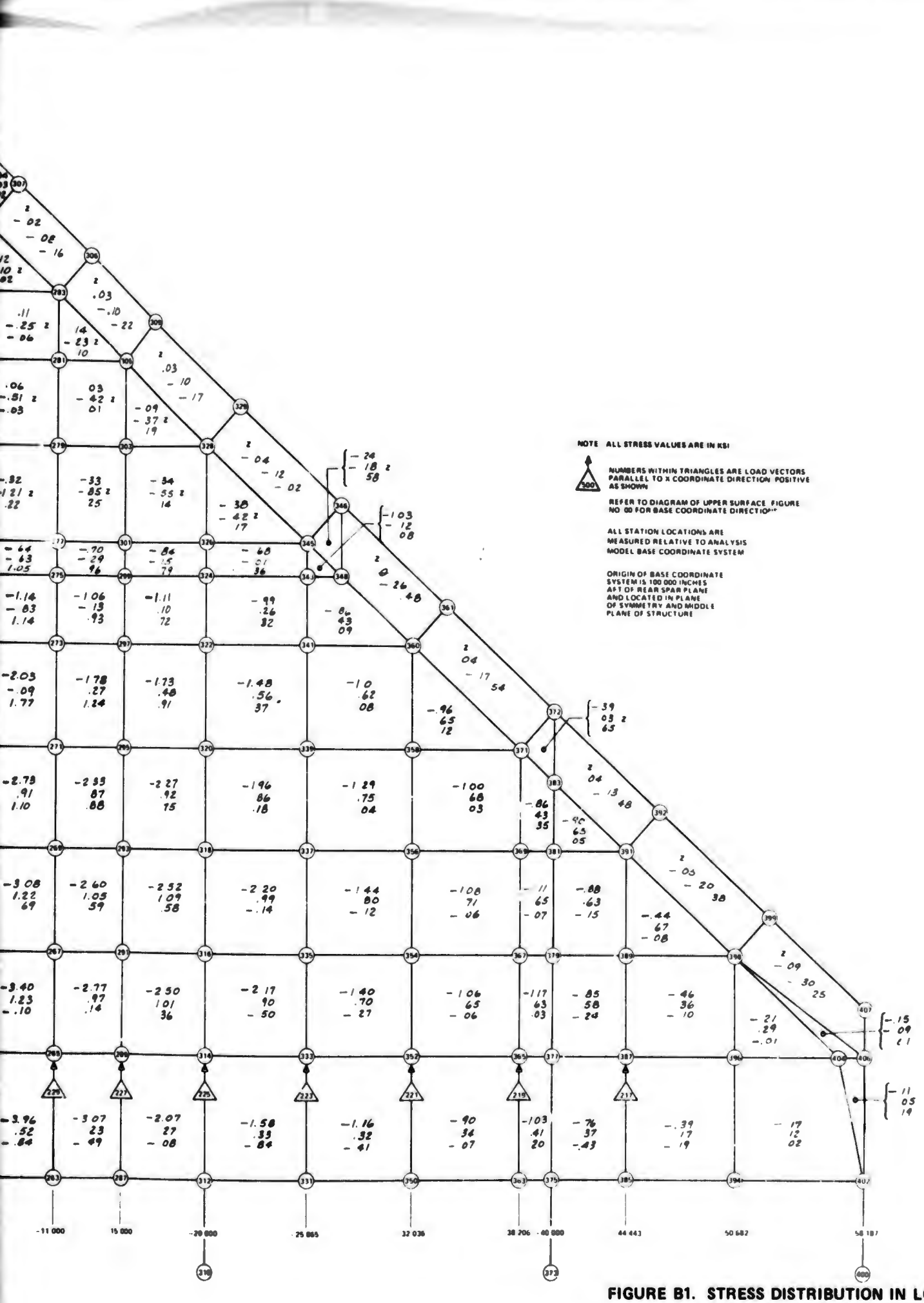

FIGURE B1. STRESS DISTRIBUTION IN LOWER PANEL AND LEADING EDGE – LOAD CONDITION D

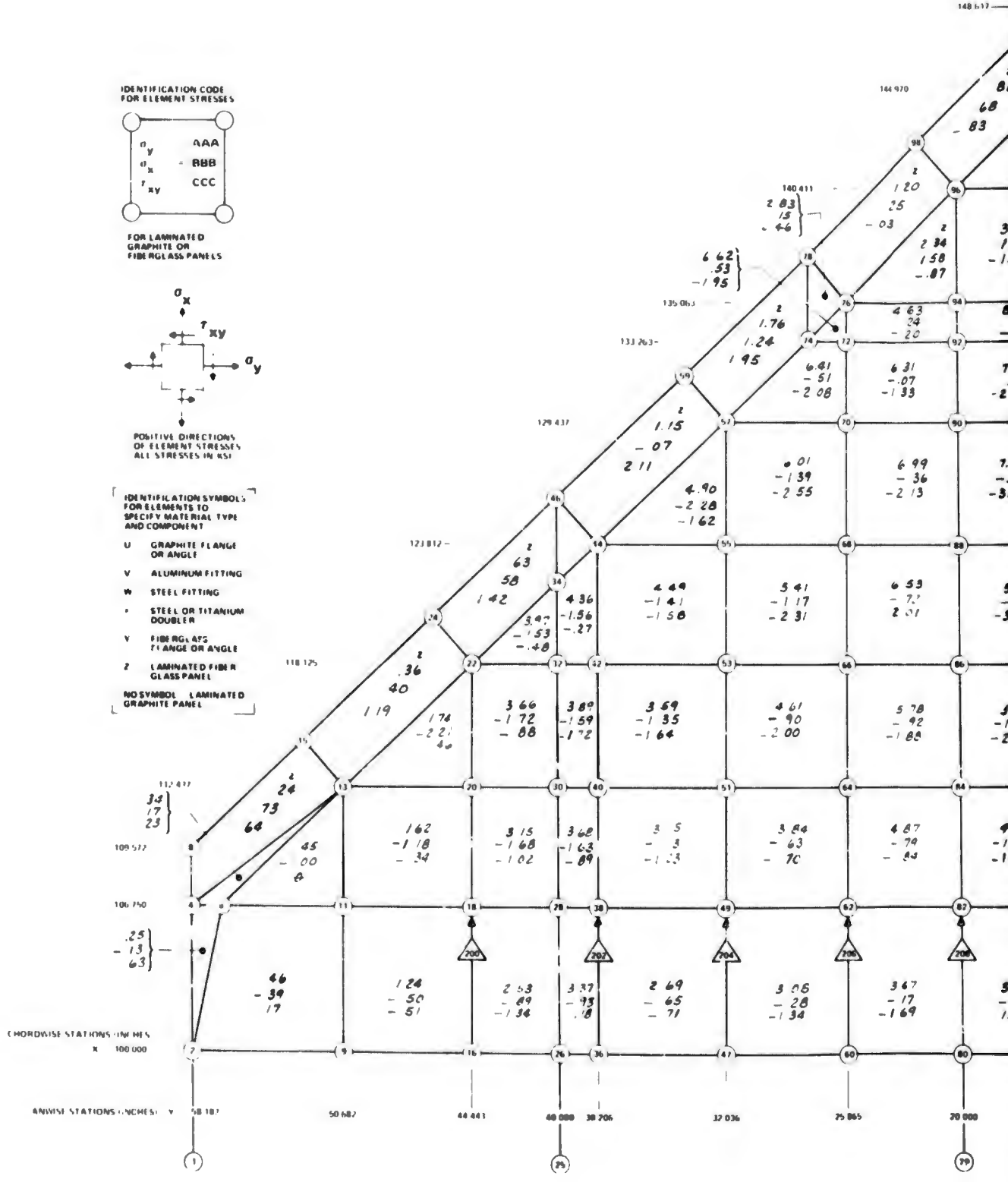
IDENTIFICATION CODE FOR ELEMENT STRESSES
AAA
BBB
CCC
FOR LAMINATED GRAPHITE OR FIBERGLASS PANELS
POSITIVE DIRECTIONS OF ELEMENT STRESSES ALL STRESSES IN KSI
IDENTIFICATION SYMBOLS FOR ELEMENTS TO SPECIFY MATERIAL TYPE AND COMPONENT
U GRAPHITE FLANGE OR ANGLE
V ALUMINUM FITTING
W STEEL FITTING
STEEL OR TITANIUM DOUBLER
Y FIBERGLASS FLANGE OR ANGLE
Z LAMINATED FIBER GLASS PANEL
NO SYMBOL LAMINATED GRAPHITE PANEL
CHORDWISE STATIONS (INCHES) X
ANWISE STATIONS (INCHES) Y

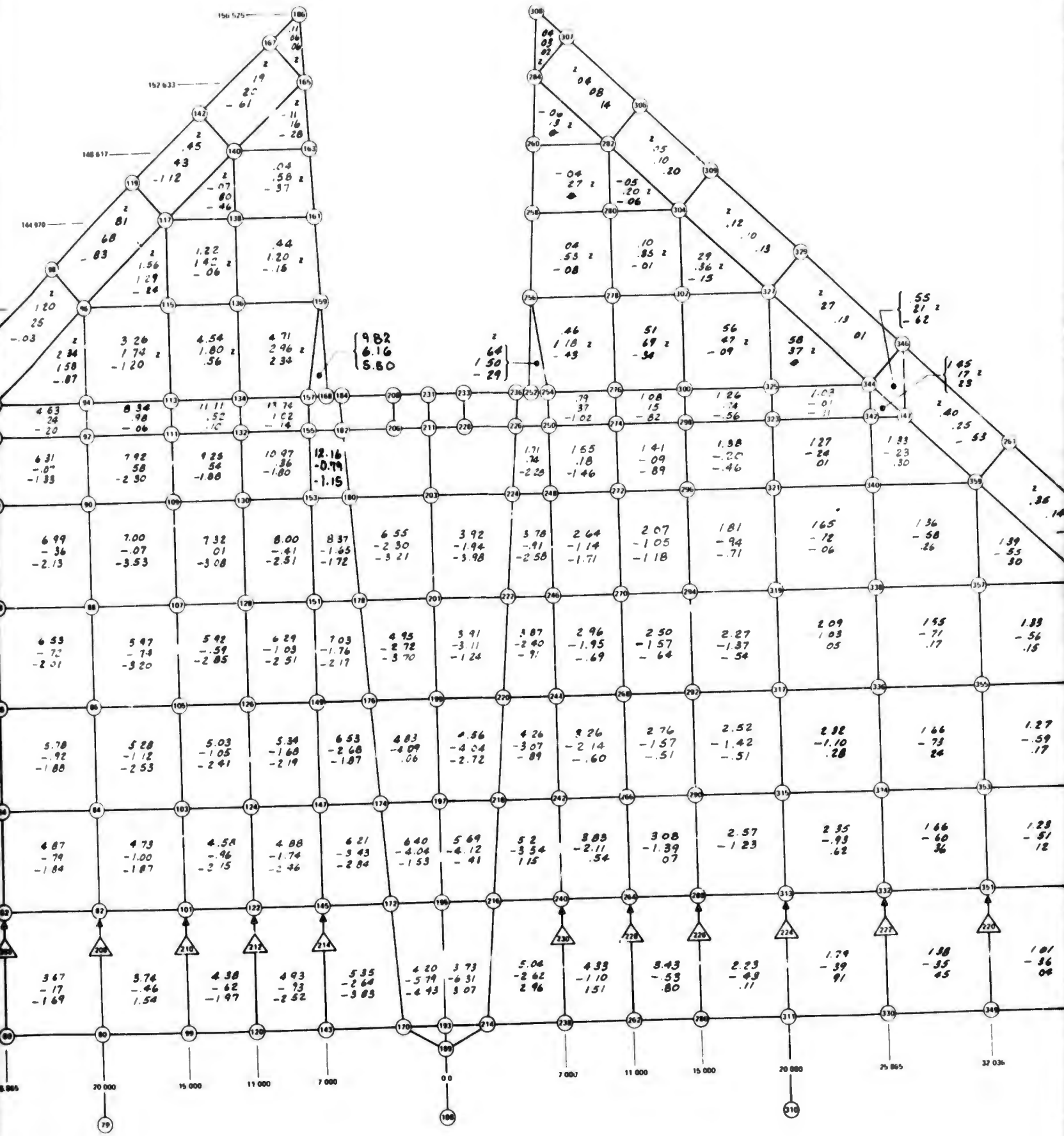

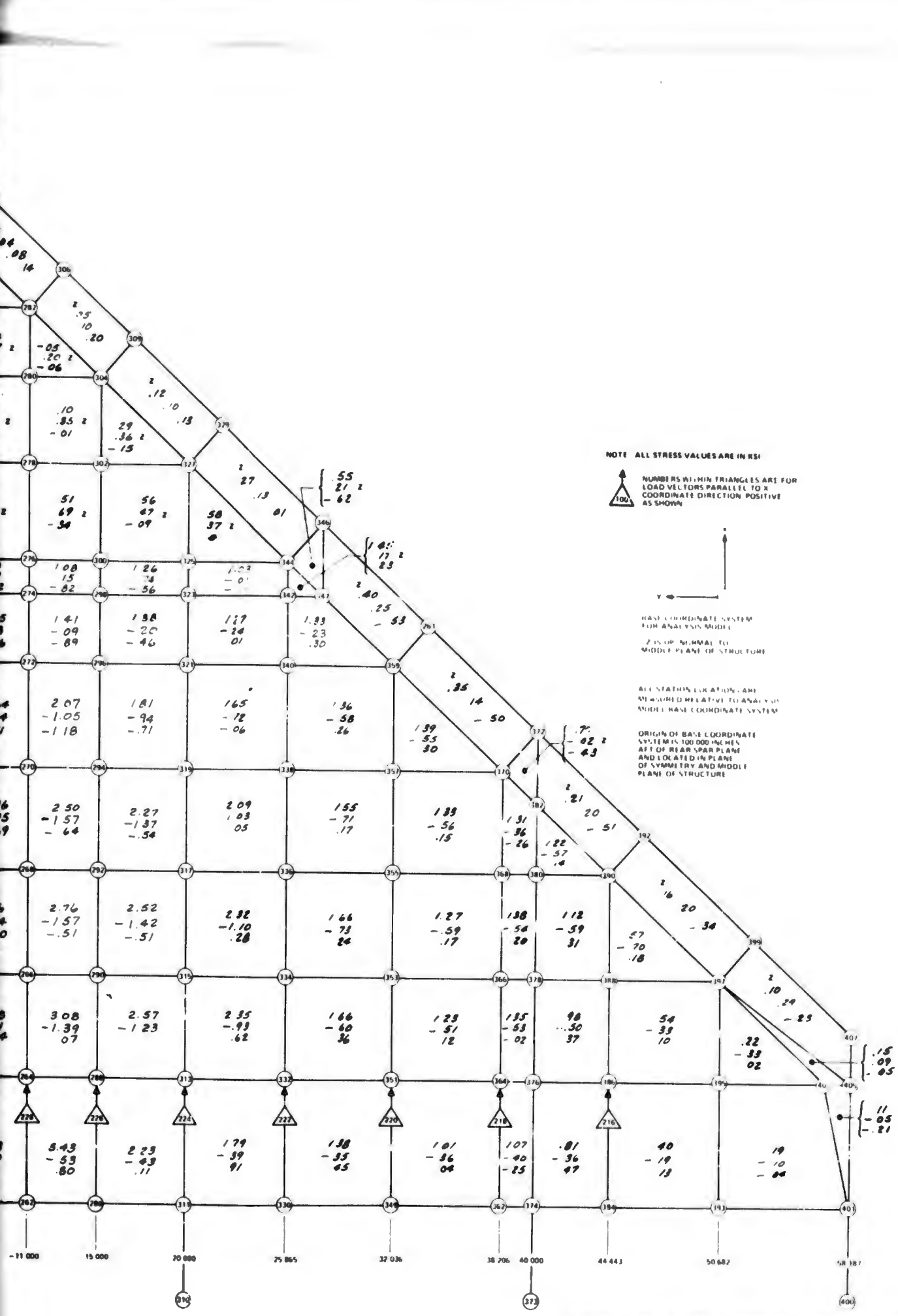

FIGURE B2. STRESS DISTRIBUTION IN UPPER PANEL AND LEADING EDGE – LOAD CONDITION D

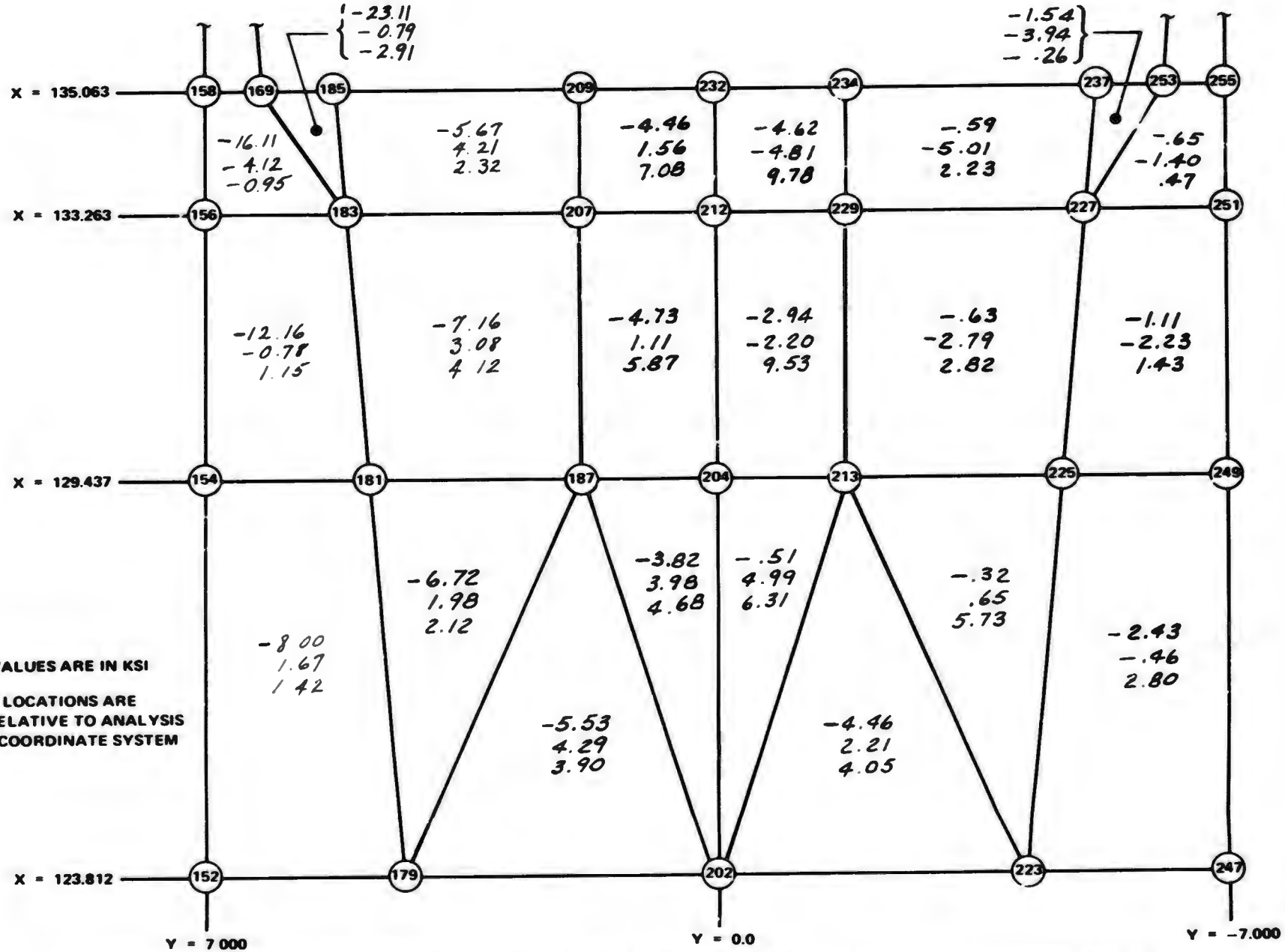

NOTE:
ALL STRESS VALUES ARE IN KSI

ALL STATION LOCATIONS ARE MEASURED RELATIVE TO ANALYSIS MODEL BASE COORDINATE SYSTEM

FIGURE B3. STRESS DISTRIBUTION IN LOWER PANEL ADJACENT TO PIVOT FITTING – LOAD CONDITION D

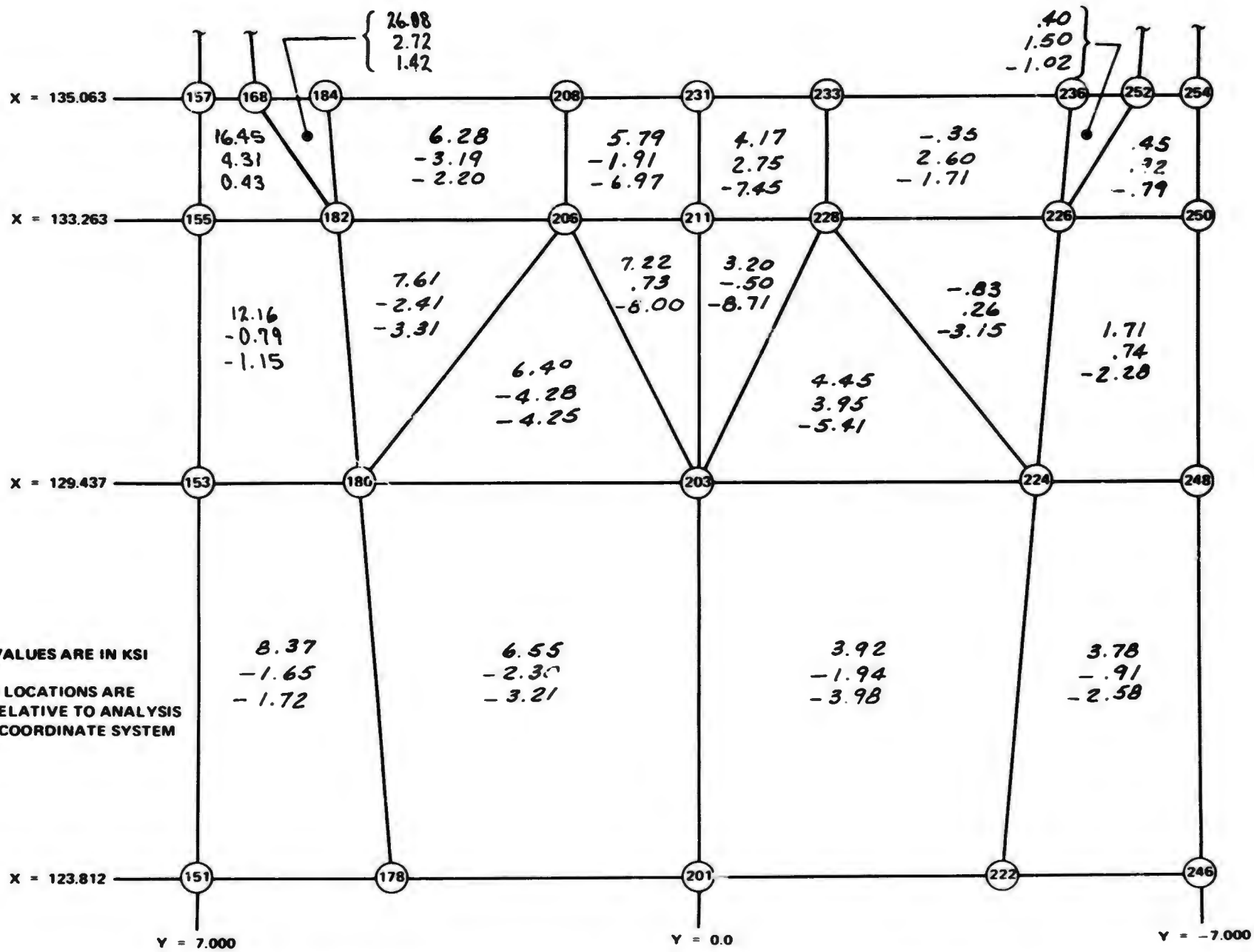

FIGURE B4. STRESS DISTRIBUTION IN UPPER PANEL ADJACENT TO PIVOT FITTING – LOAD CONDITION D

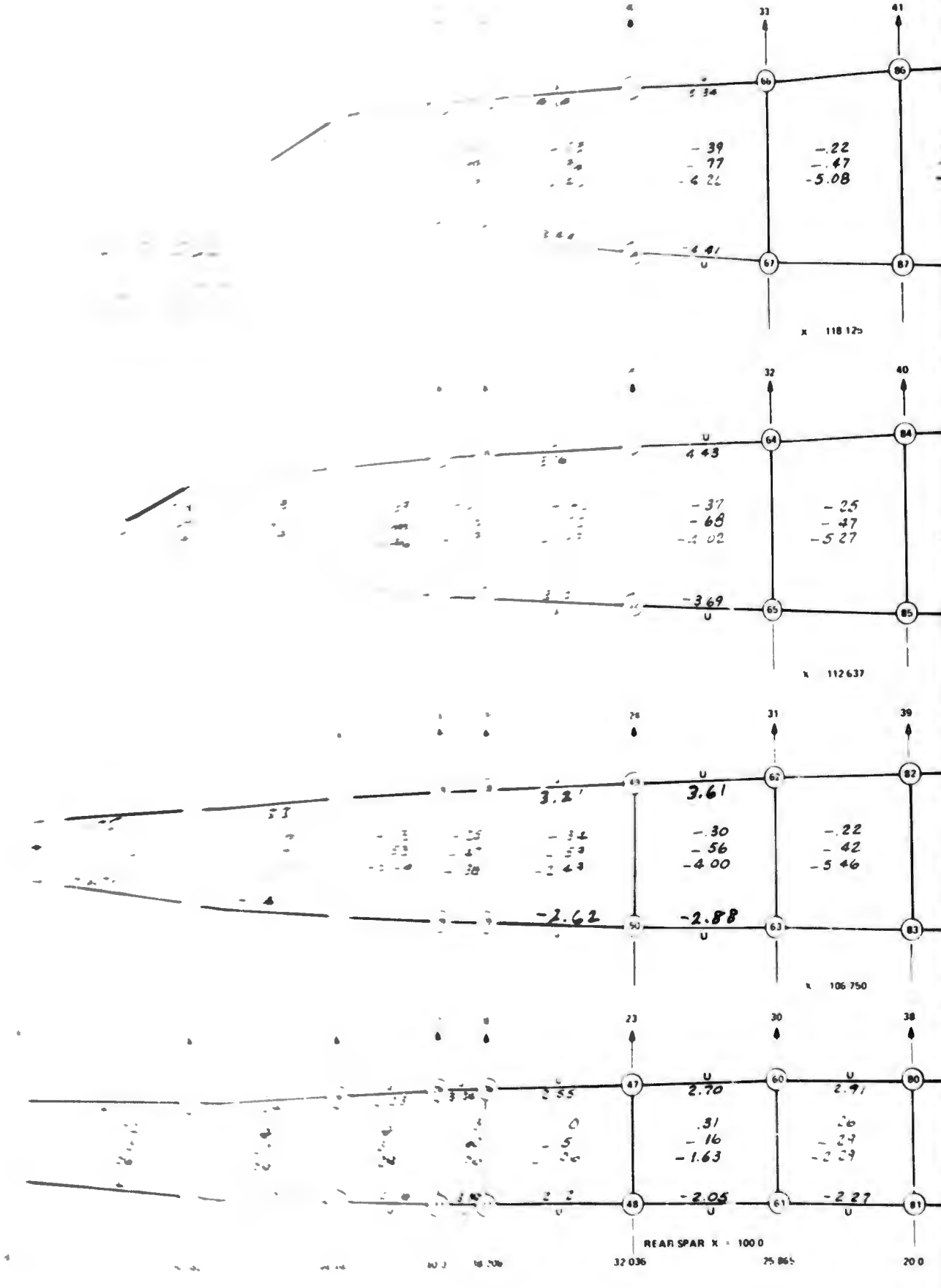
33
41
66
86
-.39
-.77
-6.26
-.22
-.47
-5.08
-4.81
U
67
87
X 118.125
32
40
64
84
U
4.43
-.37
-.68
-4.02
-.25
-.47
-5.27
-3.69
U
65
85
X 112.637
31
39
62
82
U
3.61
-.30
-.56
-4.00
-.22
-.42
-5.46
-2.62
-2.88
U
63
83
X 106.750
30
38
U
2.70
U
2.91
.31
-.16
-1.63
-2.05
U
61
X 100.0
32.036
25.865
20.0

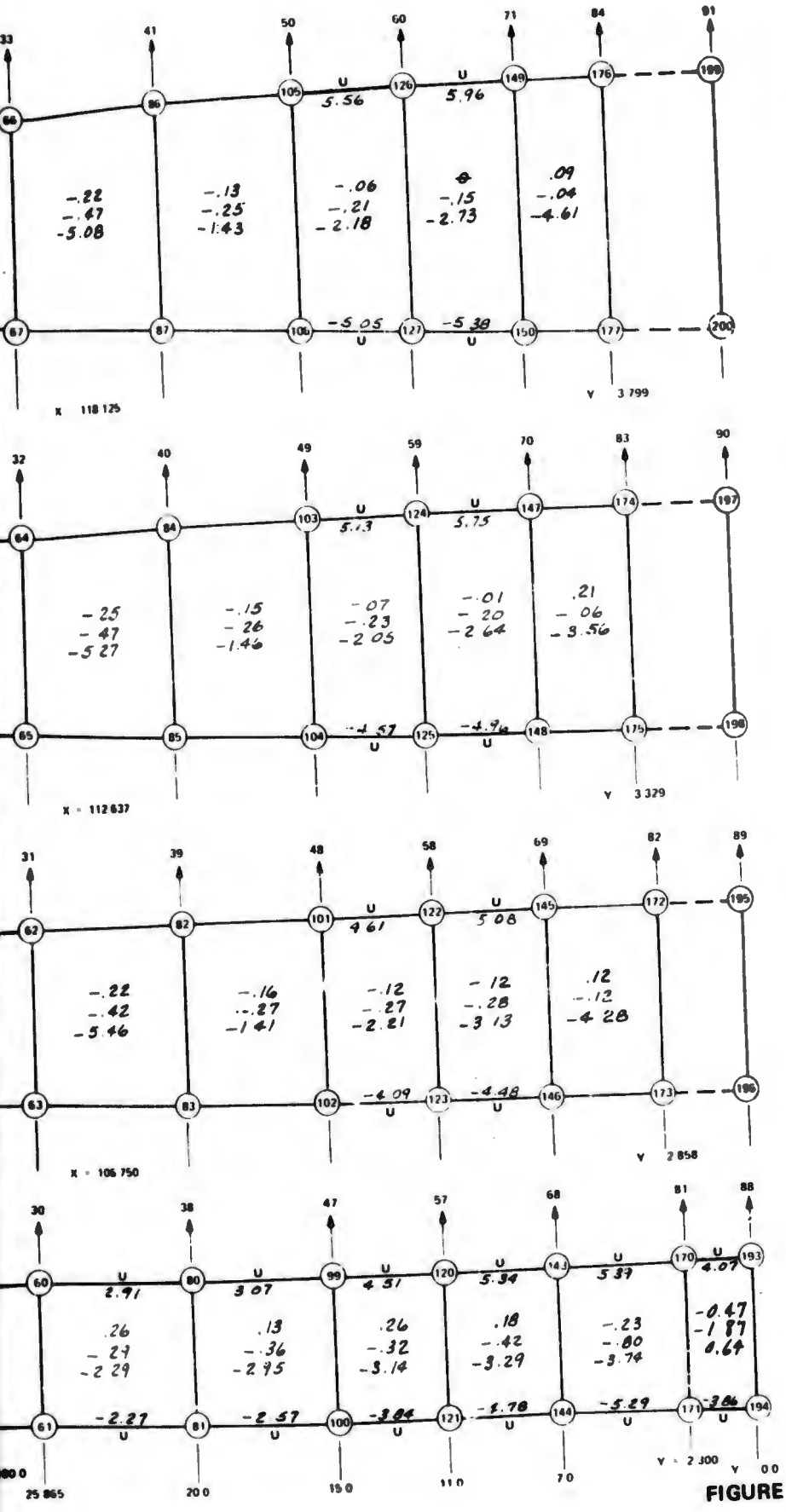

IDENTIFICATION CODE FOR ELEMENT STRESSES

σ_y = AAA
σ_z = BBB
τ_{yz} = CCC

FOR LAMINATED GRAPHITE OR FIBERGLASS PANELS

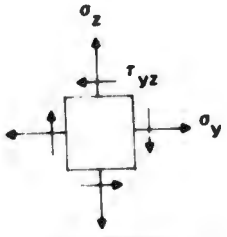

POSITIVE DIRECTIONS OF ELEMENT STRESSES ALL STRESSES IN KSI

IDENTIFICATION SYMBOLS FOR ELEMENTS TO SPECIFY MATERIAL TYPE AND COMPONENT

- U – GRAPHITE FLANGE OR ANGLE
- V – ALUMINUM FITTING
- W – STEEL FITTING
- X – STEEL OR TITANIUM DOUBLER
- Y – FIBERGLASS FLANGE OR ANGLE
- Z – LAMINATED FIBER GLASS PANEL

NO SYMBOL – LAMINATED GRAPHITE PANEL

FIGURE B5. STRESS DISTRIBUTION IN SPANWISE SPARS – LOAD CONDITION D

IDENTIFICATION CODE
FOR ELEMENT STRESSES

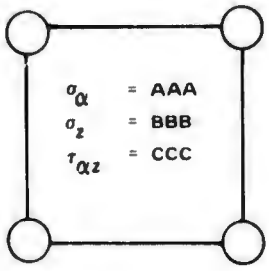

FOR LAMINATED
GRAPHITE OR
FIBERGLASS PANELS

IDENTIFICATION SYMBOLS
FOR ELEMENTS TO
SPECIFY MATERIAL TYPE
AND COMPONENT:

- U – GRAPHITE FLANGE OR ANGLE
- V – ALUMINUM FITTING
- W – STEEL FITTING
- X – STEEL OR TITANIUM DOUBLER
- Y – FIBERGLASS FLANGE OR ANGLE
- Z – LAMINATED FIBER GLASS PANEL

NO SYMBOL LAMINATED
GRAPHITE PANEL

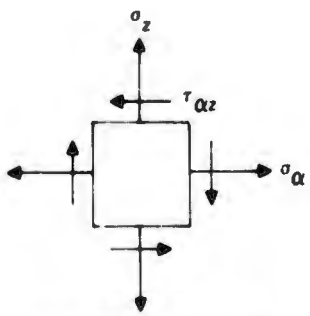

POSITIVE DIRECTIONS
OF ELEMENT STRESSES
ALL STRESSES IN KSI
α IS COORDINATE DIRECTION
PARALLEL TO CENTERLINE
OF RIB OR SPAR

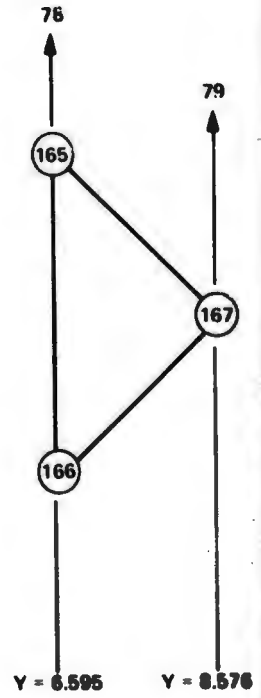

CROSS SECTION THROUGH LEADING EDGE

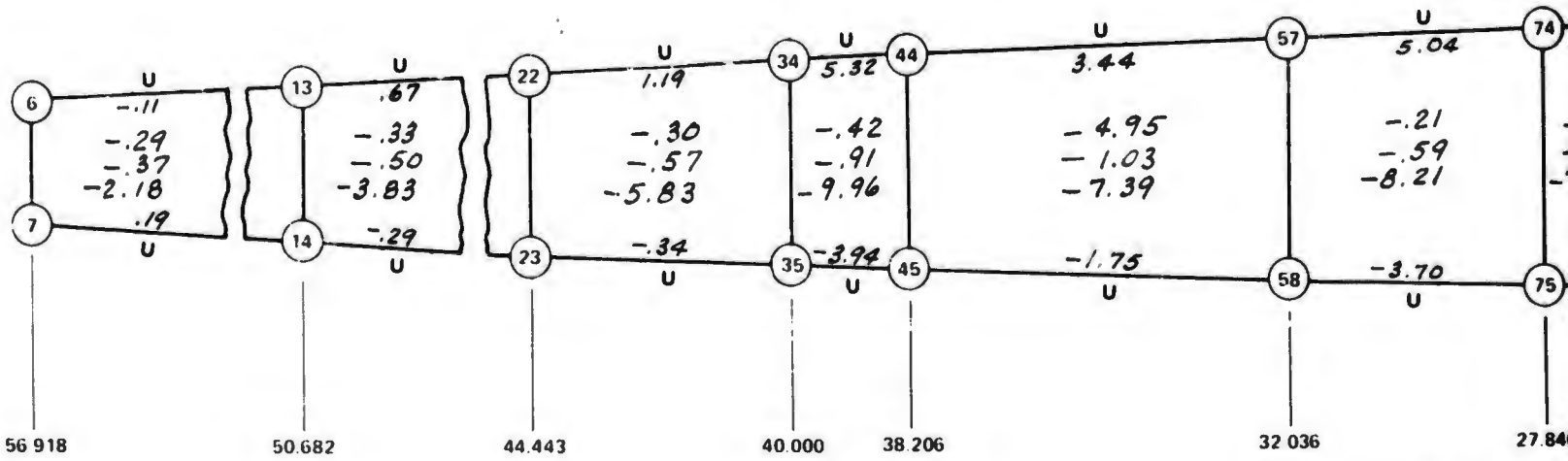

LEADING EDGE SPAR MEMBER

ALL STATION LOCATIONS ARE
MEASURED RELATIVE TO ANALYSIS
MODEL BASE COORDINATE SYSTEM

POSITIVE DIRECTIONS FOR
LOAD VECTORS ARE SHOWN

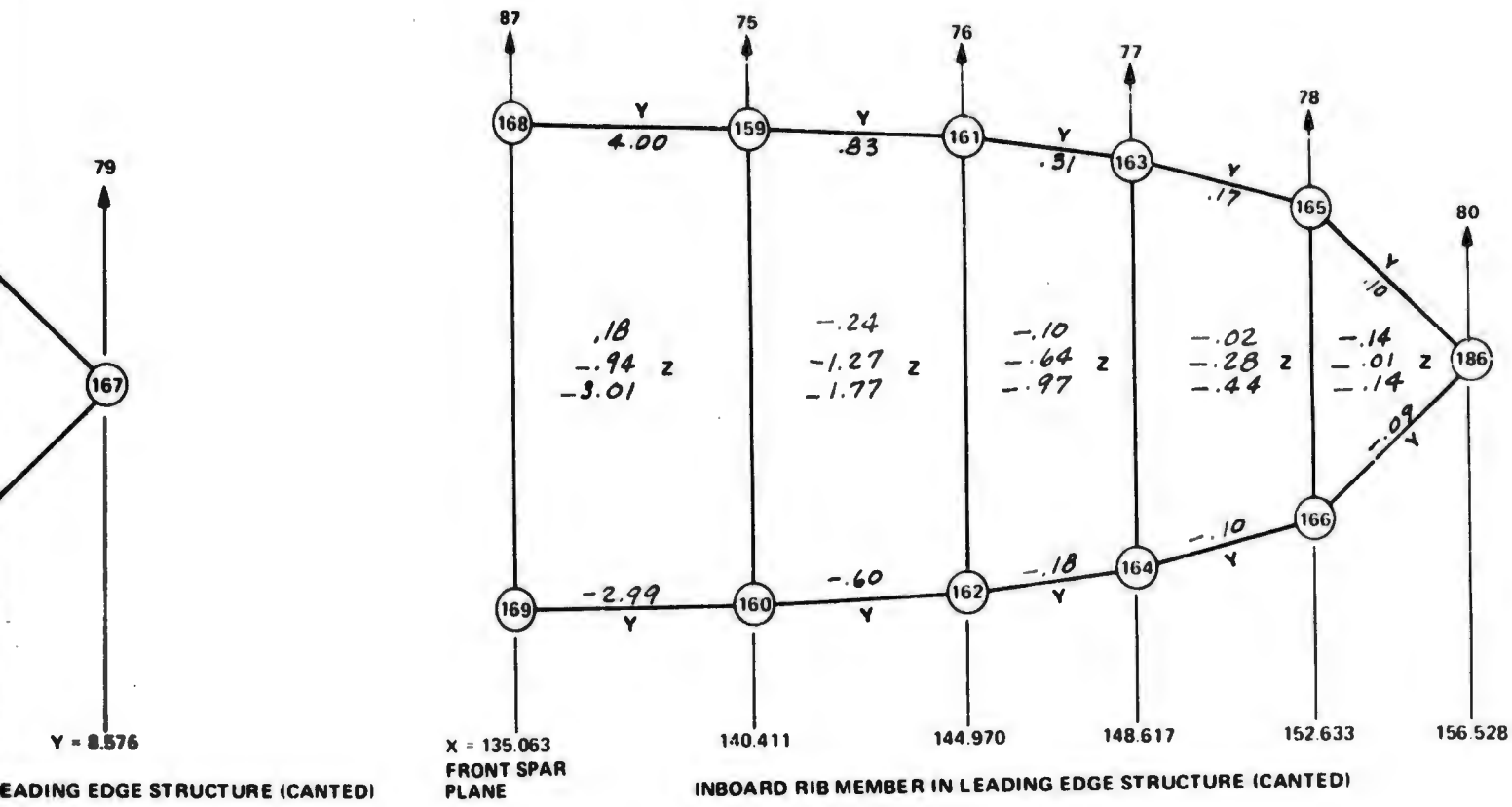

EADING EDGE STRUCTURE (CANTED)

INBOARD RIB MEMBER IN LEADING EDGE STRUCTURE (CANTED)

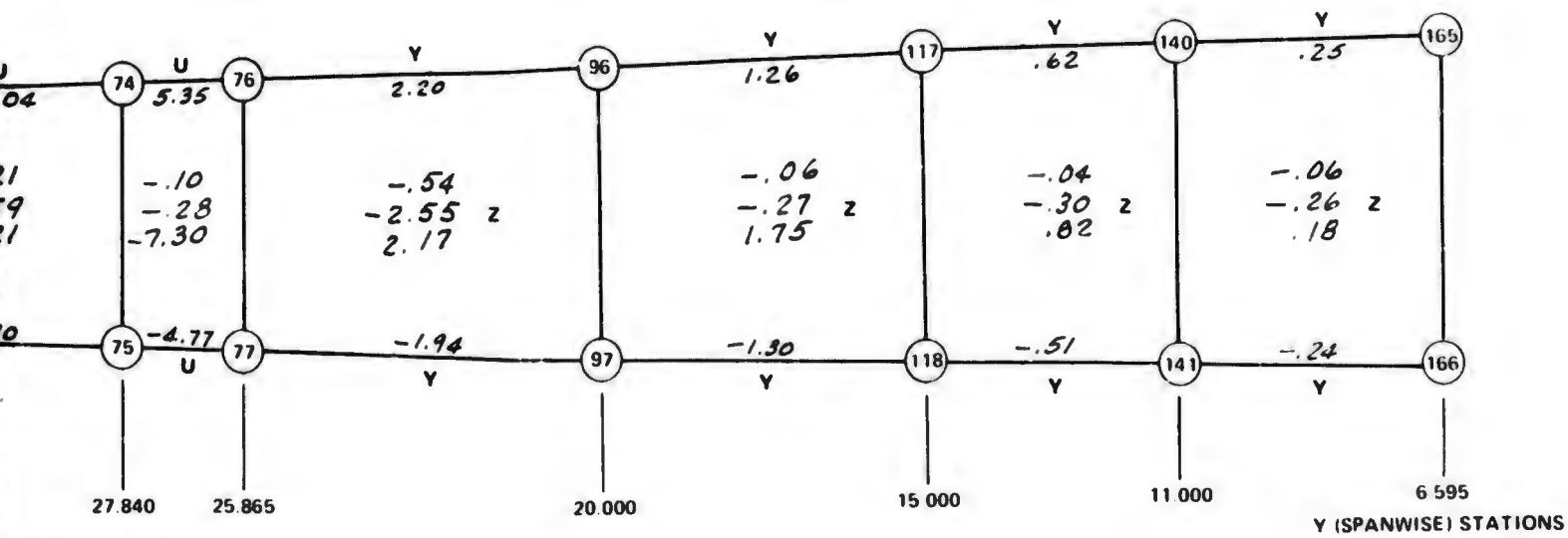

PAR MEMBER (CANTED)

FIGURE B6. STRESS DISTRIBUTION IN LEADING EDGE SPAR AND INBOARD RIB – LOAD CONDITION D

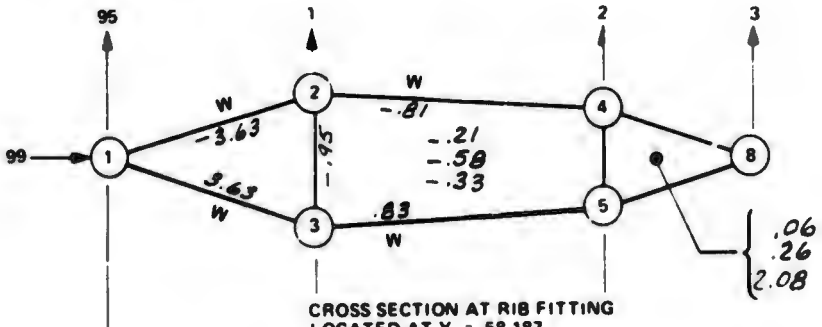

CROSS SECTION AT RIB FITTING
LOCATED AT Y = 58.187

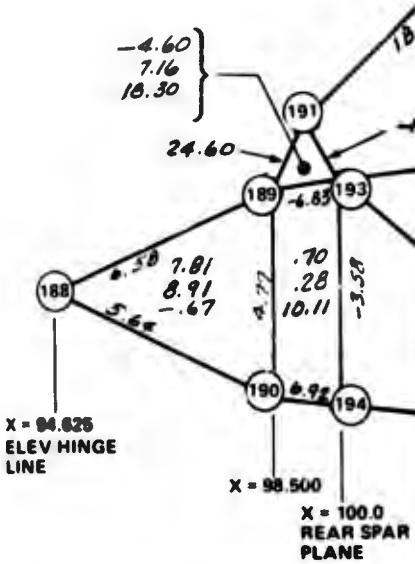

ALL STATION LOCATIONS ARE
MEASURED RELATIVE TO ANALYSIS
MODEL BASE COORDINATE SYSTEM

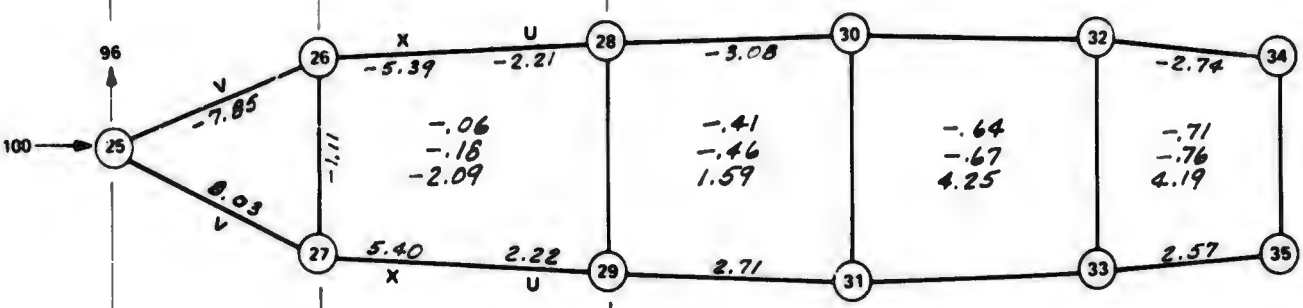

CROSS SECTION AT Y = 40.000 RIB

X = 94.625
ELEV HINGE
LINE

X = 100.00
REAR SPAR
PLANE

106.750

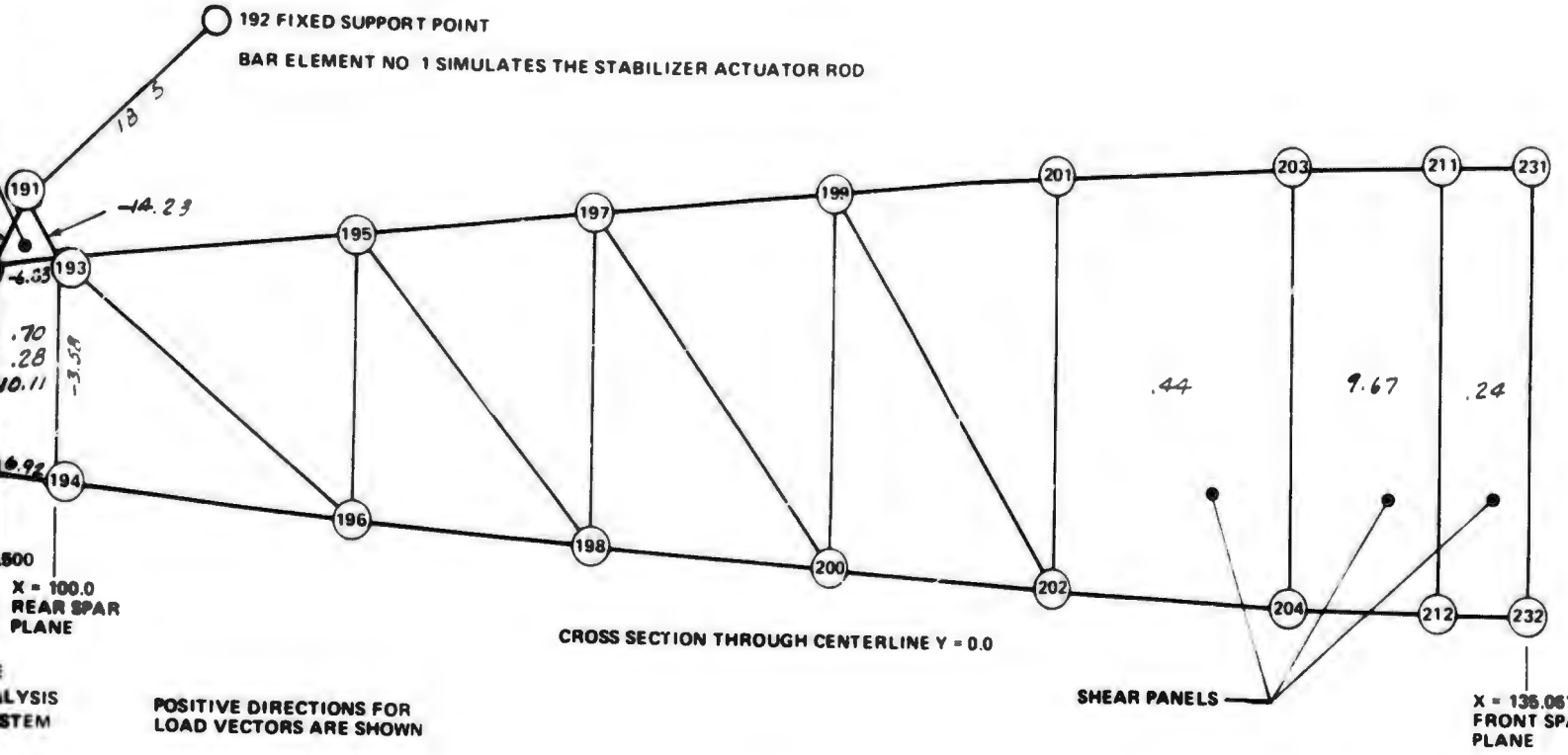

ALYSIS
STEM

POSITIVE DIRECTIONS FOR
LOAD VECTORS ARE SHOWN

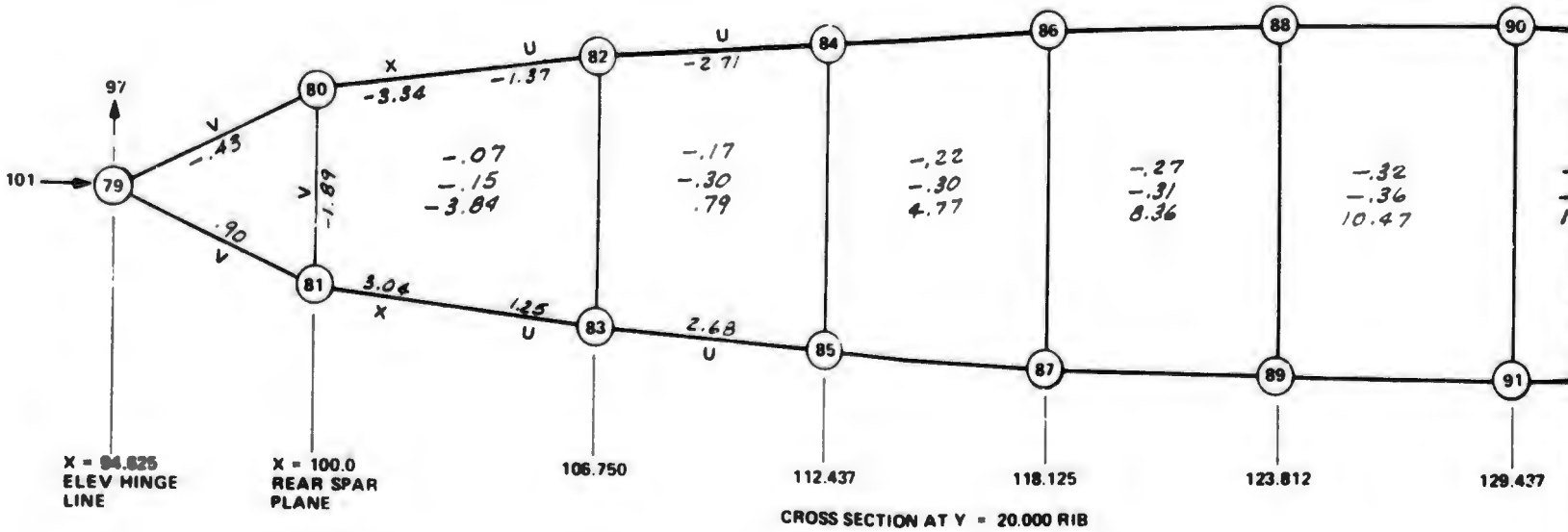

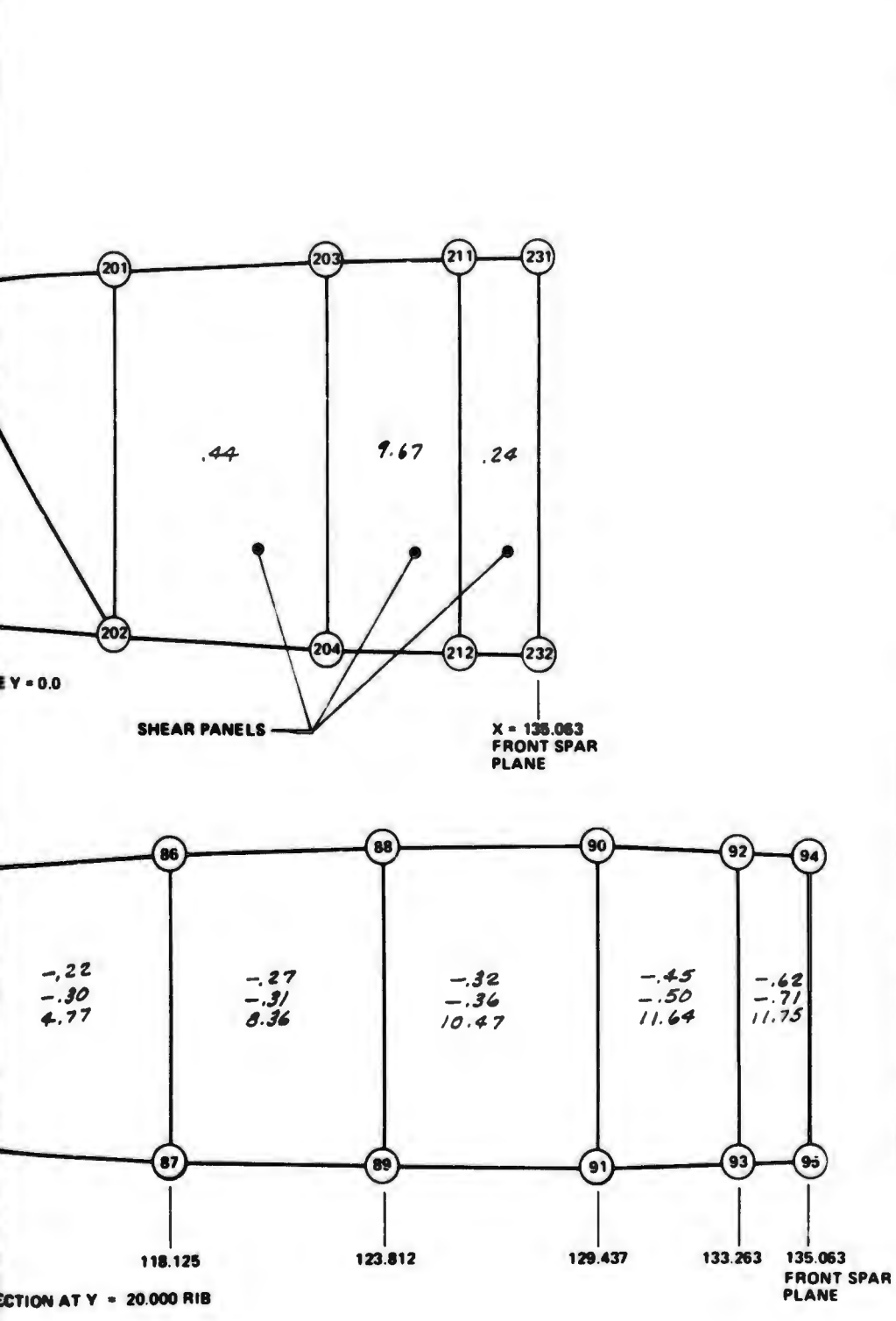

FIGURE B7. STRESS DISTRIBUTION IN CHORDWISE RIBS – LOAD CONDITION D

IDENTIFICATION CODE
FOR ELEMENT STRESSES

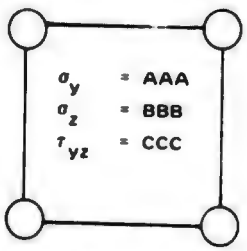

FOR LAMINATED
GRAPHITE OR
FIBERGLASS PANELS

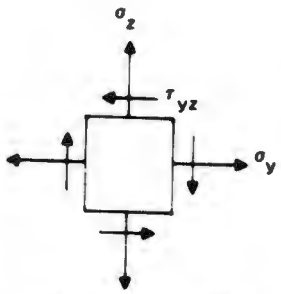

POSITIVE DIRECTIONS
OF ELEMENT STRESSES
ALL STRESSES IN KSI
(NOT APPLICABLE TO
CANTED RIB)

ALL STATION LOCATIONS ARE
MEASURED RELATIVE TO ANALYSIS
MODEL BASE COORDINATE SYSTEM

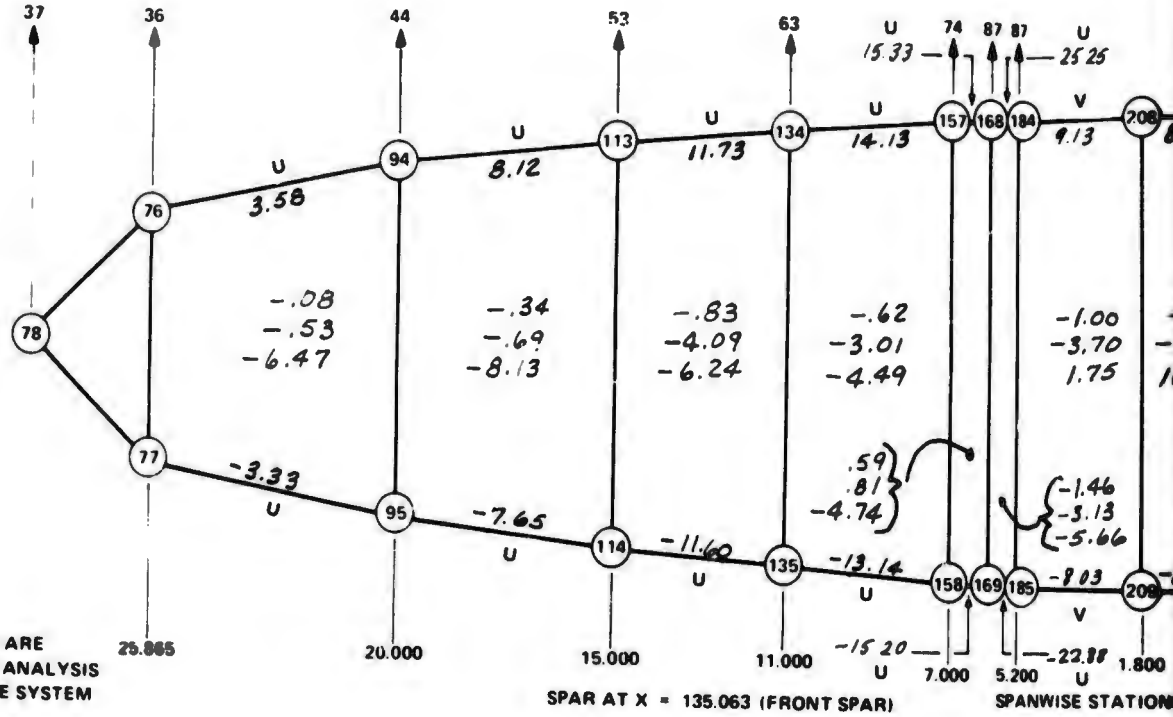

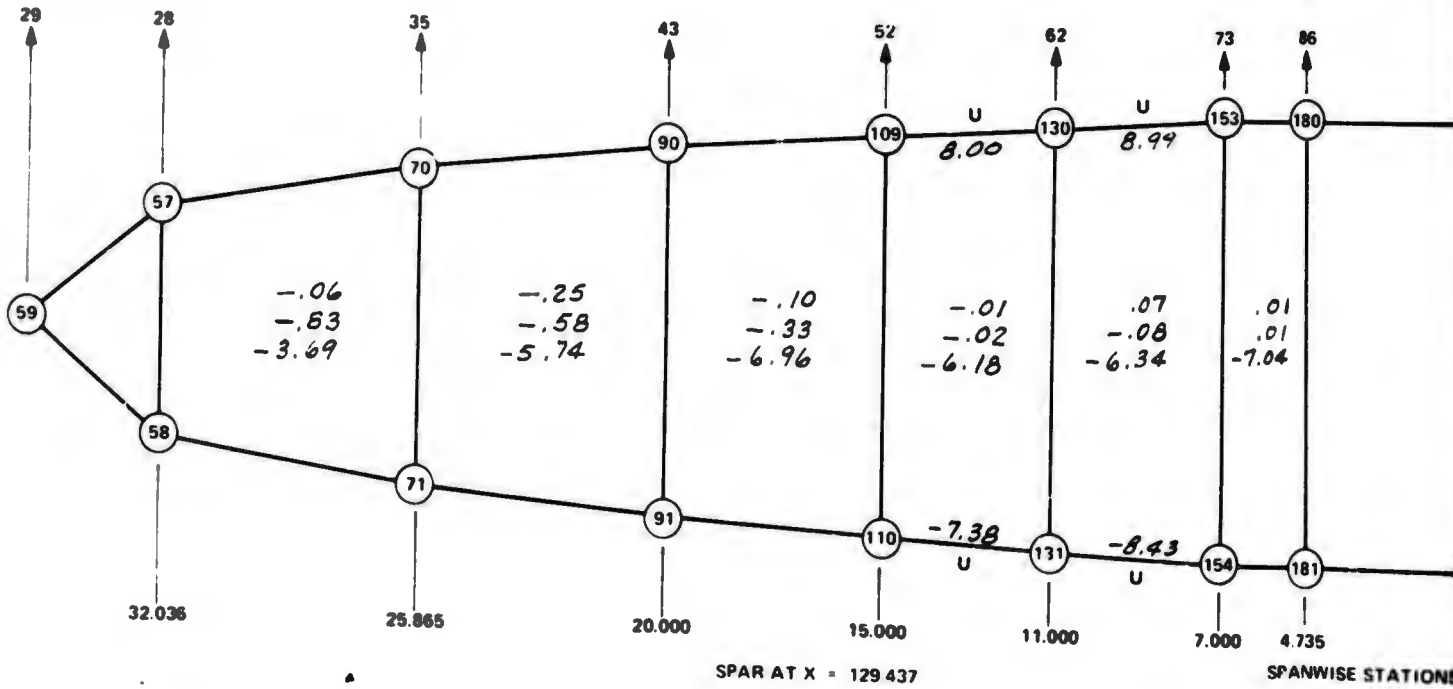

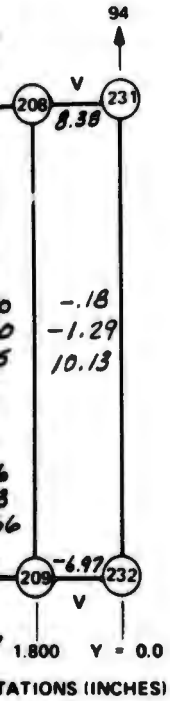

TATIONS (INCHES)

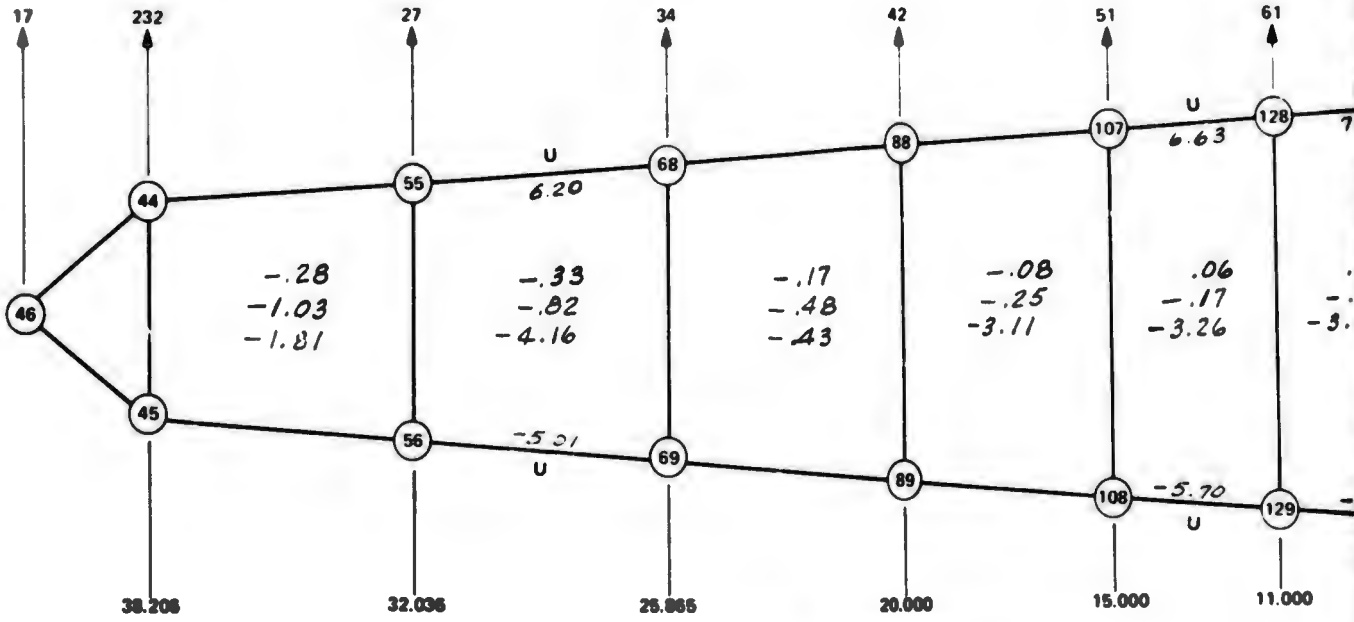

SPAR AT X = 123.612

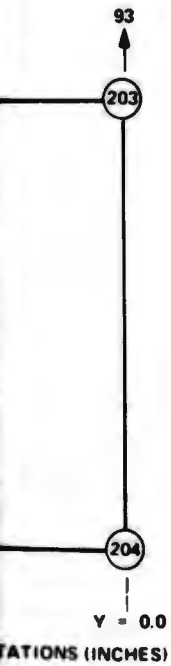

TATIONS (INCHES)

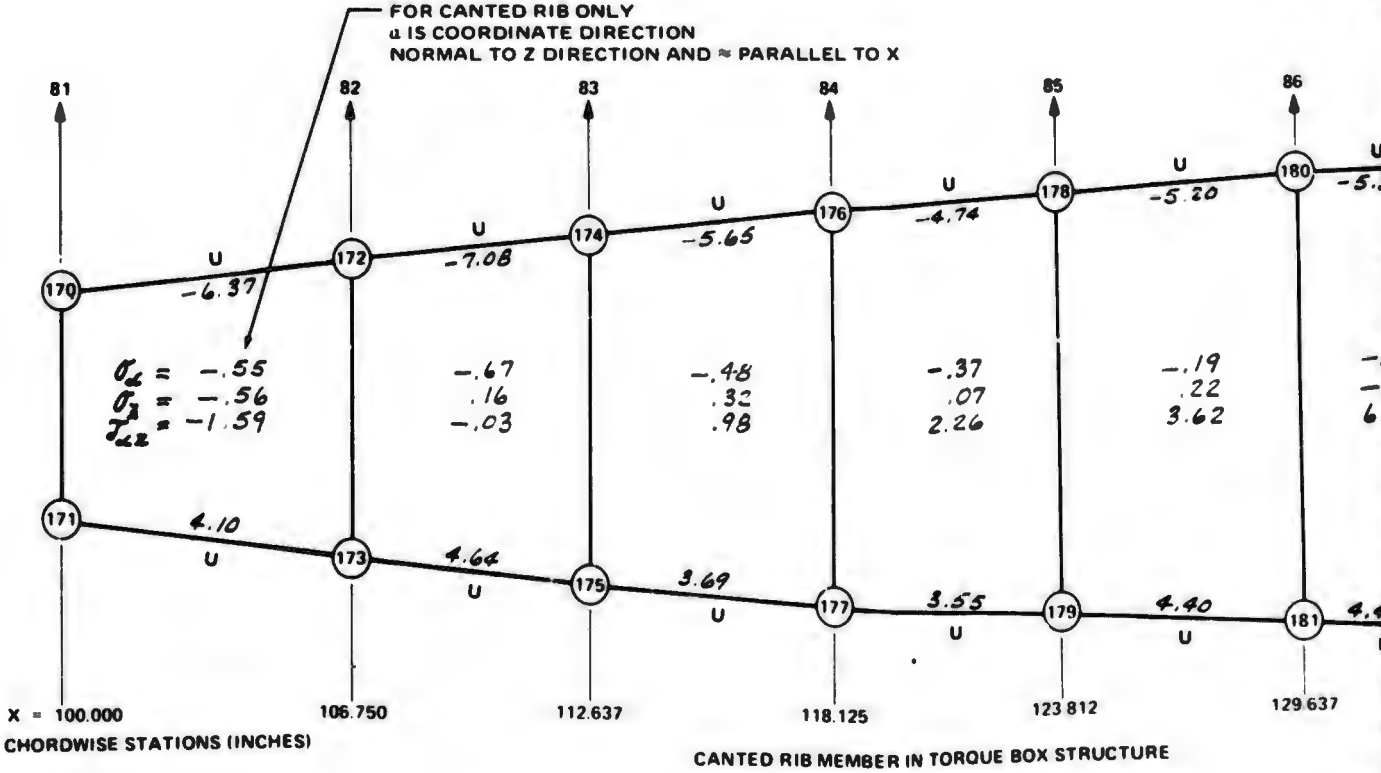

CHORDWISE STATIONS (INCHES)

CANTED RIB MEMBER IN TORQUE BOX STRUCTURE

FIGU

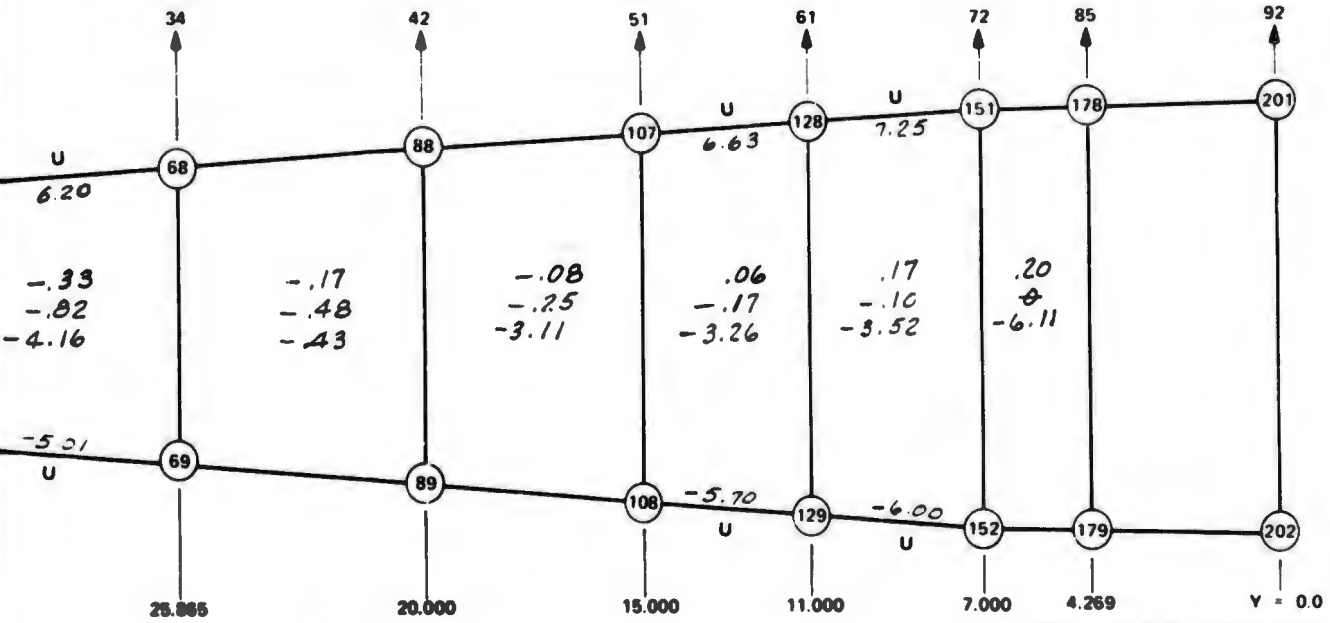

SPAR AT X = 123.612

D RIB ONLY
NATE DIRECTION
Z DIRECTION AND ≈ PARALLEL TO X

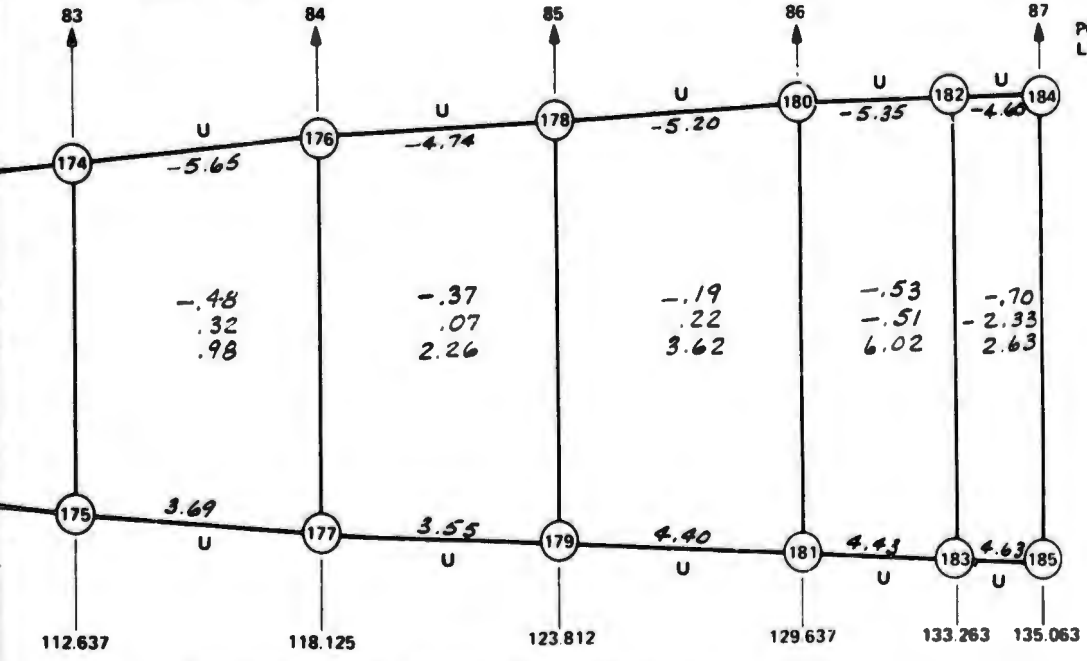

CANTED RIB MEMBER IN TORQUE BOX STRUCTURE

POSITIVE DIRECTIONS FOR LOAD VECTORS ARE SHOWN

IDENTIFICATION SYMBOLS FOR ELEMENTS TO SPECIFY MATERIAL TYPE AND COMPONENT:

- U – GRAPHITE FLANGE OR ANGLE
- V – ALUMINUM FITTING
- W – STEEL FITTING
- X – STEEL OR TITANIUM DOUBLER
- Y – FIBERGLASS FLANGE OR ANGLE
- Z – LAMINATED FIBERGLASS PANEL

NO SYMBOL – LAMINATED GRAPHITE PANEL

FIGURE B8. STRESS DISTRIBUTION IN RIBS AND SPARS – LOAD CONDITION D

BOTTOM VIEW

NOTE ALL STRESS VALUES ARE IN KSI

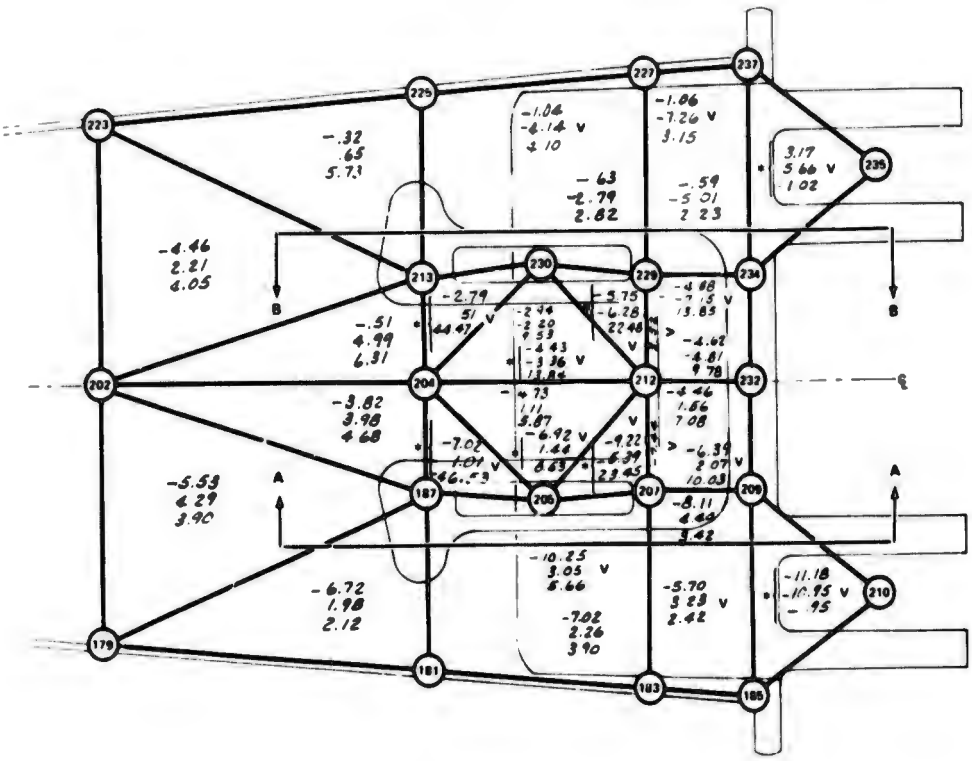

IDENTIFICATION SYMBOLS FOR ELEMENTS TO SPECIFY MATERIAL TYPE AND COMPONENT

U	GRAPHITE FLANGE OR ANGLE
V	ALUMINUM FITTING
W	STEEL FITTING
X	STEEL OR TITANIUM DOUBLER
Y	FIBERGLASS FLANGE OR ANGLE
ℓ	LAMINATED FIBER GLASS PANEL

NO SYMBOL LAMINATED GRAPHITE PANEL

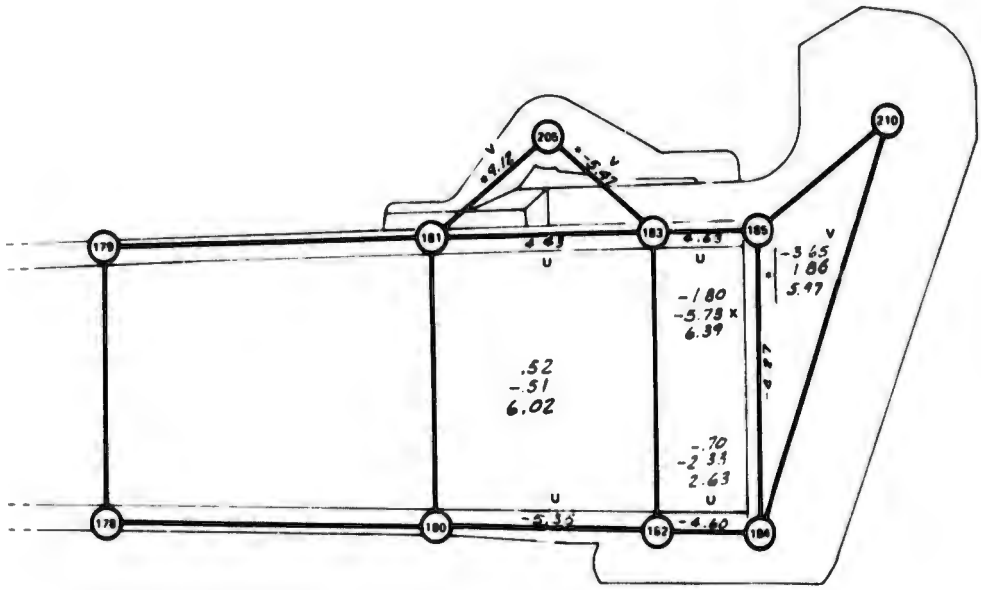

ORIENTATION OF STRESSES
TYPICAL FOR TOP AND
BOTTOM VIEWS

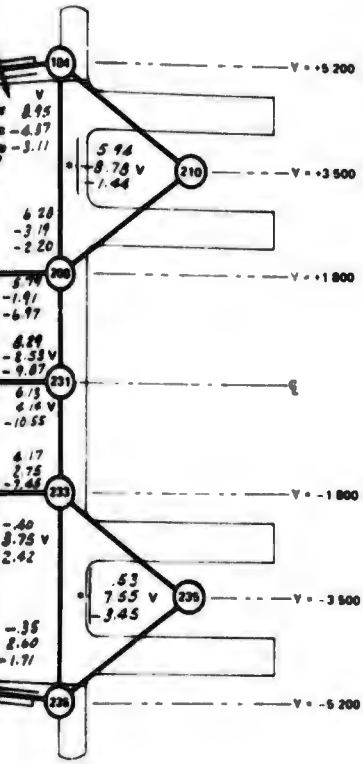

NOTES

QUANTITIES MARKED * REPRESENT STRESSES IN THE LUG AREA OF THE PIVOT POINT FITTING AND THE ELEVATOR MECHANISM ATTACH FITTING

SINCE THESE AREAS ARE HIGHLY IDEALIZED, THESE VALUES ARE NOT REPRESENTATAIVE OF THE ACTUAL STRESS FIELD IN THE FITTINGS AND ARE LISTED FOR REFERENCE ONLY

NODES NO 210 AND 236 ARE FIXED SUPPORT POINTS

ALL STATION LOCATIONS ARE MEASURED RELATIVE TO ANALYSIS MODEL BASE COORDINATE SYSTEM

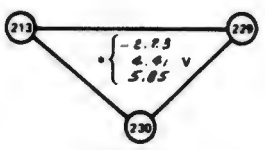

SECTION B B

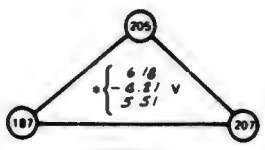

SECTION A A

FOR LEFT
HT VIEWS α IS
IATE – DIRECTION
OF ELEMENT
MAL TO Z COORDINATE

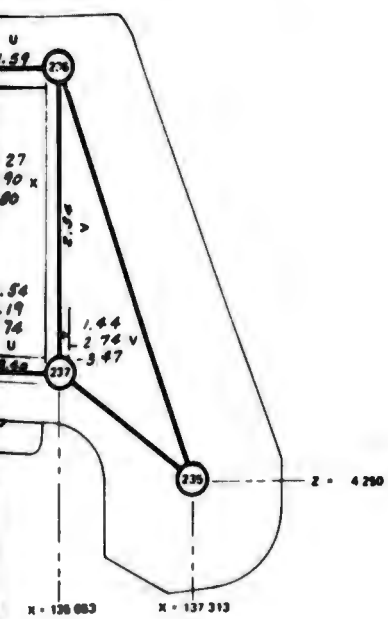

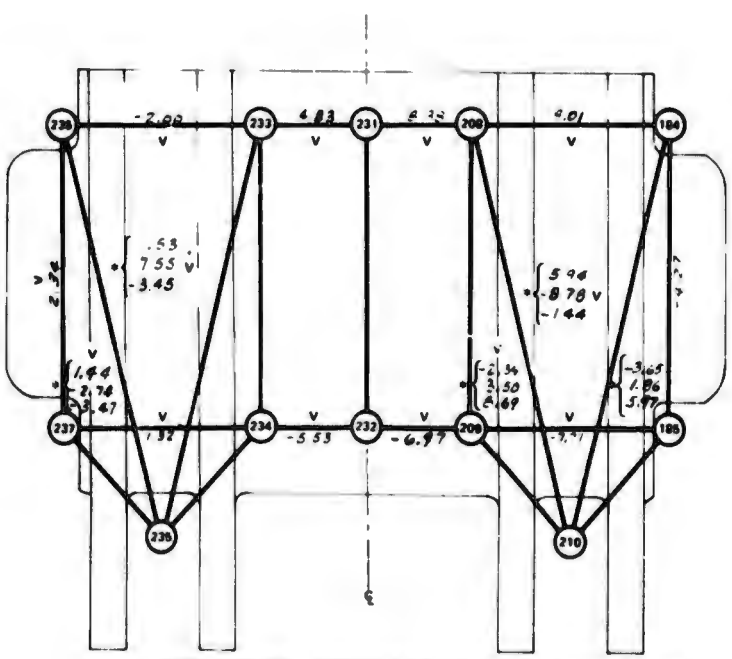

FIGURE B9. STRESSES IN IDEALIZED PIVOT FITTING AND ADJACENT STRUCTURE – LOAD CONDITION D

NOTE ALL STRESS VALUES ARE IN KSI

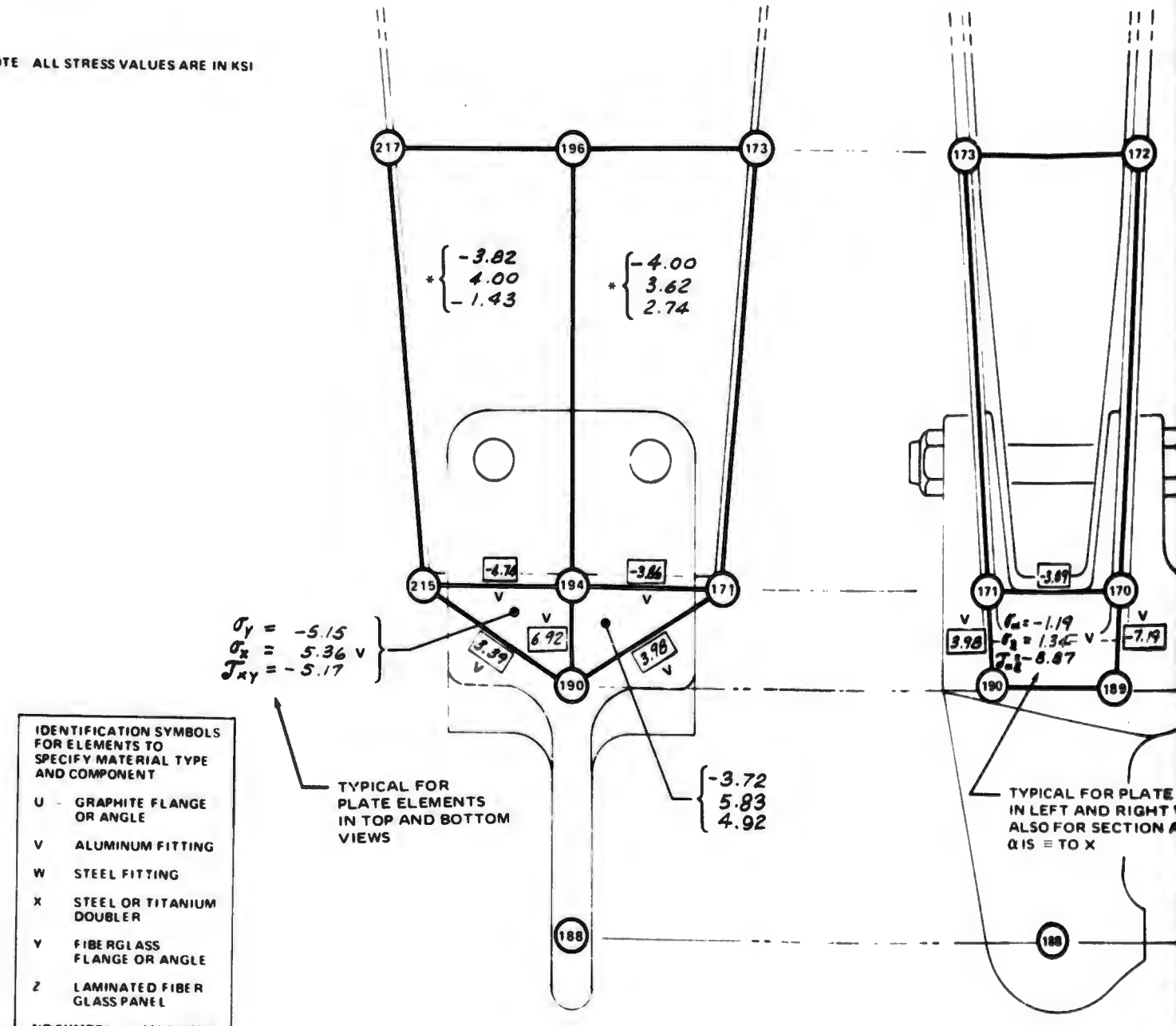

IDENTIFICATION SYMBOLS FOR ELEMENTS TO SPECIFY MATERIAL TYPE AND COMPONENT

U	GRAPHITE FLANGE OR ANGLE
V	ALUMINUM FITTING
W	STEEL FITTING
X	STEEL OR TITANIUM DOUBLER
Y	FIBERGLASS FLANGE OR ANGLE
Z	LAMINATED FIBER GLASS PANEL

NO SYMBOL LAMINATED GRAPHITE PANEL

BOTTOM VIEW

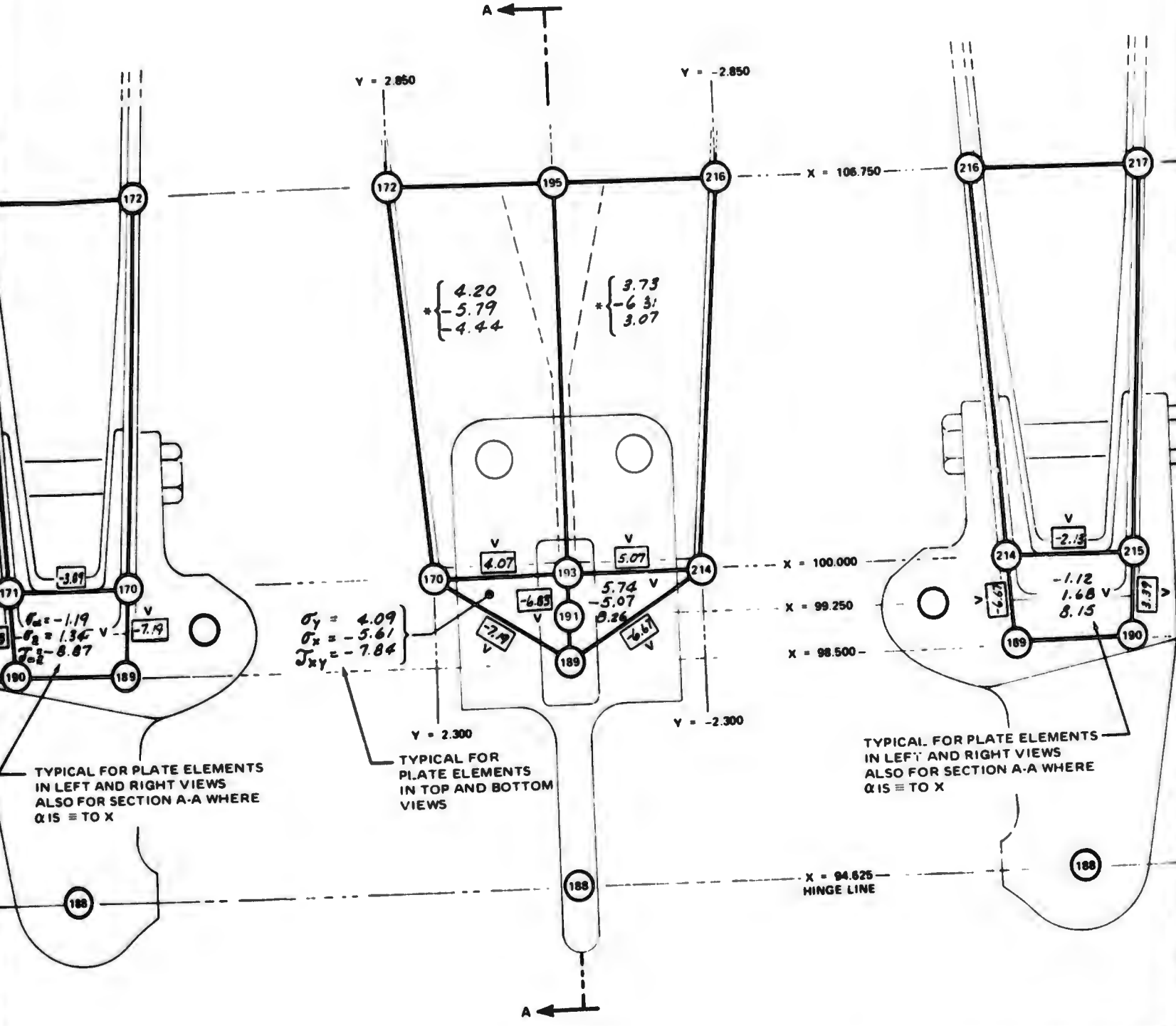

TOP VIEW

*THESE QUANTITIES ARE STRESSES IN THE CANT RIB

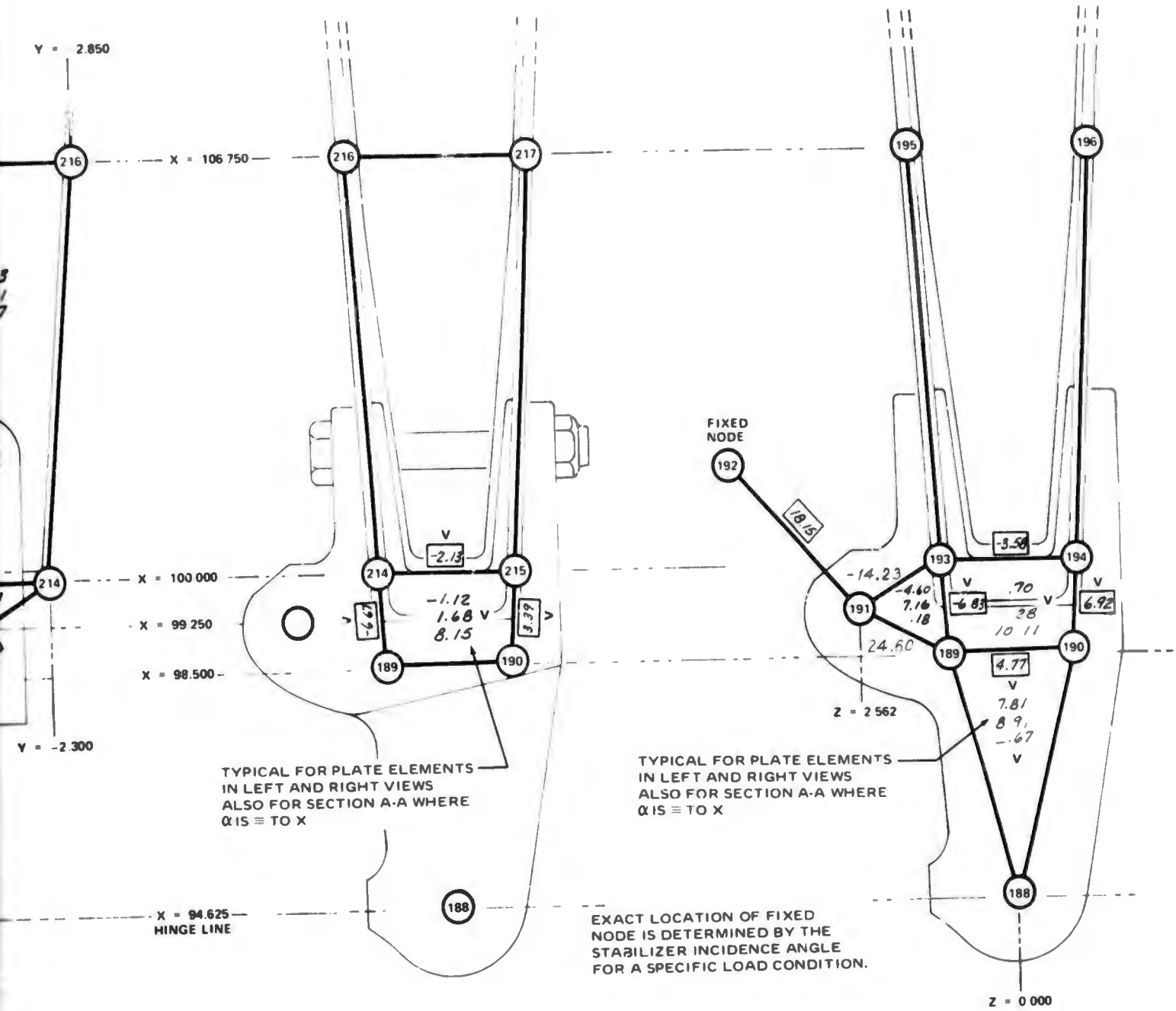

*THESE QUANTITIES ARE STRESSES IN THE CANT RIB FLANGES.

SECTION A-A

ALL STATION LOCATIONS ARE
MEASURED RELATIVE TO ANALYSIS
MODEL BASE COORDINATE SYSTEM

FIGURE B10. STRESSES IN IDEALIZED ACTUATOR FITTING AND ADJACENT STRUCTURE – LOAD CONDITION D

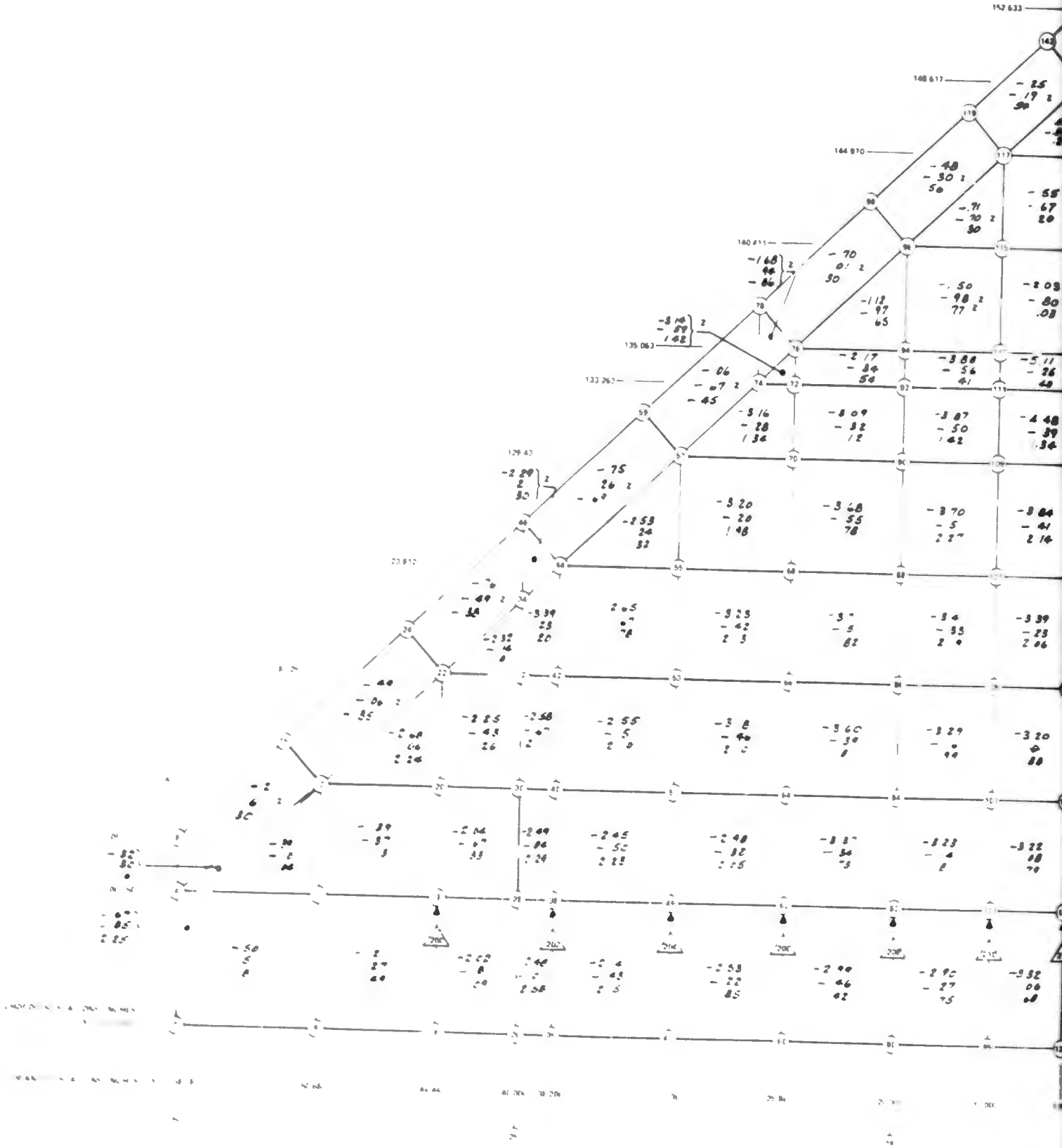

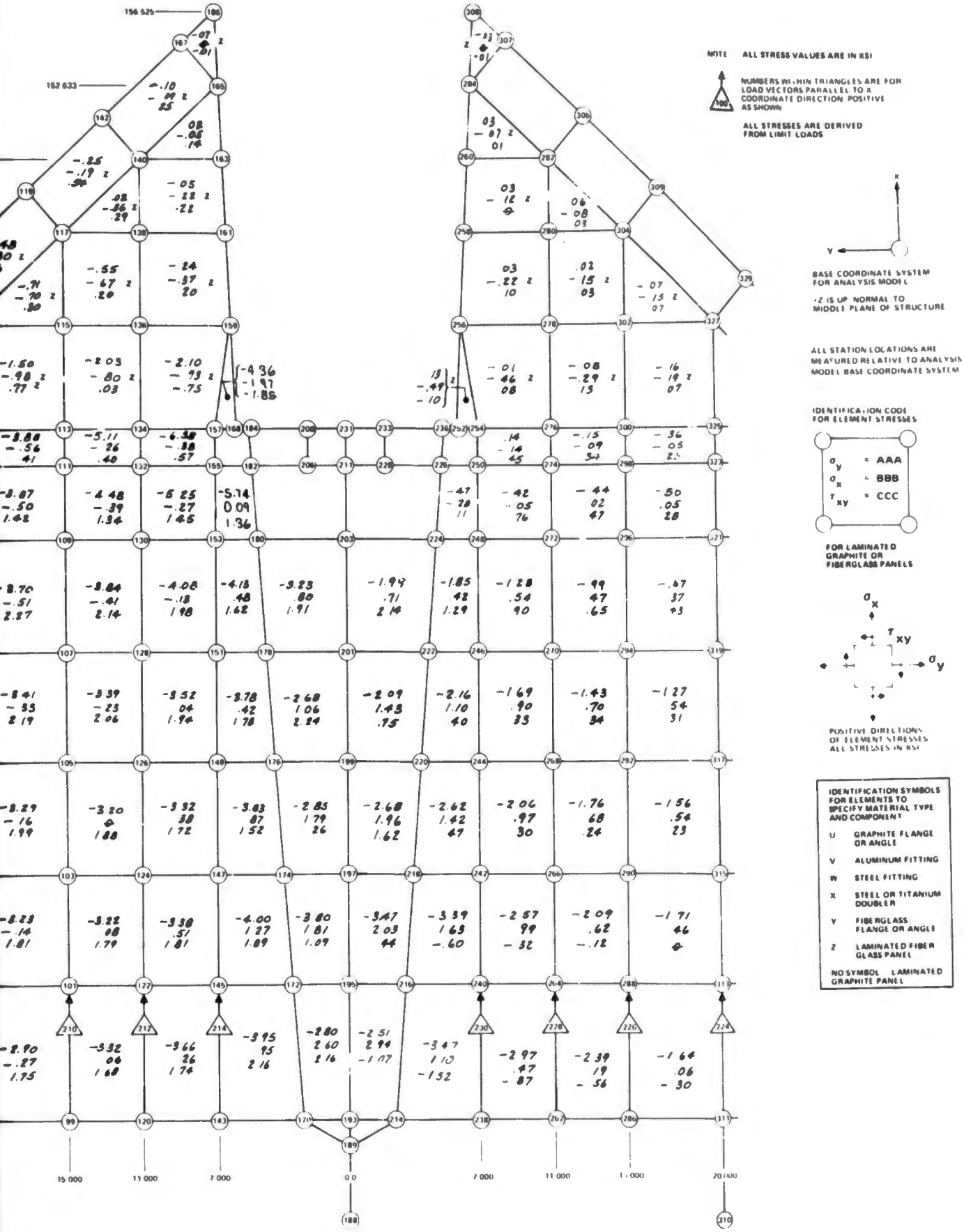

FIGURE B11. STRESS DISTRIBUTION IN UPPER PANEL AND LEADING EDGE – LOAD CONDITION F

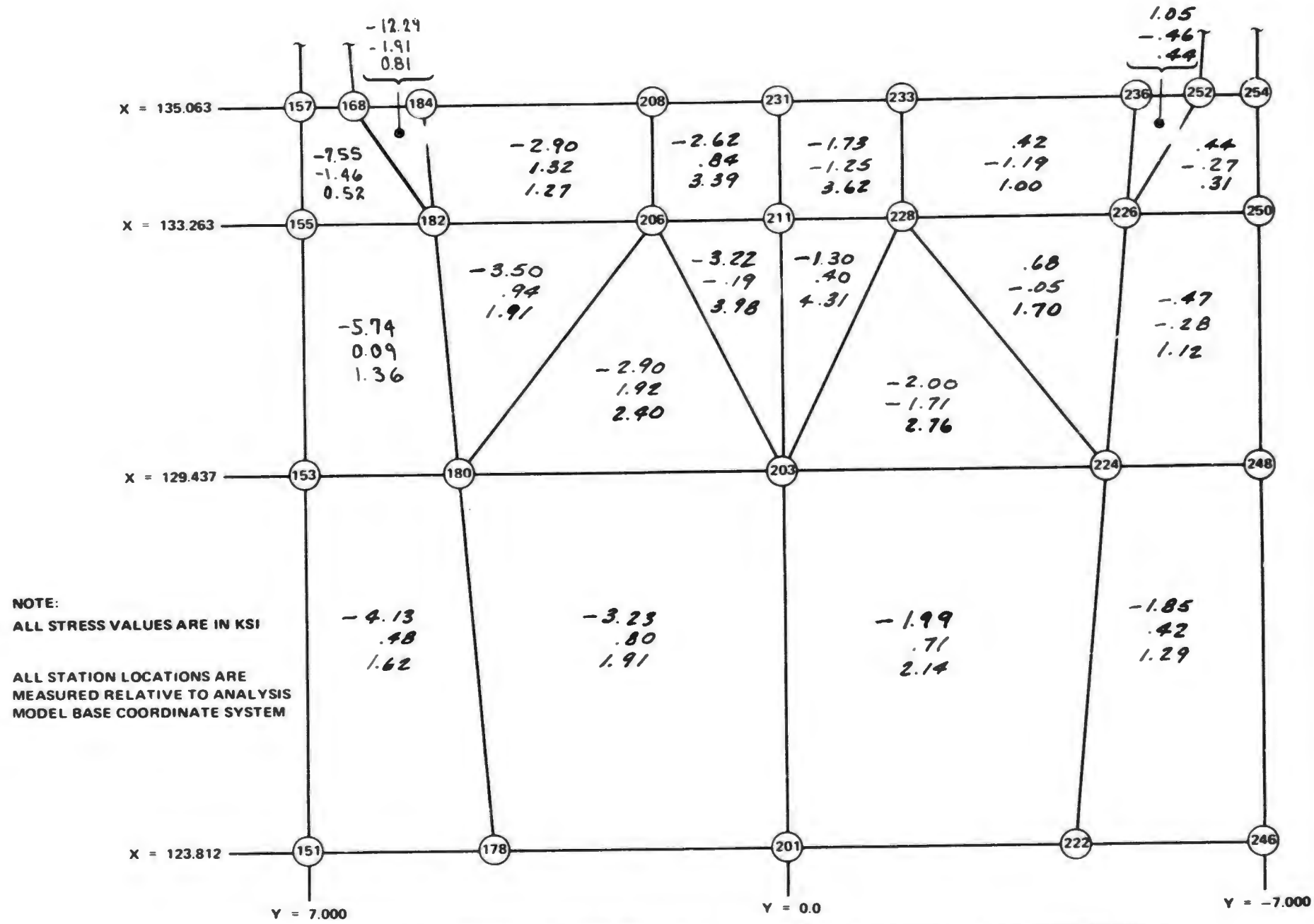

FIGURE B12. STRESS DISTRIBUTION IN UPPER PANEL ADJACENT TO PIVOT FITTING – LOAD CONDITION F

THIS PAGE LEFT BLANK INTENTIONALLY.

APPENDIX C

INCOMING MATERIAL, IN-PROCESS, AND NONDESTRUCTIVE TEST RESULTS

Incoming material and in-process coupon test results are tabulated in this appendix together with the discussion and intepretation of the nondestructive tests conducted on the stabilizer graphite-epoxy skins and bond assemblies.

INCOMING MATERIAL AND IN-PROCESS TEST RESULTS

Incoming material tests were conducted on seven lots of Modmor II/5206 graphite prepreg during the reporting period. Material receipts are summarized in Table CI. Acceptance test results are summarized in Tables CII through CVIII.

In-process test results for skin panels, attach angles, and leading-edge details of stabilier unit one are presented in Tables CIX and CX. In-process test results for the rear-spar and cant-ribs of stabilizer unit 2 are presented in Table CXI.

The in-process test results in flexure and interlaminar shear for the fabricated stabilizer parts were compared to the results obtained from the intermediate component I-beam and box-beam skin panels (see Reference 2). The in-process test results from the fabricated stabilizer parts were significantly lower than the corresponding values measured on the intermediate component skins, especially in interlaminar shear where strength reductions ranged between 13% and 47%. The strength and modulus reductions were attributed to higher void contents in the stabilizer parts (up to about 2% actual void volume) in comparison to the essentially void-free intermediate component skins. The reasons for the higher void volumes in the stabilizer parts have not been fully investigated but they may have been influenced by the following differences in processing. These processing differences were necessitated by the relative part complexities and heat-sink capacities of the full-scale tooling.

ITEM	INTERMEDIATE COMPONENT SKINS	STABILIZER PARTS
Layup Time	1-2 days	3-4 days
Debulking Stages	None	3 or 4 debulk cycles
Heat-up Rate during Cure	5°F per minute	1° - 2°F per minute

TABLE CI

SUMMARY OF GRAPHITE PREPREG MATERIAL RECEIPTS

LOT OR BATCH	TYPE MATERIAL	DATE RECEIVED	AMOUNT (LB)
60C	METER LENGTH SHEETS	4/22/71	15.35
81B	METER LENGTH SHEETS	3/18/71	9.57
81C	METER LENGTH SHEETS	4/22/71	25.38
98	METER LENGTH SHEETS	6/29/71	27.00
317	3-INCH TAPE	7/16/71	27.45
319	3-INCH TAPE	7/16/71	23.24
320	3-INCH TAPE	7/1/71	32.35
		TOTAL	160.34

TABLE
PREPREG QUALITY CONTROL REC

MATERIAL MODMOR II/5206

VENDOR NARMCO

QUANTITY RECEIVED 15.35 LB NUMBER OF UNITS _____ UNIT SI

TEST / UNIT IDENTITY	PREPREG PROPERTIES									
	RESIN CONTENT WT. %	VOLATILE CONTENT WT. %	GEL TIME MINUTES	VISUAL	HANDLING		TENSILE STRENGTH 10^3 PSI	TENSILE MODULUS 10^6 PSI	RESIN CONTENT WT. %	
DMS _____ REQ'TS	39 To 45.0	3.0 Max.	18 To 26	—	—		145.0 Min.	19.0 Min.	28 To 34	
VENDOR AVERAGE RESULTS	43.1									
SHEET__-1 246 -2 -3 -4 -5 AVE.	____	____	____	____	____	____	216.3 166.6 183.6 222.6 228.2 193.5	24.4 24.8 24.5 25.3 26.2 25.0	____	
SHEET__-1 278 -2 -3 -4 -5 AVE.	____	____	____	____	____	____	185.7 193.5 208.6 147.3 200.5 187.1	23.9 24.1 20.7 23.1 24.7 23.3	____	
SHEET__-1 311 -2 -3 -4 -5 AVE.	____	____	____	____	____	____	236.1 226.9 231.8 255.6 222.4 234.5	22.2 26.3 25.1 23.5 24.2 24.3	____	
SHEET__-1 325 -2 -3 -4 -5 AVE.	____	____	____	____	____	____	186.6 186.8 181.6 127.8 188.5 174.2	23.6 22.5 21.8 23.0 24.1 23.0	____	
SHEET__-1 -2 -3 -4 -5 AVE.	____	____	____	____	____	____	____	____	____	

REMARKS:

TABLE CII
OL RECEIVING INSPECTION REPORT

LOT NUMBER 60C DMS 1936A PAGE 1 OF 1

DATE OF MANUFACTURER 12-17-70 DATE RECEIVED 4-22-71

IT SIZE METER S/O 16105411 P/O OCY-665602-9

LAMINATE PROPERTIES									
SIN TENT %	VOID CONTENT Vol. %	FLEXURAL STRENGTH 10^3PSI	FLEXURAL MODULUS 10^6 PSI	SHEAR STRENGTH 10^3 PSI	RESIN CONTENT WT. %	VOID CONTENT VOL. %	THICKNESS PER PLY INCHES		COMMENTS
8 to 4	1 Max.	195.0 Min.	17.5 Min.	14.0 Min.	28 to 34	1 Max.			
		250.0		18.1					
		204.3 220.9 212.6	19.1 19.2 19.2	14.5 17.0 16.6 16.0					
		200.7 204.5 202.6	21.1 19.3 20.2	16.6 17.2 17.0 16.9					

MEETS SPEC. ☒ DOES NOT MEET SPEC ☐

MEETS P.O. ☒ DOES NOT MEET P.O. ☐

Q.C. REPRESENTATIVE H. M. Tillness

DATE: 7-7-71

TABLE CIII
PREPREG QUALITY CONTROL RECEIVING I

MATERIAL MODMOR II/5206 LOT NUM

VENDOR NARMCO DATE OF

QUANTITY RECEIVED 9.574 LB NUMBER OF UNITS AN 88, 91-144 UNIT SIZE MET

TEST / UNIT IDENTITY	PREPREG PROPERTIES: RESIN CONTENT WT. %	VOLATILE CONTENT WT. %	GEL TIME MINUTES	VISUAL	HANDLING		TENSILE STRENGTH 10^3 PSI	TENSILE MODULUS 10^6 PSI	RESIN CONTENT WT. %	VOID CONTENT Vol. %
DMS REQ'TS	39 To 45.0	3.0 Max.	18 To 26	—	—		145.0 Min.	19.0 Min.	28 To 34	1 Max.
VENDOR AVERAGE RESULTS	42.7									
SHEET 99 -1	45.3	0.56	25:21				200.8	23.6		
-2	44.4		26:07				176.5	22.6		
-3	46.1						163.6	23.0		
-4							208.9	22.8		
-5							173.2	22.5		
AVE.	45.3	0.56	25:44				184.6	22.9		
SHEET 119 -1	44.08	0.50	24:48				166.0	20.9		
-2	42.7		24:07				181.0	21.4		
-3	43.2						197.4	21.4		
-4							190.5	19.5		
-5							212.8	22.4		
AVE.	43.3	0.50	24:28				189.5	21.1		
SHEET -1										
-2										
-3										
-4										
-5										
AVE.										
SHEET -1										
-2										
-3										
-4										
-5										
AVE.										
SHEET -1										
-2										
-3										
-4										
-5										
AVE.										

REMARKS:

BLE CIII
RECEIVING INSPECTION REPORT

LOT NUMBER 81B DMS 1936B PAGE 1 OF 1

DATE OF MANUFACTURER 3-5-71 DATE RECEIVED 3-18-71

SIZE METER S/O 16105411 P/O OCY-665602-9

	LAMINATE PROPERTIES								
	VOID CONTENT Vol. %	FLEXURAL STRENGTH 10^3PSI	FLEXURAL MODULUS 10^6 PSI	SHEAR STRENGTH 10^3 PSI	RESIN CONTENT WT. %	VOID CONTENT VOL. %	THICKNESS PER PLY INCHES		COMMENTS
	1 Max.	195.0 Min.	17.5 Min.	14.0 Min.	28 to 34	1 Max.			
		221.0		15.9					
		235.0	21.2	18.2	28.5	−0.6	0.00567		
		236.3	20.9	16.5	28.8	−0.6	0.00567		
		235.8	22.4	17.4	28.4	−0.6	0.00557		
		235.7	21.5	17.4	28.4	−0.6	0.00560		

MEETS SPEC. ☒ DOES NOT MEET SPEC ☐

MEETS P.O. ☒ DOES NOT MEET P.O. ☐

Q.C. REPRESENTATIVE H. M Toellner

DATE: 4-9-71

TABLE C
PREPREG QUALITY CONTROL REC

MATERIAL MODMOR II/5206

VENDOR NARMCO

QUANTITY RECEIVED 25.384 LB NUMBER OF UNITS SH 145-286 UNIT SIZE

TEST / UNIT IDENTITY	PREPREG PROPERTIES									
	RESIN CONTENT WT. %	VOLATILE CONTENT WT. %	GEL TIME MINUTES	VISUAL	HANDLING		TENSILE STRENGTH 10^3 PSI	TENSILE MODULUS 10^6 PSI	RESIN CONTENT WT. %	V C
DMS _____ REQ'TS	39 To 45.0	3.0 Max.	18 To 26	—	—		145.0 Min.	19.0 Min.	28 To 34	
VENDOR AVERAGE RESULTS	42.9									
SHEET__-1	47.78	1.12					214.1	23.5		
228 -2	45.52						207.1	21.0		
-3	46.82						245.6	22.4		
-4							202.8	20.0		
-5							151.7	23.1		
AVE.	46.71	1.1					204.3	22.0		
SHEET__-1							179.6	21.6		
233 -2							224.1	20.2		
-3							195.9	20.4		
-4							181.7	20.4		
-5							162.5	21.5		
AVE.							188.8	20.8		
SHEET__-1							177.2	21.8		
238 -2							161.2	21.3		
-3							170.9	21.8		
-4							175.9	22.8		
-5							165.7	23.1		
AVE.							170.2	22.2		
SHEET__-1							207.3	23.3		
242 -2							178.0	22.3		
-3							211.3	21.9		
-4							183.5	22.7		
-5							145.7	21.7		
AVE.							185.2	22.4		
SHEET__-1							232.8	21.0		
247 -2							188.2	19.3		
-3							201.7	19.2		
-4							216.9	21.9		
-5							205.7	20.5		
AVE.							209.1	20.4		

REMARKS: APPROVED ON AVERAGE FLEXURAL MODULUS DUE TO HIGHER THAN TYPICAL STRUCTUR

TABLE CIV
Y CONTROL RECEIVING INSPECTION REPORT

LOT NUMBER 81C DMS 1936B PAGE 1 OF 2

DATE OF MANUFACTURER 3-5-71 DATE RECEIVED 4-22-71

UNIT SIZE METER S/O 16105411 P/O OCY-665602-9

LAMINATE PROPERTIES									COMMENTS
RESIN CONTENT WT. %	VOID CONTENT Vol. %	FLEXURAL STRENGTH 10^3PSI	FLEXURAL MODULUS 10^6 PSI	SHEAR STRENGTH 10^3 PSI	RESIN CONTENT WT. %	VOID CONTENT VOL. %	THICKNESS PER PLY INCHES		
28 To 34	1 Max.	195.0 Min.	17.5 Min.	14.0 Min.	28 to 34	1 Max.			
		221.0		15.9					
		217.6	17.5	17.6	28.4	−0.7	0.00497		
		266.6	19.8	17.0	29.0	−0.7	0.00497		
		269.4	21.0	17.5	29.5	−0.6	0.00499		
				17.3	29.7	−0.5			
		251.2	19.4	17.3	29.2	−0.6	0.00498		
		213.8	16.3	17.4	29.4	−0.5	0.00547		
		224.4	17.0	17.6	29.9	−0.5	0.00531		
		235.6	17.7	17.8	28.6	−0.5	0.00507		
				17.1	28.6	−0.5			
		224.6	17.0	17.5	29.1	−0.5	0.00528		

STRUCTURAL PROPERTIES ON THE OTHER TESTS.

MEETS SPEC. ☐ DOES NOT MEET SPEC ☒
MEETS P.O. ☒ DOES NOT MEET P.O. ☐
Q.C. REPRESENTATIVE H.M. Toelbner
DATE: 7-7-71

MATERIAL MODMOR II/5206 LOT NUMB

VENDOR NARMCO DATE OF

QUANTITY RECEIVED 25.384 LB NUMBER OF UNITS SH 145-282 UNIT SIZE METE

TEST / UNIT IDENTITY	PREPREG PROPERTIES										
	RESIN CONTENT WT. %	VOLATILE CONTENT WT. %	GEL TIME MINUTES	VISUAL	HANDLING		TENSILE STRENGTH 10^3 PSI	TENSILE MODULUS 10^6 PSI	RESIN CONTENT WT. %	VOID CONTENT Vol. %	F S
DMS REQ'TS	39 To 45.0	3.0 Max.	18 To 26	—	—		145.0 Min.	19.0 Min.	28 To 34	1 Max.	
VENDOR AVERAGE RESULTS											
SHEET 245 -1			21' 30"				185,047	22.196			
-2			23' 00"				195,755	24.610			
-3			24' 30"				161,429	23.376			
-4							202,830	23.008			
-5											
AVE.							186,265	23.318			
SHEET __ -1											
-2											
-3											
-4											
-5											
AVE.											
SHEET __ -1											
-2											
-3											
-4											
-5											
AVE.											
SHEET __ -1											
-2											
-3											
-4											
-5											
AVE.											
SHEET __ -1											
-2											
-3											
-4											
-5											
AVE.											

REMARKS:

LOT NUMBER 81C DMS 1936B PAGE 2 OF 2

DATE OF MANUFACTURER 3-5-71 DATE RECEIVED 4-22-71

SIZE METER S/O 16105411 P/O OCY-665602-9

LAMINATE PROPERTIES								COMMENTS
VOID CONTENT Vol. %	FLEXURAL STRENGTH 10^3PSI	FLEXURAL MODULUS 10^6 PSI	SHEAR STRENGTH 10^3 PSI	RESIN CONTENT WT. %	VOID CONTENT VOL. %	THICKNESS PER PLY INCHES		
1 Max.	195.0 Min.	17.5 Min.	14.0 Min.	28 to 34	1 Max.			
	194.6 228.7 220.0	20.2 20.3 19.7	14.8 15.1 17.1			0.0053 0.0053 0.0052		
	214.6	20.08	15.7			0.0053		

MEETS SPEC. ☐ DOES NOT MEET SPEC ☐

MEETS P.O. ☐ DOES NOT MEET P.O. ☐

Q.C. REPRESENTATIVE _____

DATE: _____

TABLE CV
PREPREG QUALITY CONTROL RECEIVING INSPE

MATERIAL MODMOR II/5206 LOT NUMBER
VENDOR NARMCO DATE OF MA
QUANTITY RECEIVED 27 LB NUMBER OF UNITS UNIT SIZE METER

TEST / UNIT IDENTITY	PREPREG PROPERTIES										
	RESIN CONTENT WT. %	VOLATILE CONTENT WT. %	GEL TIME MINUTES	VISUAL	HANDLING		TENSILE STRENGTH 10^3 PSI	TENSILE MODULUS 10^6 PSI	RESIN CONTENT WT. %	VOID CONTENT Vol. %	FLE STR 1C
DMS _____ REQ'TS	39 To 45.0	3.0 Max.	18 To 26	—	—		145.0 Min.	19.0 Min.	28 To 34	1 Max.	1 M
VENDOR AVERAGE RESULTS	≅43.5										21
SHEET 13 -1	43.61	1.324	21:48				191.8	22.4			
-2	44.33						203.5	22.6			
-3	37.22						237.0	22.8			
-4							233.2	23.2			
-5							189.0	22.8			
AVE.	41.72	1.324	21:48				210.9	22.8			
SHEET 24 -1	43.59	0.910					225.0	22.2			
-2	40.86						196.9	20.8			
-3	38.19						237.3	22.2			
-4							255.5	21.4			
-5							231.9	22.3			
AVE.	40.88	0.910					229.3	21.8			
SHEET 77 -1	42.44	1.026	20:14				204.8	22.3			
-2	39.89						166.9	21.5			
-3	39.96						231.0	21.2			
-4							201.5	21.4			
-5							208.1	21.6			
AVE.	40.76	1.026	20:14				202.5	21.6			
SHEET 107 -1	38.16	0.930	20:43				230.1	22.7			
-2	38.35						223.9	22.7			
-3	33.12						214.2	22.2			
-4							236.0	22.7			
-5							214.1	22.5			
AVE.	39.88	0.930	20:43				223.7	22.6			
SHEET 144 -1	35.32	0.845					154.7	21.4			2
-2	41.48						198.4	21.9			2
-3	34.43						194.5	21.6			2
-4							189.6	21.1			
-5							223.8	22.2			
AVE.	38.08	0.845					192.2	21.6			2

REMARKS:

TABLE CV
CONTROL RECEIVING INSPECTION REPORT

LOT NUMBER 98 DMS 1936B PAGE 1 OF 2

DATE OF MANUFACTURER 6-1-71 DATE RECEIVED 6-29-71

UNIT SIZE METER S/O 16105411 P/O OCY-665602-9

LAMINATE PROPERTIES									COMMENTS
RESIN CONTENT WT. %	VOID CONTENT Vol. %	FLEXURAL STRENGTH 10^3PSI	FLEXURAL MODULUS 10^6 PSI	SHEAR STRENGTH 10^3 PSI	RESIN CONTENT WT. %	VOID CONTENT VOL. %	THICKNESS PER PLY INCHES		
28 To 34	1 Max.	195.0 Min.	17.5 Min.	14.0 Min.	28 to 34	1 Max.			
		218.9	16.8						
							0.0055 0.0052 0.0053 0.0058 0.0055 0.00546		
		230.4 215.2 216.5 220.7	17.7 18.0 17.8 17.8	16.0 16.1 16.0 16.0					

MEETS SPEC. ☒ DOES NOT MEET SPEC ☐

MEETS P.O. ☒ DOES NOT MEET P.O. ☐

Q.C. REPRESENTATIVE H. M. Troellner

DATE: 8-6-71

MATERIAL MODMOR II/5206 LOT NUMBER

VENDOR DATE OF MANU

QUANTITY RECEIVED NUMBER OF UNITS UNIT SIZE

TEST / UNIT IDENTITY	PREPREG PROPERTIES						LA				
	RESIN CONTENT WT. %	VOLATILE CONTENT WT. %	GEL TIME MINUTES	VISUAL	HANDLING		TENSILE STRENGTH 10^3 PSI	TENSILE MODULUS 10^6 PSI	RESIN CONTENT WT. %	VOID CONTENT Vol. %	FLEXU STREN 10^3
DMS _____ REQ'TS	39 To 45.0	3.0 Max.	18 To 26	—	—		145.0 Min.	19.0 Min.	28 To 34	1 Max.	195 Min
VENDOR AVERAGE RESULTS											
SHEET__-1 178 -2 -3 -4 -5 AVE.	42.04 38.84 42.39 41.09	0.880 0.880	19:57 19:57				232.0 238.4 239.6 225.8 246.4 236.4	23.0 21.9 21.6 21.4 22.1 22.0			
SHEET__-1 202 -2 -3 -4 -5 AVE.	34.93 43.47 43.01 40.47	0.783 0.783	20:42 20:42				165.9 176.0 204.0 207.7 194.6 189.6	21.7 21.6 21.8 20.8 21.6 21.5			
SHEET__-1 79 -2 -3 -4 -5 AVE.											22 22 20 22
SHEET__-1 -2 -3 -4 -5 AVE.											
SHEET__-1 -2 -3 -4 -5 AVE.											

REMARKS:

LOT NUMBER 98 DMS 1936B PAGE 2 OF 2

DATE OF MANUFACTURER _____ DATE RECEIVED _____

SIZE _____ S/O _____ P/O _____

	LAMINATE PROPERTIES								
T	VOID CONTENT Vol. %	FLEXURAL STRENGTH 10^3PSI	FLEXURAL MODULUS 10^6 PSI	SHEAR STRENGTH 10^3 PSI	RESIN CONTENT WT. %	VOID CONTENT VOL. %	THICKNESS PER PLY INCHES		COMMENTS
	1 Max.	195.0 Min.	17.5 Min.	14.0 Min.	28 to 34	1 Max.			
-	____	____	____	____	____	____	____	____	
-	____	____	____	____	____	____	____	____	
		229.1	18.1	16.6					
		229.2	17.5	16.6					
		209.7	17.3	16.2					
-	____	____	____	____	____	____	____	____	
		222.7	17.6	16.5					
-	____	____	____	____	____	____	____	____	
-	____	____	____	____	____	____	____	____	

MEETS SPEC. ☐ DOES NOT MEET SPEC ☐

MEETS P.O. ☐ DOES NOT MEET P.O. ☐

Q.C. REPRESENTATIVE _____

DATE: _____

TABLE CVI
PREPREG QUALITY CONTROL RECEIVI

MATERIAL MODMOR II/5206 LOT

VENDOR NARMCO DAT

QUANTITY RECEIVED 27.45 LB NUMBER OF UNITS 27 UNIT SIZE

TEST / UNIT IDENTITY	PREPREG PROPERTIES										
	RESIN CONTENT WT. %	VOLATILE CONTENT WT. %	GEL TIME MINUTES	VISUAL	HANDLING		TENSILE STRENGTH 10^3 PSI	TENSILE MODULUS 10^6 PSI	RESIN CONTENT WT. %	VOID CONTE Vol.
DMS _____ REQ'TS	39 To 45.0	3.0 Max.	18 To 26	—	—		145.0 Min.	19.0 Min.	28 To 34	1 Max
VENDOR AVERAGE RESULTS	≅43.0									
SHEET 4 -1	40.31	0.776	22:17				207.4	23.8		
-2	40.82						183.3	22.9		
-3							193.6	22.8		
-4							184.5	22.4		
-5							200.3	23.8		
AVE.	40.57	0.776	22:17				193.8	23.1		
SHEET 8 -1	41.34	1.300	22:43				215.2	24.1		
-2	43.18						215.2	21.8		
-3	42.40						206.5	22.4		
-4							187.3	21.4		
-5							198.5	23.3		
AVE.	42.31	1.300	22:43				204.5	22 6		
SHEET 12 -1	39.71	0.565	23:26				191.9	21.9		
-2	45.21						209.3	22.3		
-3							195.7	22.6		
-4							167.6	20.8		
-5							202.9	23.0		
AVE.	42.46	0.565	23:26				193.5	22.1		
SHEET 16 -1	43.37	1.211					200.6	23.2		
-2	42.26						191.5	23.9		
-3							174.0	21.2		
-4							154.2	21.8		
-5							179.6	23.3		
AVE.	42.82	1.211					180.0	22.7		
SHEET 20 -1	40.82		21:08				203.8	21.7		
-2	39.18						206.3	22.2		
-3							196.3	21.8		
-4							184.0	21.4		
-5							185.8	22.5		
AVE.	40.41		21:08				195.2	21.9		

REMARKS:

TABLE CVI
CONTROL RECEIVING INSPECTION REPORT

LOT NUMBER 317 DMS 1936B PAGE 1 OF 2

DATE OF MANUFACTURER 6-21-71 DATE RECEIVED 7-6-71

UNIT SIZE 3" TAPE S/O 16105411 P/O OCY-665603-9

LAMINATE PROPERTIES									
RESIN CONTENT WT. %	VOID CONTENT Vol. %	FLEXURAL STRENGTH 10^3PSI	FLEXURAL MODULUS 10^6 PSI	SHEAR STRENGTH 10^3 PSI	RESIN CONTENT WT. %	VOID CONTENT VOL. %	THICKNESS PER PLY INCHES		COMMENTS
28 To 34	1 Max.	195.0 Min.	17.5 Min.	14.0 Min.	28 to 34	1 Max.			
		204.9		15.7					
		215.4 215.2 211.7	18.6 18.4 18.5	15.6 14.0 15.4			0.00566 0.00562 0.00560		
		214.1	18.5	15.0			0.00563		

MEETS SPEC. ☒ DOES NOT MEET SPEC ☐

MEETS P.O. ☒ DOES NOT MEET P.O. ☐

Q.C. REPRESENTATIVE H m. Toellner

DATE: 8-13-71

TABLE CVI

MATERIAL MODMOR II/5206 LO

VENDOR DA

QUANTITY RECEIVED ______ NUMBER OF UNITS ______ UNIT SIZE ______

TEST / UNIT IDENTITY	PREPREG PROPERTIES RESIN CONTENT WT. %	VOLATILE CONTENT WT. %	GEL TIME MINUTES	VISUAL	HANDLING		TENSILE STRENGTH 10^3 PSI	TENSILE MODULUS 10^6 PSI	RESIN CONTENT WT. %	VOI CONT Vo
DMS REQ'TS	39 To 45.0	3.0 Max.	18 To 26	—	—		145.0 Min.	19.0 Min.	28 To 34	I Ma
VENDOR AVERAGE RESULTS										
SHEET 24 -1	39.51	0.900	19:44				211.4	24.4		
-2	38.72						191.8	22.1		
-3							202.9	22.5		
-4							193.2	21.9		
-5							221.6	23.3		
AVE.	39.12	0.900	19:44				204.2	22.8		
SHEET 19 -1										
-2										
-3										
-4										
-5										
AVE.										
SHEET__ -1										
-2										
-3										
-4										
-5										
AVE.										
SHEET__ -1										
-2										
-3										
-4										
-5										
AVE.										
SHEET__ -1										
-2										
-3										
-4										
-5										
AVE.										

REMARKS:

LE CVI (CONTINUED)

LOT NUMBER 317 DMS 1936B PAGE 2 OF 2

DATE OF MANUFACTURER _____ DATE RECEIVED _____

IZE _____ S/O _____ P/O _____

LAMINATE PROPERTIES								COMMENTS
VOID CONTENT Vol. %	FLEXURAL STRENGTH 10^3PSI	FLEXURAL MODULUS 10^6 PSI	SHEAR STRENGTH 10^3 PSI	RESIN CONTENT WT. %	VOID CONTENT VOL. %	THICKNESS PER PLY INCHES		
1 Max.	195.0 Min.	17.5 Min.	14.0 Min.	28 to 34	1 Max.			
	208.2* 218.2* 205.0* 210.5*	18.9* 18.7* 19.1* 18.9*	15.3 15.6 12.8 14.6					

MEETS SPEC. ☐ DOES NOT MEET SPEC ☐

MEETS P.O. ☐ DOES NOT MEET P.O. ☐

Q.C. REPRESENTATIVE _____

DATE: _____

TABLE CVII
PREPREG QUALITY CONTROL RECEIVI

MATERIAL MODMOR II/5206 LOT

VENDOR NARMCO DAT

QUANTITY RECEIVED 23.24 LB NUMBER OF UNITS 8 UNIT SIZE

TEST / UNIT IDENTITY	PREPREG PROPERTIES									
	RESIN CONTENT WT. %	VOLATILE CONTENT WT. %	GEL TIME MINUTES	VISUAL	HANDLING		TENSILE STRENGTH 10^3 PSI	TENSILE MODULUS 10^6 PSI	RESIN CONTENT WT. %	VOID CONTE Vol.
DMS REQ'TS	39 To 45.0	3.0 Max.	18 To 26	—	—		145.0 Min.	19.0 Min.	28 To 34	1 Max
VENDOR AVERAGE RESULTS	≅43.0									
SHEET__-1	40.03	0.742	21:19				200.7	23.7		
1 -2	40.47						111.4	23.3		
-3							111.8	22.9		
-4							128.9	22.6		
-5							172.2	23.4		
AVE.	40.25	0.742	21:19				145.0	23.2		
SHEET__-1	46.46	0.671	21:54				183.8	23.1		
3 -2	43.40						168.3	22.3		
-3	43.30						193.0	22.8		
-4							183.4	21.4		
-5							192.7	23.3		
AVE.	44.39	0.671	21:54				184.2	22.6		
SHEET__-1	41.78	0.510	20:26				210.9	23.0		
4 -2	39.73						192.3	22.4		
-3	44.27						175.6	21.1		
-4							211.2	22.2		
-5							203.5	23.4		
AVE.	40.76	0.510	20:26				198.7	22.4		
SHEET__-1	44.27	0.650	22:58				218.8	23.8		
5 -2	43.07						193.1	22.7		
-3	46.20						203.0	22.3		
-4							201.2	23.5		
-5							174.7	22.4		
AVE.	44.51	0.650	22:58				198.2	23.0		
SHEET__-1	43.59	0.629	21:59				187.0	21.1		
7 -2	44.28						189.8	21.6		
-3							178.3	21.3		
-4							179.6	21.0		
-5							195.7	22.0		
AVE.	43.94	0.629	21:59				186.1	21.4		

REMARKS:

TABLE CVII
CONTROL RECEIVING INSPECTION REPORT

LOT NUMBER 319 DMS 1936B PAGE 1 OF 1

DATE OF MANUFACTURER 6-29-71 DATE RECEIVED 7-6-71

UNIT SIZE 3" TAPE S/O 16105411 P/O OCY-665603-9

LAMINATE PROPERTIES									COMMENTS
RESIN CONTENT WT. %	VOID CONTENT Vol. %	FLEXURAL STRENGTH 10^3PSI	FLEXURAL MODULUS 10^6 PSI	SHEAR STRENGTH 10^3 PSI	RESIN CONTENT WT. %	VOID CONTENT VOL. %	THICKNESS PER PLY INCHES		
28 To 34	1 Max.	195.0 Min.	17.5 Min.	14.0 Min.	28 to 34	1 Max.			
		201.1		15.4					
		200.3 184.6 203.4 196.1	18.1 18.0 18.6 18.2	14.5 15.2 15.0 14.9			0.00568 0.00565 0.00567 0.00567		
		189.2 214.0 202.4 201.9	19.6 19.4 19.3 19.4	15.4 15.4 14.8 15.2					

MEETS SPEC. ☒ DOES NOT MEET SPEC ☐

MEETS P.O. ☒ DOES NOT MEET P.O. ☐

Q.C. REPRESENTATIVE H. M Toellner

DATE: 8-13-71

TABLE CVIII
PREPREG QUALITY CONTROL RECEIVING I

MATERIAL MODMOR II/5206 LOT NUM

VENDOR NARMCO DATE OF

QUANTITY RECEIVED 32.35 LB NUMBER OF UNITS 12 UNIT SIZE 3" T

TEST / UNIT IDENTITY	PREPREG PROPERTIES									
	RESIN CONTENT WT. %	VOLATILE CONTENT WT. %	GEL TIME MINUTES	VISUAL	HANDLING		TENSILE STRENGTH 10^3 PSI	TENSILE MODULUS 10^6 PSI	RESIN CONTENT WT. %	VOID CONTENT Vol. %
DMS _____ REQ'TS	39 To 45.0	3.0 Max.	18 To 26	—	—		145.0 Min.	19.0 Min.	28 To 34	1 Max.
VENDOR AVERAGE RESULTS	≅41.5									
SHEET 12 -1	39.34	1.397	22:39				187.2	23.3		
-2	40.56						182.5	21.5		
-3							174.8	21.2		
-4							165.0	22.3		
-5							202.4	24.2		
AVE.	39.95	1.397	22:39				182.4	22.5		
SHEET 14 -1	40.13						187.2	21.7		
-2	39.23						193.8	22.3		
-3							198.7	22.2		
-4							196.6	22.0		
-5							193.1	23.3		
AVE.	39.68						193.9	22.3		
SHEET 16 -1	42.50	1.408	21:52				175.3	22.1		
-2	40.82						168.3	20.9		
-3	41.52						166.1	22.3		
-4							174.9	21.6		
-5							178.2	22.8		
AVE.	41.61	1.408	21:52				172.6	21.9		
SHEET 18 -1	41.57						196.5	23.2		
-2	40.75						179.1	21.9		
-3							184.6	21.5		
-4							132.8	20.6		
-5							169.0	19.8		
AVE.	41.16						172.4	21.4		
SHEET 19 -1	44.71	1.575	20:39				178.9	21.1		
-2	39.79						184.1	22.7		
-3							186.7	22.3		
-4							166.2	20.5		
-5							196.9	22.5		
AVE.	42.25	1.575	20:39				182.6	21.8		

REMARKS:

CVIII
ECEIVING INSPECTION REPORT

LOT NUMBER 320 DMS 1936B PAGE 1 OF 2

DATE OF MANUFACTURER 7-1-71 DATE RECEIVED 7-6-71

ZE 3" TAPE S/O 16105411 P/O OCY-665603-9

LAMINATE PROPERTIES								
VOID CONTENT Vol. %	FLEXURAL STRENGTH 10^3PSI	FLEXURAL MODULUS 10^6 PSI	SHEAR STRENGTH 10^3 PSI	RESIN CONTENT WT. %	VOID CONTENT VOL. %	THICKNESS PER PLY INCHES		COMMENTS
1 Max.	195.0 Min.	17.5 Min.	14.0 Min.	28 to 34	1 Max.			
	197.5		17.1					
						0.0059 0.0056 0.0061		
						0.0055		
	215.9 188.0 201.0	18.4 18.0 19.2	14.0 14.6 14.0					
	201.6	18.5	14.2					

MEETS SPEC. ☒ DOES NOT MEET SPEC ☐

MEETS P.O. ☒ DOES NOT MEET P.O. ☐

Q.C. REPRESENTATIVE H. M. Tollner

DATE: 8-12-71

TABLE CVIII (

MATERIAL MODMOR II/5206 LOT

VENDOR DAT

QUANTITY RECEIVED NUMBER OF UNITS UNIT SIZE

TEST / UNIT IDENTITY	PREPREG PROPERTIES									
	RESIN CONTENT WT. %	VOLATILE CONTENT WT. %	GEL TIME MINUTES	VISUAL	HANDLING		TENSILE STRENGTH 10^3 PSI	TENSILE MODULUS 10^6 PSI	RESIN CONTENT WT. %	VOID CONTE Vol.
DMS REQ'TS	39 To 45.0	3.0 Max.	18 To 26	—	—		145.0 Min.	19.0 Min.	28 To 34	1 Max
VENDOR AVERAGE RESULTS										
SHEET 11 -1	40.63	1.600	22:27				198.3	22.9		
-2	41.87						173.9	21.2		
-3	41.90						171.9	21.2		
-4							186.6	21.2		
-5							152.8	18.2		
AVE.	41.47	1.600	22:27				176.7	20.9		
SHEET 13 -1	42.09	1.456	21:10				188.4	21.4		
-2	40.58						176.5	20.1		
-3							191.4	21.0		
-4							154.0	20.9		
-5							167.9	22.8		
AVE.	41.34	1.456	21:10				175.7	21.2		
SHEET__ -1										
-2										
-3										
-4										
-5										
AVE.										
SHEET__ -1										
-2										
-3										
-4										
-5										
AVE.										
SHEET__ -1										
-2										
-3										
-4										
-5										
AVE.										

REMARKS:

TABLE CVIII (CONTINUED)

LOT NUMBER 320 DMS 1936B PAGE 2 OF 2

DATE OF MANUFACTURER _____ DATE RECEIVED _____

UNIT SIZE _____ S/O _____ P/O _____

LAMINATE PROPERTIES

RESIN CONTENT WT. %	VOID CONTENT Vol. %	FLEXURAL STRENGTH 10^3PSI	FLEXURAL MODULUS 10^6 PSI	SHEAR STRENGTH 10^3 PSI	RESIN CONTENT WT. %	VOID CONTENT VOL. %	THICKNESS PER PLY INCHES		COMMENTS
28 To 34	1 Max.	195.0 Min.	17.5 Min.	14.0 Min.	28 to 34	1 Max.			
		201.6 208.5 177.1 195.7	18.1 18.3 17.9 18.1	14.4 13.8 14.3 14.1					
							0.0063 0.0056 0.0059 0.0056 0.0049 0.0057		

MEETS SPEC. ☐ DOES NOT MEET SPEC ☐

MEETS P.O. ☐ DOES NOT MEET P.O. ☐

Q.C. REPRESENTATIVE _____

DATE: _____

TABLE C-IX
IN-PROCESS QUALITY CONTROL TESTS – STABILIZER UNIT ONE
GRAPHITE COMPONENTS

PROPERTY	REAR SPAR		CANT RIB NO. 1		CANT RIB NO. 2		SKINS				ATTACH ANGLES[1]	
							UPPER		LOWER			
	UPPER FLANGE	LOWER FLANGE	UPPER FLANGE	LOWER FLANGE	UPPER FLANGE	LOWER FLANGE	LEFT	RIGHT	LEFT	RIGHT	UPPER	LOWER
FLEXURAL STRENGTH, PSI	73,500	73,600	66,200	66,700	70,700	65,500	69,200	74,000	79,900	65,400	179,600	181,600
FLEXURAL MODULUS, PSI x 10^{-6}	6.6	7.0	6.1	6.5	8.2	7.9	6.2	6.1	5.4	6.0	16.3	17.6
SHORT BEAM SHEAR, PSI	11,400	11,500	7,100	7,800	7,900	8,200	9,600	7,800	7,000	8,000	14,100	13,600
RESIN CONTENT, WEIGHT PERCENT	36.4	36.5	36.2	35.0	35.5	35.7	35.6	34.5	33.1	33.8		34.1
VOID CONTENT, VOLUME PERCENT	–0.95	–1.03	–0.31	–0.04	0.31	0.54	–0.03	0.17	1.18	0.67		0.84
TENSILE LAP SHEAR (ADHESIVE)	–	–	–	–	–	–	–	–	–	–	2,710	2,450

[1] DATA ON UNIDIRECTIONAL PANEL AND TENSILE LAP SHEAR ADHESIVE COUPONS CURED WITH PART.

TABLE C-X

IN-PROCESS QUALITY CONTROL TESTS – STABILIZER UNIT ONE FIBERGLASS LEADING-EDGE COMPONENTS

TEST	COMPONENT NO.								
	-13[1]	-14[1]	-17 NO. 1	-17 NO. 2	-19 NO. 1	-19 NO. 2	-33[1]	-35 NO. 1	-35 NO. 2
RESIN CONTENT, PERCENT BY WEIGHT	19.6	19.0	15.9	16.9	16.8	15.4	17.1	16.8	18.6
VOID CONTENT, PERCENT BY VOLUME	2.9	3.3	1.5	1.2	1.7	2.4	1.4	1.8	1.7

[1] 2 PARTS MADE -1 PART TESTED

TABLE C-XI

IN-PROCESS QUALITY CONTROL TESTS – STABILIZER UNIT TWO

PROPERTY		CANT-RIB NO. 3		CANT-RIB NO. 4		REAR-SPAR	
		UPPER FLANGE	LOWER FLANGE	UPPER FLANGE	LOWER FLANGE	UPPER FLANGE	LOWER FLANGE
FLEXURAL STRENGTH (PSI)	1	68,800	70,900	82,400	73,400	65,200	65,100
	2	61,000	63,100	56,800	63,000	64,200	75,900
	AVG.	64,900	67,000	69,600	68,200	64,700	70,500
FLEXURAL MODULUS (10^6 psi)	1	7.12	7.76	7.69	8.06	7.79	8.41
	2	7.32	6.39	7.51	7.86	8.01	7.79
	AVG.	7.22	7.08	7.60	7.96	7.90	8.10
SHORT BEAM SHEAR (PSI)	1	8,500	8,240	9,690	8,470	9,550	8,460
	2	9,540	9,480	9,200	9,420	10,320	9,730
	3	8,600	8,360	10,620	10,570		
	AVG.	8,880	8,690	9,830	9,480	9,940	9,100
RESIN CONTENT (WT PERCENT)	1	32.5	31.8	31.9	32.8	35.1	34.3
	2	33.4	32.6	32.5	32.8	37.6	35.9
	3	32.9	32.4	33.5	32.3		
	AVG.	32.9	32.3	32.6	32.6	36.4	35.1
VOID CONTENT (VOL PERCENT)	1	0.01	0.01	0.51	0.31	0.15	0.09
	2	0.01	0.01	0.02	0.39	0.61	0.26
	3	0.01	0.01	0.41	0.21		
	AVG.	0.01	0.01	0.31	0.30	0.38	0.18

The structural performance of the stabilizer parts is more dependent on in-plane properties than on flexural properties. The assessment of the effects of voids on structural performance will therefore be performed on completion of the static tests of the stabilizer assembly.

NONDESTRUCTIVE TESTS

The skin panels and various adhesive bonds in the stabilizer structure were nondestructively tested using ultrasonic and radiographic techniques. The upper and lower graphite-epoxy skin panels were tested using the ultrasonic pulse-echo, ultrasonic C-scan, and X-ray techniques. Reference standard specimens were fabricated to represent the various pattern and thickness combinations in the stabilizer which were joined by adhesive bonding. These specimens were then used to determine the presentations on the various items of testing equipment for both high and low quality bonds.

The upper and lower skin panels were ultrasonically inspected by the pulse-echo (loss of back-surface signal) technique at 5 MHZ using a 1/2 inch diameter SPZ contact search-unit. Areas exhibiting more than 75% loss of back-surface signal (indicative of low resin or porous conditions) were observed in relatively thick laminates (48 layers or greater) and in areas adjacent to the bonded titanium doublers (Figures C1 and C2). These areas were subsequently X-rayed using 100 KVP, 5 ma, GEVAERT D4 film. The X-ray photographs indicated fiber patterns in the areas exhibiting loss of back-surface signal. Graphite composite skins exhibiting good ultrasonic transmission are generally homogeneous and do not reveal fiber orientations when radiographed. The upper skin was also inspected using the ultrasonic C-scan technique. A highly damped, 5 MHZ short-focus search-unit was used to make a C-scan record at the forward center section and at the aft hinge at x = -20. Light areas in C-scan record corresponded to locations on the panel exhibiting more than 75% loss of back-surface signal.

The NDT results for the stabilizer skins are qualitative in nature and are not conclusive from the standpoint of accepting or rejecting of the parts involved. The results appear consistent with the indications of laminate voids from the previously discussed in-process tests. Validity of the NDT results will be assessed during the post-static test analysis of the stabilizer.

The lower skin (Z5569974) was bonded to the honeycomb ribs using graphite attach-angles. Both sides of the bond assembly were accessible for inspection since the upper panel was not in place at this time. The bond assembly was located in the assembly jig in the vertical position. The graphite angle-to-skin and angle-to-honeycomb bond quality was checked by tap test, contact pulse-echo ultrasonic, and Fokker bond tester. No bond discontinuities were indicated.

The ultrasonic test was conducted using contact pulse-echo techniques at 2.25 and 5.0 MHZ using a 3/8 inch diameter SFZ search-unit. Reference standards representing no-bond and good-bond between the angle to skin,

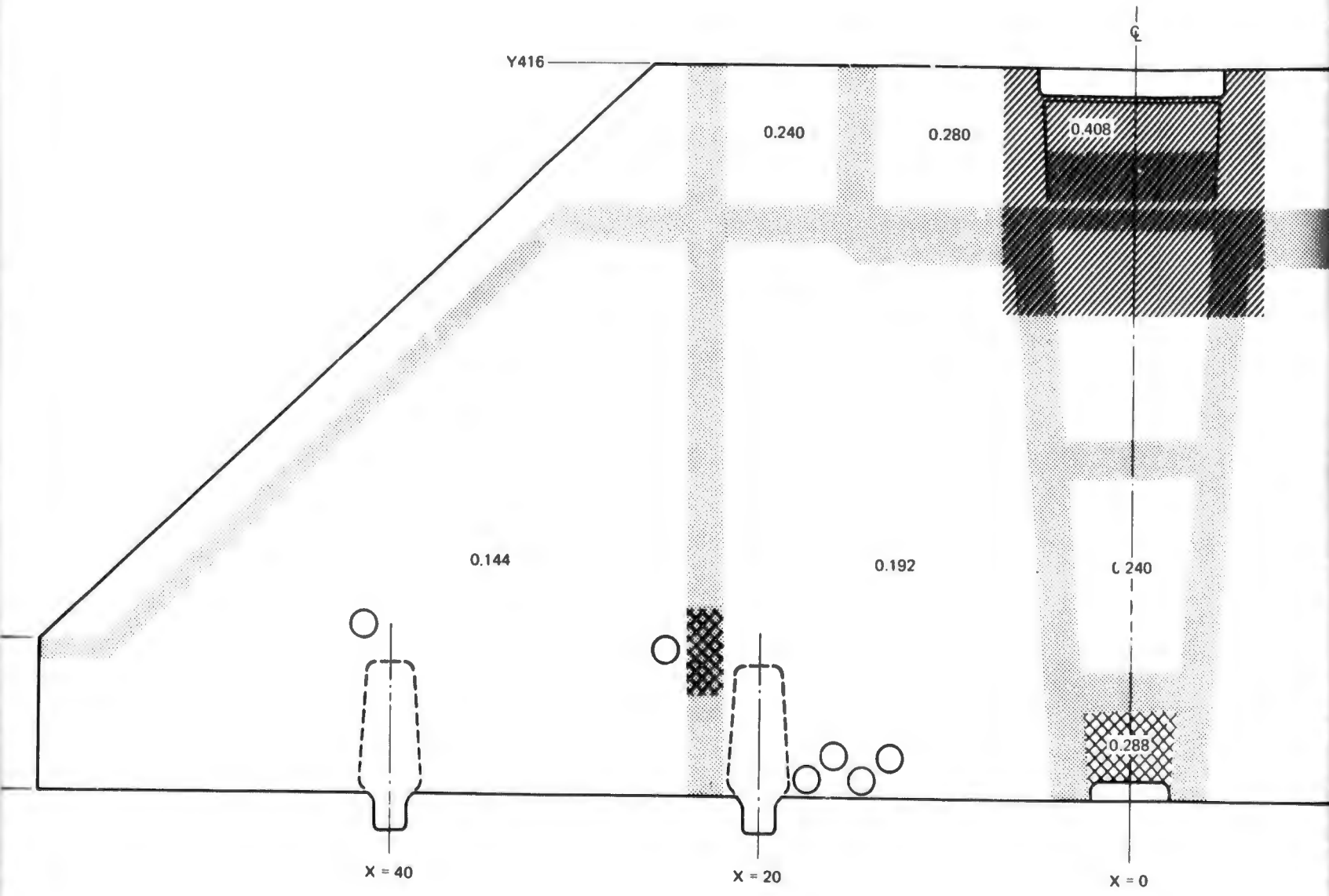

Z5569973
UPPER SKIN
LOOKING DOWN

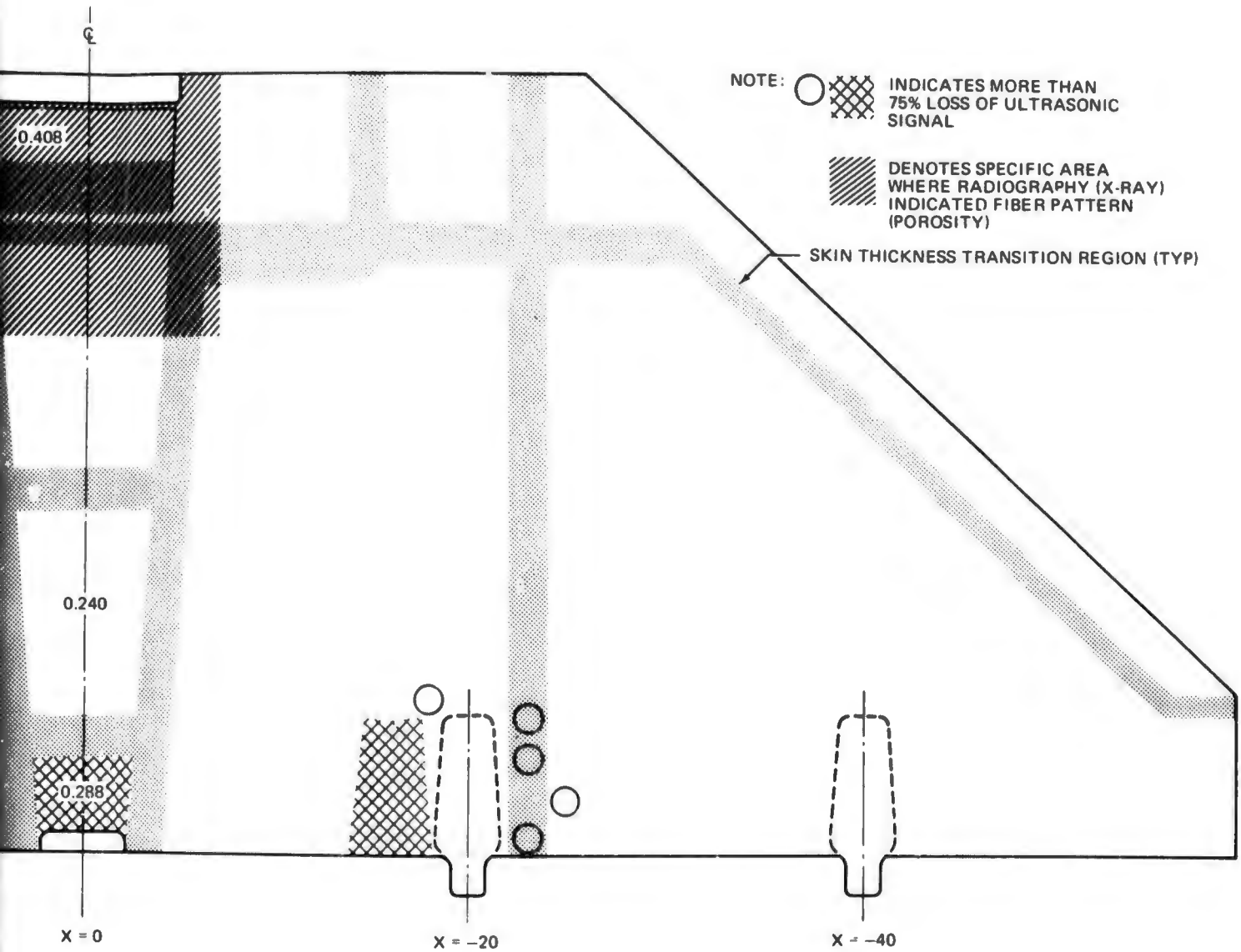

FIGURE C-1. NONDESTRUCTIVE TEST RESULTS FOR UPPER SKIN

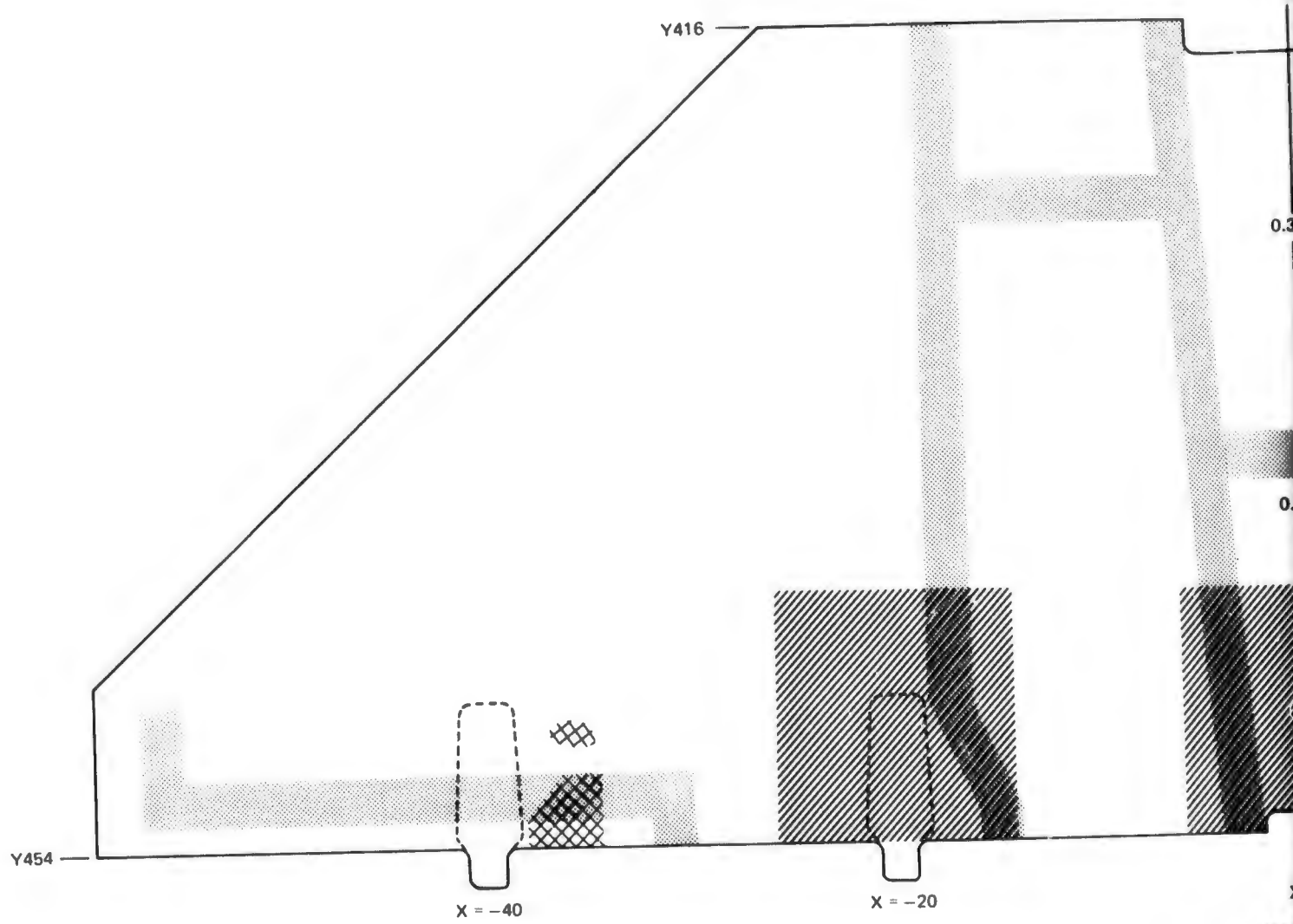
Y416
Y454
X = −40
X = −20

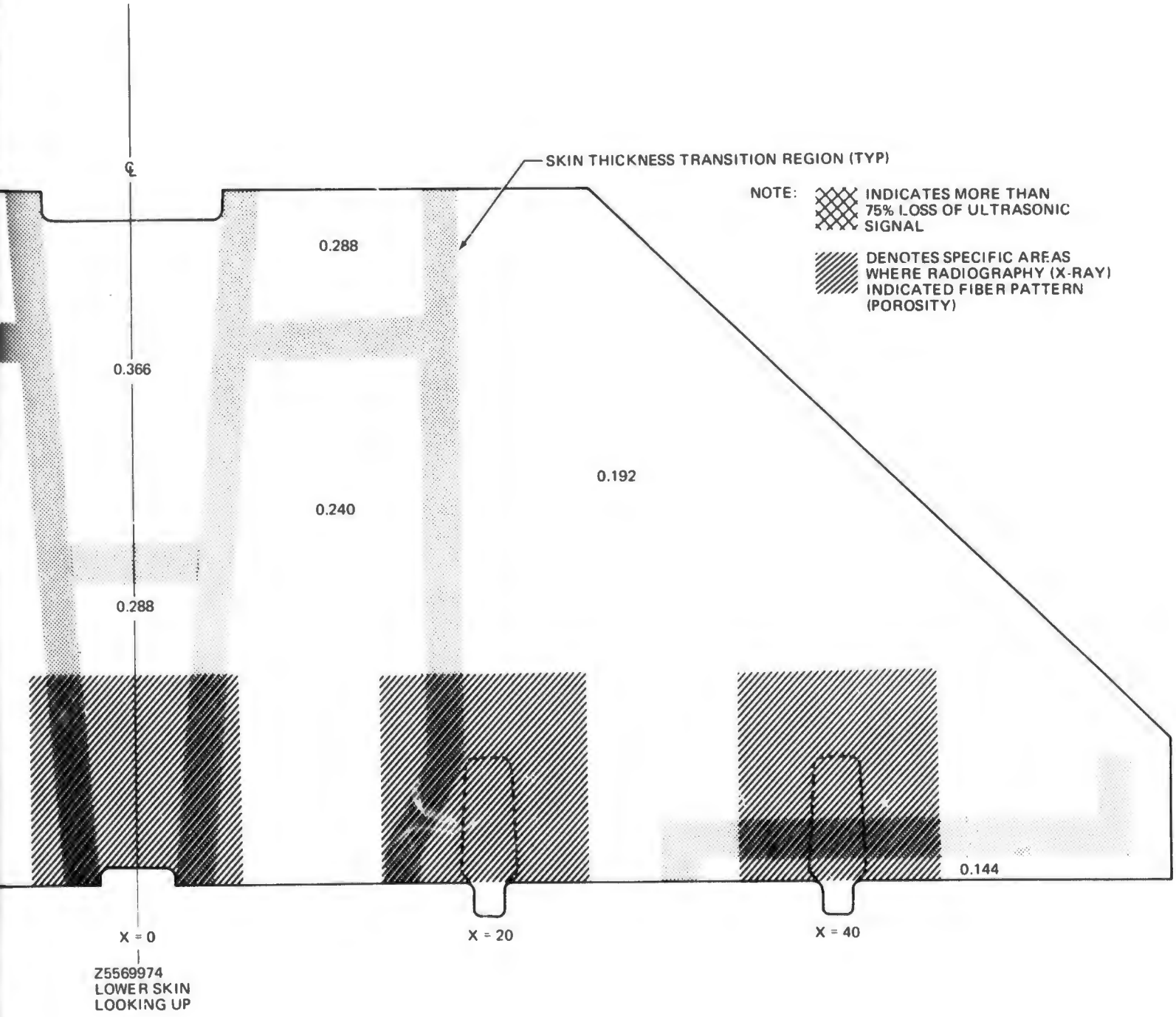

FIGURE C-2. NONDESTRUCTIVE TEST RESULTS FOR LOWER SKIN

and angle to honeycomb were prepared. The cathode ray tube (CRT) presentations of the ultrasonic test results at 5 MHZ for various test response are shown in Figure C3. The structure was tested from the inner surface with the probe placed on the individual angles. No bond discontinuities were indicated.

The Fokker bond tester was also calibrated on the applicable reference standards. Various probes and frequency settings were evaluated. The final selection for optimum response was Probe No. 1214-0518 (1/2 inch diameter). Fokker bond tester fluid was used as a couplant for all tests. Results obtained from angle-to-honeycomb bond quality are shown in Figure C4. The angle-to-honeycomb bond quality was checked from the accessible side with no lack-of-bond indicated.

The instrument was then calibrated to the angle-to-skin standards yielding results shown in Figure C5. The angle-to-lower-skin bond was tested from the inner surface. During testing, it was observed that the Fokker A-scope and B-meter readings changed when the probe was placed on variable thickness areas of the skin. Figure C2 shows five changes of thickness in the lower skin ranging from 0.144 to 0.366 inch. Figure C6 shows the change in Fokker readings as the probe was placed over two variations in skin thickness. Note that the same reading are obtained for a skin-to-angle bond 0.242 inch thick, and for skin only 0.240 thick (Figure C6-(2), (3)).

Based on the foregoing findings, a second set of reference standard specimens, Figure C7, were fabricated. Evaluation of the bond joint between the upper skin and graphite angles was performed from the outer surface of the upper skin since the interior of the structure was inaccessible. Because of this fact, the reference standards specimens were designed to represent the variations in the upper skin thickness as shown on drawing number Z5569973. The design for the three reference standards is shown in Figure C7. Specimen A (3 x 9 inches) is typical of the adhesive system used to bond the upper skin to upper attach-angles. Specimen B (2 x 9 inches) is typical of the adhesive system used to bond the upper skin to upper attach-angles, except it was cured in an autoclave. Specimen C (2 x 9 inches) is typical of the actual adhesive system with bolt-pressure bonding of the upper skin to upper attach-angles. Specimen C is typical of the actual condition used on the horizontal stabilizer upper skin to upper attach-angle bond joints. All three specimens had six thickness steps of 24, 32, 40, 48, 56, and 68 plies. Precured angle layers of 8 and 16 plies were bonded to each of the three specimens as shown. Specimen A represents a condition of bare skin (no-bond) and also 8 and 16 ply bonded angles.

After the specimens were fabricated, they were evaluated by radiography and immersed ultrasonic C-scan recording at 5 MHZ. Radiography showed no discontinuities in the specimens. The results by ultrasonic C-scan recording shown in Figure C8 indicate good bond quality for all three specimens. The ultrasonic C-scan system is shown in Figure C9. The specimens were also

(A) CRT PRESENTATIONS FOR ANGLE TO SKIN BOND QUALITY

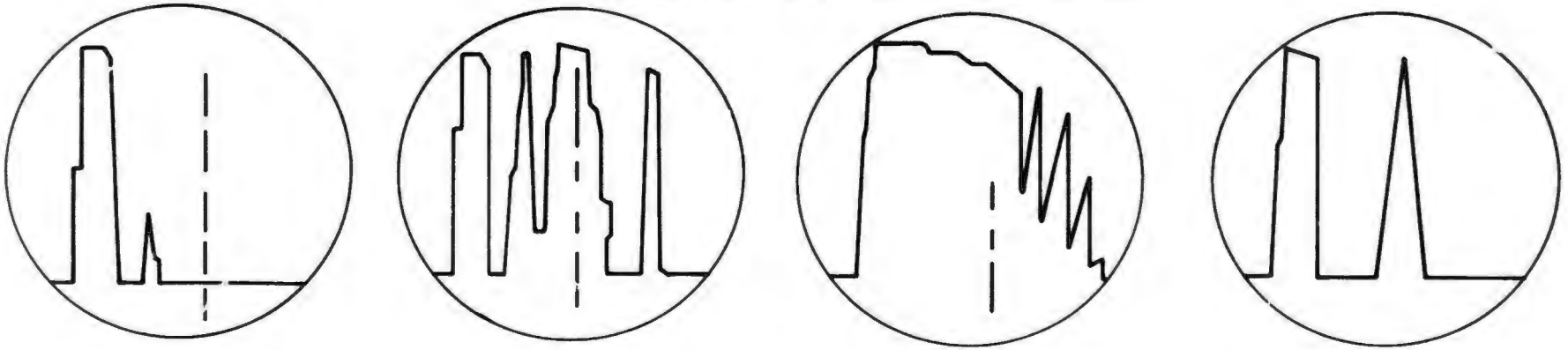

(1) PROBE IN AIR

(2) PROBE ON SKIN

(3) PROBE ON ANGLE ONLY (NO BOND)

(4) PROBE ON ANGLE TO SKIN (GOOD BOND)

(B) CRT PRESENTATIONS FOR ANGLE TO HONEYCOMB BOND QUALITY

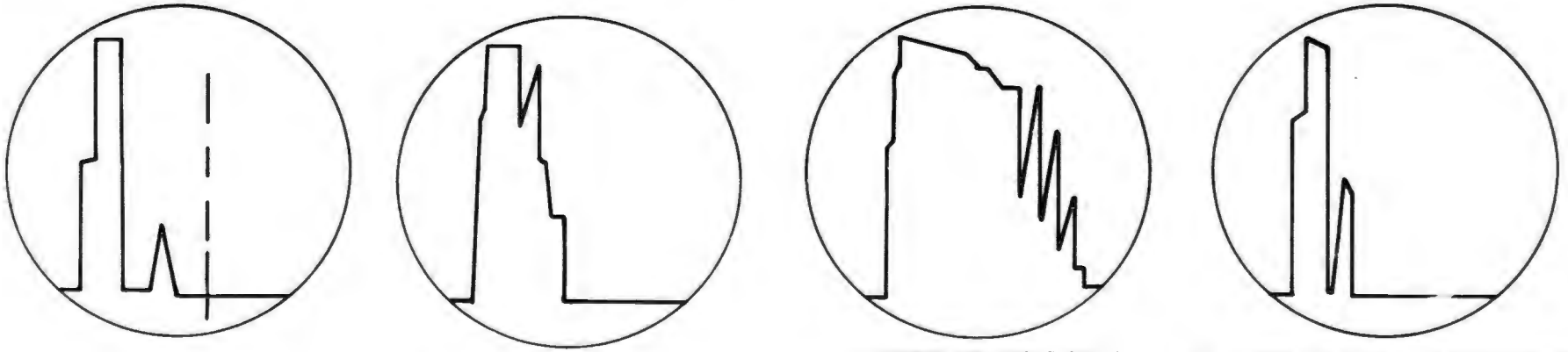

(1) PROBE IN AIR

(2) PROBE ON HONEYCOMB ONLY

(3) PROBE ON ANGLE ONLY (NO BOND)

(4) PROBE ON ANGLE TO HONEYCOMB (GOOD BOND)

FIGURE C-3. CONTACT PULSE-ECHO ULTRASONIC TEST RESULTS AT 5 MHz FOR LOWER ATTACH-ANGLE BOND

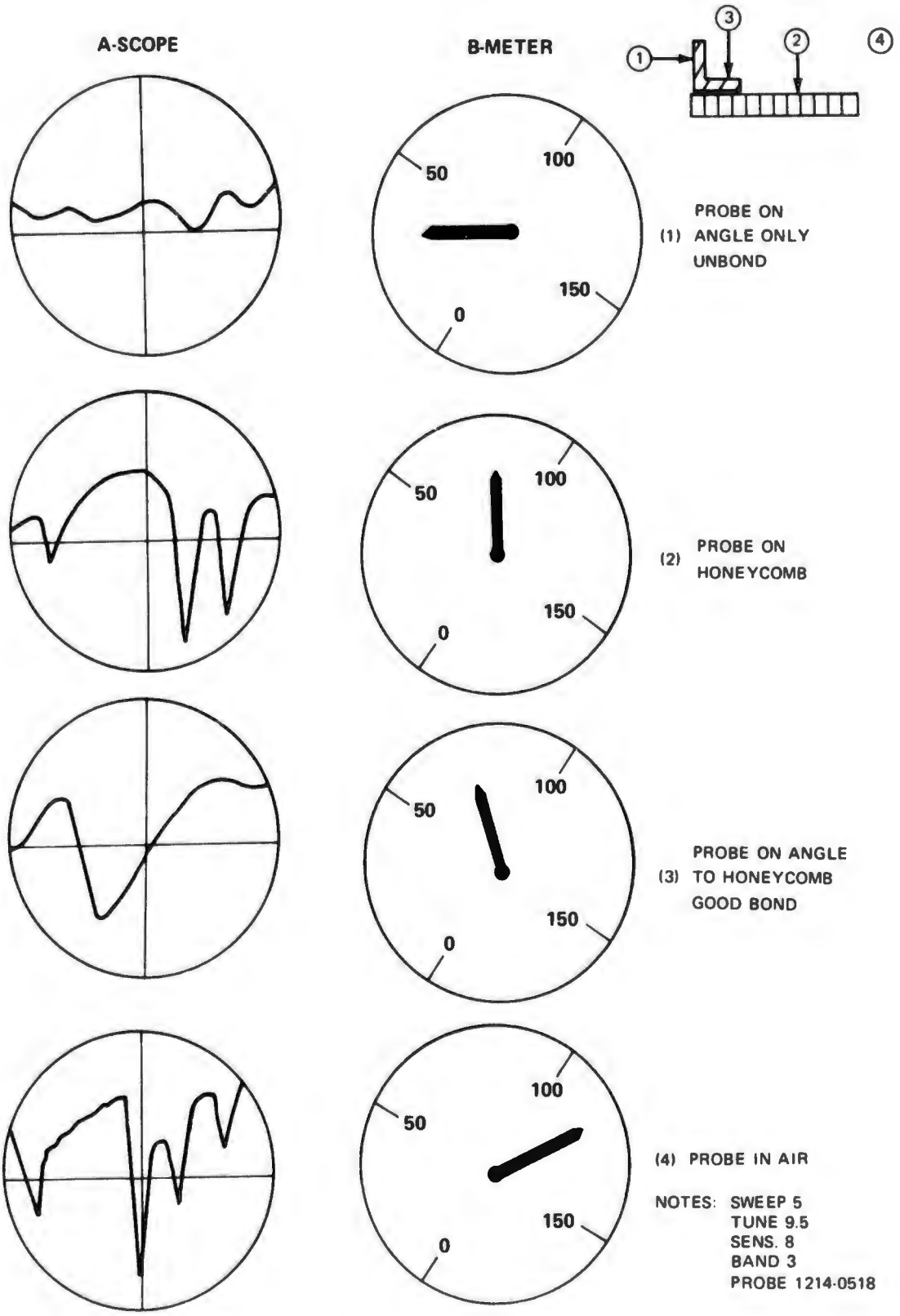

FIGURE C-4. FOKKER BOND TESTER PRESENTATIONS FOR ATTACH-ANGLE TO HONEYCOMB BOND QUALITY

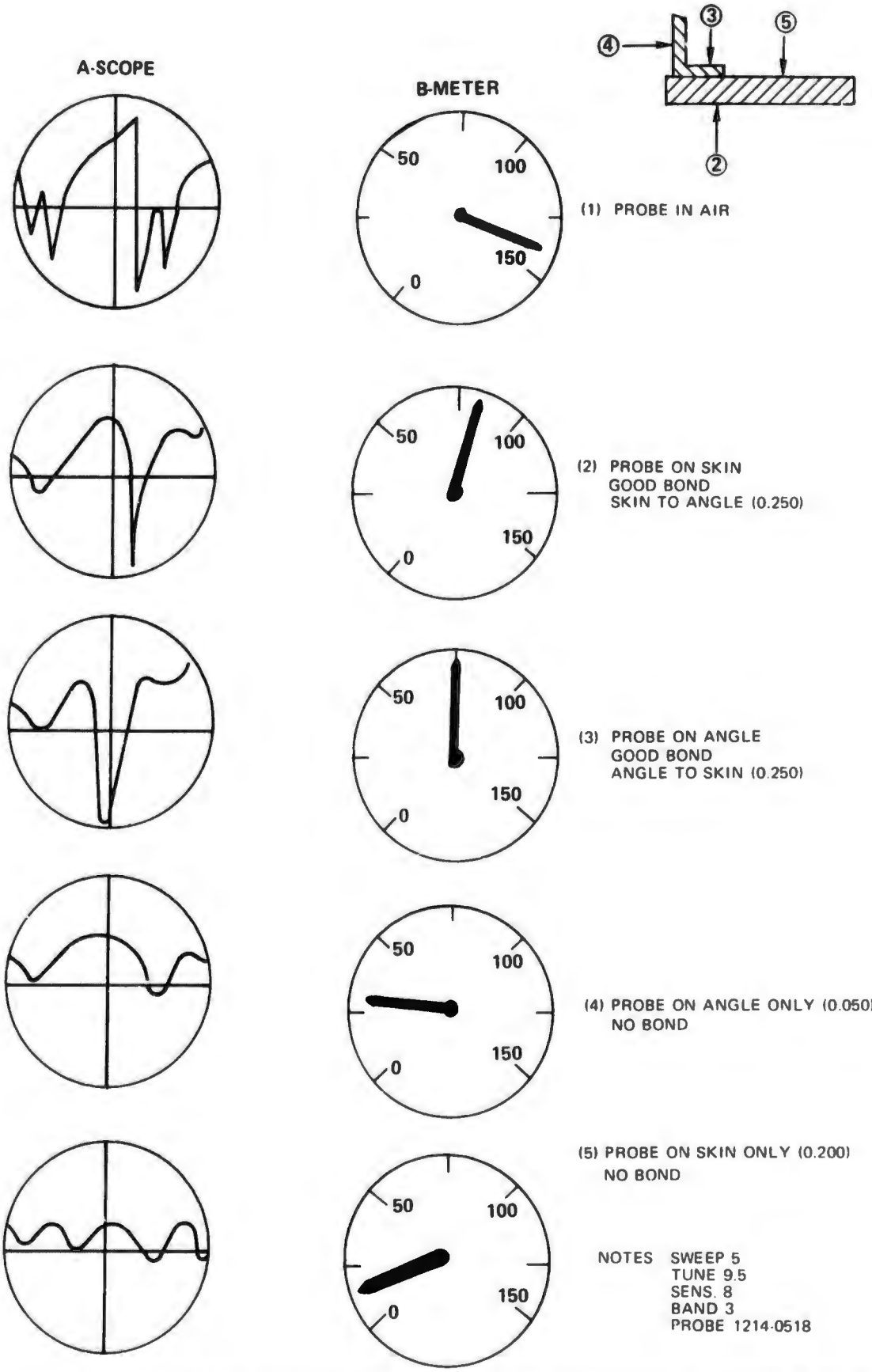

FIGURE C-5. FOKKER BOND TESTER PRESENTATIONS FOR ATTACH-ANGLE TO SKIN BOND QUALITY

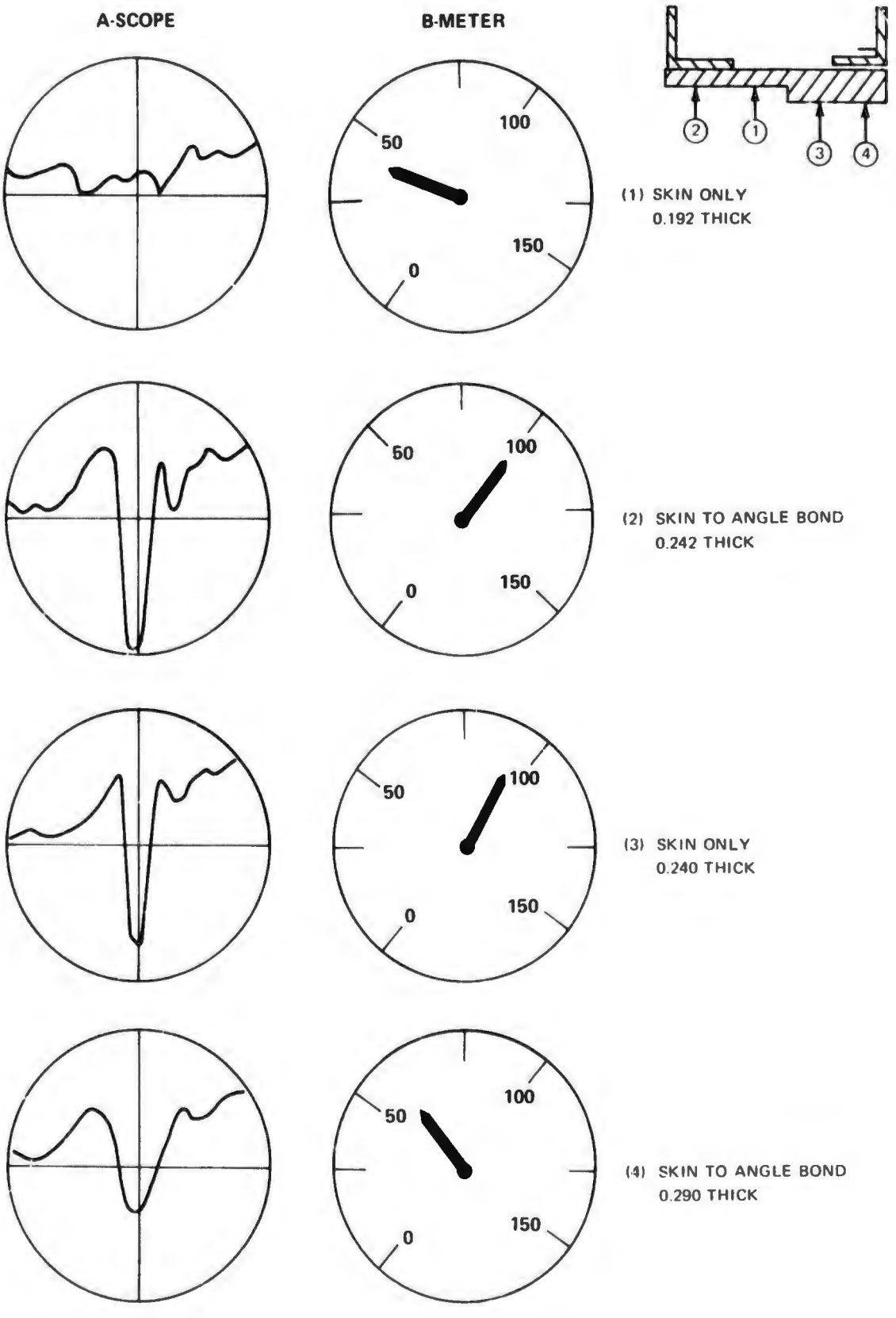

FIGURE C-6. FOKKER BOND TESTER READINGS VS GRAPHITE COMPOSITE THICKNESS

SPECIMEN A. COCURE AND BONDED (NARMCO 329 ADHESIVE)

BOTTOM SKIN ONLY

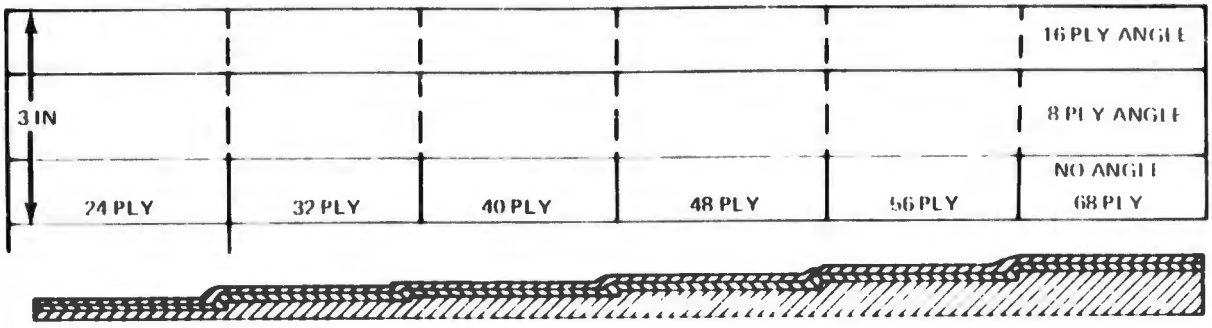

SPECIMEN B. PRECURED ANGLE (BONDED WITH HYSOL EA 951) AUTOCLAVE

TOP SKIN SIMULATION NOT USED

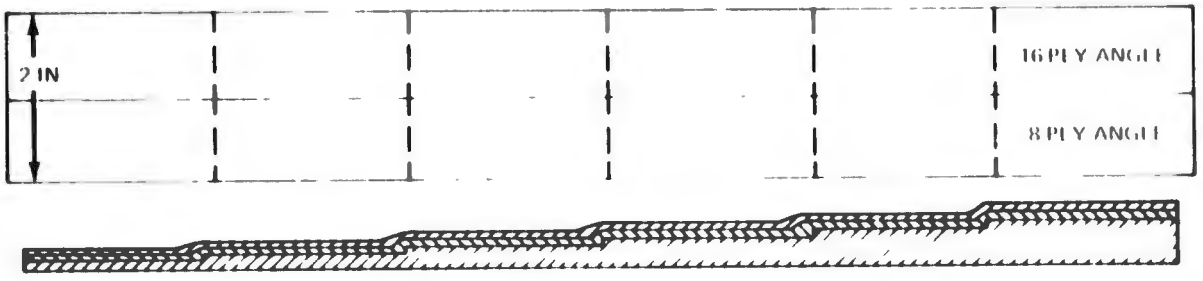

SPECIMEN C PRECURED ANGLE LEG (BONDED WITH HYSOL EA 951) BOLT PRESSURE

TOP SKIN ONLY ACTUAL BOND

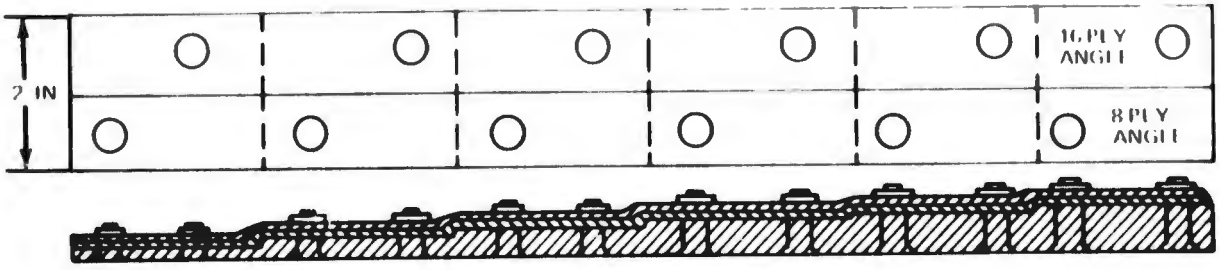

FIGURE C 7. NDT STANDARD SPECIMENS FOR EVALUATING SKIN TO ATTACH ANGLE BOND QUALITY

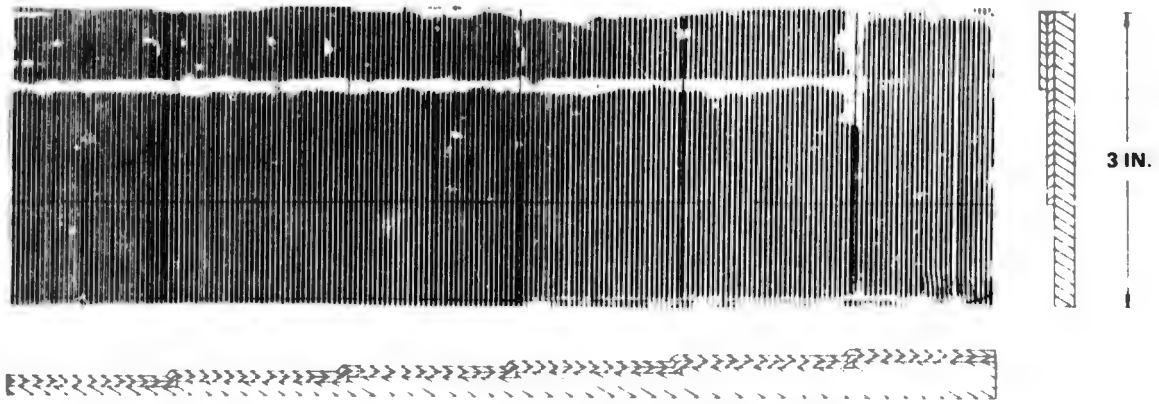

SPECIMEN A. CO CURE AND BONDED WITH 1 PLY NARMCO 329 ADHESIVE

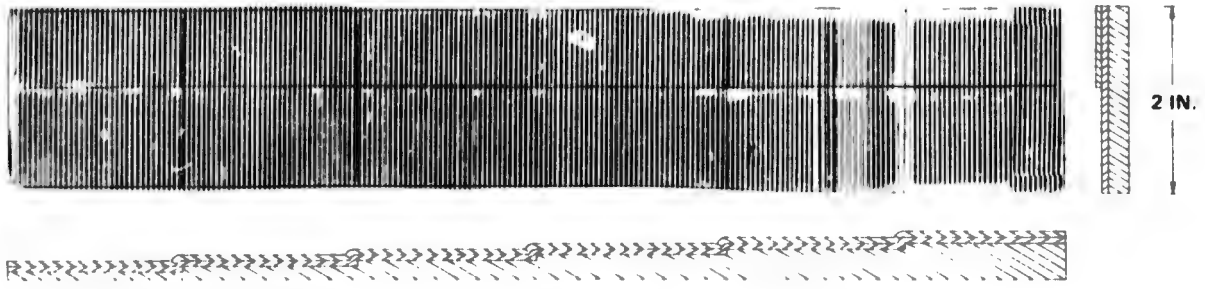

SPECIMEN B. PRECURED ANGLE LEG BONDED WITH SHELL EA-951 ADHESIVE (AUTOCLAVE)

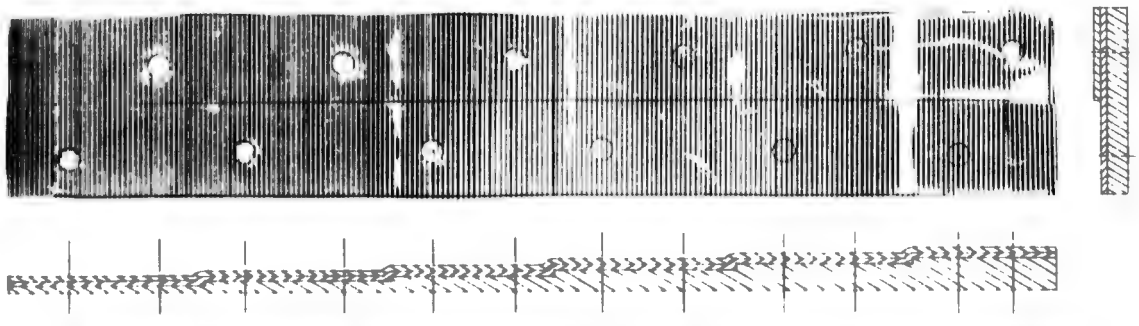

SPECIMEN C. PRECURED ANGLE LEG BONDED WITH SHELL EA-951 ADHESIVE (BOLT PRESSURE)

FIGURE C-8. ULTRASONIC C-SCAN RECORDINGS OF NDT STANDARD SPECIMENS

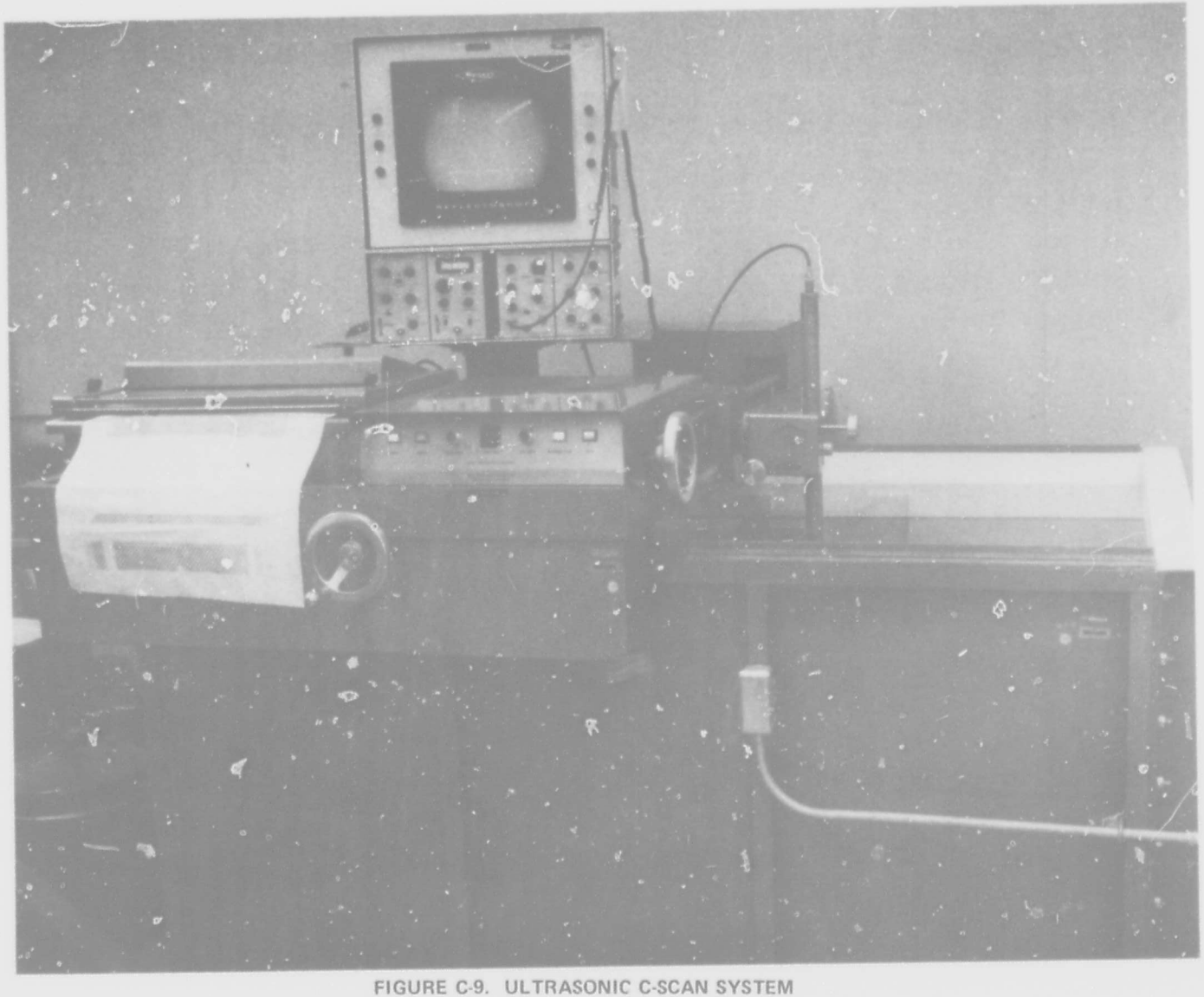

FIGURE C-9. ULTRASONIC C-SCAN SYSTEM

evaluated using contact pulse-echo ultrasonic tests. A Reflectoscope (Figure C10) was used in conjunction with a 3/8 inch diameter SFZ, 5 MHZ search unit with Fokker bond test fluid as a couplant. The search unit was placed on each step of Specimen A (Figure C7) and the CRT presentation was photographed. The results of this test were recorded to facilitate interpretation of the change in signal spacing with changes in thickness. The difference in response between a bond and no-bond condition was evaluated by comparing the bare skin (no-bond) condition with a bonded condition for an 8 ply angle and for a 16 ply angle.

The specimens were also evaluated using the Fokker bond tester, Figure C11. The Fokker probe was placed on each step of Specimen A and the results indicated by the A-scope (CRT) and B-meter readings were recorded (see Figure C12). There was an obvious and distinct variation in response between the bond and no-bond conditions. The instrument settings were also recorded in Figure C12. Specimen A was tested with the probe placed both on the skin side (Figure C12) and on the angle side (Figure C13). Comparison of Figures C12 and C13 indicate similar results.

Each of the three specimens were then tested to evaluate the Fokker response regarding differences in adhesive (i.e., Narmco 329 and Hysol EA951) or differences in curing (i.e., Specimen B, autoclave versus Specimen C, oven cured using bolt pressure). The Fokker results for the bonded 8 ply angle on the three specimens show a marked similarity, Figure C14. The test was repeated on the bonded 16 ply angle on all three specimens. The results illustrated in Figure C15, again showed a similarity of response.

Having established the test criteria from the reference standards, the actual bond joints on the horizontal stabilizer were evaluated. The Fokker was calibrated to the specific thickness step of the test standard prior to evaluating that thickness in the horizontal stabilizer. Each upper skin constant thickness section of the stabilizer was checked for bond to the upper attach-angles and the results were indicated on a drawing of the part. The results are shown in Figure C16 (LH side) and Figure C17 (RH side). The Fokker probe was moved along each angle between the fasteners and the results were indicated as good bond, partial bond, or poor bond. The good and poor bond responses were compared directly to the reference standards. The partial-bond response was one which did not correlate directly to the applicable reference standard. The bond quality as determined by the Fokker was also evaluated in specific areas using the contact pulse-echo technique. The bond versus unbond responses correlated with results of the ultrasonic test. The partially bonded areas showed an erratic bond response associated with a decrease in signal amplitude when evaluated by the pulse-echo technique.

Reference standards for evaluating the bond at the skin to rear-spar and skin leading-edge-to-angle were not available. The skin leading-edge-to-angle bond joint consists of a skin thickness of 0.084 inch (14 ply) bonded to the -45 (8 ply) angle. To evaluate the joint, a piece of skin material 0.088

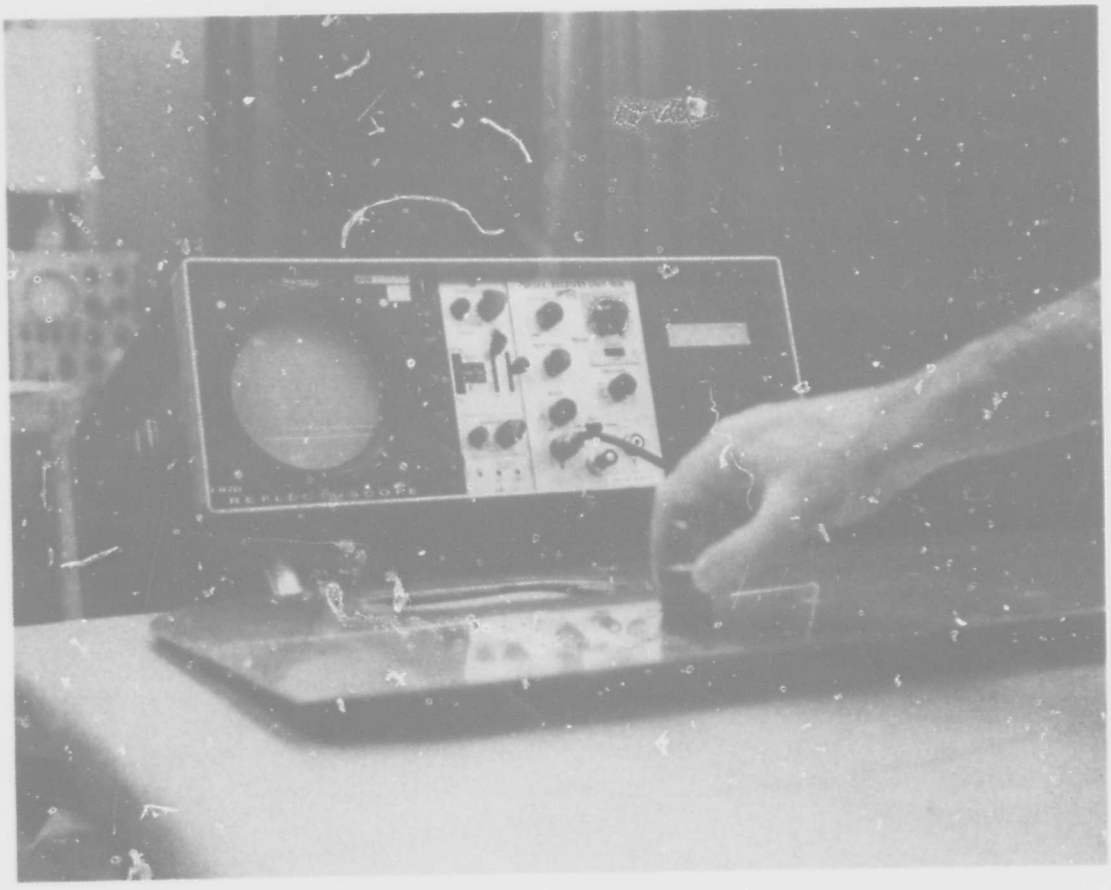

FIGURE C-10. ULTRASONIC TEST INSTRUMENT

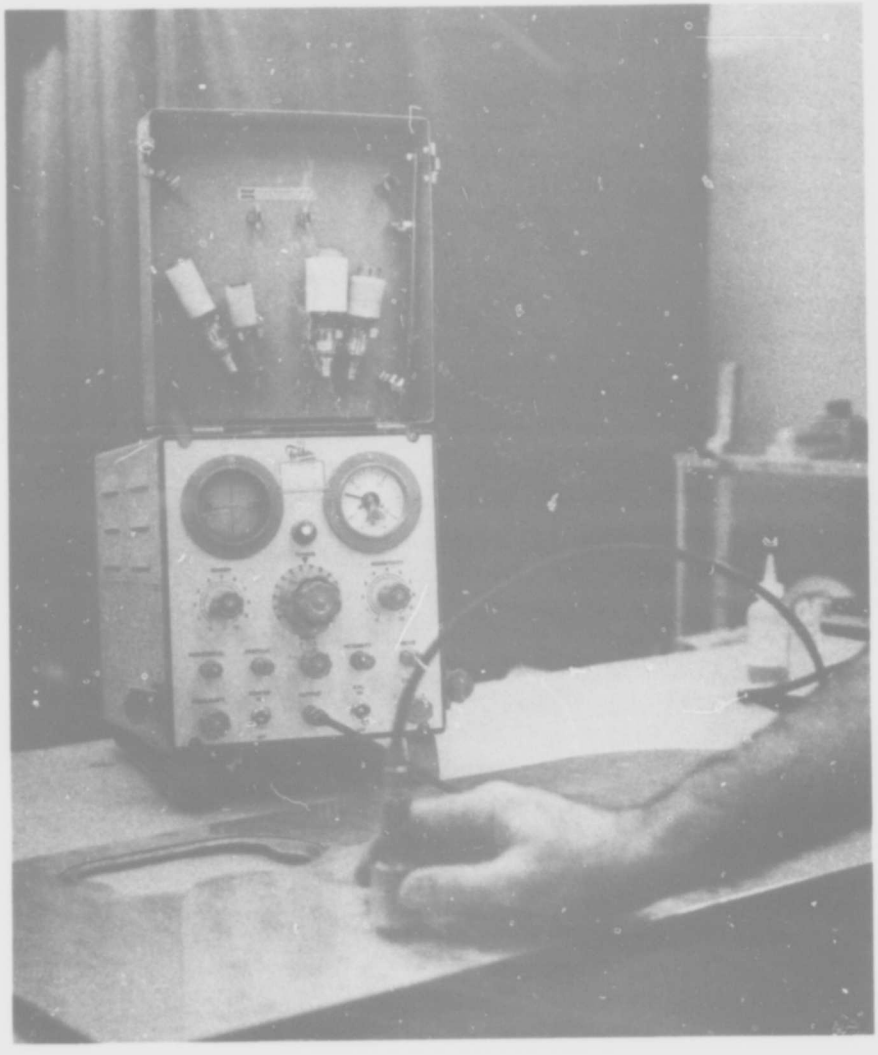

FIGURE C-11. FOKKER BOND TESTER

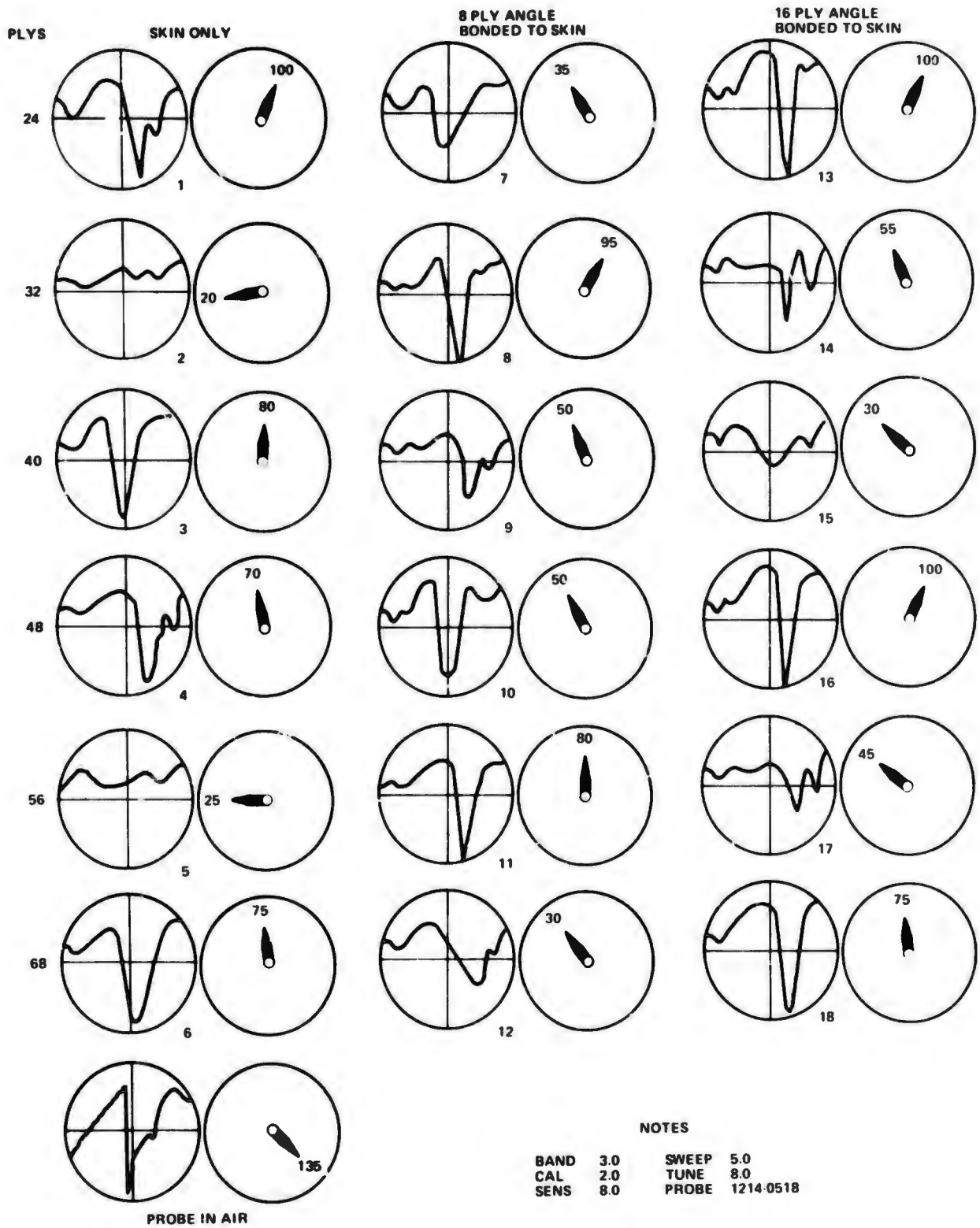

FIGURE C-12. FOKKER BOND TESTER PRESENTATIONS FOR SPECIMEN A FROM SKIN SIDE

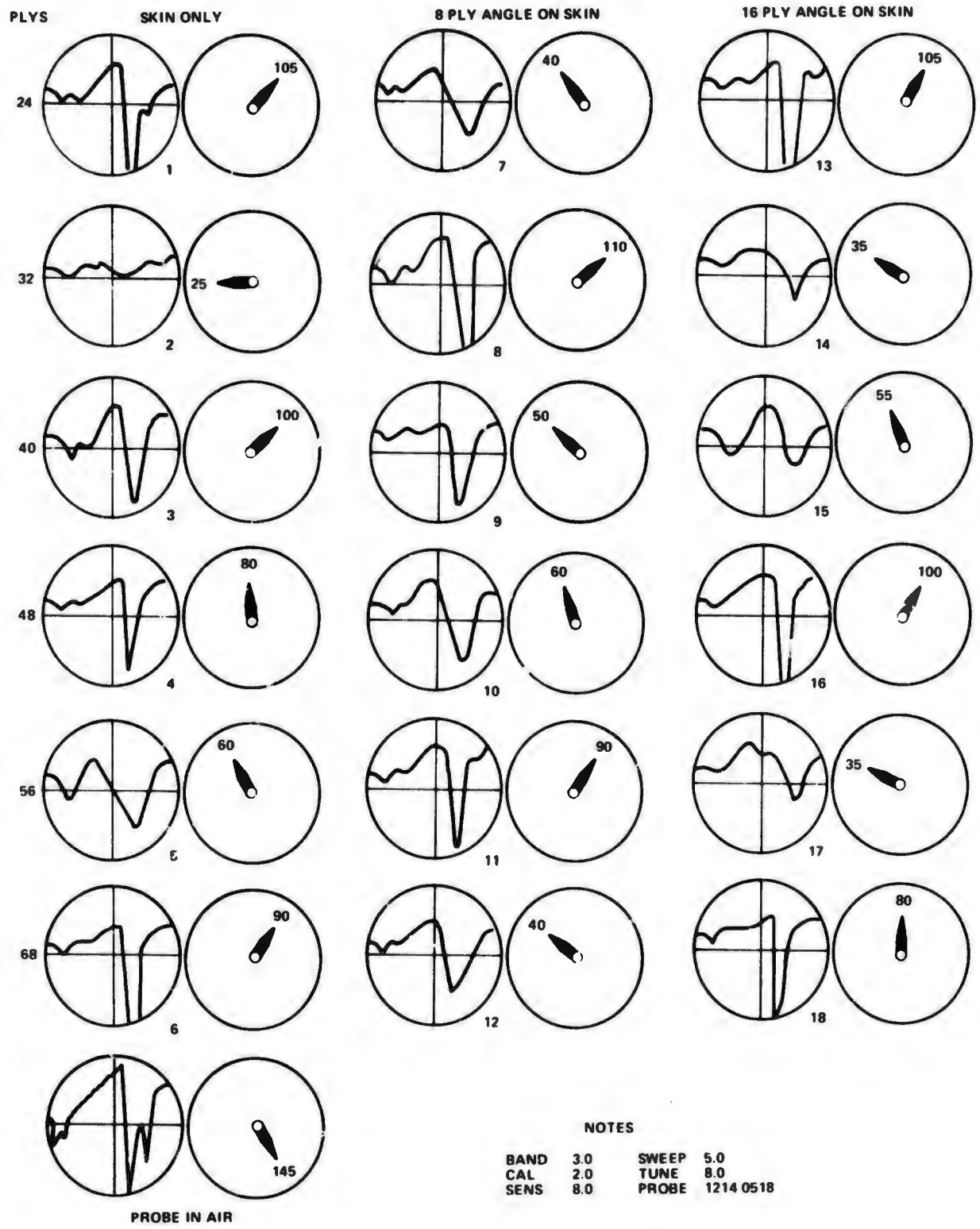

FIGURE C-13. FOKKER BOND TESTER PRESENTATIONS FOR SPECIMEN A FROM ANGI E SIDE

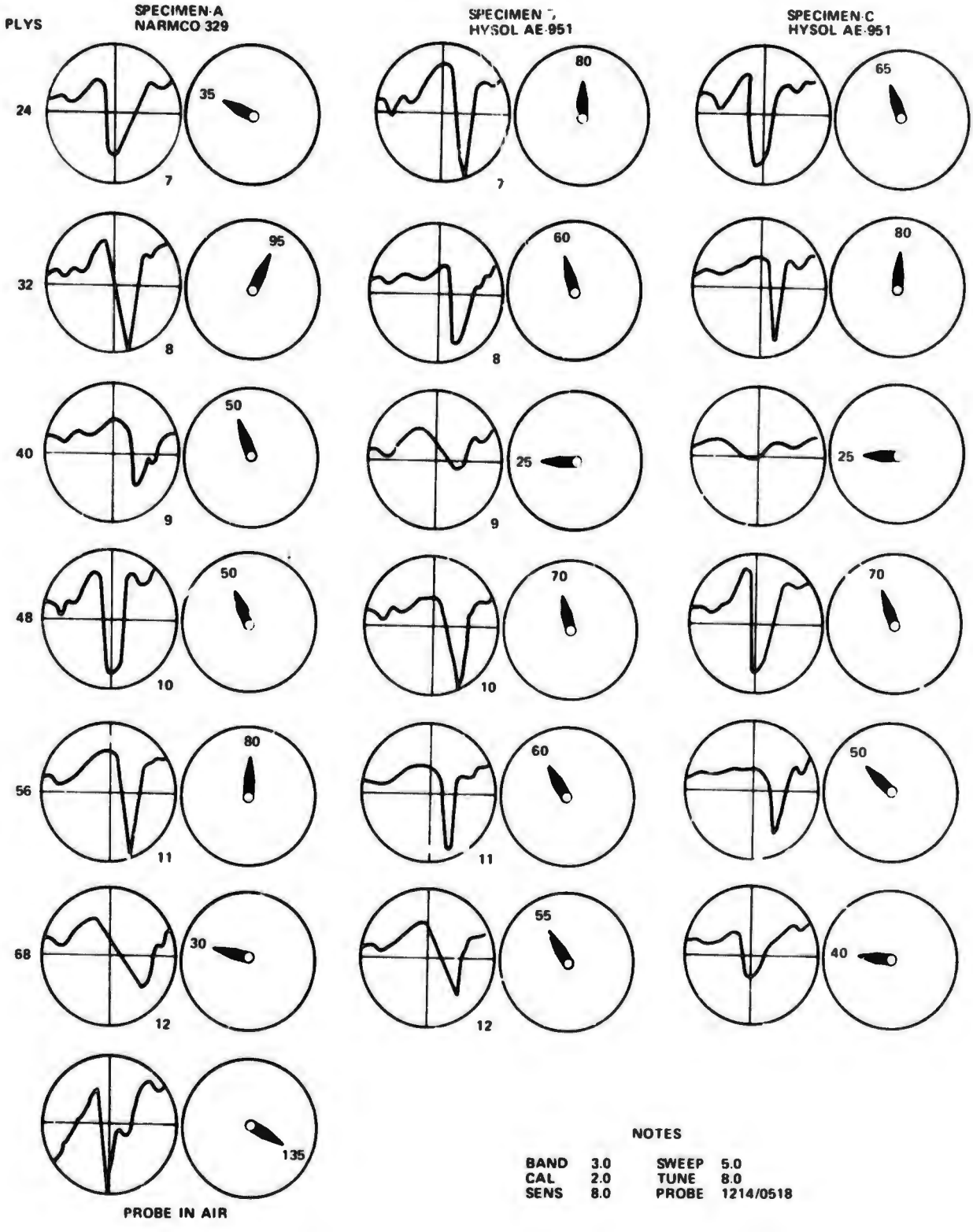

FIGURE C-14. FOKKER BOND TESTER PRESENTATIONS FOR SPECIMENS A, B, AND C WITH 8-PLY ANGLE

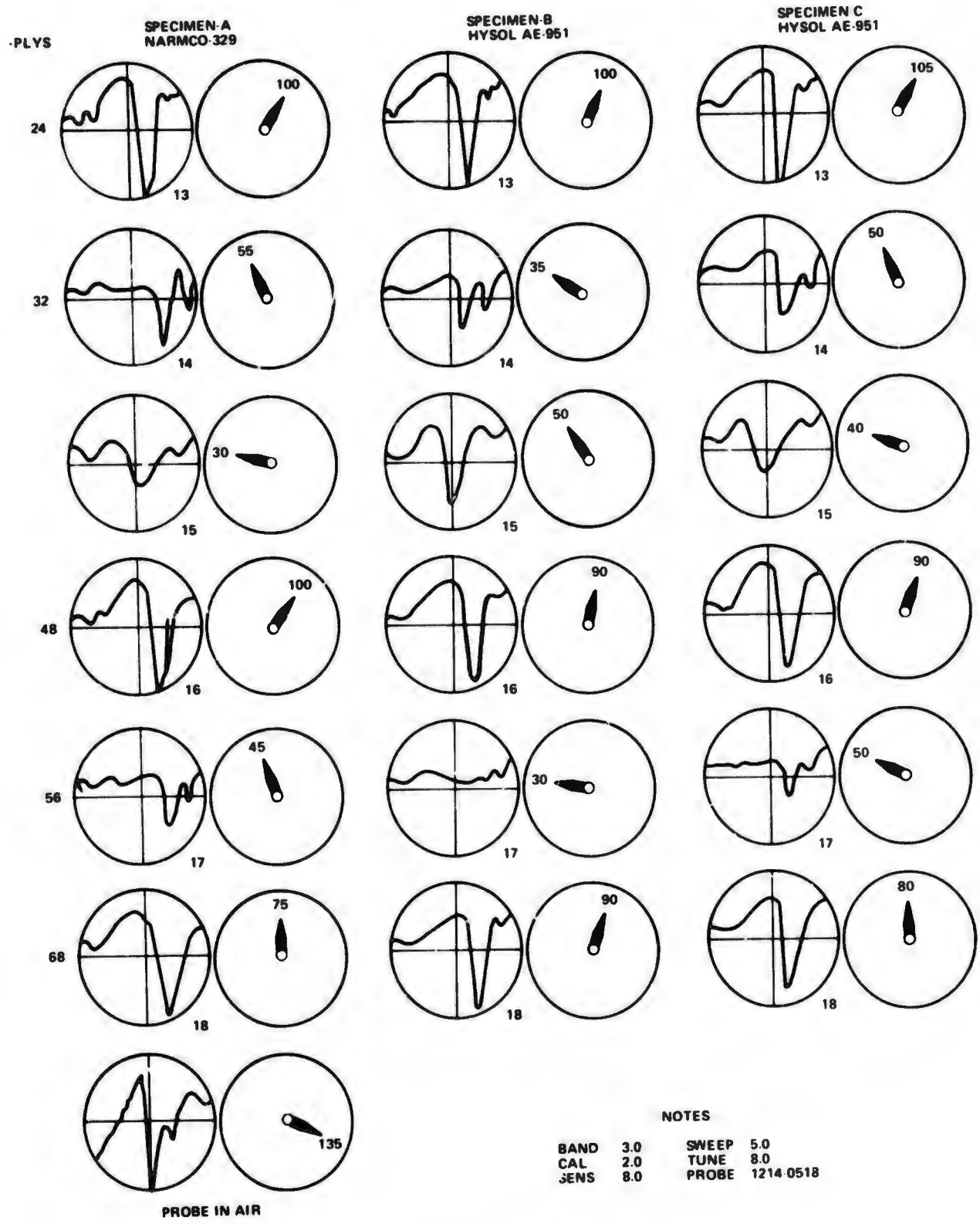

FIGURE C-15. FOKKER BOND TESTER PRESENTATIONS FOR SPECIMENS A, B, AND C WITH 16-PLY ANGLE

Z5569966
TOP SKIN PLAN VIEW
FOKKER TEST RESULTS

● INDICATES GOOD BOND QUALITY

▮▮▮▮▮▮▮ INDICATES POOR BOND QUALITY

\# INDICATES MARGINAL BOND QUALITY

▭ INDICATES TAPER IN SKIN THICKNESS

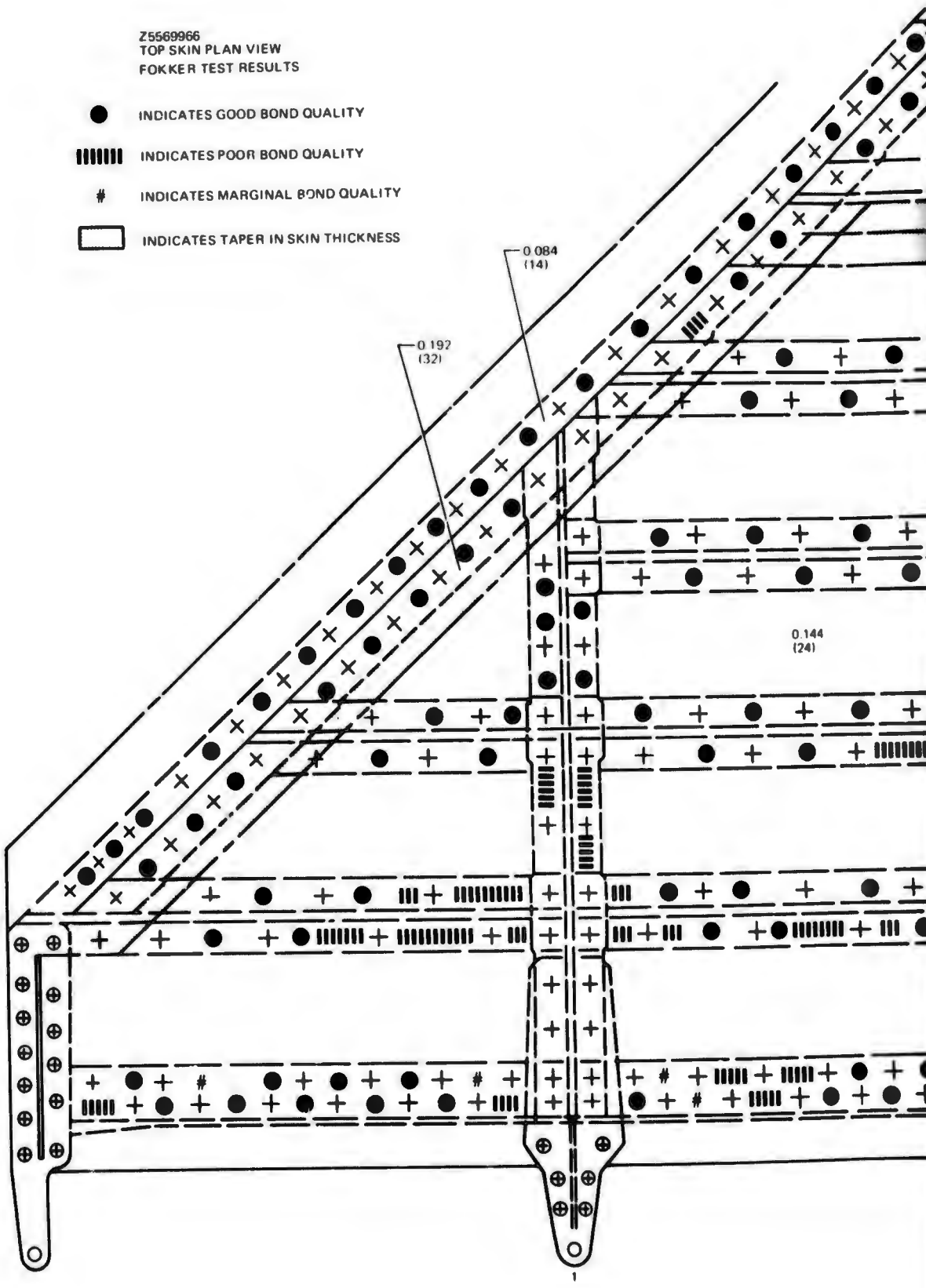

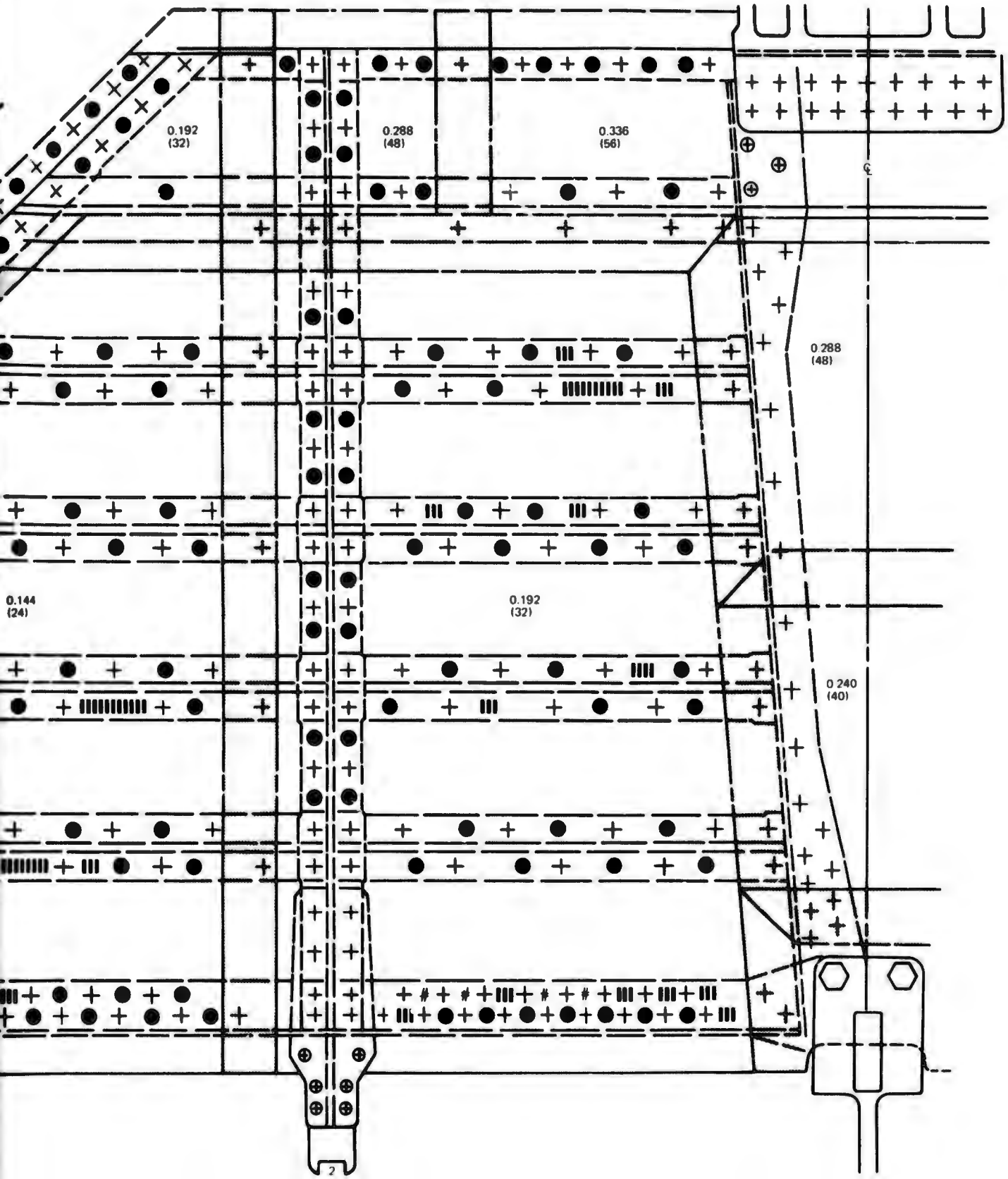

FIGURE C-16. FOKKER BOND TEST RESULTS FOR UPPER SKIN TO ATTACH-ANGLE BOND – LH SIDE

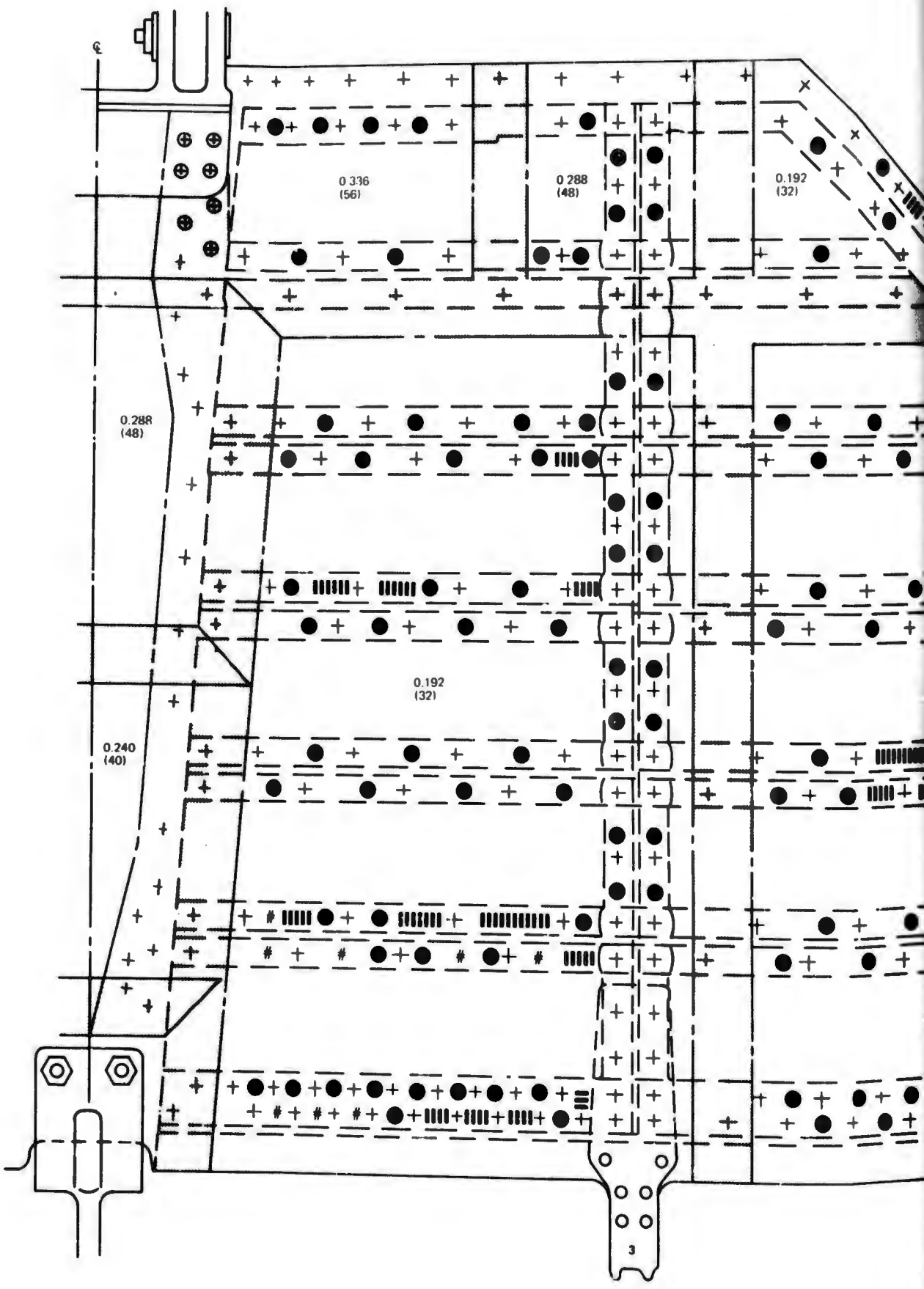
0.336
(56)
0.288
(48)
0.192
(32)
0.288
(48)
0.192
(32)
0.240
(40)
3

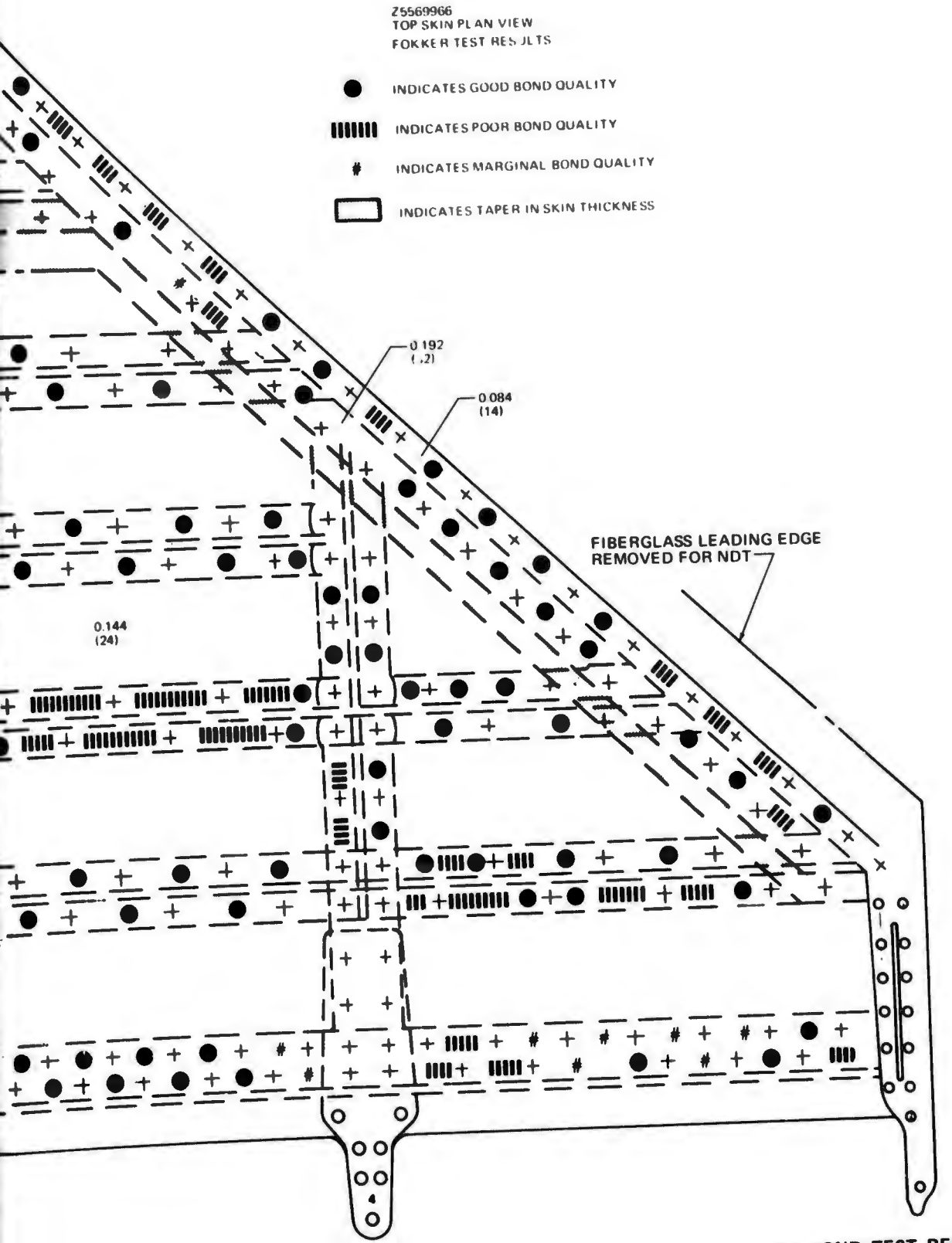

FIGURE C-17. FOKKER BOND TEST RESULTS FOR UPPER SKIN TO ATTACH-ANGLE BOND – RH SIDE

inch thick was obtained to determine the Fokker response for this thickness which represents a no-bond condition. The probe was placed on the part and the response was noted (see Figure C17). The left hand side showed a good bond response along the full length. Partial unbond was shown along the right hand side. The skin to rear-spar was checked by calibrating the Fokker to Specimen A (24 and 32 plies) which represented no-bond along the rear-spar. The probe was scanned along the rear-spar and readings shown in Figure C18 were obtained. Test results are shown in Figures C16 and C17. Hinges 1 through 4 were checked by setting up to the Specimen A (24 and 32 plies) standards which represented a non-bond condition. No lack of bond was detected in any of the hinge areas.

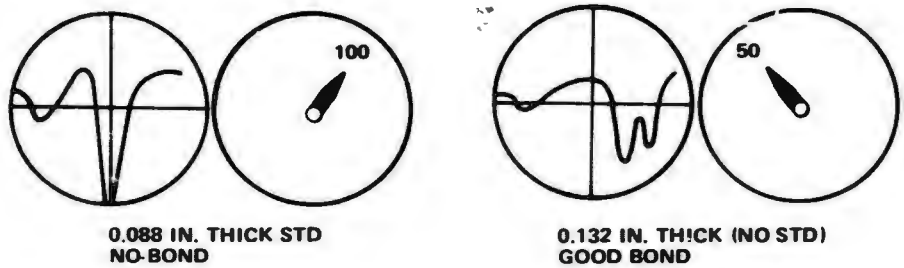

A. SKIN LEADING EDGE TO DOUBLER BOND JOINT

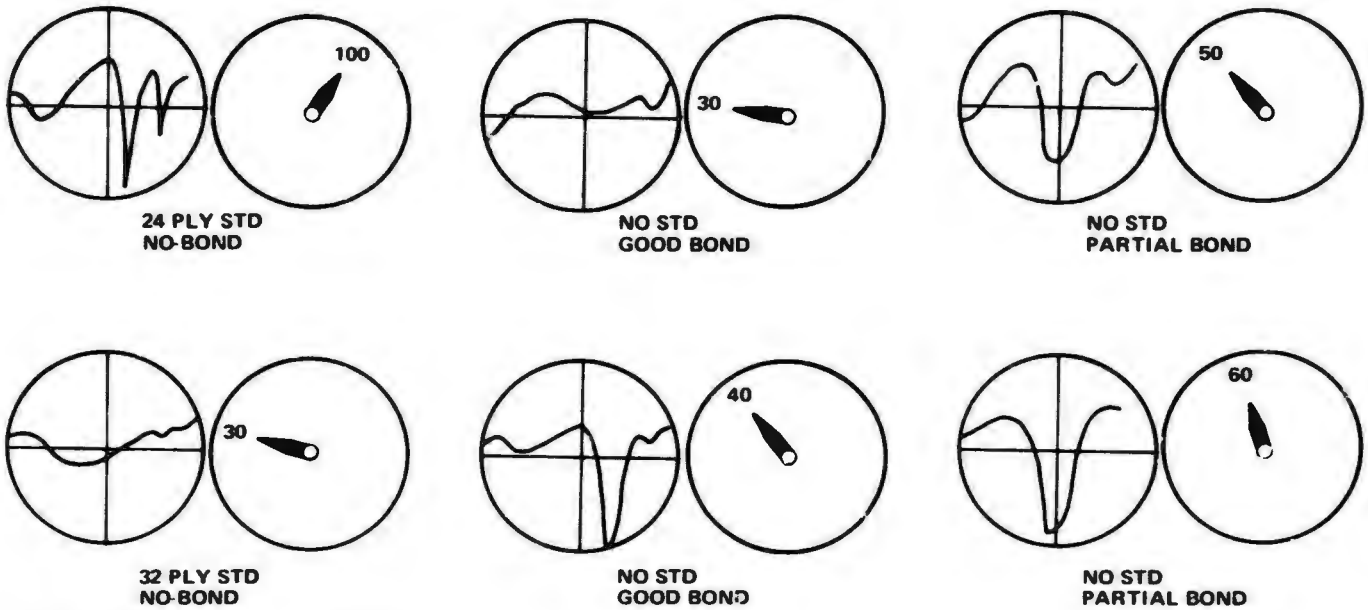

B. SKIN TO REAR SPAR BOND JOINT

FIGURE C-18. FOKKER BOND TESTER PRESENTATIONS FOR SECTIONS TESTED WITHOUT STANDARD SPECIMENS

APPENDIX D

FABRICATION PROCEDURES

This appendix describes fabrication and assembly procedures used in the manufacture of the horizontal stabilizer. Step-by-step procedures are presented for laminate layup and curing, machining, bonding, and in-process quality testing of details and assemblies. Tooling, materials, and processes required during detail part fabrication and assembly are defined.

In-process quality test specimens were made during each cure and bond cycle. The types, numbers, and locations of specimens are indicated in the panel cutting and identification diagrams included in the fabrication procedures. Test data were recorded on a Fabrication and Control Traveller (FACT) sheet which accompanied each component during fabrication.

STABILIZER ASSEMBLY

Fabrication Procedure Summary

The upper and lower surface graphite-epoxy attach angles were laid-up in the "B" stage, debulked, trimmed to length, and stored at 0°F until needed during assembly bonding. The substructure assembly was machined to contour at the upper and lower surfaces using machining templates (plaster back-casts) taken directly from the inner surfaces of the mating skin panels. The first assembly bond cycle was accomplished in the autoclave to co-cure and bond the upper surface attach angles to the substructure assembly. The upper skin panel (suitably protected with a teflon film to preclude bonding) was used as the mold surface to insure the proper bevels and contours on the attach angle skin flanges. The second assembly bond cycle was also accomplished in the autoclave to co-cure and bond the lower surface attach angles to both the substructure assembly and the lower surface panel. The resulting bond assembly was installed in the assembly-jig and fastener holes were prepared for the skin panels, the leading-edge, and the various fitting attachments. The lower surface attachments were installed, and nutplates were located and bonded at the upper surface, leading-edge, and fitting attach holes. The upper skin panel was bolted in place with an adhesive film at the faying surface between the panel and the attach angle flanges. The adhesive film was subsequently oven-cured using the bolt pre-load to supply bonding pressure to the adhesive. The leading-edge assemblies and the various fittings were then installed to complete the horizontal stabilizer assembly.

Applicable Drawings

Z5569970	Substructure Assembly-Graphite Composite Horizontal Stabilizer
Z5569966	Horizontal Stabilizer Assembly-Graphite Composite
Z5569975	Structure Installation-Graphite Composite Horizontal Stabilizer Leading Edge

Special Tooling

Z5669970-BONJ	Substructure Assembly Bonding Jig
C6652-Z5569973-3ET1	Plaster Back Cast - Upper
C6652-Z5569974-3ET1	Plaster Back Cast - Lower
C6652-Z5823615-35BJI	Attach Angle Mandrel
C6652-Z5569973-3PLM1	Laminating and Bonding Mold
C6652-Z5569973-3ET2	Bonding Pressure Plate
C6652-Z5569966-1AJ1	Assembly Jig
C6652-Z5569966-AT1	Drill Template
C6652-Z5569975-17LT1	Rivet Layout Template
C6652-Z5569975-25LT1	Bolt Layout Template
C6652-Z5569966-1ATP1	Drill Template
C6652-Z3569977-1LT1	Bolt Layout Template
C6652-Z5569975-27AT1	Trim and Drill Template

Materials

- Narmco 5206 graphite/epoxy, DMS1936, Type II (Narmco)
- 5-3008 Epoxy Filler (Organoceram Company)
- Prekote 87-76 Mold Release (Ram Chemical Company)
- Mockburg Bleeder Paper CW-1850 (West Coast Paper Company)
- EA951 Adhesive Film, MMM-A-132, (Dexter Corporation, Hysol Division)
- ADX 228 Adhesive Primer (Dexter Corporation, Hysol Division)
- EA9306 Adhesive, (Dexter Corporation, Hysol Division)
- Metlbond 329 Adhesive, MMM-A-132, Type II, 0.070 lb/sq.ft. (Narmco)
- Armalon Permeable Release Cloth, Type 403F-DPM3463 (Hastings Plastic)
- Coreprene DK-153 Edge Dam (Western Gasket and Packing Company)

Methods and Processes

1. "B" Stage Attach Angle Fabrication

   a. Layup the upper and lower surface "B" stage attach angles on the attach angle mandrel (C6652-Z5823615-35BJ1) in accordance with Tables DI and DII, respectively.

   b. Debulk each layup at 100 psi and 150°F for 10 minutes in the autoclave.

   c. After debulking, cut the attach angles to length as indicated in Tables D1 and DII.

   d. Apply Metlbond 329 adhesive film to the external surfact of the tapered leg only of the upper surface attach angles (Table DI).

   e. Apply Metlbond 329 adhesive film to the external surfaces of both legs of the lower surface attach angles (Table DII).

TABLE DI

UPPER SURFACE "B" STAGE
ATTACH ANGLE LAYUP SUMMARY

PATTERN	LAYUP LENGTH (IN.)	NUMBER OF LAYUPS REQD	PARTS CUT FROM EACH LAYUP		
			5569966 DASH NO.	QTY	LENGTH (IN.)
$(0^{o}/45^{o}/-45^{o}/90^{o})2S$ (16 PLY)	38.00	2	–5 –51	1 1	14.50 23.00
$(0^{o}/45^{o}/-45^{o}/90^{o})S$ (8 PLY)	44.50	1	–3	8	5.50
	50.00	2	–3	9	5.50
	50.00	1	–13	3	16.50
	52.50	1	–13 –15 –37	1 1 2	16.50 17.00 9.25
	57.25	2	–19 –45 –49	1 1 1	6.50 43.50 6.75
	57.50	1	–21	6	9.50
	58.50	1	–17 (STA 20) –17 (STA 40)	4 4	6.75 7.75
	58.50	1	–23 –25 –27	2 2 2	11.50 13.00 4.50
	59.50	1	–29 –43	2 2	17.75 11.75
	59.50	1	–31 –41	2 2	19.25 10.25
	59.75	4	–35	3	19.75
	61.00	1	–15 –33	3 2	17.00 4.75
	61.00	1	–39 –47	2 2	13.75 16.75
	61.50	1	–7	4	15.25
	62.50	1	–9	4	15.50
	64.50	1	–11	4	16.00

TABLE DII

LOWER SURFACE "B" STAGE
ATTACH ANGLE LAYUP SUMMARY

PATTERN	LAYUP LENGTH (IN.)	NUMBER OF LAYUPS REQD	PARTS CUT FROM EACH LAYUP		
			5569966 DASH NO.	QTY	LENGTH (IN.)
$(0^{o}/45^{o}/-45^{o}/90^{o})2S$ 16 PLY	38.00	2	-55	1	14.50
			-53	1	23.00
$(0^{o}/45^{o}/-45^{o}/90^{o})S$ 8 PLY	44.50	1	-63	8	5.50
	50.00	2	-63	9	5.50
	50.00	1	-69	3	16.50
	52.50	1	-69	1	16.50
			-71	1	17.00
			-93	2	9.25
	57.25	2	-57	1	6.50
			-59	1	43.50
			-101	1	6.75
	57.50	1	-75	6	9.50
	58.50	1	-89 (STA 20)	4	6.75
			-89 (STA 40)	4	7.75
	58.50	1	-77	2	11.50
			-79	2	13.00
			-83	2	4.50
	59.50	1	-73	2	17.75
			-97	2	11.75
	59.50	1	85	2	19.25
			-95	2	10.25
	59.75	4	-87	3	19.75
	61.00	1	-71	3	17.00
			-81	2	4.75
	61.00	1	-91	2	13.75
			-99	2	16.75
	61.50	1	-61	4	15.25
	62.50	1	-65	4	15.50
	65.50	1	-67	4	16.00

f. Wrap the attach angles and adhesive in a moisture proof film, identify (dash number) each angle, and store at 0°F until needed during the stabilizer assembly bonding.

2. Substructure Machining

a. Using the substructure bonding jig (BONJ) as a holding fixture, mount the Z5569970 substructure assembly on the Rockford Profile Milling Machine. Index the upper surface plaster back-cast (C6652-Z5569973-3ET1) to the substructure.

b. Machine the rear-spar and cant-rib flanges to contour using a four-flute carbide end-mill (1/2 inch diameter, 3600 rpm). See drawing number Z5569966 for flange thickness and dimensional restraints. Conduct the machining operations dry (without cutting fluid) to protect the honeycomb panel edges.

c. Machine the honeycomb sandwich facings one face at a time without cutting fluid using a diamond router (1/4 inch diameter, 3600 rpm).

d. Invert the Z5569970 substructure assembly and reinstall it in the holding fixture (BONJ). Index the lower surface plaster back cast (C6652-Z5569974-3ET1) to the substructure.

e. Machine the lower surface to contour as in steps (b) and (c) above.

3. First Bond Cycle - Upper Attach Angles to Substructure

a. Locate the upper skin panel on the C6652-Z5569973-3PLM1 Laminating and Bonding Mold.

b. Completely cover the inner surface of the skin panel with a 5 mil teflon film to preclude adhesion to the panel during the first bond cycle.

c. Prepare the Z5569970 substructure assembly for bonding by grit-blasting and/or scuff-sanding a one-inch wide strip along the upper edge of the web assemblies. Areas not to be cleaned shall be protected with masking tape.

d. Carefully vacuum-clean the substructure assembly to remove the grit-blast residue.

e. Locate the substructure assembly on the bonding mold against the teflon film on the upper skin panel.

f. Apply a bead of Organoceram 5-3008 at the junctions of the sub-structure web assemblies and the teflon film (upper panel) and form a fillet with a concave radius of 0.103 to 0.134 inch.

g. Cure the Organoceram 5-3008 fillets at room temperature for 24 hours.

h. Remove the "B" stage upper-surface attach angles (Table DI) from cold storage and warm to room-temperature before opening the sealed package.

i. Locate the upper attach angles on the bonding mold with the adhesive against the webs of the substructure assembly in accordance with drawing number Z5569966, view A, zone 9.

j. Fit all attach angles into place and press down firmly to assure intimate contact between the angles, the web skins, and the teflon film (upper skin) so the proper skin bevels and contours will be attained during the cure cycle.

k. Layup a graphite-epoxy quality control panel (Figure D1) and the adhesive test coupons (Figure D2) and position them on the mold surface between the right and left-hand cant-rib flanges so the panel and adhesive will cure during the autoclave cycle.

l. After all angles are fitted in place, apply edge dams at both edges of each angle. Use teflon tape for edge dam at the tapered leg of the angle, and Coreprene at the edge of the skin flange and around the edges of the quality control panel. Cut and apply a teflon coated nylon stripper-ply to the skin flange of each attach-angle.

m. Cut Armalon to fit over all the angles. Apply the Armalon in two strips, one on the vertical (tapered) leg of the angle, and one on the skin flange of each angle. Two pieces are required to preclude bridging at the corners of the angles. Apply one layer of Armalon to the quality control panel.

n. Cut Mockburg bleeder paper into strips in a similar manner and apply one strip to the vertical (tapered) leg of the angle and two strips to the skin flange of each angle. Apply Mockburg bleeder paper to the quality control panel at a ratio of one layer of bleeder to four layers of laminate.

o. Cover the bleeder paper with teflon film and seal the edges of film with tape. Allow sufficient slack in the teflon film to allow it to slide into the apex of the attach angles without bridging. Apply leather fillets in all corners of the substructure to prevent bridging of the vacuum-bag in these areas.

p. Fit the bonding pressure plate (C6652-Z5569973-3ET2) on the top of the substructure assembly to prevent direct pressure application of the edges of the honeycomb webs.

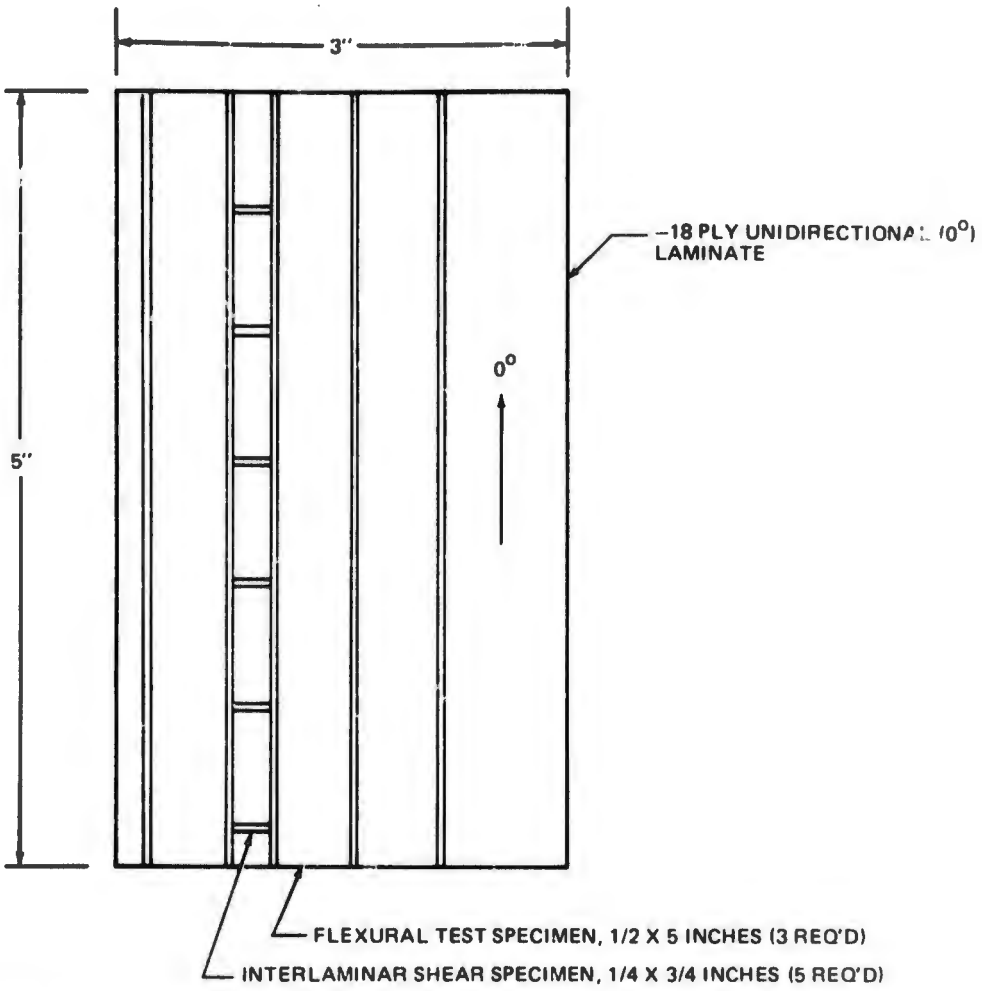

FIGURE D1. LAMINATE QUALITY CONTROL PANEL AND CUTTING DIAGRAM

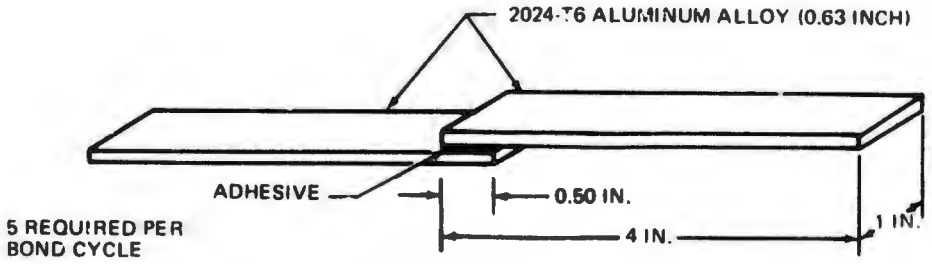

FIGURE D2. IN-PROCESS ADHESIVE TEST COUPON

q. Apply fiberglass bleeder cloth to the assembly taking care to assure that the bleeder cloth reaches all areas of the assembly and that sufficient material is used to allow 50 psi pressure to be applied without any bridging. Pay particular attention to the lower corners of the assembly so that the total area of the "B" stage angles receives full pressure.

r. Vacuum-bag the entire assembly with a large sheet of nylon bagging material. Fit the nylon bag carefully into each cavity so that no wrinkles occur over the prepreg angles. Seal the edges of the bag and apply vacuum.

s. With vacuum applied to the assembly, check for leaks and recheck the position of bag. Reposition the bag if necessary to insure that there is no wrinkling or bridging in the areas of the prepreg angles. When the bag position and vacuum are satisfactory, place the assembly in the autoclave for cure.

t. Cure in autoclave using the following cure cycle sequence:

   (1) Apply vacuum pressure

   (2) Turn on autoclave with temperature setting at 285°F.

   (3) When part temperature reaches 275°F or after autoclave has been at 275°F or higher for three hours, whichever occurs first, apply 50 psi pressure (using nitrogen) and vent vacuum to atmosphere.

   (4) Increase part temperature to 350°F.

   (5) Cure two hours at 350°F and 50 psi.

   (6) Cool under pressure to less than 150°F and remove from autoclave.

   (7) Record the cure cycle on the FACT sheet.

u. Remove the bag and clean the substructure assembly as required.

v. Cut quality-control flexure, interlaminar shear, resin, and void-content coupons from the QC panel as shown in Figure D1. Record test results on the FACT sheet together with the adhesive test coupon results.

w. Inspect the adhesive bond lines visually and with a Fokker Bond Tester and record observations and results on the FACT sheet.

4. Second Bond Cycle - Lower Attach Angles to Substructure and Lower Panel.

a. Locate the lower skin panel on the C6652-Z5569973-3PLM1 Laminating and Bonding Mold.

b. Prepare the inner surface of the lower skin panel (Z5569974) for bonding by grit-blasting and/or scuff-sanding in areas where bonding is required. Areas not to be cleaned shall be protected with masking tape.

c. Prepare the Z5569970 substructure assembly for bonding by grit-blasting and/or scuff-sanding a one-inch wide strip along the lower edge of the web assemblies. Areas not to be cleaned shall be protected with masking tape.

d. Carefully vacuum-clean the substructure assembly and the lower skin panel to remove the grit-blast residue.

e. Locate the substructure assembly on the bonding mold against the lower skin panel.

f. Apply a bead of Organoceram 5-3008 at the junctions of the substructure web assemblies and the lower skin panel and form a fillet with a concave radius of 0.103 to 0.134 inch.

g. Cure the Organoceram 5-3008 fillets at room temperature for 24 hours.

h. Remove the "B" stage lower-surface attach angles (Table DII) from cold storage and warm to room-temperature before opening the sealed package.

i. Locate the lower attach angles on the bonding mold with the adhesive against the webs of the substructure assembly and the lower skin panel in accordance with drawing number Z5569966, view A, zone 9.

j. Fit all attach angles into place and press down firmly to assure intimate contact between the angles, the web skins, and the lower skin panel so the proper skin bevels and contours will be attained during the cure cycle.

k. Layup a graphite-epoxy quality control panel (Figure D1) and the adhesive test coupons (Figure D2) and position them on the mold surface between the right and left-hand cant-rib flanges so the panel and adhesive will cure during the autoclave cycle.

l. After all angles are fitted in place, apply edge dams at both edges of each angle. Use teflon tape for edge dam at the tapered leg of the angle, and Coreprene at the edge of the skin flange and around the edges of the quality control panel. Cut and apply a teflon coated nylon stripper-ply to the skin flange of each attach-angle.

m. Cut Armalon to fit over all the angles. Apply the Armalon in two strips, one on the vertical (tapered) leg of the angle, and one on the skin flange of each angle. Two pieces are required to preclude bridging at the corners of the angles. Apply one layer of Armalon to the quality control panel.

n. Cut Mockburg bleeder paper into strips in a similar manner and apply one strip to the vertical (tapered) leg of the angle and two strips to the skin flange of each angle. Apply Mockburg bleeder paper to the quality control panel at a ratio of one layer of bleeder to four layers of laminate.

o. Cover the bleeder paper with teflon film and seal the edges of film with tape. Allow sufficient slack in the teflon film to allow it to slide into the apex of the attach angles without bridging. Apply leather fillets in all corners of the substructure to prevent bridging of the vacuum-bag in these areas.

p. Fit the bonding pressure plate (C6652-Z5569973-3ET2) on the top of the substructure assembly.

q. Apply fiberglass bleeder cloth to the assembly taking care to assure that the bleeder cloth reaches all areas of the assembly and that sufficient material is used to allow 50 psi pressure to be applied without any bridging. Pay particular attention to the lower corners of the assembly so that the total area of the "B" stage angles receives full pressure.

r. Vacuum-bag the entire assembly with a large sheet of nylon material. Fit the nylon bag carefully into each cavity and position such that no wrinkles occur over the prepreg angles. Seal the edges of the bag and apply vacuum.

s. With vacuum applied to the assembly, check for leaks and recheck the position of bag. Reposition the bag if necessary to insure that there is no wrinkling or bridging in the areas of the prepreg angles. When the bag position and vacuum are satisfactory, place the assembly in the autoclave for cure.

t. Cure in autoclave using the following cure cycle sequence:

(1) Apply vacuum pressure

(2) Turn on autoclave with temperature setting at 285°F

(3) When part temperature reaches 275°F or after autoclave has been at 275°F or higher for three hours, whichever occurs first, apply 50 psi pressure (using nitrogen) and vent vacuum to atmosphere

(4) Increase part temperature to 350°F

(5) Cure two hours at 350°F and 50 psi

(6) Cool under pressure to less than 150°F and remove from autoclave

(7) Record the cure cycle on the FACT sheet

u. Remove the bag and clean the substructure assembly as required.

v. Cut quality-control flexure, interlaminar shear, resin, and void-content coupons from the QC panel as shown in Figure A1. Record test results on the FACT sheet together with the adhesive test coupon results.

w. Inspect the adhesive bond lines visually and with a Fokker Bond Tester and record observations and results on the FACT sheet.

5. Fastener Hole Preparation and Installation - Lower Panel

a. Locate the substructure to lower skin bond assembly (Z5569970 and Z5569974) in the C6652-Z5569966-1AJ1 assembly jig (AJ) with the open upper surface facing inward toward the AJ frame structure.

b. Insert two tooling pins through the rear spar web tooling holes at stations X = ±32.560 and Y = 453.125.

c. Install a third tooling pin through the front spar web at station X = 0, on the stabilizer centerline at station Y = 418.062.

d. Install tooling pins through the Z3569971 hinge brackets at stations X = ±58.187 and Y = 457.250.

e. Locate and identify the stabilizer chord plane (horizontal plane) through two tooling holes located at station X = ±32.560 in the rear spar web.

f. Locate and identify bracket location points at stations X = ±20.000 and ±40.000.

g. Locate and identify all hole locations on rear spar web for the aerodynamic seal attachment.

h. Locate and clamp the appropriate drill bushings to rear spar outer surface and 1/2-inch thick aluminum blocks against the corresponding inner surface for drilling the aerodynamic seal attach holes.

i. Hand drill the holes using an air-motor at 2400 rpm. Remove all drill chips from the substructure assembly.

j. On the lower skin (Z5569974) complete drilling of two 1/8-inch diameter coordinating holes through the attach angles. These holes were previously located and drilled in the skin at stations X = 30.000 and Y = 447.135, prior to bonding attach angles.

k. Check coordinating holes for proper distance from datum surface of -31 web at station Y = 446.375 (Z5569970).

l. Locate the C6652-Z5569966-AT1 drill template (AT1) in the AJ against the lower skin through the two coordinating holes at stations X = +30.000 and Y = 447.135. Support the weight of the AT1 at bracket stations X = +20.000 and +40.000 and along AT1 trailing edge. Clamp edges of AT1 to the lower skin.

m. Insert a 0.128 inch inside diameter (ID)/0.500 inch outside diameter (OD) bushing in one of the AT1 holes and drill a pilot hole. Check for proper hole location on the attach angles per Z5569966. Relocate bushing in same bolt line, drill, and check again. Repeat pilot hold drilling and checking as necessary.

n. Insert 0.1875 inch ID/0.500 inch OD bushing in AT1 and drill hole with 3/16 inch diameter carbide spade insert drill at 2400 rpm using an air-motor. Drill all 0.1875 inch ID holes in Z5569974 lower skin, except in Z3569971 bracket fitting. Drill the latter holes with same carbide spade drill mounted in a 450 to 600 rpm air-motor.

o. Ream all appropriate holes with a 0.1895 inch diameter body reamer with an 0.1875 inch diameter pilot mounted in a 450 to 600 rpm air-motor.

p. Adjust a countersink stop gage to the proper depth with a 100° countersink cutter and a number 12 pilot. Mount in an air-motor and countersink all appropriate 0.1895 inch diameter holes using 450 to 600 rpm per note 10 of Z5569966. Start with a high-speed-steel cutter and finish with a carbide cutter.

q. Adjust a countersink stop gage to the proper depth with a 100° countersink cutter and a 0.250 inch diameter pilot. Mount in an air-motor and countersink all appropriate 0.250 inch diameter holes using 450 to 600 rpm, per note 10 of Z5569966. Start with a high-speed-steel cutter and finish with a carbide cutter.

r. Grind the vertical flange portions of the attach angles to allow proper fit of the Z3569977 pivot fitting web flanges. Make 3 x 5 inch oval cutout in the front-spar web per Z5569966, View K-K.

s. Locate and install the Z3569977 pivot fitting and the AJ-230 assembly as shown in View B of the tool drawing, C6652-Z5569966-AJ1.

t. Install the 5547524 actuator fitting in the AJ1 and on the horizontal stabilizer so that it is symmetrical about the centerline and is aligned with the chord plane.

u. Apply a release coat to the appropriate side of one each of the -109, -111, and -113 shims per Z5569966, General Note 16. Insert shims and apply adhesive per General Note 16 and bond shims to the rear-spar or lower skin.

v. Install and clamp the -3 and -5 assemblies of C6652-Z5569966-1ATP1 in place on the AT1. Use a low speed 450 to 600 rpm air-motor for the following operations.

w. Use a number 12 (0.1875 inch diameter or a 3/16 inch diameter) carbide bit and a number 10 bushing to drill the 24 required holes through the lower skin and each cant-rib flange. Remove the -3 part of the -1 ATP1 from the AT1 drill template. Ream the 48 holes using a 0.1895/0.1915 inch diameter reamer with a 0.1875 inch diameter pilot.

x. Use a 0.421 (27/64) inch diameter carbide bit and bushing in the 1ATP1-5 to drill 17 holes through the pivot fitting flange and the lower skin.

y. Remove the -5 part of the 1ATP1 from the AT1. Ream the 17 holes using a 0.4370/0.4390 inch diameter reamer with 0.421 inch diameter pilot.

z. Install bolts, washers, and nuts in the lower skin (excluding the pivot and actuator fitting bolts) and torque in accordance with the instructions on Z5569966.

6. Fastener Hole Preparation-Upper Panel.

a. Remove the bond assembly from AJ1, rotate 180°, and relocate and pin in AJ1.

b. Insert two tooling pins through the rear spar web tooling holes at stations X = ±32.560 and Y = 453.125. Install a third tooling pin through the front spar web at Station X =) on the stabilizer centerline at station Y = 418.062. Install tooling pins through the Z3569971 brackets at stations X - ±58.187 and Y = 457.250.

c. Locate and identify stations X = +30.000 and Y = 447.735 on the top side of upper attach angles -35 and -87.

d. Install drill breakout surface material (peel-ply) for actuator and pivot fittings and between cant-rib flanges. Locate the upper skin (Z5569973) in the AJ so that the corresponding coordinating holes at station X = ±30.00 are centered over the station lines identified above.

e. Locate the C6652-Z5569966-AT1 drill template (AT1) in the AJ against the upper skin through the two coordinating holes at stations X = ±30.000 and Y = 447.135. Support the weight of the AT1 at bracket stations X = ±20.000 and ±40.000 and along AT1 trailing edge. Clamp edges of AT1 to the lower skin.

f. Insert a 0.128 inch ID/0.500 inch OD bushing in one of the AT1 holes and drill a pilot hole. Check for proper hole location on the attach angles per Z5569966. Relocate bushing in same bolt line, drill and check again. Repeat pilot hole drilling and checking as necessary.

g. Insert 0.1875 inch ID/0.5000 inch OD bushing in AT1 and drill hole with 3/16 inch diameter carbide spade insert drill at 2400 rpm using an air-motor. Drill all 0.1875 inch diameter holes in Z5569973 upper skin and attach angles except in the Z3569971 bracket fitting. Drill these holes with the same carbide spade drill mounted in a 450 to 600 rpm air-motor.

h. Ream all the holes with a 0.1895 inch diameter body reamer with a 0.1875 inch diameter pilot mounted in a 450 to 600 rpm air-motor.

i. Adjust a countersink stop gage to the proper depth with a 100° countersink cutter and a number 12 pilot. Mount in an air-motor and countersink all appropriate holes using 450 to 600 rpm per note 10 of Z5569966. Start with a high-speed steel cutter and finish with a carbide cutter.

j. Adjust a countersink stop gage to the proper depth with a 100° countersink cutter and a 0.250 inch diameter pilot. Mount in an air-motor and countersink all appropriate holes using 450 to 600 rpm per note 10 of Z5569966. Start with a high-speed steel cutter and finish with a carbide cutter.

k. Locate and install the Z3569977 pivot fitting and the AJ-230 assembly as shown in View B of the tool drawing, C6652-Z5569966-AJ1.

l. Install the 5547524 actuator fitting in the AJ1 and on the horizontal stabilizer so that is is symmetrical about the centerline and is aligned with the chord plane.

m. Install and clamp the -3 and -5 of the Z5569966-1ATP1 in place on the AT1. Use a 450 to 600 rpm air-motor for the following operations.

n. Use a number 12 (0.1875 inch diameter or a 3/16 inch diameter) carbide bit and a number 10 bushing to drill the 24 required holes through the upper skin and each cant-rib flange. Remove the -3 part of the -1 ATP1 from the AT1 drill template.

o. Ream the 48 holes using a 0.1895/0.1915 inch diameter reamer with a 0.1875 inch diameter pilot.

p. Use a 0.3594 (23/64) inch diameter carbide bit and bushing in the 1ATP1-5 to drill 18 holes through the pivot fitting flange and the upper skin.

q. Remove the -5 part of the 1ATP1 from the AT1.

r. Ream the 18 holes using a 0.3745/0.3765 inch diameter reamer and a 0.3594 inch diameter pilot.

s. Remove the AT1 drill template from the upper skin.

7. Fastener Hole Preparation - Fittings

a. Layout the 12 hole centers on the pivot fitting web as shown in Zone 4, View E-E on drawing Z5569966.

b. Drill the 12 pilot holes (0.125 inch diameter) through the fitting web and front-spar using layout template C6652-Z356997-1LT with a carbide drill.

c. Use a 0.2969 (19/64) inch diameter drill with a 0.125 inch diameter pilot to enlarge the 12 holes.

d. Ream the 12 holes through the pivot fitting web and the front-spar web using a 0.3125 inch diameter reamer with a 0.2969 inch diameter pilot.

e. Use a 0.375 inch diameter carbide drill and a drill-table bushing aligned with the pilot hole in the actuator fitting 5547524 and drill the two pilot holes through the upper skin and cant-rib flanges, View E-E of 75569966. Do not drill normal to the lower skin contour.

f. In a similar manner, drill the two 0.375 inch diameter holes through the actuator fitting and the rear-spar.

g. Ream the two holes through the actuator fitting and the rear-spar using a 0.5000 inch diameter reamer with a 0.4844 inch diameter pilot.

h. Install the Z3569978 and Z3569979 brackets with a release agent on the shim surfaces which contact the brackets. Locate a -105 shim against the lower skin inner surface and a -107 shim against the rear spar web outer surface at stations X = +20.000 and +40.000. Fill the gaps between shims and skin with adhesive per Note 6 of Z5569966 just prior to installing the tooling pins which locate the Z3569978 and Z3569979 brackets. Cure the adhesive at room temperature.

i. Using the two 0.190/0.194 inch diameter pilot holes in each bracket, drill the pilot holes through the rear spar web with a number 10 high speed steel drill 1-1/2 inches long, mounted in a 2800 rpm right angle drive(American Pneumatic Drill Motor-Model #810).

j. Drill 0.234 inch diameter holes through the pilot holes in the bracket from the rear-spar web inner surface with a 0.234 inch diameter drill body with a 0.190 inch diameter pilot.

k. Ream from the rear-spar web inner surface with a 0.232 inch diameter left hand spiral-piloted reamer. Operate the reamer at 450 rpm.

l. Remove shavings and clean the rear-spar and brackets.

m. Install NAS6404U-8 and -9 bolts through the bracket web holes and the adjacent rear-spar holes at Stations X = +20.00 and +40.000. Install 1252416H washers per Z5569966 and MS21075-L4 nutplates. Torque the bolts to 50-70 inch pounds in accordance with DP2.70-2.

n. Drill all 0.234 inch diameter holes through the lower skin shims, doublers, and bracket fittings at stations X = ±20.000 and ±40.000 with a high speed steel drill mounted in a 450 to 600 rpm air-motor.

o. Ream the holes with a 0.250/0.254 inch diameter body reamer and a 0.234 inch diameter pilot rotating at 450 to 600 rpm.

p. Install the upper skin panel and the -105 shims in the AJ and repeat steps n and o for the upper panel hinge bracket attachments.

q. Remove the upper skin panel from the AJ and strip all drill breakout material (peel ply) from the skin panel and substructure assembly.

8. Fastener Hole Preparation - Leading Edge

a. Locate a Z5569975-13 (lower right) and a -14 (lower left) panel assembly against the AT1 with the inboard leading edge in place between the AT1 loft line contour and the Z5569974 lower panel leading edge recess.

b. Locate the other -13 (upper left) and the -14 (upper right) panel assemblies against the AJ-525 contour boards and clamp in place.

c. Insert a .1875 inch diameter handle or flanged drill bushing with a .500 inch OD into one of the inboard leading edge positions of the AT1 on the lower surface. Drill a hole with a 3/16-inch diameter carbide spade insert drill mounted in a 2400 rpm air-motor.

d. Relocate the bushing and complete drilling the holes through the -13 and -14 panels, the lower skin panel, and attach angles Z5569966-51 and -53.

e. Ream the holes with a 0.1895/0.1915 inch diameter body reamer with a 0.1875 inch diameter pilot rotating at 450 to 600 rpm.

f. At stations X = ±5.750 (ref.) and Y = 417.232 insert a 0.234 inch ID/0.500 inch OD drill bushing. Drill two 0.234 inch diameter holes with a 2400 rpm air-motor. Remove the bushings and ream the two holes with a 0.250/0.254 inch diameter body reamer with a 0.234 inch diameter pilot rotating at 450 to 600 rpm.

g. Adjust a countersink stop gage to the proper depth with a 100° countersink cutter and a number 12 pilot. Mount in an air-motor and countersink all appropriate holes using 450 to 600 rpm. Start with a high-speed-steel cutter and finish with a carbide cutter.

h. Repeat steps (c) through (g) for the upper surface Z5569975-13 and -14 panels.

i. Place the Z5569975-27 leading edge skin so that its net trimmed inboard edge fits around the Z5569975-17/-19 rib assembly and along entire left hand leading edge to the net trimmed outboard end at X = 58.968. Scribe upper and lower edge trim lines. Remove the -27 leading edge skin and trim.

j. Place the -27 in the C6652-Z5569975-27AT1 and drill 0.125 inch diameter pilot holes in the upper and lower edges.

k. Fit the left-hand -27 leading edge skin in place, clamp, and drill all holes through the -27 and the lower and upper skins with a 0.1875 (3/16) inch diameter carbide drill aligned with a drill table bushing and the pilot hole in the -27.

l. Adjust a countersink stop gage to the proper depth with a 100° countersink cutter and a number 12 pilot. Mount in an air-motor and countersink all holes using 450 to 600 rpm. Start with a high-speed-steel cutter and finish with a carbide cutter.

m. Repeat steps (i) through (l) for the right-hand leading edge.

9. Third Bond Cycle - Upper Panel to Attach Angles

a. Place the substructure to lower skin bond assembly in the C6652-Z5569973-1PLM1 laminating and bonding mold for the upper panel fit check.

b. Locate the upper panel on the substructure with a layer of uncured silicone rubber between two 0.002 mil teflon films at the faying surfaces between substructure and upper panel.

c. Cure the silicone rubber layer 24 hours at room temperature.

d. Remove the upper panel and measure the thickness of the rubber sheet with a micrometer over the planform area of the stabilizer. Note thickness variations on the FACT sheet.

e. Locate the substructure to lower skin bond assembly in the AJ with the closed (lower) surface facing the AJ frame structure.

f. Install tooling pins through the Z3569971 hinge brackets at stations X = ±58.187 and Y = 457.250.

g. Prepare all laminate bonding surfaces for internal nutplates by light scuff-sanding and solvent (MEK) wipe.

h. Locate all internal nutplates for the pivot and actuator fittings and the hinge-bracket fittings (stations ±20.000, +40.000, and +58.187). Locate the nutplates on EA951 adhesive film and secure in place for bonding with setup screws of appropriate diameter. Coat the setup screws with mold-release prior to installation.

i. Locate all internal nutplates for the upper panel to the cant-rib, rear-spar, and upper attach angle fasteners. Locate the nutplates on EA951 adhesive film and secure in place for bonding with setup screws or Cleco-clamps of appropriate diameter. Coat the setup screws with mold-release prior to installation.

j. Remove the bond assembly from the AJ and place it on the C6652-Z5569973-1PLM1 laminating and bonding mold. Cure the nutplate adhesive in a circulating air oven at 350°F for two hours.

k. After removal of the bond assembly from the oven, remove all setup screws and Cleco-clamps from the nutplates. Test the nutplate bonds by installing a screw of appropriate diameter in each nutplate.

l. Clean the internal surface of the upper skin panel and the mating flanges of the upper attach angles using light scuff-sand and/or grit blast. Remove the sanding or grit-blast residue using a clean cloth. Prime the cleaned surfaces using Hysol ADX228 primer. Also relocate all nutplates unbonded during step (k) above. Relocate these nutplates using Hysol EA 9306 adhesive and secure in place for rebonding with setup screws of appropriate diameter.

m. Cure the adhesive primer and nutplate bonds in a circulating air oven at 250°F for two hours.

n. After removal of the bond assembly from the oven, remove the setup screws from the rebonded nutplates.

o. Cut and fit EA951 adhesive film on the faying surface of each upper surface attach flange for the rear-spar, cant-ribs, and attach angles. Cut and fit additional local layers to bridge gaps noted during step (d) above.

p. Locate the upper surface panel on the substructure assembly taking care not to displace the adhesive film at the faying surface.

q. Install and torque the upper surface fasteners, (excepting those for the pivot fitting) per instructions on drawing number Z5569966.

r. Locate ten 3/8 inch diameter nutplates for the pivot fitting on the inner surface of the upper panel between the cant-rib flanges. Locate the nutplates on EA951 adhesive film and secure in place using 3/8 inch diameter setup screws. Coat the setup screws with mold-release prior to installation.

s. Cure the adhesive film in a circulating air oven at 350°F for two hours.

t. Inspect the bond with a Fokker Bond Tester and record observations and results on the FACT sheet.

10. Fitting and Leading Edge Installation

a. Locate the structural bond assembly in the AJ and install tooling pins through the Z3569971 hinge brackets at stations X = ±58.187 and Y = 457.250.

b. Locate the pivot and actuator fittings (Z3569977 and 5547524, respectively). Install and torque all attaching hardware per instructions on drawing number Z5569966, excepting the six 5/16 inch diameter bolts through the front-spar web, the Z3569977 fitting, and the Z5569975-25 angles.

c. Locate the Z5569975-13 (lower right and upper left) and -14 (lower left and upper right) panel assemblies in the AJ and index the previously drilled holes to the hole pattern in the structural bond assembly.

d. Install the left-hand Z5569975-19 rib angle against the AJ-515 locator bar with the flanges facing inboard. Place a .007-inch thick adhesive bondline spacer (2 and 5 mil mylar sheets) on the -19 attach flanges and clamp the -19 rib to the -13 panel.

e. Install the left-hand Z5569975-17 rib channel against the -19 rib angle webs with a .007 mylar adhesive bondline spacer located on both the web and attach flanges that bond to the -14 panel assemblies. Clamp the -17 rib channel to the -19 rib angle and the -14 panel.

f. Using a caliper, measure a 0.82 ± .030-inch from the front spar and scribe cut off lines on the -17 rib channel and the -19 rib angle.

g. Identify hole vertical centerline as shown in Zone 8 of Z5569975 and extend lines .75-inch forward of the vertical centerline. Bolt centers are +0.50 and ±1.44 inches from the horizontal stabilizer chord line.

h. Remove -17 and -19 from the AJ. Cut to scribe net size at the lines.

i. Relocate the left-hand -17 and -19 in position in the AJ.

j. Locate the C6652-Z5569975-17 LTI rivet layout template against the -17 rib channel, clamp in place with a drill breakout surface (peel ply and bleeder cloth or aluminum plate) against the exposed -19 rib angle web surface.

k. Drill the 0.128-inch diameter (#30 drill) holes in the rib web for the MS20470AD4 rivets with a high-speed-steel or carbide drill mounted in a 2400 rpm air motor.

l. Install the left-hand Z5569975-25 angle against the -19 rib angle as shown in Zone 8 of drawing Z5569975. Install and torque the three 5/16-inch diameter bolts through the -25 angle, the Z3569977 fitting, and the frontspar web per instructions on drawing number Z5569976.

m. Locate and clamp the C6652-Z5569975-25 LTI so that its centerline aligns with the holes centerline on the -19 rib angle.

n. Drill the two 0.190/0.194 inch diameter holes through the -19 rib angle and -25 angle with a 450 to 600 rpm air motor. Remove the -25 LTI.

o. Locate the -25 LTI on the -17 rib channel and drill two 0.190/0.194 inch diameter holes through the -17 and -25 angle.

p. Locate a Z5569975-35 leading edge zee against the lower left -17 panel forward edge so that its vertical inboard web flange rests against the -19 rib angle. Install 0.007 inch bondline spacers between the -14 panel, -19 rib and the -35 zee flanges. Clamp the -35 zee in place.

q. Locate a -33 leading edge channel against the upper left -13 panel forward edge, the -35 web, and the substructure front-spar (Z5569970-43) extension. Insert the -31 spacer, view G-G, Z5569975, Zone 5. Place a 7 mil adhesive bondline spacer between -33 and -13 and between -33 and -35.

r. Layout the -33 and -35 leading edge rib web hole pattern on ribs as shown in view M-M of drawing number Z5569975. Provide a backup surface for drill breakout and drill the required holes using a #30 drill (0.128 inch diameter) mounted in a 2400 rpm air motor.

s. Remove -17, -19, -33, and -35 from the AJ and bond -17 to -19 and -33 to -35 in accordance with general note 14 on drawing number Z5569975. Install the MS20426AD4 rivets through the rib and channel webs in accordance with drawing number Z5569975. Install rivets through the rib and channel webs in accordance with drawing number Z5569975. Install rivets per standards drawing S-5076260.

t. Install the bonded -17/-19 rib assembly and the -33/-35 channel assembly against the -13 and -14 panels. Locate the -17/-19 rib assembly against the -25 angle and install the four NAS6403U-5 bolts through the -25 angle and rib. Torque to 20-25 inch-pounds.

u. Bond the -17/-19 and the -33/-35 assemblies to the -13 and -14 panels in accordance with general note 14 on drawing number Z5569975.

v. Install the MS20426AD4 rivets though -13 and -14 panels and lower flanges of the -17 and -19 ribs per standards drawing S-5076260.

w. Install the torque the six NAS4903U-3 bolts in the rib to 20-25 inch-pounds.

x. Install the left-hand -27 leading edge using the previously drilled holes. Install and torque the attaching screws to 20-25 inch-pounds.

y. Locate and clamp a Z5569975-29 rib in the end of the -27 leading edge skin against the Z4569980 tee. Layout the centerline on Station X = 57.968, per view E-E on drawing number Z5569975.

z. Drill a 0.125 inch diameter pilot hole through each centerline location on the -29 and the Z4569980 tee. Enlarge with a 3/16 inch diameter carbide drill guided by a drill table. Ream with a -.190 inch diameter reamer with a -.1875 inch diameter pilot.

aa. Layout the six MS20426AD4 rivet centerlines on -27 leading edge skin for the -29 rib. Use a #30 (0.128 inch diameter drill) mounted in a 450-600 rpm air-motor and a drill table to drill the holes.

ab. Adjust a countersink stop gage to the proper depth with a 100° countersink cutter and a #30 pilot. Countersink the rivet holes using 450 to 600 air motor. Install the rivets per standards drawing S-5076260.

ac. Repeat steps (d) through (ab) for the right-hand leading edge installation. Note that Z5569975-34 replaces -33 for the right-hand inboard leading edge assembly (-4).

ad. Remove the completed stabilizer assembly from the AJ.

REFERENCES

1. "Development of a Graphite Horizontal Stabilizer", contract N00156-70-C-1321, Interim Technical Report, McDonnell Douglas Report MDC J5169, July 1971.

2. "Development of a Graphite Horizontal Stabilizer", contract N00156-70-C-1321, Interim Technical Report, McDonnell Douglas Report MDC J0945, December 1970.

3. "Development of a Graphite Horizontal Stabilizer", contract N00156-70-C-1321, Interim Technical Report, McDonnell Douglas Report MDC J1435, June 1970.

4. Anon, "Metallic Materials and Elements for Flight Vehicle Structures", Mil-Hdbk-5A, 1968.

5. Lehman, G. M. et al, "Investigation of Joints in Advanced Fibrous Composites for Aircraft Structures", McDonnell Douglas Corporation, Douglas Aircraft Company, Technical Report, AFFDL-TR-69-43, Volume I, June 1969.

6. Allen, F. C. et al, "Stress Analysis-Model A-4 Graphite Composite Horizontal Stabilizer", contract N00156-70-C-1321, McDonnell Douglas Report MDC J5316, October 1971.

7. Rutishauser, A., "Algurithmus 1 - Lineares Gleichungs System Mit Symmetrischer Positiv-Definiter Bandmatrix Nach Cholesky, Computing (Archives for Electronic Computing), Volume 1, ISS 1 (1966), pg 77-78.

8. Mikkelson, P. T., "Computerized Analysis of Non-Isotropic Structures", Douglas Paper 5617, McDonnell Douglas Corporation, Douglas Aircraft Company, November 1969.

9. "Empennage Loads - Volume III, Horizontal Surface and Control System Loads", Technical Report ES 17192, McDonnell Douglas Corporation, Douglas Aircraft Company, September 1955.

10. Smith, S., "Structural Tests - Tail Group", McDonnell Douglas Corporation, Douglas Aircraft Company, Technical Report ES 17155, Volume II, December 1957.

THIS PAGE LEFT BLANK INTENTIONALLY.